DISTRIBUTED CONTROL OF TENSION IN MULTI-SPAN WEB TRANSPORT SYSTEMS

By

KEE-HYUN SHIN

Bachelor of Science in Engineering
Seoul National University
Seoul, Korea
1981

Master of Science
Oklahoma State University
Stillwater, Oklahoma
1987

Submitted to the faculty of the Graduate College of
the Oklahoma State University
in partial fulfilment of the requirements
for the degree of
DOCTOR OF PHILOSOPHY
May, 1991

DISTRIBUTED CONTROL OF TENSION IN MULTI-SPAN WEB TRANSPORT SYSTEMS

Thesis Approved:

Karl N. Reid

Thesis Adviser

Lawrence J. Haberack

Gary E. Young

John D. Shelton

Carl D. Latta

Norman N. Durham

Dean of the Graduate College

ACKNOWLEDGEMENTS

I wish to express sincere appreciation to Dr. Karl N. Reid for his encouragement, understanding, and advice throughout my graduate program. Dr. John J. Shelton 's encouragement and direction have been very helpful. Many thanks also go to Dr. Lawrence L. Hoberock, Dr. Gary E. Young, and Dr. Martin Hagan for serving on my graduate committee. Their teaching, suggestions, and support were very helpful throughout the study.

I appreciate the support of Mobil Chemical and the efforts of D. Gibben in carrying out my experiment. I sincerely appreciate the financial support of Miwon Group and Rinnai Korea Corporation during these difficult years.

This thesis would have been impossible without God's abundant grace and love. Glory to God! My parents, Young-Kyu Shin and Jin-Joo Hong, and my parents in-law, Kee-Duck Yoo and Man-Soon Suh, encouraged and supported me all the way and helped me keep the end goal constantly in sight. The endless support, love, and prayers of Aeran and Patrick is sincerely appreciated. Without friends like Glenna Banks, John and Marius Green, Dr. Ron Delahoussaye, Dr. Taejoon Um, and Bang-Eop Lee, this endeavor would not have been as stimulating. I extend a sincere thank-you to all of these people.

TABLE OF CONTENTS

LIST OF TABLES

LIST OF FIGURES

NOMENCLATURE

A	Cross-sectional area of web
A_n	System matrix of the n-th open-loop auxiliary model
A_u	Cross-sectional area of unstretched web
A_{nm}	Interconnection matrix of open-loop auxiliary model
$\overline{A}_n$	System matrix of the n-th closed-loop auxiliary model
$\overline{A}_{nm}$	Interconnection matrix of closed-loop auxiliary model
a_n	Constants
B_{fn}	Rotary friction constants of bearing
B_n	Input matrix
b	Viscosity
b_c, b_n	Constants
C_n	Output matrix
c, c_c, c_n	Constants
$c(t)$	Creep function
d, d_n, d_{mn}	Width of web
E, E_1	Modulus of elasticity

E_R	Relaxed elastic modulus
E_2	Viscosity factor in web
e_{ss}	Steady-state error
F_n	Feedback gain vector
F_{n2}	Effective normal force
$F_i(t)$	Temperature of web
F_{i0}	Initial temperature of web
F_{f2}	Effective frictional force
$f(t)$	Time dependent forcing function
f_n^m	Elements in feedback gain F_n vector
G	Shear modulus
G_n	Feedforward control gains
$g_n(t)$	Translation of web due to eccentricities of roller or roll
H_n	Feedback control gains
$H_i(t)$	Moisture of web
H_{i0}	Initial moisture of web
h, h_n, h_{mn}	Thickness of web
I	Unit matrix
J_n	Polar moment of inertia of roll or roller

K_d	Derivative gain of PID controller
K_i	Integral gain of PID controller
K_n	Constants
K_p	Proportional gain of PID controller
k_r	Constants
k, k_s, k_{sn}	Spring constant
k_μ	μ_{20}/μ
$k(t)$	Relaxation function
L, L_n	Length of web span
L_{rn}	Length of roll or roller
M	A matrix
m	Mass of roll or roller
m_w	Mass of the web per unit length
P	A diagonal matrix
Q	A matrix
q_{nm}	Constants
R, R_n	Radius of roll or roller
R_b	Build-up ratio
$\overline{R}$, $\overline{R}_n$	Average radius of roll or roller
R_{cn}	Radius of core of roll

$\overline{R}_{cn}$	Average radius of core of roll
R^n	Real vector
R^{mn}	Real matrix
r_t	Real root
s	Laplace operator
T	Tension (Chapter 2.7)
T_L, T_n, T_x	Change in web tension from a steady-state operating value
T_{nc}	Reference tension in the n-th subsystem
t	Time
t_{n0}	Steady-state operating value for tension
t_n	Tension in web = $t_{n0} + T_n$
U_n	Change in input to a subsystem from a steady-state operating value
$U_{n\,n-1}$	Difference between inputs to motor at the ends of the web span
U_{nc}	Reference input to a subsystem
V_n	Change in web velocity from a steady-state operating value
V_{nm}	Difference between web velocities at the ends of a web span
v_n	Velocity of web = $v_{n0} + V_n$
v_{n0}	Steady-state operating value for web velocity

$\bar{v}$, $\bar{v}_n$	Average transport velocity of web
W_n	Change in roller tangential velocity from a steady-state operating value
w_n	Tangential velocity of roller = $w_{n0} + W_n$
w_{n0}	Steady-state operating value for roller tangential velocity
X_n, x_{21}	State variables
X_{n0}	Initial values of X_n
x_2	Vertical displacement of a dancer
Y_n	Outputs
y_2	State variable (angular displacement θ)
y_{21}	State variable (angular velocity)
α	Coefficient of expansion with temperature
α_n	Absolute value of the real part of the eigenvalue of the mathematical model of the n-th closed-loop subsystem
β	Coefficient of expansion with moisture
β_n	Constants
δ	Phase angle by which the stress lags the strain due to the viscoelastic properties
δ_{nc}	Constants
$\delta(t)$	Unit impulse function
$\delta(x)$	Kronecker delta function in section 3.6.
ε_n	Strain = $\varepsilon_{n0} + \in_n$
ε_{n0}	Steady-state operating value of web strain

ϵ^m	Change in hygroscopic strain
ϵ^t	Change in thermal strain
ϵ_i	Total change in web strain (Chapter 3)
ϵ_i^e	Change in elastic web strain (Chapter 3)
ϵ_i^t	Change in thermal web strain (Chapter 3)
ϵ_i^m	Change in hygroscopic web strain (Chapter 3)
ϵ_{id}^e	Change in elastic web strain due to the difference between web velocities at the ends of a web span. (Chapter 3)
ϵ_{iv}^e	Change in elastic web strain due to the vertical displacement of the dancer roll (Chapter 3)
ϵ_{ia}^e	Change in elastic web strain due to the angular displacement of the dancer roll (Chapter 3)
μ	Friction coefficient between web and roller
μ_0	Static friction coefficient between web and roller
μ_{n0}	Coulomb friction coefficient between web and roller
ν	Poisson's ratio
θ	Angular displacement
θ_a	Angle for a region of adhesion within a wrap angle
θ_s	Angle for a region of slip within a wrap angle
θ_w	Wrap angle of a web on a roller
θ_T	Temperature change from a steady-state operating point
σ	Normal stress

γ	Shear strain
τ	Shear stress
τ_e	External torque applied to the roll
τ_ε	Time of relaxation of load
τ_σ	Time of relaxation of strain
ω	Circular frequency
ω_r	Natural frequency associated with rotational inertia and effective elastic spring constant of the web entering and exiting the dancer roll
ω_s	Natural frequency associated with web transport system without the dancer
ω_t	Natural frequency associated with translational inertia and spring in the dancer
ξ	A dummy variable
ζ	Damping coefficient
Ω	Angular velocity
Ψ	Complex modulus of a viscoelastic material
ϕ_n	Transition matrix of the n-th subsystem

Subscripts:

c	Reference
d	Disturbance
0	Steady-state operating condition
f	Friction
i, j, m, n,	0,1,2,3, . . .

mo	Moisture
u	Condition in unstretched web
x,y,z	Cartesian coordinate

Superscripts:

e	Elastic
h	Hygroscopic (Chapter 3)
m	Integer
n	Integer
t	Thermal (Chapter 3)

CHAPTER I

INTRODUCTION

Background

The term "web" refers to any material in a continuous flexible strip form which is either endless or very long compared to its width, and very wide compared to its thickness. There are, however, a host of other terms for a web in common use, e.g., film, belt, foil, strip, thread, fabric, etc.

Many types of material are most economically manufactured or processed in the form of a web, e.g., paper, plastic film, textiles, thin metals, etc. Figure 1 shows schematically a web processing line in an Oklahoma plant that involves slitting and electrical treating of a polypropylene web. A thick polypropylene web is formed upstream, and is stretched in the lateral direction (cross-machine direction, CMD) and longitudinal direction (machine direction, MD) before it reaches the entering section shown in Figure 1. The web is slitted in half and trimmed at roller #4, and electrically treated at rollers #10, #11, and #11A respectively. Rollers #1, #5, #10, #11A, and the mill rolls are driven by motors in order to control the velocity/torque of the rollers/rolls for the control of longitudinal tension in the various web spans. Rollers #2, #8,

#9A, #16 and #18A are equipped with tension measuring devices (load cells) to facilitate the accurate measurement and control of longitudinal tension in the corresponding web spans.

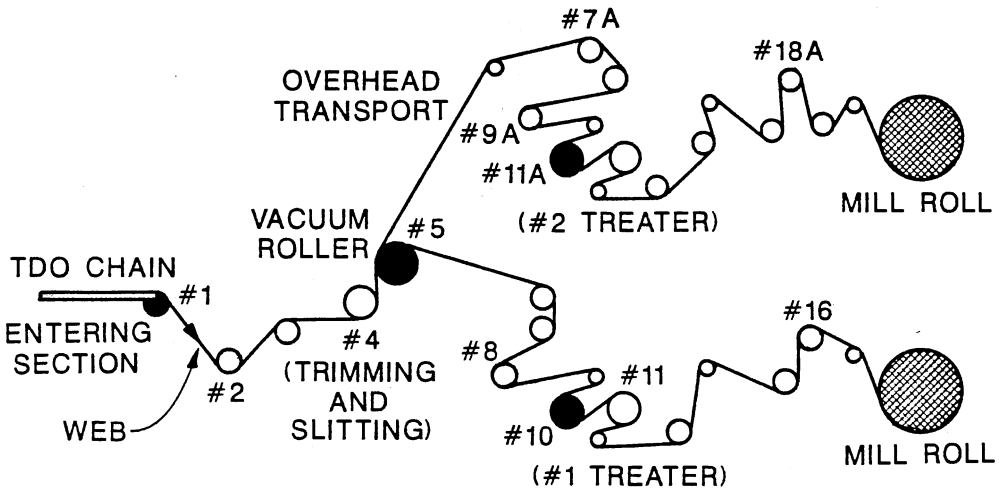

#2, #8, #9A, #16 and #18A are rollers
equipped for tension measurement (load cell)

Figure 1. Slitting and Electrical Treating of a Polypropylene Web with Tension Control

A multi-span web transport system (e.g., Figure1) consists of several types of mechanical components (e.g., rollers, rolls, measuring devices, driving motors, etc.) and web spans. The dynamic characteristics of the mechanical components and the physical properties of the web material affect the steady-state and dynamic behavior of the web in the longitudinal (MD) direction. Tension variations in the web in the longitudinal (MD) direction are common. Variations in the physical characteristics of the web material in the longitudinal direction (MD) and in the transverse direction (CMD), and the high sensitivity of the web material characteristics to environmental changes (e.g., temperature, moisture, etc.), make accurate control of tension in a moving web more difficult. The trend toward thinner webs of material being handled at higher speeds makes problems associated with tension variations more critical.

The web material may have to pass through several consecutive processing sections (e.g., cleaning, coating, drying, etc.) in the manufacture of an intermediate or final product. An example structure of a multi-span web transport system which has three different processing sections is shown schematically in Figure 2. Different web tension levels and accuracies may be required in the different processing sections. If severe tension variations occur, rupture of the material during processing or degradation of product quality may occur, resulting in significant economic losses due to machine damage and slowed production. Therefore, in order to minimize these losses, it is very important to monitor and control the tension[1] within the desired limit within each span.

---

1. Unless stated otherwise throughout this thesis, the term "tension" refers to the longitudinal tension in a web span.

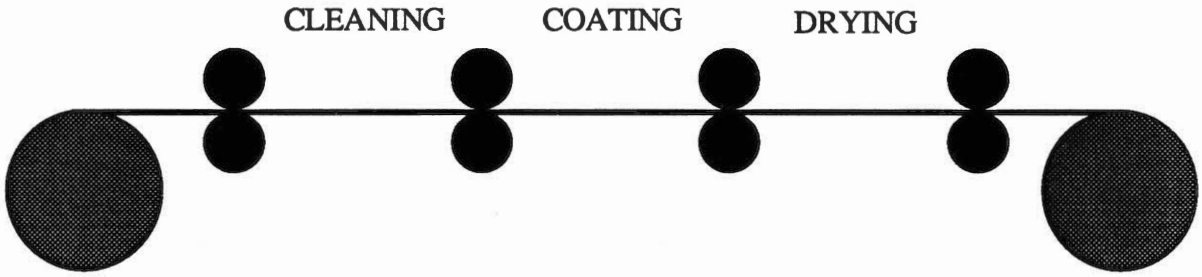

Figure 2. A Multi-Span Web Transport System with Several Consecutive Processing Sections

The advantages of accurate tension control within a moving web include [1]:

(1) avoidance of wrinkles, slack regions, breakage, and lateral movement, especially with thin webs and low tension levels,

(2) minimization of knitting together of two rolls wound from a slit web,

(3) elimination of air pockets under the web entering blade coaters,

(4) maintenance of good web contact with dryer drums,

(5) avoidance of slippage resulting from excess tension at pull rolls feeding a web cutter,

(6) maintenance of proper hardness of wound-up rolls.

There are two control schemes in general use: the centralized control scheme and the distributed (or decentralized) control scheme. In the centralized control scheme, all the information about the system model ("off line" or priori information) and the system response ("on line" or measured/estimated information) are used in the design of a control

system. In the distributed control scheme, a subset of the information about the system model and the system response is used in the design of a control system.

As the number of processing sections increases, the order of the overall system mathematical model increases rapidly. For the high order system with a structure which is a cascade of interconnected web spans, the distributed control scheme is easy to implement compared to the centralized control scheme [25][26]. In this study, the distributed control scheme will be adopted in the development of a design method of a tension control system for a multi-span web transport system.

Previous Studies

A thorough understanding of longitudinal dynamics, as well as the structure of the mathematical model of the system, are crucial to designing a distributed control system for the control of tension in a multi-span web transport system.

There is quite an extensive literature concerning web tension control and mathematical models of web transport systems for tension control [1] - [4], [35], [36], [54]-[59], [66], [67]. Brandenburg [2], Campbell [3], King [4], and Shelton [66] conducted fundamental background studies of the longitudinal dynamics of a moving web. Working early in the field, Campbell did not consider the tension of the web in the entering span when he developed his mathematical model for a web transport system. Thus, his model could not predict "tension transfer". In contrast, King,

Brandenburg, and Shelton considered the tension of the web in the entering span when they developed mathematical models for web tension. Brandenburg and Shelton assumed that the strain in the web is very small, but, King did not. Campbell, King, and Shelton did not take into account "non-ideal effects" (e.g., changes in cross-sectional area, temperature, and moisture in the web; viscoelastic characteristics of the web; slippage between the web and rollers, etc.) on tension variations in the development of the mathematical models. Brandenburg considered the effects of area-change resulting from strain change, the effect of temperature change, and the effect of register error on strain change.

Literature concerning the control of web tension includes [5], [26], [37], [59] - [61], [66]. The most relevant study related to tension control in a multi-span web transport system was reported by W. Wolfermann and D. Schroder [5] in 1987. In their technique, optimal output feedback was applied to control the speed of driven rollers in a multi-span system. A decentral observer which is able to decouple the drives from the web forces was designed. This observer reconstructs the web forces acting on the driven rollers. The reconstructed web forces are used to improve the speed control of the driven rollers. This method leads to considerable improvement in the speed responses of the driven rollers in multi-span web transport systems [5]. However, Wolfermann and Schroder used the desired "speeds of the driven rollers" rather than the desired "tensions" in the web spans for reference inputs in their control system. That is, the web tensions were controlled in open loop by the relation of the speeds of the driven rollers. This control method cannot reject disturbances due to "tension transfer" from adjacent web spans and due to interactions between adjacent

web spans through an intermediate driven roller.

Studies related to the stabilization of an overall distributed closed-loop control system were conducted by various researchers including M. Aoki [6], S. H. Wang and E. J. Davision [7], D. D. Siljak and M. B. Vukcevic [8], B. S. Chen and H. C. Lu [9], and M. E. Sezer and O. Huseyn [10]. In each study, local constant or dynamic output feedback or state feedback was used to stabilize a certain class of interconnected systems. This class of interconnected systems has a particular structure in a manner of interconnections of subsystems and providing inputs to subsystems. But the structure of interconnections in web transport systems is different from those classes of problems studied by [6], [7], [8], [9], [10], and these previous methods do not apply.

In summary, a review of the literature cited above revealed that:

(1) Mathematical models are needed for certain primitive elements and subsystems found in web transport systems which describe the effects of moisture, viscoelastic properties of web materials, slippage between the web and the roller etc. on tension variation. The availability of these models facilitates the design of a distributed system for tension control in multi-span systems.

(2) The fundamental behavior of the web in the multi-span system (e.g., tension transfer, interaction between adjacent web spans) was not considered in the design of distributed control systems [5].

(3) No study on the stability of an overall web transport system with closed-loop control has been reported.

The Tension Control Problem

An important control problem in a multi-span web transport system is maintaining the precise longitudinal tension level required in each processing section, and at same time stabilizing the overall web handling system. Two primary techniques are commonly used in web processing industries for tension control; they are either open-loop "draw control" or closed-loop tension control based on a "progressive set-point coordination" scheme.

In the "draw control" scheme, tension in a web span is controlled in an open-loop fashion by controlling the velocities of rollers at either end of a free web span. Tension variation is very sensitive to the velocity difference between the ends of the web span. For example, a velocity difference of 0.1 % of the nominal velocity for a Polypropylene web (Young's modulus = 350,000 lbs/in^2, thickness = 0.001 inch, width = 120 inch) results in a tension variation of 42 lbs. Indeed, control of web tension using the draw control requires extremely accurate control of the velocities of the driven rollers, a requirement which may be very difficult or expensive. Also, it will be shown in a later section that when open-loop draw control is used, a disturbance from the adjacent web spans cannot be rejected.

In order to illustrate the difficulties of open-loop draw control of tension in a multi-span web transport system, consider the two-span system shown in Figure 3 below. By assuming no slip between the web and the rollers, a linearized mathematical model for the tension T_2 and T_3 can be

written as shown in equations (1) and (2) (see Chapter 2 for a detailed derivation).

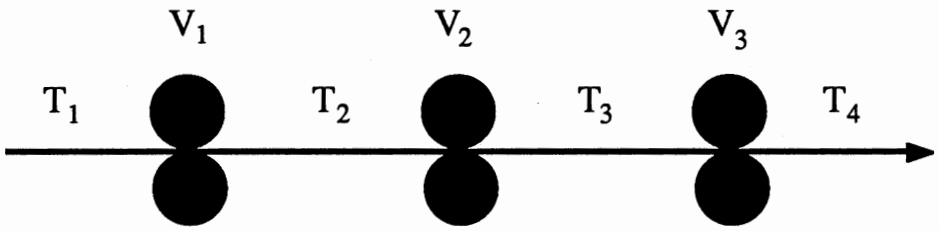

Figure 3. A Two-Span Web Transport System

All variables shown in Figure 3 are changes from the initial steady-state operating conditions. That is,

where

$$t_n = t_{n0} + T_n, \qquad v_n = v_{n0} + V_n$$

and

t_n : Web tension, v_n : Web velocity

t_{n0} : Steady-state operating value for web tension

v_{n0} : Steady-state operating value for web velocity

T_n : Change in web tension from a steady-state operating value

V_n : Change in web velocity from a steady-state operating value.

$$\frac{dT_2}{dt} = -\frac{v_{20}}{L_2}T_2 + \frac{v_{10}}{L_2}T_1 + \frac{AE}{L_2}(V_2 - V_1). \qquad (1)$$

$$\frac{dT_3}{dt} = -\frac{v_{30}}{L_3}T_3 + \frac{v_{20}}{L_3}T_2 + \frac{AE}{L_3}(V_3 - V_2). \qquad (2)$$

In equation (1), the tension change T_2 is function of T_1, V_1, V_2. That is, a change in the tension in the entering span (e.g., T_1 in Figure 3) affects the tension in the following span (e.g., T_2 in Figure 3). This behavior is called "tension transfer". No matter how accurately the velocities of the rollers can be controlled, open-loop draw control cannot provide accurate control of tension in a span because of "tension transfer" from the upstream span to the downstream span.

A numerical example will illustrate the effect of tension transfer in open-loop draw control. Consider the simple two-span web transport system shown in Figure 3. The tangential velocities of the rollers (V_n, n= 1, 2, 3) are assumed to be controlled. Suppose the control purpose is to maintain t_3 at a certain tension level lower than the initial operating tension (t_{30}) by providing the velocity difference, $(V_3 - V_2) = -0.06$ ft/min. With $V_1 = V_3 = 0$, equations (1) and (2) were solved with $V_2 = 0.06$ ft/min as a step input to the second roller in Figure 3. The operating conditions and parameter values in Table 1 were used for computer simulation. Computer simulation results are shown in Figure 4. The tension t_3 could not be maintained at a certain level below the initial operating tension even though the negative velocity difference ($V_3 - V_2 = -0.06$ ft/min) was provided. T_3 returned to zero due to the tension transfer from the entering span.

TABLE 1

PARAMETER VALUES AND SYSTEM CONDITIONS
FOR SIMULATION IN SECTION 1.3

System Conditions

$T_n(0^-) = 0.0$ (lbf), n = 1,...,4

$V_n(0^-) = 0.0$ (ft/sec), n = 0,...,4

Parameter Values

A = 0.12 (in^2)

E = 350,000 (lbf/in^2)

J_n = 94.0 (lbf in sec^2), n=0,...,4

L_n = 120 (in), n=1,...,2

v_{n0} = 1,000 (ft/min), n=0,...,3

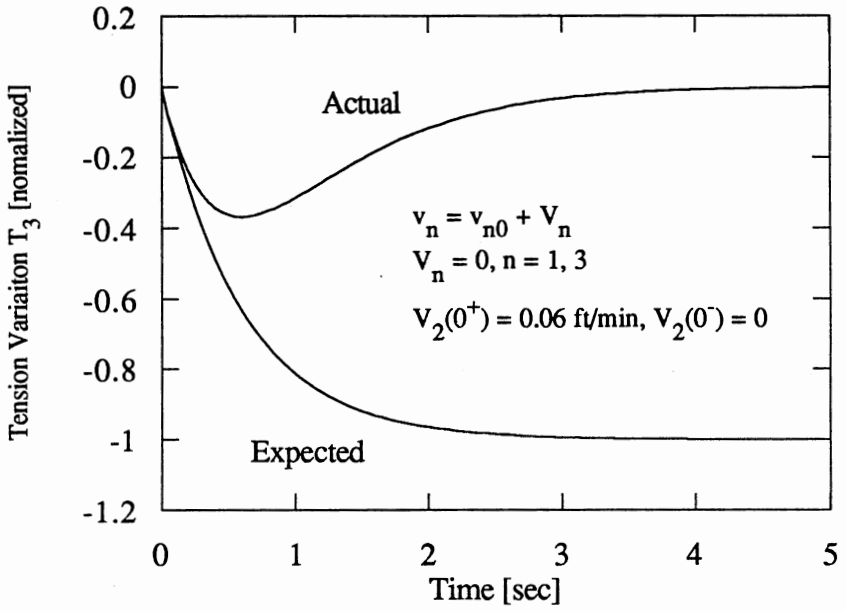

Figure 4. Tension Variation: T_3

In a multi-span web transport system, driven rollers are interconnected through a continuous web span. Interaction occurs between adjacent web spans. Equations (1) and (2) indicate that a velocity change in a particular driven roller (say V_2 in Figure 3) changes not only the tension in the upstream span (T_2 in Figure 3) but also the tension in the downstream span (T_3) with respect to that roller. In order to compensate for the unwanted tension change (T_3) in the downstream span, "progressive set point coordination" control scheme is commonly used. For example,

once an input is provided to an upstream driven roller, an input of the same magnitude is automatically provided to each of the driven rollers which follow downstream.

The progressive set-point coordination control scheme is effective for the start-up or shut-down of a system. But this is not a desirable scheme for a normal operation since it forces tensions in the downstream web spans to be automatically changed when the tension only in the upstream web span needs to be changed. That is, it is impossible to control the tension in each web span independently in a multi-span web transport system using progressive set-point coordination.

Following conclusions were drawn from the study.

(1) A disturbance in an upstream span is propagated into the downstream span; i.e., tension is transferred. Open-loop draw control may not be sufficient in a multi-span system, even with extremely accurate control of the tangential velocities of the rollers, because of tension transfer.

(2) Interaction occurs between adjacent web spans. It is impossible to control the tension in each web span independently in a multi-span web transport system using progressive set-point coordination.

Objectives

The objectives of this study were:

(1) to develop models for the "primitive elements" and "subsystems"

that occur in multi-span web transport systems,

(2) to develop a control algorithm that allows precise control of tension in multi-span web transport systems, and

(3) to develop a computer-based analysis and design program for multi-span web transport systems (WTS).

Principal Results

This thesis concerns itself with aspects of the longitudinal dynamic behavior of a straight moving web between parallel cylindrical rollers/rolls.

The concept of a "primitive element" and a "subsystem" was introduced to facilitate the modeling and the analysis of web transport systems. Steady-state and dynamic models for important primitive elements or combinations of primitive elements (subsystems) were also developed. The derivation of open-loop mathematical models for longitudinal dynamics and the analysis of non-ideal effects on tension variation were carried out. Fundamental analyses of interactions between adjacent web spans and between the web and mechanical components were emphasized, so that these analysis results can be used in the design of closed-loop control systems for multi-span web transport systems. Various non-ideal effects (e.g., temperature change, moisture change, viscoelastic properties of the web material) on tension variation and the effect of slippage between the web and rollers on tension variation were investigated. Results indicated that the effect of temperature change on tension variation is

significant in plastic film and the effect of moisture change is significant in paper. The effects of the viscoelastic properties of the web material on tension variation were shown to be relatively insignificant if the duration time of the web in a processing section is very short (a few seconds). The effect of slippage between the web and the roller on tension variation was found to be significant.

The mathematical model for a free span was validated through experiments on a production system in an Oklahoma plant. The significant effects of slippage between the web and the roller and the effect of temperature on tension variation in plastic film were also confirmed through experimentation. "Tension transfer" in a multi-span system was confirmed through simulation of the derived mathematical model and through experiments.

The derivation of a "unified" open-loop dynamic model for an important sub-system which includes a dancer is also a significant result. It was assumed that there is no slippage between the web and the dancer roll. This model includes the combined effects of slippage, temperature variation, and moisture variation. Using the model, a dancer subsystem was evaluated as a tension measuring system and as a disturbance minimizing system. Typical web material (Polypropylene) characteristics and typical web transport system operating conditions were used for the evaluation. Conclusions from the evaluation are as follows:

(a) When the dancer is to be used for tension measurement, the dancer should be designed such that:

$$\omega_t > 3\omega_s \quad \text{and} \quad \omega_r > 3\omega_s$$

where

ω_r is the natural frequency associated with the rotational inertia of the dancer roll and the effective elastic spring constant of the web entering and exiting the dancer roll,

ω_s is the natural frequency of the web transport system without the dancer,

ω_t is the natural frequency associated with the translational inertia of the dancer roll and the dancer system spring.

(b) When the dancer is to be used for minimizing the effects of disturbances, the dancer should be designed such that:

$$\text{If } \omega_d < \omega_s, \text{ then } \omega_t > 3\omega_s, \ \omega_r < \frac{1}{3}\omega_d$$

$$\text{If } \omega_d > \omega_s, \text{ then } \omega_t > 3\omega_d, \ \omega_r < \frac{1}{3}\omega_s$$

where

ω_d is the frequency of the disturbance.

The most significant contribution of this thesis was the development of a method for the design of a distributed tension control system for a multi-span web transport system (see Chapter VII). It was demonstrated that the asymptotic stability of an overall closed-loop distributed control system depends on the gains of the local controllers, the magnitude of the local inputs, and the degree of interconnections between subsystems. In multi-span web transport systems, a disturbance in an upstream is propagated into the downstream span (i.e., tension is transferred), and

interactions occur between adjacent web spans. The distributed control system designed by using the method developed in this study can reject disturbances due to the tension transfer and interactions of web spans.

In a production plant, the tension in a given web span often is controlled by using a fixed-gain PID controller. Such a controller fails when the system has time-varying parameters, and when certain types of disturbances are present. It was demonstrated that a variable-gain PID controller would produce an "optimum" solution for a system with time-varying parameters (i.e., a winding roll with increasing radius). Further it was demonstrated that feedforward control could reject some types of disturbances and improve the dynamic performance of the closed-loop control system.

This thesis is also concerned with the development of a computer-based program for the analysis and design of a web transport system (WTS). The functions of WTS include (1) automatic assembly of primitive elements into a web transport system (configuration of the system), (2) automatic generation of the mathematical model for the configured system, (3) steady-state analysis, and (4) dynamic analysis of the configured (assembled) system.

CHAPTER II

ANALYSES OF PRIMITIVE ELEMENTS

To facilitate the modeling and analysis of web transport systems, the concept of a "primitive element" was established. Examples of primitive elements are a free web span, various types of rollers and rolls, a web interacting with roller, etc., as shown in Figure 5. A web transport system can be thought of as a combination of primitive elements.

In this chapter, mathematical models will be derived for a free web span, a roller, and a web interacting with a roller. Then, non-ideal effects (change in cross-sectional area, temperature, and moisture of the web; viscoelastic properties of the web; slippage between the web and a roller) on tension variation will be investigated by using the mathematical models developed.

Analysis of a Free Web Span

Strain -Web Velocity Relationship

The free web span shown in Figure 6 is the most fundamental primitive element found in web processing systems. This element is

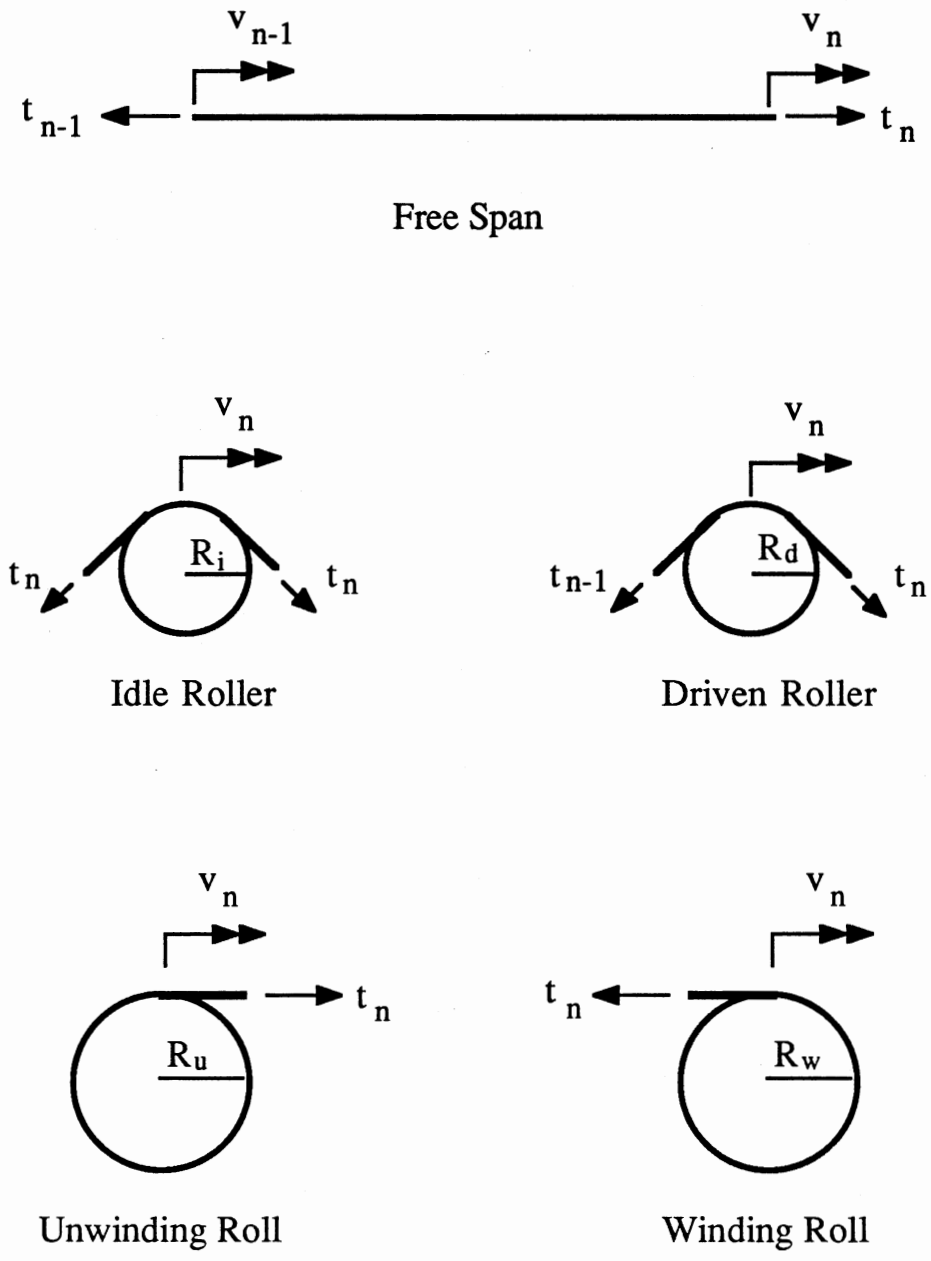

Figure 5. Some Primitive Elements

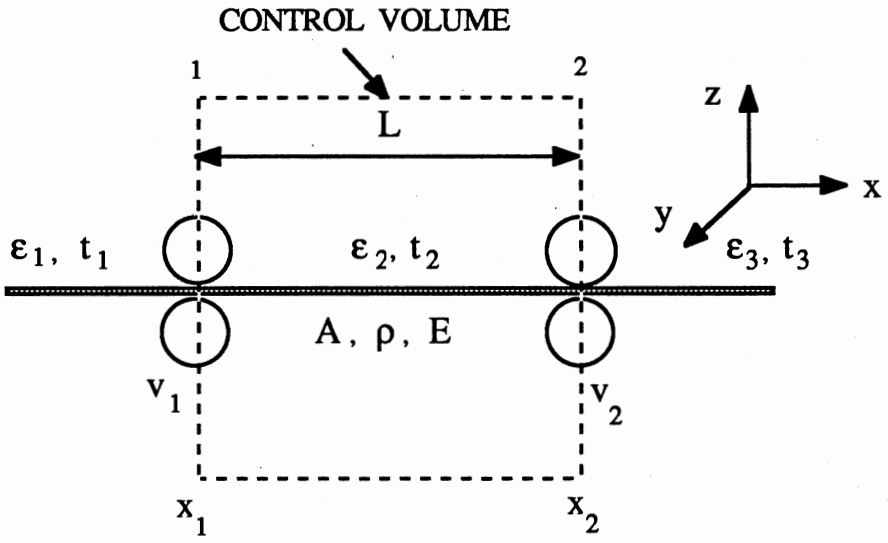

A : Cross-sectional area of web
E : Young's modulus
L : Length of web
t : Tension in web
v : Tangential velocity of roller
ε : Strain in web
ρ : Mass density of web
σ : Stress in web

Subscripts:

u : Designates unstretched condition
x : Distance measured from section 1
0 : Initial value of variable
1, 2 : Conditions at section 1 and 2.

Figure 6. A Free Web Span

terminated by a roller(s) (or roll) at each end of the span. A mathematical model for the longitudinal dynamic behavior of a free web span is developed in this section. The web is assumed to be a continuum. Other assumptions are as follows:

(1) The length of contact region between the web material and a roller is negligible compared to the length of free web span between the rollers (i.e., the strain variations in the contact region are negligible),

(2) The thickness of the web is very small compared with the radius of rollers over which the web is wrapped,

(3) There is no slippage between the web material and the rollers,

(4) There is no mass transfer between the web material and the environment (i.e., no humidification or evaporation),

(5) The strain in the web is small (much less than unity),

(6) The strain is uniform within the web span,

(7) The web cross-section in the unstretched state does not vary along the web,

(8) The density and the modulus of elasticity of the web in the unstretched state are constant over the cross-section,

(9) The web is perfectly elastic,

(10) The web material is isotropic, so that (MD) stress prevails. That is,

$\sigma_x \neq 0, \sigma_y = \sigma_z = 0$,

(11) The web properties do not change with temperature or humidity.

Under assumption (1), a control volume can be drawn as shown in Figure 6. Under the assumption (4), the law of conservation of mass for the control volume shown in the Figure 6 can be written as follows:

$$\frac{d}{dt}\left[\int_{x_1}^{x_2} \rho(x,t)A(x,t)dx\right] = \rho_1(t)A_1(t)v_1(t) - \rho_2(t)A_2(t)v_2(t). \quad (3)$$

Considerable mathematical simplification can be achieved if the mass terms (e.g., $\rho(x,t)A(x,t)dx$) in equation (3) can be described in the unstretched web condition. The web is considered to be unstretched when it is free from external forces. From the definition of strain, the relationship between the stretched length and unstretched length of the element shown in Figure 7 can be written as follows:

$$dx = (1 + \varepsilon_x)\, dx_u, \quad (4)$$

$$d = (1 + \varepsilon_y)\, d_u, \quad (5)$$

$$h = (1 + \varepsilon_z)\, h_u, \quad (6)$$

where the subscript u indicates the unstretched state of the web.

In the infinitesimal element shown in Figure 7, the mass of the infinitesimal element is constant. Thus, the following relationship can be written.

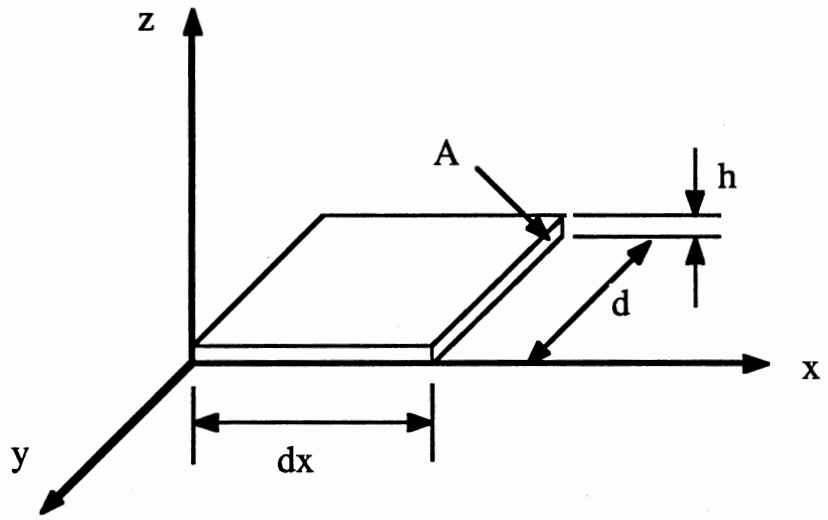

Figure 7. An Infinitesimal Element out of a Web Span

$$dm = \rho\, d\, h\, dx = \rho_u\, d_u\, h_u\, dx_u\,. \tag{7}$$

Combining equations (4) and (7) gives

$$\frac{\rho\, d\, h}{\rho_u d_u h_u} = \frac{dx_u}{dx} = \frac{dx_u}{(1+\varepsilon_x)dx_u} = \frac{1}{1+\varepsilon_x}. \tag{8}$$

or since $d \times h = A$ and $d_u \times h_u = A_u$,

$$\frac{\rho(x,t)\ A(x,t)}{\rho_u(x,t)\ A_u(x,t)} = \frac{1}{1+\varepsilon_x(x,t)}. \tag{9}$$

With assumption (10), the subscript x in the strain[1], ε_x,which means x-coordinate will be dropped for simplicity from this point on. Combining equations (3) and (9) gives

$$\frac{d}{dt}\left[\int_{x_1}^{x_2} \frac{\rho_u(x,t)\, A_u(x,t)}{1+\varepsilon_2(x,t)}\, dx\right] = \frac{\rho_{1u}(x,t)\, A_{1u}(x,t)\, v_1(t)}{1+\varepsilon_1(x,t)} - \frac{\rho_{2u}(x,t)\, A_{2u}(x,t)\, v_2(t)}{1+\varepsilon_2(x,t)}. \quad (10)$$

Under assumptions (7), (8), and (11), equation (10) can be written as

$$\rho_u A_u \frac{d}{dt}\left[\int_0^1 \frac{1}{1+\varepsilon_2(x,t)}\, dx\right] = \frac{\rho_u A_u v_1(t)}{1+\varepsilon_1(x,t)} - \frac{\rho_u A_u v_2(t)}{1+\varepsilon_2(x,t)}. \quad (11)$$

or

$$\frac{d}{dt}\left[\int_0^1 \frac{1}{1+\varepsilon_2(x,t)}\, dx\right] = \frac{v_1(t)}{1+\varepsilon_1(x,t)} - \frac{v_2(t)}{1+\varepsilon_2(x,t)}. \quad (12)$$

With assumption (6), equation (12) can be written as

$$L \frac{d}{dt}\left[\frac{1}{1+\varepsilon_2(t)}\right] = \frac{v_1(t)}{1+\varepsilon_1(t)} - \frac{v_2(t)}{1+\varepsilon_2(t)}. \quad (13)$$

By using assumption (5), i.e. for small ε:

$$\frac{1}{1+\varepsilon} \cong 1 - \varepsilon. \quad (14)$$

1. Unless stated otherwise throughout this thesis, the term "strain" refers to the longitudinal strain (x-coordinate in Figure 6) in a web span.

Considerable mathematical simplification can be obtained by using equation (14) in equation (13) as follows:

$$L \frac{d}{dt} [1 - \varepsilon_2(t)] = [1 - \varepsilon_1(t)] v_1(t) - [1 - \varepsilon_2(t)] v_2(t). \qquad (15)$$

Rearranging equation (15) gives

$$L \frac{d}{dt}[\varepsilon_2(t)] = - v_1(t) + v_2(t) + \varepsilon_1(t) v_1(t) - \varepsilon_2(t) v_2(t). \qquad (16)$$

The mathematical model represented by equation (16) is nonlinear. The nonlinear equation can be linearized by using the perturbation method.

$$\text{Let} \quad \in \equiv \varepsilon - \varepsilon_0 \text{ and } V \equiv v - v_0. \qquad (17)$$

Equation (16) must be satisfied at the initial steady-state operating condition, i.e.,

$$0 = - v_{10} + v_{20} + \varepsilon_{10} v_{10} - \varepsilon_{20} v_{20}. \qquad (18)$$

The following linearized model results from applying equations (17) and (18) with equation (16), and dropping second order terms:

$$\frac{d}{dt} [\in_2(t)] = - \frac{v_{20}}{L} \in_2(t) + \frac{v_{10}}{L} \in_1(t) - \frac{[1 - \varepsilon_{10}]}{L} V_1(t) + \frac{[1 - \varepsilon_{20}]}{L} V_2(t). \qquad (19)$$

Since $\varepsilon_{10} << 1$ and, $\varepsilon_{20} << 1$, equation (19) can be written as:

$$\frac{d}{dt}[\epsilon_2(t)] = -\frac{v_{20}}{L}\epsilon_2(t) + \frac{v_{10}}{L}\epsilon_1(t) - \frac{V_1(t)}{L} + \frac{V_2(t)}{L}. \qquad (20)$$

Equation (20) represents a linearized dynamic relationship between the changes in the web strain within the control volume, $\epsilon_2(t)$, and the changes in the velocities at the ends of the web span, $V_1(t)$ and $V_2(t)$.

Tension - Web Velocity Relationship

With assumptions (5) through (11), the force-deformation relations (Hooke's law) can be written as [14]:

$$T_1 = AE\epsilon_1 \text{ and } T_2 = AE\epsilon_2, \qquad (21)$$

where A and E are constants, and T_1 and T_2 are changes in tension from an initial steady-state operating value.

Combining equations (20) and (21) gives:

$$\frac{d}{dt}[T_2(t)] = -\frac{v_{20}}{L}T_2(t) + \frac{v_{10}}{L}T_1(t) + \frac{AE}{L}(V_2(t) - V_1(t)) . \qquad (22)$$

Equation (22) is the linearized dynamic model for the free web span.

Effect of Slippage between a Web and a Roller

A web is transported by virtue of the traction between the web and driven rollers. When there is enough traction between the web and a driven roller or idler, such that there is no slippage, the velocity of the web at the point of contact with the roller and the tangential velocity of the roller are identical. But, when there is slippage, the velocity of web and the tangential velocity of the roller are generally not equal.

Concept of Slippage within the Region of Wrap

See Townsend & Salisbury J. Mech. Transmission & Automation in Design Vol. 110, pp 303-307

(*) only if tension is changing slowly.

Consider the region of wrap on a roller as shown in Figure 8.a. If a web has the region (θ_w) of wrap on a roller, a region (θ_a) of adhesion is normally formed at the beginning part (*) of the region of wrap; this is followed by a region(θ_s) of sliding or slipping [2]. The tension is constant throughout the region of adhesion, and the web velocity is equal to the tangential velocity of the surface of the roller. In the region of slip, the tension varies in the transport direction, and the web velocity differs from the tangential velocity of the surface of the roller. Slip (creep) occurs in this region until the tension of the entering span gradually change to the tension of the exiting span.

is this true for web handling case or for the case of belts? See Whitworth, D.P.D., Ph D. Thesis

It can be shown that in the limit as the region of adhesion approaches zero [2],

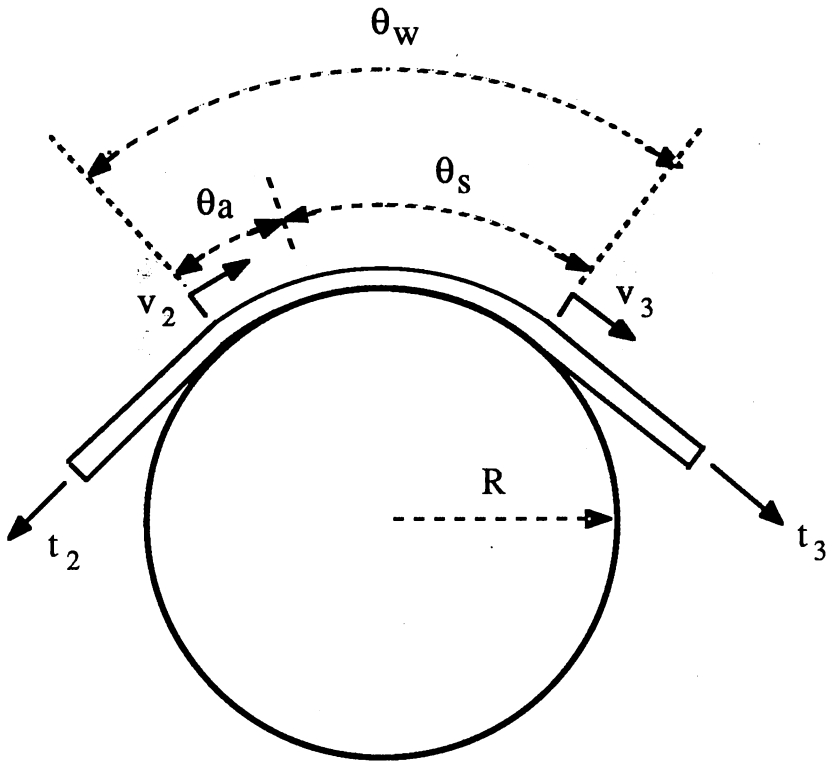

Figure 8.a. Concept of Slippage within the Region of Wrap

$$\left[\frac{t_3}{t_2}\right]_{max} = e^{\pm \mu \theta_w}, \qquad (23)$$

where

+ : $t_3 > t_2$

- : $t_3 < t_2$

μ : Friction coefficient.

At this limiting value of tension ratio, the web adheres only at one point at the beginning part in the region of wrap on the roller. A further increase in the tension ratio will make the web slip throughout the region of wrap on the roller.

Relation between the Velocity of a Web and the Tangential Velocity of a Roller

When the web slips throughout the region of wrap, the forces and velocities are as shown in the free body diagram of Figure 8.b. Using the free body diagram for the web, the force balance equations in the region of wrap lead to the following relations:

$$F_{f2} = t_2 - t_3 \quad (24)$$

$$F_{n2} = \frac{1}{\mu}(1 - e^{-\mu \theta_w})\, t_2, \quad \text{for } t_2 > t_3. \quad (25)[1]$$

Factors affecting the traction between the web and the rollers include web velocity, web tension, wrap angle, roller diameter, web width, web porosity, web moisture, web thickness, etc. [54][55]. But the mechanism of traction between a web and a roller is not well understood and is beyond the scope of this study. One possible model of traction between a web and a roller combines stiction, Coulomb friction, and viscous friction as shown in Figure 9[2].

---

1. See Appendix A for derivation
2. See Appendix B for case with Coulomb friction only

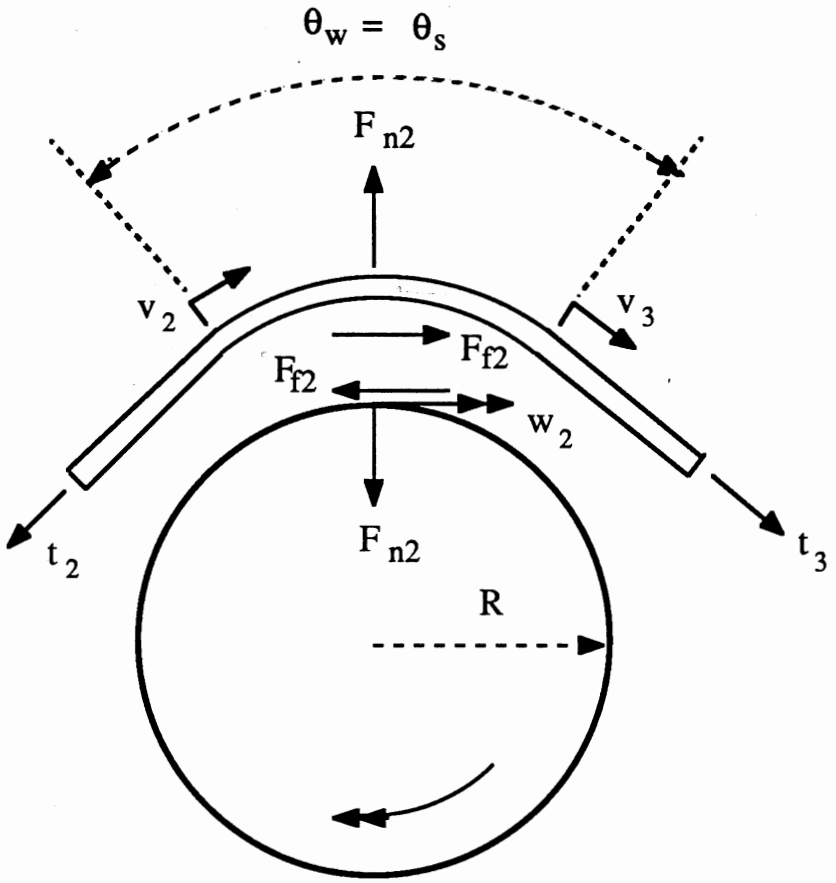

F_{f2} - Effective frictional force
F_{n2} - Effective normal force
w_2 - Tangential velocity of roller
v_n - Web velocity
t_n - Web tension

Figure 8.b. Forces and Velocities When Slippage Occurs Throughout the Region of Wrap

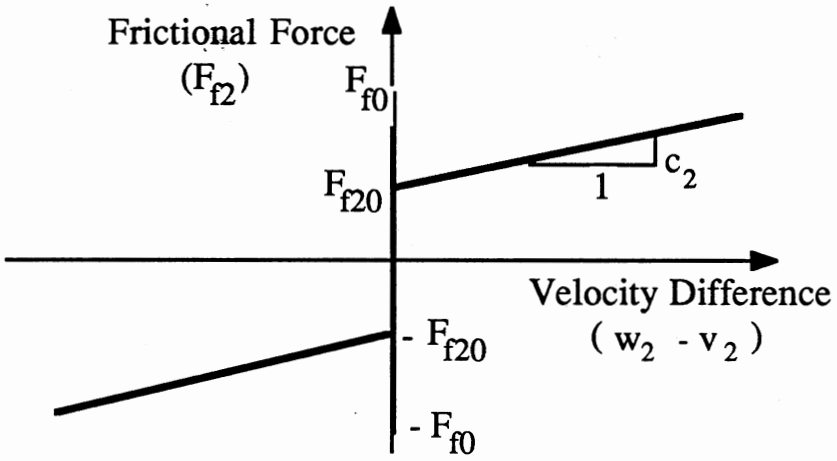

Figure 9. One Model of Friction between a Web and a Roller

The model of friction shown in Figure 9 can be expressed as:

$$F_{f2} = F_{f20}\,\text{sign}(w_2 - v_2) + c_2(w_2 - v_2) + F_{f0}\,\delta(w_2 - v_2), \qquad (26)$$

where

c_2 : Slope of friction characteristics

$F_{f20} = \mu_{20} F_{n2}$: Coulomb frictional force

$F_{f0} = \mu_0 F_{n2}$: Stiction force

$$\text{sign}(w_2 - v_2) = \begin{cases} 1 & \text{for} \quad w_2 - v_2 > 0 \\ 0 & \text{for} \quad w_2 - v_2 = 0 \\ -1 & \text{for} \quad w_2 - v_2 < 0 \end{cases}$$

$$\delta(w_2 - v_2) = \begin{cases} 1 & \text{for } w_2 - v_2 = 0 \\ 0 & \text{for } w_2 - v_2 > 0 \cdot \\ 0 & \text{for } w_2 - v_2 < 0 \end{cases}$$

Combining equations (24), (25), and (26) gives the following relation between the velocity of the web and the tangential velocity of the roller:

$$v_2 = w_2 - \frac{1}{c_2}\left[1 - k_\mu\left(1 - e^{-\mu\theta_w}\right) - \frac{t_3}{t_2}\right] t_2, \qquad (27)$$

for $t_2 > t_3$ and $w_2 > v_2$

where

$$k_\mu = \frac{\mu_{20}}{\mu}.$$

Analysis of a Single-Span System with Slippage Between the Web and a Roller

Consider the single-span system shown in Figure 10. It is assumed that there is slippage between the web and the downstream roller, i.e.:

$$v_1 = w_1 \text{ , and } v_2 \neq w_2 \text{ .} \qquad (28)$$

Equation (16) describes the longitudinal dynamics of the free span. The force - deformation relations can be written as:

$$t_1 = AE\varepsilon_1. \qquad (29)$$

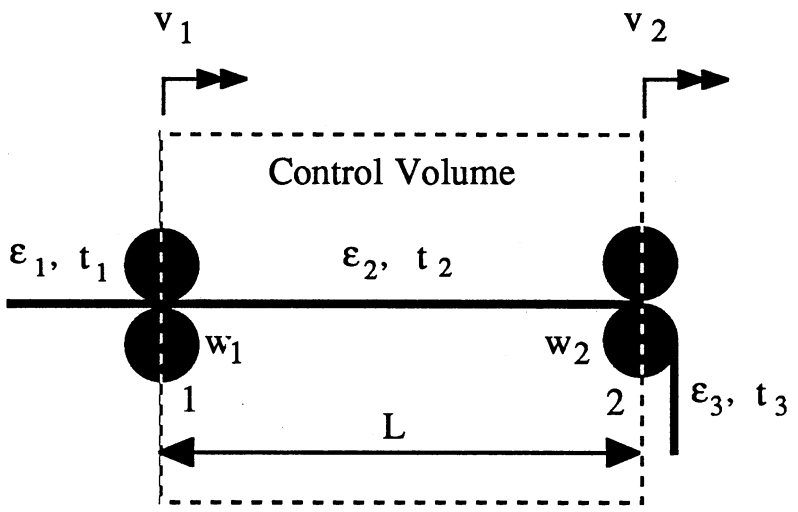

Figure 10. A Single-Span System

$$t_2 = AE\varepsilon_2. \tag{30}$$

From equation (27), the slip relation for the case when $v_2 \neq w_2$ and $t_2 > t_3$ is:

$$v_2 = w_2 - \frac{1}{c_2}\left[1 - k_\mu\left(1 - e^{-\mu\theta_w}\right) - \frac{t_3}{t_2}\right] t_2. \tag{31}$$

Equations (16) and (28) through (31) describe the dynamic behavior of the single-span system in Figure 10 with slippage between the web and downstream roller. When there is slippage between the web and the downstream roller, the tension t_2 is function of t_1, t_3, w_1, and w_2. That is,

the tension not only is transferred from an upstream span to a downstream span, but also from a downstream span to an upstream span when there is slippage between the web and the downstream roller.

Equations (16), (29), and (30) describe the dynamic behavior of the single-span system without slippage between the web and the downstream roller (i.e., if $v_2 = w_2$). When there is no slippage between the web and the downstream roller, the tension t_2 is function of t_1, w_1, and w_2. That is, the tension is only transferred from an upstream span to a downstream span.

Numerical Examples

Several examples were solved to illustrate the effect of slippage in single-span and two-span systems.

Example 1-A : Effect of % Slip on Web Tension in a Single-Span System

The % slip is defined as:

$$\% \text{ slip} = \left| \frac{\text{tangential velocity of roller - web velocity}}{\text{web velocity}} \right| \times 100. \tag{32}$$

Consider the single-span system shown in Figure 11. It is assumed that there is slippage only at the downstream roller; that is, $v_1 = w_1$ and $v_2 \neq w_2$. The dynamic behavior of the system can be described by equations

(16), and (28) through (31). The response of t_2 to a step change in w_2 for different values of % slip is shown in Figure 12. Parameter values and system conditions for simulation are given in Table 2.

When there is slippage between the web and the downstream

TABLE 2

PARAMETER VALUES AND SYSTEM CONDITIONS FOR SIMULATION IN SECTION 2.2

Parameter Values			
E	= 350,000 lbf/in^2,	c_2	= 2300 lbf-sec/ft,
L	= 10 ft	d	= 120 in
μ	= 0.1	h	= 0.001 in
μ_{20}	= 0.033	θ_w	= 3.14 rad
System Conditions			
t_1	= 42.0 lbf	$v_1 = w_1$	= 1000 ft/min
$t_2(0\text{-})$	= 42.0 lbf	$w_2(0^-)$	= 1001 ft/min
$t_3(0\text{-})$	= 42.0 lbf	$w_2(0^+)$	= 1002 ft/min

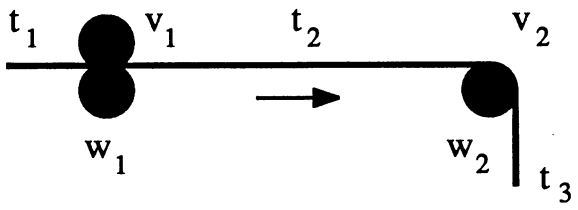

Figure 11. A Single-Span System: Example 1-A

roller and the tangential velocity of the roller w_2 is greater than the web velocity v_2, a change in the tangential velocity of the downstream roller produces a smaller change in the tension t_2 than would occur with no-slippage.

Example 1-B : Effect of Wrap Angle on Tension t_2 in the Single-Span System

Figure 13 shows the response of t_2 to a step change in w_2 for the same system as that of example 1-A but with different wrap angles. Parameter values and system conditions for simulation are given in Table 2. The example was solved for the ratio $t_3/t_2 = 0.9$. As the wrap angle gets smaller, the % slip between the web and the downstream roller increases (see equation (32)). And thus, a change in the tangential velocity of the roller produces a smaller change in the tension t_2 as the wrap angle gets smaller.

Example 2-A : Effect of Slippage on Web Tension in a Two-Span System with Step Input at w_2

Consider a two-span system as shown in Figure 14. It is assumed that there is slippage at roller 2.The two-span system shown in Figure 14 can be described by equations (34) through (38) as follows:

$$L \frac{d}{dt}[\varepsilon_2(t)] = - v_1(t) + v_2(t) + \varepsilon_1(t)\, v_1(t) - \varepsilon_2(t)\, v_2(t) . \quad (34)$$

$$L \frac{d}{dt}[\varepsilon_3(t)] = - v_2(t) + v_3(t) + \varepsilon_2(t)\, v_2(t) - \varepsilon_3(t)\, v_3(t). \quad (35)$$

$$v_1(t) = w_1(t), \quad v_3(t) = w_3(t). \quad (36)$$

$$v_2(t) = w_2(t) - \frac{1}{c_2}\left[1 - k_\mu\left(1 - e^{-\mu_0 \theta_w}\right) - \frac{t_3(t)}{t_2(t)}\right] t_2(t). \quad (37)$$

$$t_1(t) = AE\varepsilon_1(t), \quad t_2(t) = AE\varepsilon_2(t) , \quad t_3(t) = AE\varepsilon_3(t). \quad (38)$$

Responses of t_2 and t_3 to a step change in w_2 are shown in Figure 15. Parameter values and system conditions are given in Table 2. Figure 15 shows that a change in the tangential velocity of the roller w_2 produces smaller tension variations, t_2 and t_3 than would occur with no-slippage.

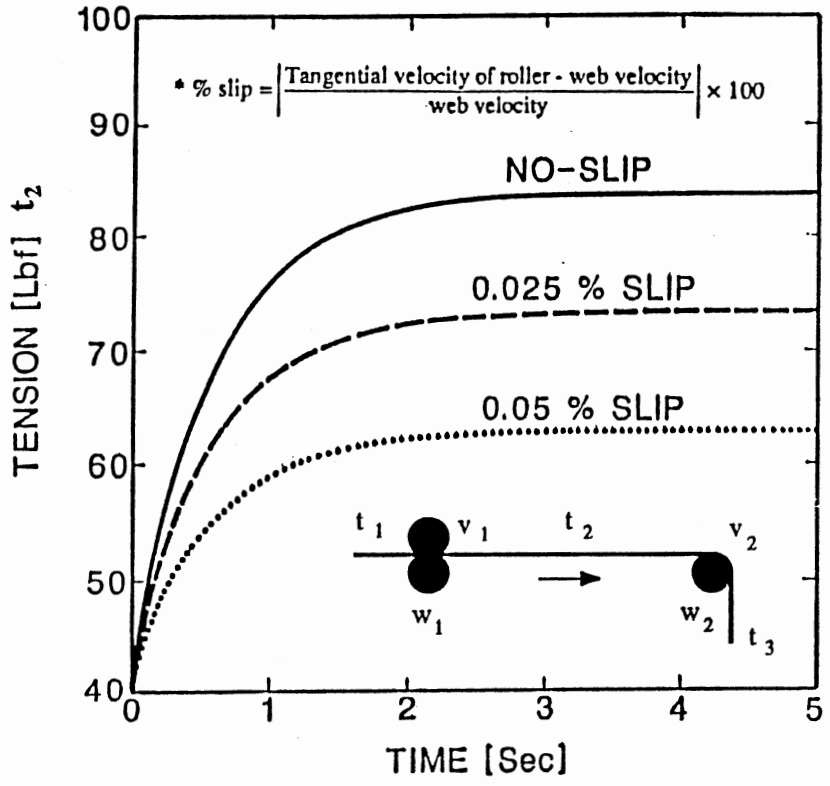

Parameter values and system conditions: see Table 2

$V_1 = W_1 = 1000$, $W_2(0^-) = 1001$, $W_2(0^+) = 1002$ ft/min

Figure 12. Response of t_2 to a Step Change in w_2 for Different % Slip

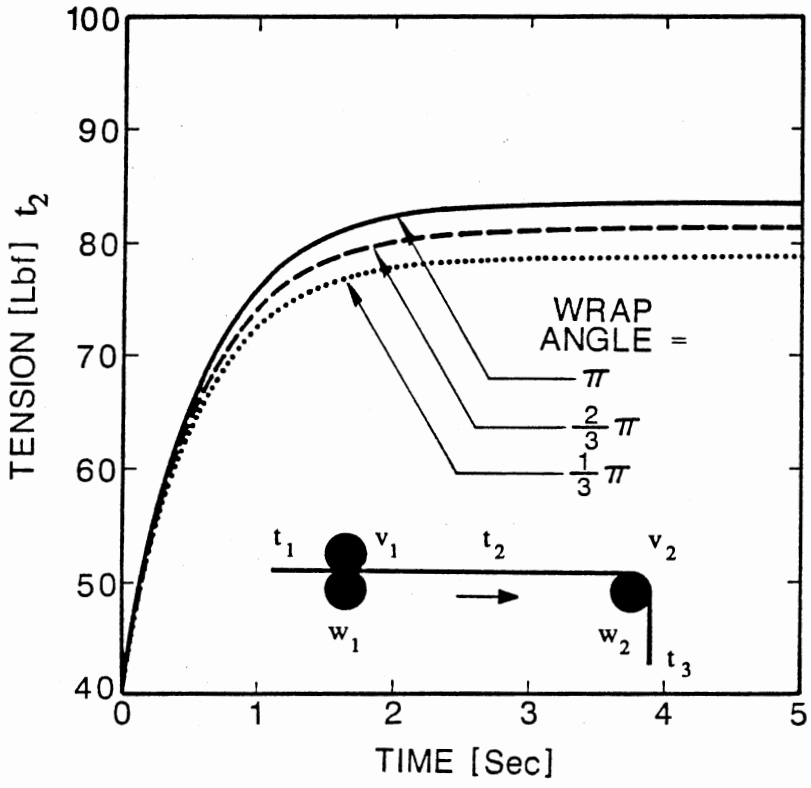

Parameter values and system conditions: $t_3/t_2 = 0.9$

and see Table 2

$V_1 = W_1 = 1000$, $W_2(0^-) = 1001$, $W_2(0^+) = 1002$ ft/min

Figure 13. Response of t_2 to a Step Change in w_2 for Different Wrap Angles

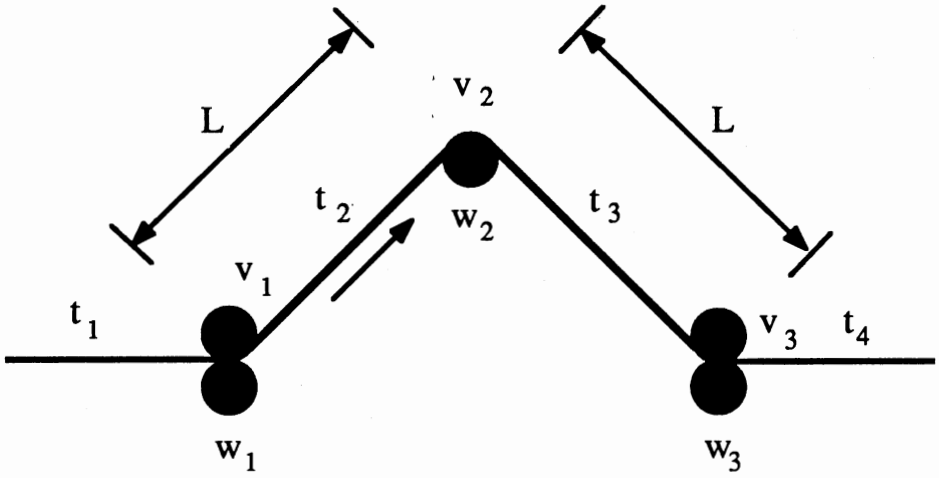

Figure 14. A Two-Span System

Example 2-B : Effect of Slippage on Web Tension in a Two-Span System with Step Input at w_3

Responses of t_2 and t_3 to a step change in w_3 are shown in Figure 16. Figure 16 shows that a change in the tangential velocity of the roller w_3 produces not only a change in tension t_3 but also a change in tension t_2, which would not occur with the case of no slippage at roller #2. This means that there is a "tension transfer[3]" from downstream to upstream when there is slippage between the web and the intermediate roller.

3. See Chapter 4

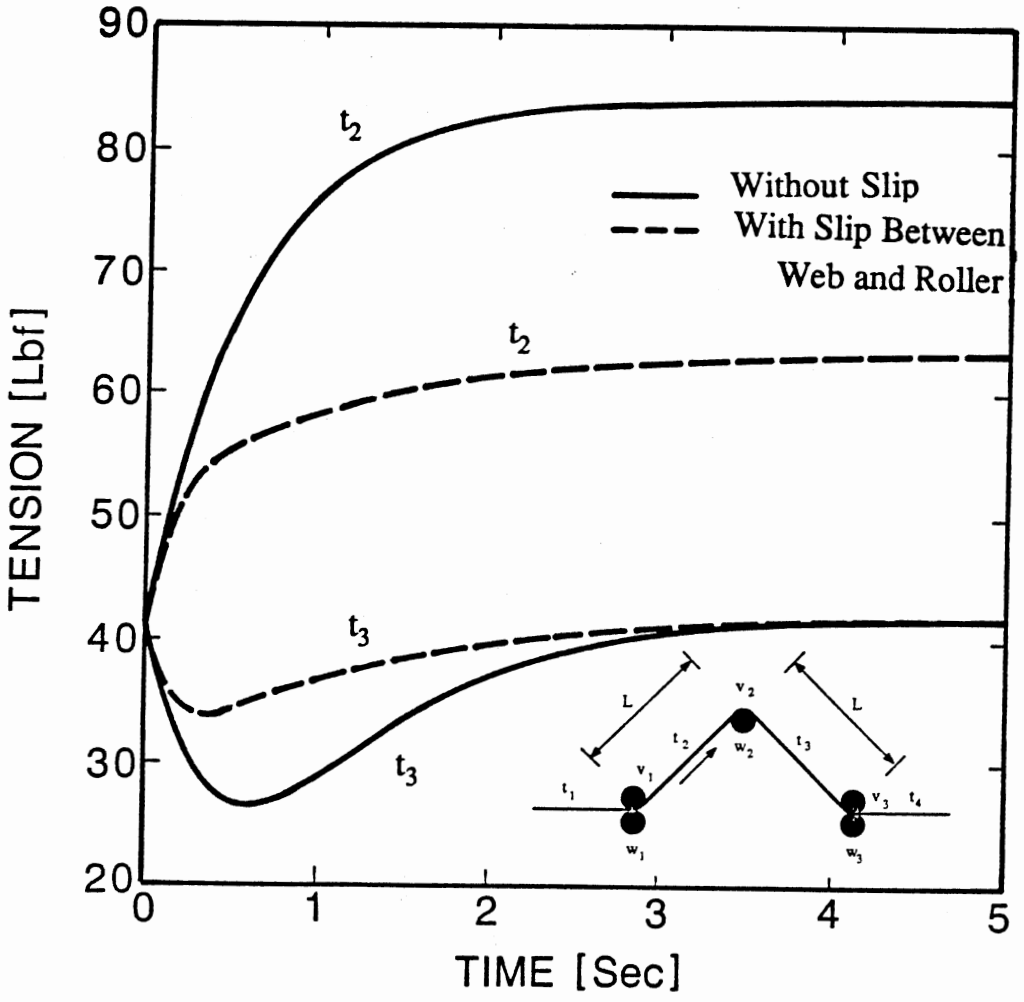

Parameter values and system conditions: see Table 2

$V_1 = W_1 = 1000$, $W_2(0^-) = 1001$, $W_2(0^+) = 1002$, $V_3 = W_3 = 1001$ ft/min

Figure 15. Responses of t_2 and t_3 to a Step Change in w_2 for the Two-Span System

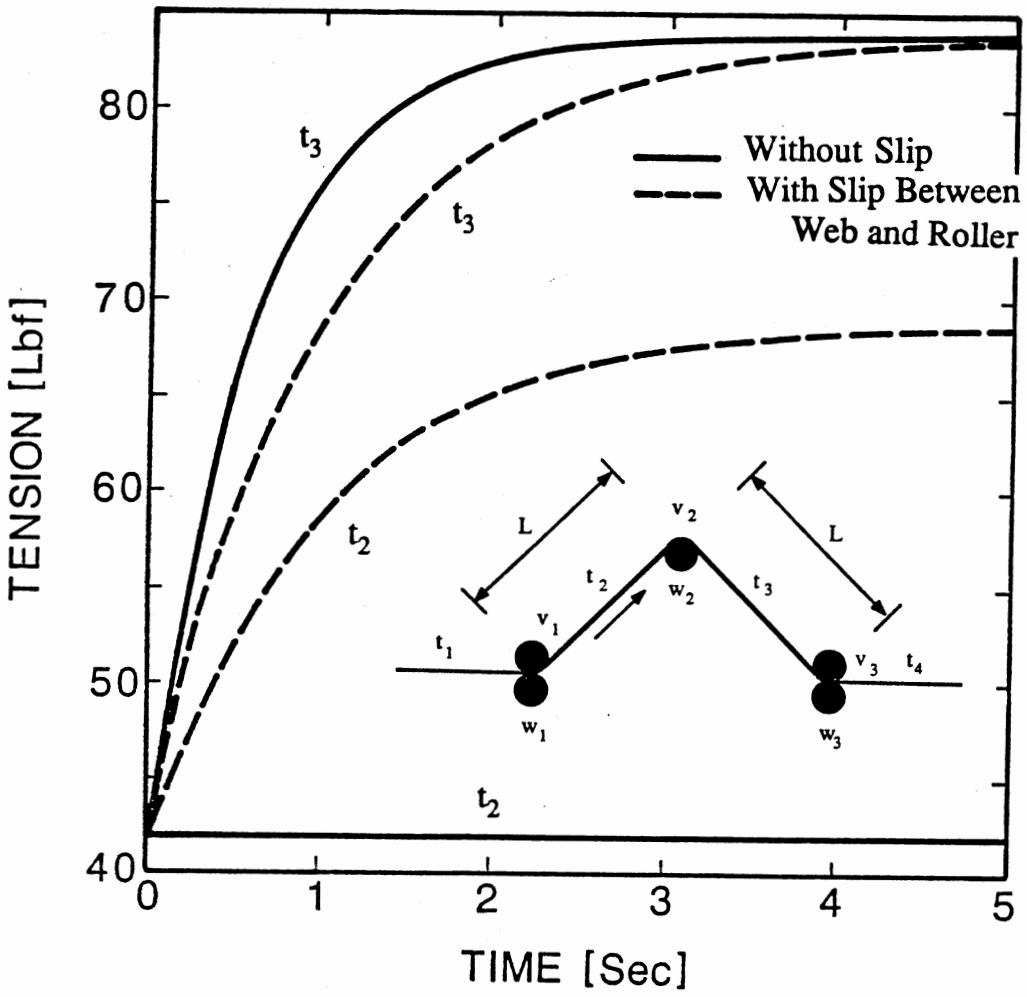

Parameter values and system conditions: see Table 2

$V_1 = W_1 = 1000$, $W_2 = 1001$, $V_3 = W_3$, $W_3(0^-) = 1001$, $W_3(0^+) = 1002$ ft/min

Figure 16. Responses of t_2 and t_3 to a Step Change in w_3 for the Two-Span System

Analysis of a Roller

Tension -Tangential Velocity of Roller Relationship

Another important primitive element is a roller. It is assumed that the rollers at both ends of the free span in Figure 6 are driven by motors and there is no change in the moment of inertia of any of the rollers. The dynamics of the driving motor generally are negligible compared to those of the rollers. A relationship between the tension in the web and the tangential velocity of the roller at position 2 in Figure 6 can be obtained from a torque balance on the roller as follows:

$$\frac{dW_2}{dt} = -\frac{B_{f2}}{J_2}W_2 + \frac{R_2^2}{J_2}(T_3 - T_2) + \frac{R_2}{J_2}K_2U_2, \qquad (38)$$

where

B_{f2} : Rotary friction constant of bearing

J_n : Polar moment of inertia of roll

K_2 : Motor constant

R_n : Radius of roller

U_2 : Change in input to the motor driving the roller at position 2

W_2 : Change in tangential velocity of the roller.

The change in the velocity (V_2) of the web in equation (22) and the change in tangential velocity of the roller (W_2) in equation (38) are identical when no slip occurs between the web and the roller (i.e, $V_2 = W_2$).

Effect of Web Cross-Sectional Area Change on Change in Tension

As the strain varies in the web material, the cross-sectional area of the web may vary from one web span to the next due to Poisson's ratio. The importance of this effect is considered below. Assuming that the material is isotropic and does not experience temperature changes, the stress-strain relationships can be written as [14]:

$$\epsilon_x = \frac{1}{E}\sigma_x, \tag{39}$$

$$\epsilon_y = -\frac{1}{E}\nu\,\sigma_x, \tag{40}$$

$$\epsilon_z = -\frac{1}{E}\nu\,\sigma_x, \tag{41}$$

where

E	: Young's modulus	σ	: Stress
ν	: Poisson's ratio	ϵ	: Strain.

Now, consider an infinitesimal element of the web as shown in Figure 17. The cross-sectional area of the web in the stretched condition is

$$\begin{aligned} A &= d \times h = \left[(1 + \epsilon_y)\, d_u\right]\left[(1 + \epsilon_z)\, h_u\right] \\ &= d_u\, h_u\, (1 + \epsilon_y + \epsilon_z + \epsilon_y\, \epsilon_z). \end{aligned} \tag{42}$$

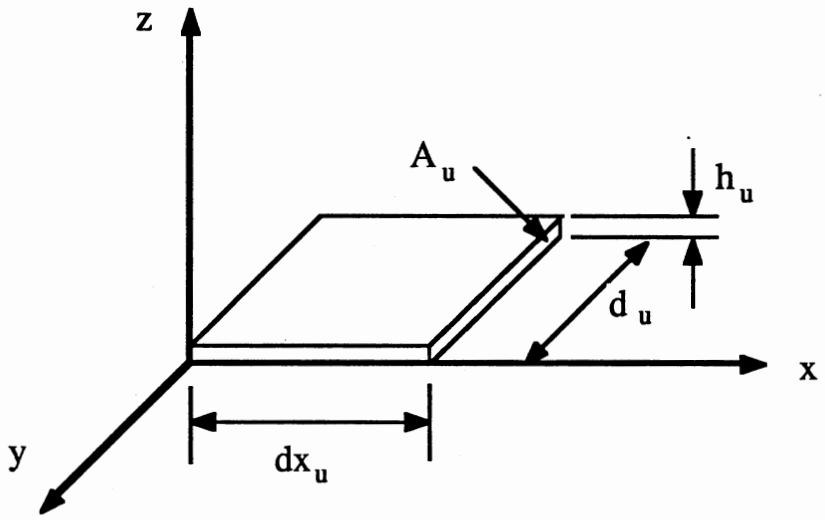

Unstretched web element

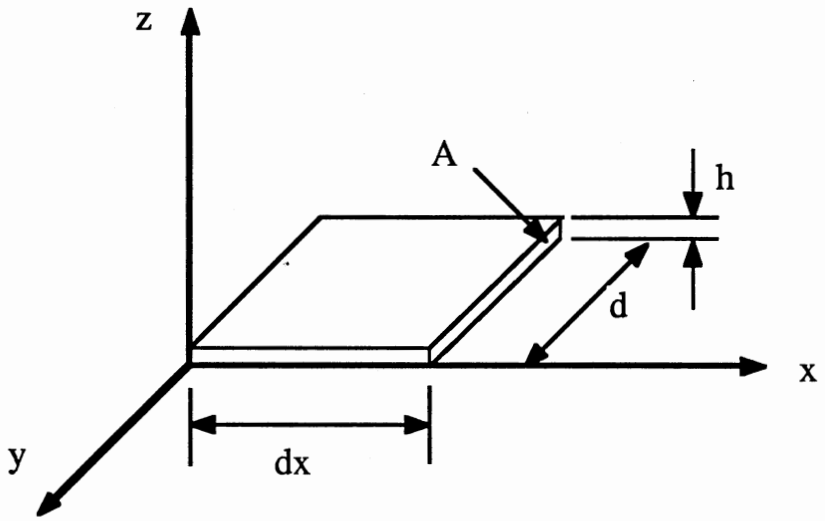

Stretched web element

Figure 17. A Mass Element out of a Web Span in the Unstretched and Stretched Conditions

Since $\epsilon_y \epsilon_z \cong 0$, equation (42) can be written as:

$$A \cong d_u h_u (1 + \epsilon_y + \epsilon_z). \tag{43}$$

Using equations (40) and (41), equation (43) can be written as:

$$A \cong d_u h_u (1 - 2 \nu \epsilon_x) = A_u (1 - 2 \nu \epsilon_x). \tag{44}$$

The longitudinal tension in the web can be written as:

$$T_x(t) = A E \epsilon_x. \tag{45}$$

Combining equations (44) and (45) gives:

$$T_x(t) = A E \epsilon_x(t) = A_u \left[1 - 2 \nu \epsilon_x(t)\right] E \epsilon_x(t). \tag{46}$$

By using equation (20) in section 2.1, the relationship between the strain in a web span and web velocities at the ends of the span (see Figure 6) can be written as:

$$\frac{d}{dt}[\epsilon_2(t)] = -\frac{v_{20}}{L_2}\epsilon_2(t) + \frac{v_{10}}{L_2}\epsilon_1(t) + \frac{V_2(t)}{L_2} - \frac{V_1(t)}{L_2}. \tag{47}$$

The algebraic equation (46) can be solved simultaneously with the differential equation (47) to evaluate the tension variation in a span when the change in the cross-sectional area is taken into consideration.

A numerical example is solved to show the effect of a change in the cross-sectional area of the web on the tension variation. Consider a two-span web transport system as shown in Figure 18. The cross-sectional areas A_2 and A_3 change with the change in strains ϵ_2 and ϵ_3. By using equations (46) and (47), the dynamic equations for the two-span system can be written as:

$$\frac{d}{dt}[\epsilon_2(t)] = -\frac{v_{20}}{L_2}\epsilon_2(t) + \frac{v_{10}}{L_2}\epsilon_1(t) + \frac{V_2(t)}{L_2} - \frac{V_1(t)}{L_2}. \qquad (48)$$

$$T_2(t) = A_{2u}\,[1 - 2\nu\,\epsilon_2(t)]\,E\,\epsilon_2(t). \qquad (49)$$

$$\frac{d}{dt}[\epsilon_3(t)] = -\frac{v_{30}}{L_3}\epsilon_3(t) + \frac{v_{20}}{L_3}\epsilon_2(t) + \frac{V_3(t)}{L_3} - \frac{V_2(t)}{L_3}. \qquad (50)$$

$$T_3(t) = A_{3u}\,[1 - 2\nu\,\epsilon_3(t)]\,E\,\epsilon_3(t). \qquad (51)$$

It is assumed that tangential velocities of rollers (V_1, V_2, V_3) are perfectly controlled. Equations (48) through (51) were solved for the conditions and parameters shown in Table 3 for ν=0.2 and ν=0.4.

In the steady-state, equations (48) through (51) becomes:

$$0 = -v_{20}\,\epsilon_2 + v_{10}\,\epsilon_1 + V_2 - V_1. \qquad (52)$$

$$T_2 = A_{2u}\,[1 - 2\nu\,\epsilon_2]\,E\,\epsilon_2 = A_2\,E\,\epsilon_2\,. \qquad (53)$$

$$0 = -v_{30}\,\epsilon_3 + v_{20}\,\epsilon_2 + V_3 - V_2. \qquad (54)$$

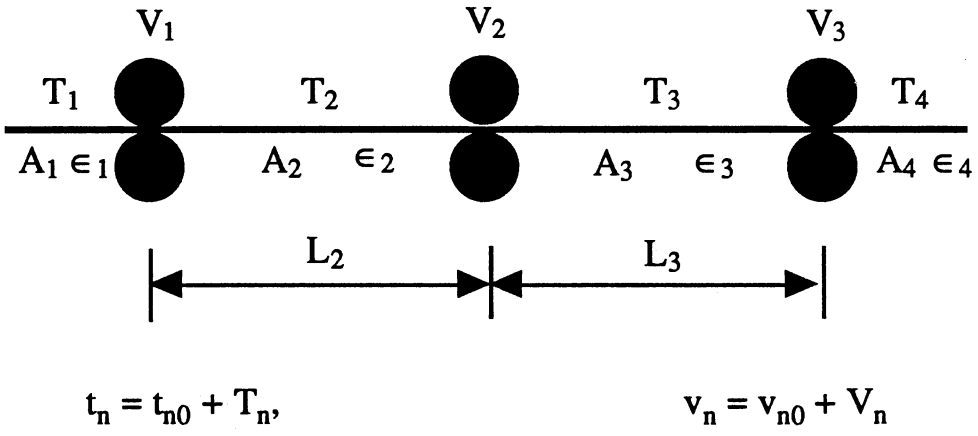

Figure 18. A Two-Span Web Transport System

$$T_3 = A_{3u}\,[1 - 2\,\nu\,\epsilon_3]\,E\,\epsilon_3 = A_3\,E\,\epsilon_3\ . \qquad (55)$$

And, $T_1 = A_1\,E\,\epsilon_1$ in the steady state. Solving equations (52) through (55) for T_2 and T_3 gives:

$$T_2 = \frac{A_2}{A_1}\frac{v_{10}}{v_{20}}\,T_1 + \frac{A_2\,E}{v_{20}}(V_2 - V_1). \qquad (56)$$

$$T_3 = \frac{A_3}{A_2}\frac{v_{20}}{v_{30}}\,T_2 + \frac{A_3\,E}{v_{30}}(V_3 - V_2). \qquad (57)$$

$$A_1 = A_{1u}\,[1 - 2\,\nu\,\epsilon_1]. \qquad (58)$$

$$A_2 = A_{2u}\,[1 - 2\,\nu\,\epsilon_2]. \qquad (59)$$

$$A_3 = A_{3u}\,[1 - 2\,\nu\,\epsilon_3]. \qquad (60)$$

TABLE 3

PARAMETER VALUES AND SYSTEM CONDITIONS
FOR SIMULATION IN SECTION 2.4

Conditions

Initial steady-state operating tension $t_{30} = 42$ (Lbf)

Initial steady-state operating velocity $v_{n0} = 1{,}000$ (ft/min),

$n = 1, 2, 3$

$V_3 = 0.06$ (ft/min), @ $t = 0^+$; $V_3 = 0$, @ $t = 0^-$

Parameter Values

$A_{nu} = 0.12$ (in^2), $n = 2, 3$

$d = 120$ (in)

$E = 350{,}000$ (Lbf/in^2)

$L_n = 120$ (in), $n = 1, 2, 3$

Combining equations (56) and (57) gives:

$$T_3 = \frac{A_3}{A_2}\frac{v_{20}}{v_{30}}\left[\frac{A_2}{A_1}\frac{v_{10}}{v_{20}}T_1 + \frac{A_2 E}{v_{20}}(V_2 - V_1)\right] + \frac{A_3 E}{v_{30}}(V_3 - V_2). \tag{61}$$

Assuming $T_1 = 0$, and $V_1 = V_2 = 0$, equation (61) can be written as:

$$T_3 = \frac{A_3 E}{v_{30}}(V_3 - V_2), \tag{62}$$

where $A_3 = A_{3u}\,[1 - 2\,\nu\,\epsilon_3]$ from equation (60).

Results for the steady-state analysis for two different values of Poisson's Ratio are as follows:

Cross-sectional area	Tension Variation ,T_3, (lbf)	
	Poisson's Ratio (ν)	
	$\nu = 0.2$,	$\nu = 0.4$
Constant	2.5199	2.5199
Varied	2.5189	2.5178

($A_3 = A_{3u}\,(1 - 2\,\nu\epsilon_3)$)

Figure 19 shows the results of a dynamic analysis for two values of Poisson's ratio computed using equations (48) - (51). A step input (i.e., $V_3 = 0.06$ (ft/min), @ $t = 0^+$; $V_3 = 0$, @ $t = 0^-$) was provided to the two

span system.

In conclusion, the effect of area change on the tension variation is not significant if the magnitude of the tension variation is small.

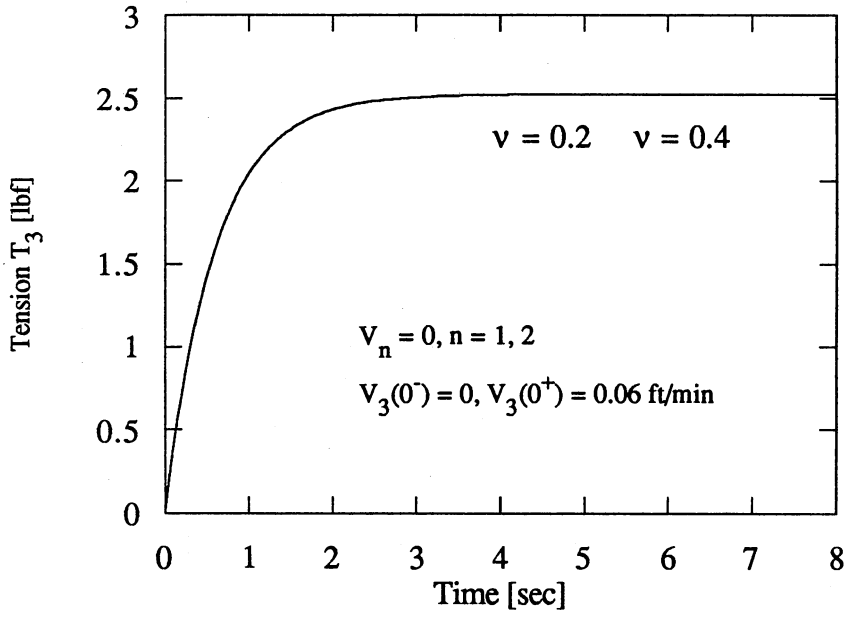

Figure 19. Effect of Web Cross-sectional Area Change on Dynamic Tension Variation

Effect of Temperature Change on Change in Tension

It is very common for the temperature conditions to differ in the various processing sections in a web transport line. Changes in temperature affect the strain in the web in two ways [14]: first, by directly producing a strain even in the absence of stress (thermal-strain) and, second, by causing a modification in the value of the Young's modulus.

Effect of a Change in Temperature on Strain

The thermal strain is almost linear in the temperature change of 100 - 200 (^{O}F). For an isotropic material, there is no shear-strain due to thermal expansion (contraction), but only pure elongation or contraction [14]. Thus, the thermal-strain due to the temperature change, θ_T, can be written as (see Figure 6):

$$\epsilon_x^t = \epsilon_y^t = \epsilon_z^t = \alpha\, \theta_T, \tag{63}$$

$$\gamma_{xy}^t = \gamma_{yz}^t = \gamma_{zx}^t = 0, \tag{64}$$

where

α is the coefficient of linear expansion

ϵ^t is the thermal strain

γ^t is the thermal shear strain

The subscripts indicate the coordinate.

The total strain in a rigid body is the sum of the strain due to the stress and the temperature. Let ϵ^e be the elastic-strain and ϵ^t be the thermal- strain. Then, the total strain can be written as [14]:

$$\epsilon = \epsilon^e + \epsilon^t. \tag{65}$$

It is assumed that uniaxial (MD) stress prevails, that is, $\sigma_x \neq 0$, $\sigma_y = \sigma_z = 0$ (see Figure 6). Assuming there are changes in the temperature within the web material, the stress-strain-temperature relationships can be written as [14]:

$$\epsilon_2(t) = \frac{1}{E}\sigma_2(t) + \alpha\,\theta_T(t)\,. \tag{66}$$

The stress-tension relationship is:

$$T_2(t) = A\,\sigma_2(t). \tag{67}$$

Combining equations (66) and (67) gives:

$$T_2(t) = A\,E\,\{\epsilon_2(t) - \alpha\,\theta_T(t)\}. \tag{68}$$

Recall equation (20) which shows the relationship between the longitudinal strain and web velocity for the web span shown in Figure 6.

$$\frac{d}{dt}[\epsilon_2(t)] = -\frac{v_{20}}{L}\epsilon_2(t) + \frac{v_{10}}{L}\epsilon_1(t) - \frac{V_1(t)}{L} + \frac{V_2(t)}{L}. \qquad (69)$$

Equations (68) and (69) can be used to illustrate the effect of a change in temperature on tension variation.

An example is solved to illustrate the effect of a change in temperature on tension in the steady state. In the steady state, assuming $\epsilon_1 = 0$, the equation (69) can be written as:

$$\epsilon_2 = \frac{V_2 - V_1}{v_{20}}. \qquad (70)$$

Combining equations (68) and (70) gives:

$$T_2 = A\,E\left\{\frac{V_2 - V_1}{v_{20}} - \alpha\,\theta_T\right\}. \qquad (71)$$

Example:

Conditions: web material is polypropylene

A (cross-sectional area of web) = 0.12 in^2

E (Young's modulus of web material) = 350,000 psi

v_{20} (average web transport speed) = 400 ft/min

$V_2 - V_1$ (velocity difference) = 1 ft/min (0.25 % of v_{20})

θ_T (temperature change) = 18.5 ^oC (33.4 ^oF)

α (thermal expansion coeff.) = $1.35 \times 10^{-4}\ ^oC^{-1}$

(in the temperature range of 20^o - 80^o C) [15].

For these conditions,

$$\frac{V_2 - V_1}{v_{20}} = \alpha \theta_T$$

, i.e., velocity difference effect is of the same order as the thermal effect.

In conclusion, change of temperature in a polypropylene web significantly affects tension.

The Effect of a Change in Temperature on Young's Modulus

For many materials (e.g., steel), temperature changes of a few hundreds degrees Fahrenheit result in very small changes in Young's modulus [14]. But, for some materials (e.g., polypropylene), the Young's modulus is reduced by half for temperature increases of less than one hundred degrees Fahrenheit (see Figure 11). In order to study the effect of Young's modulus for materials on tension variation, recall the mathematical model for a web span as shown in equations (68) and (69). Once Young's modulus is determined experimentally or statistically as a function of temperature for a given web material, equations (68) and (69) can be used to predict the change in web tension when there is a temperature change within the web span.

Effect of Moisture Change on Change in Tension

Some web processes (e.g., drying, printing) significantly change the moisture content of the web material. The effect of moisture on strain in the elastic region appears in two ways: (1) by directly producing a strain even in the absence of stress (hygroscopic strain), and (2), by causing a modification in the values of Young's modulus.

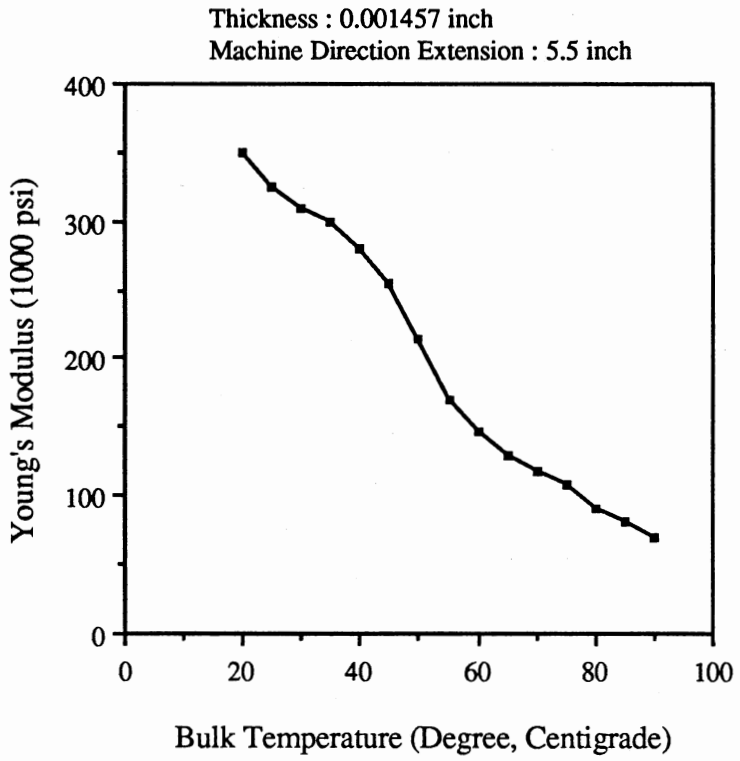

Figure 20. Temperature Effect on Young's Modulus for Polypropylene

The Effect of a Change in Moisture on Strain

The change in strain due to moisture change is approximately proportional (linear) with small changes of moisture in a web material (4 - 5 %). For an isotropic material, there is no shear-strain due to hygroscopic effect; there is only pure elongation or contraction. Without considering temperature effects, and with the assumption that MD stress prevails, the stress-strain-moisture relationship can be written as:

$$\epsilon_2 = \frac{1}{E}\sigma_2 + \epsilon^m, \qquad (72)$$

where ϵ^m is longitudinal strain due to moisture absorption (hygroscopic strain).

The total strain in a rigid body at a constant temperature is assumed to be the sum of the elastic strain and hygroscopic strain as follows:

$$\epsilon = \epsilon^e + \epsilon^m, \qquad (73)$$

where

ϵ^e : Elastic strain

ϵ^m : Hygroscopic strain.

The stress-tension relationship can be written as [14]:

$$T_2 = A\,\sigma_2. \qquad (74)$$

Combining equations (72) through (74) gives the tension - strain relationship:

$$T_2(t) = A\, E_2(t) \{\epsilon_2(t) - \epsilon^m(t)\}. \qquad (75)$$

Equations (69) and (75) can be solved simultaneously to obtain the tension variation, T_2, when there is a moisture change within a web span shown.

An example is solved to illustrate the effect of moisture change on tension variation in a web span. In the steady state, assuming $\epsilon_1 = 0$, combining equations (70) and (75) gives:

$$T_2 = A\, E \left\{ \frac{V_2 - V_1}{v_{20}} - \epsilon^m \right\}. \qquad (76)$$

Example:

Conditions: web material is fine paper

v_{20} (average web transport speed) = 400 ft/min

$V_2 - V_1$ (velocity difference) = 1 ft/min (0.25 % of v_{20})

Moisture change = 3.8 % [32].

For these conditions $\dfrac{V_2 - V_1}{v_{20}} = \epsilon^m$,

i.e., velocity difference effect is of the same order as the hygroscopic strain effect.

In conclusion, moisture absorption in a fine paper web significantly affects strain, and thus the tension.

The Effect of a Change in Moisture on Young's Modulus

The effect on the elastic constants for many materials (e.g., steel) may be small for moisture changes. But for some material (e.g., paper), the modulus of elasticity is very sensitive to the moisture change. Once Young's modulus is determined experimentally or statistically as a function of moisture, equations (69) and (75) can be used to predict the change in web tension when there is a change in the moisture within a web span.

Effect of Viscoelastic Properties on Change in Tension

The degree of change in viscoelastic properties varies from one web material to another material, and depends highly on the state of the material (e.g., degree of moisture content in the material, the temperature of material). The viscoelastic properties of a web may be very important for both the process operation and the properties of the final product. For example, the output rate of a paper machine in general, and newsprint, in particular, is most heavily dependent on the viscoelastic properties of the wet web under dynamic condition [16]. The stress relaxation in the web due to the viscoelastic property of web in the longitudinal direction may also affect the tension control in the web transport systems. In this section, the effect of viscoelastic properties of web on the longitudinal tension variation will be investigated. But the effect of temperature and moisture in material on viscoelastic properties of web will not be included in the investigation.

Consider a free web span fixed at one end and subjected to a motion (elongation) in the direction of the axis at the other end as shown in Figure 21. Let the elongation at time t be u(t) and the total tension in the web span be T(t). It will be assumed that web material retains linearity between load and elongation, but the linear relationship depends on a third parameter, time also.

For this class of material, the present state of deformation cannot be determined completely unless the entire history of loading (elongation) is known [17]. The tension T(t) is caused by the total history of the loading up (elongation instead of applied force) to the time t. If the function u(t) is

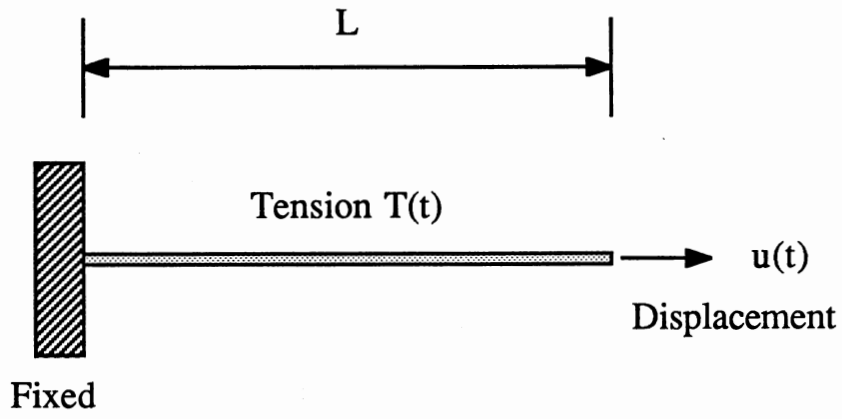

Figure 21. A Free Web Span Subject to Motion (Elongation)

continuous and differentiable, then in a small interval $d\tau$ at time τ the increment of elongation is $(du/dt)d\tau$. This increment continues to act on the free web span and contributes an element dT(t) to the tension in the web

span at the time t, with a proportionality constant k depending on the time interval t - τ. Hence, a tension dT(t) at the time t can be written [17]:

$$dT(t) = k(t-\tau) \frac{du}{dt}(\tau)\, d\tau. \qquad (77)$$

Let the origin of the time be taken at the beginning of loading. On summing over the entire history,

$$T(t) = \int_0^t k(t-\tau) \frac{du}{dt}(\tau)\, d\tau, \qquad (78)$$

where

$\frac{du}{dt}(\tau)$ means the value of du/dt evaluated at the $t = \tau$.

A similar argument, with the role of u and T interchanged, gives:

$$u(t) = \int_0^t c(t-\tau) \frac{dT}{dt}(\tau)\, d\tau, \qquad (79)$$

where

$\frac{dT}{dt}(\tau)$ means the value of dT/dt evaluated at the $t = \tau$.

Equations (78) and (79) are the forms of Boltzmann's formulation of the constitutive equation [17], in the case of a simple bar, for a material which has a linear load-deflection relationship. The function k(t) is called the "relaxation function". The function c(t) is called the "creep function". These are characteristic functions of the material. Physically, k(t) is the

force that must be applied in order to produce an elongation which changes at t = 0 from zero to unity and remains unity thereafter. Similarly, c(t) is the elongation produced by a sudden application at t = 0 of a constant force of magnitude unity; i.e., a unit-step forcing function.

Three models for the viscoelastic material have been introduced [17], namely, the Maxwell model, the Voigt model, and the "standard linear" model, all of which are composed of combinations of linear springs with spring constant k_s and dashpots with coefficient of viscosity b (see Figure 22).

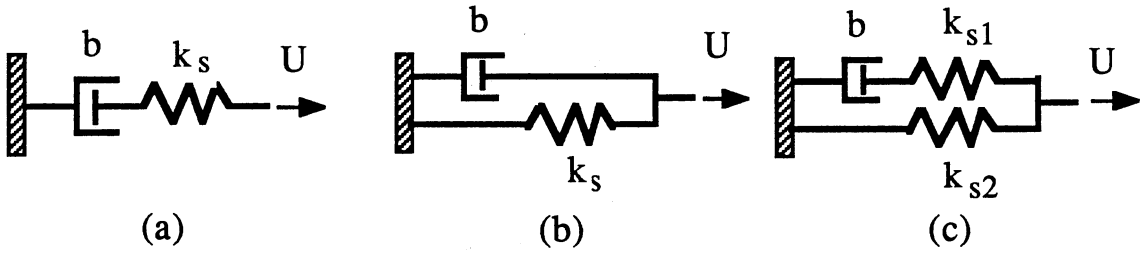

Figure 22. Models of Linear Viscoelasticity: (a) Maxwell, (b) Voigt, (c) Standard Linear Model

The load-deflection relationship for these models are

$$\text{Maxwell model: } \dot{u} = \frac{\dot{T}}{k_s} + \frac{T}{b} \quad , \quad u(0) = \frac{T(0)}{k_s}. \tag{80}$$

$$\text{Voigt model: } T = k_s u + b \dot{u} \quad , \quad u(0) = 0. \tag{81}$$

Standard linear model:

$$T + \tau_\varepsilon \dot{T} = E_R (u + \tau_\sigma \dot{u}) \ , \ \tau_\varepsilon T(0) = E_R \tau_\sigma u(0), \qquad (82)$$

where

τ_ε : time of relaxation of load under the condition of constant deflection.

τ_σ : time of relaxation of deflection under condition of constant load.

E_R : relaxed elastic modulus (load-deflection relation of spring as $t \rightarrow \infty$).

The relaxation function can be derived by solving equations (80) - (82) for T(t) when an elongation u(t) is a unit-step function 1(t) as follows [17].

$$\text{Maxwell solid: } k(t) = k_s e^{-(k_s/b)\, t}\, 1(t), \qquad (83)$$

$$\text{Voigt solid: } k(t) = b\, \delta(t) + k_s\, 1(t), \qquad (84)$$

$$\text{Standard linear solid: } k(t) = E_R \left[1 - \left(1 - \frac{\tau_\sigma}{\tau_\varepsilon}\right) e^{-t/\tau_\varepsilon}\right] 1(t), \qquad (85)$$

where

$\delta(t)$ indicates the unit-impulse function.

The function k(t) is illustrated in Figure 23.

For the Maxwell solid, a sudden deformation produces an immediate reaction by the spring, which is followed by stress relaxation according to

an exponential law expressed by equation (83). The factor b/k_s , with dimension of time, may be called a relaxation time: it characterizes the rate of force decay.

For the standard linear solid, a similar interpretation is applicable. The constant τ_ε is the time constant of load relaxation under the condition of constant deflection (see equation (85)). As $t \rightarrow \infty$, the dashpot is completely relaxed, and the load-deflection relation becomes that of the springs, as is characterized by the constant E_R, "relaxed elastic modulus".

It is highly possible for a web span to be exposed to the harmonic disturbances due to the imperfect roller/roll conditions. It might be interesting to obtain the steady-state relationship between load and

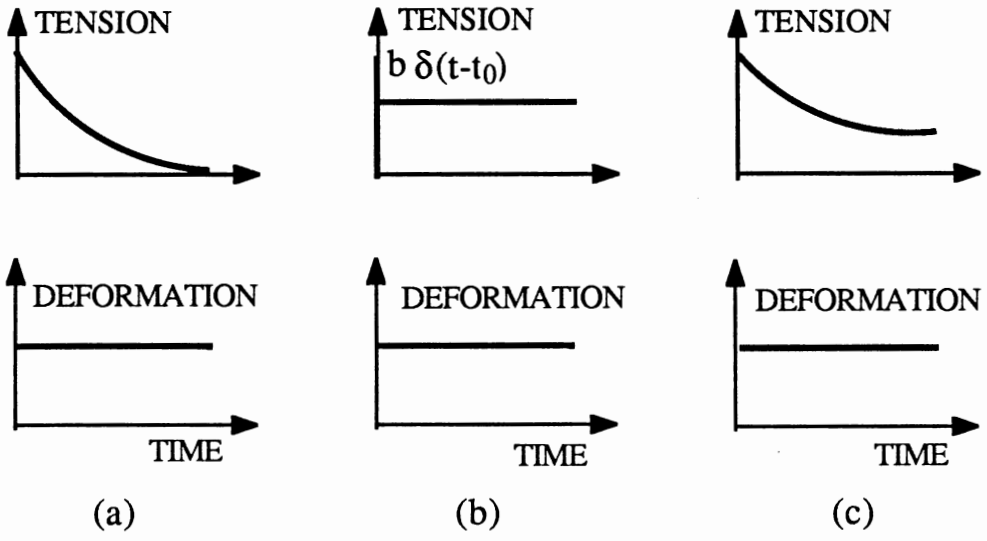

Figure 23. Relaxation Functions of (a) Maxwell, (b) Voigt, (c) Standard Linear Model

deflection when the web span is forced to perform simple harmonic oscillations. It will be convenient to put the beginning of motion at time $-\infty$ since the lower limit of equation (78) can be replaced by $-\infty$. Using complex representation for sinusoidal oscillations, let

$$u(t) = u_0 e^{i\omega t} . \tag{86}$$

And let

$$t - \tau = \xi. \tag{87}$$

Using equation (87) in equation (78) gives:

$$T(t) = \int_0^{\infty} k(\xi) \frac{du}{dt}(t - \xi)\, d\xi. \tag{88}$$

Using equation (86) in equation (88) gives:

$$T(t) = \int_0^{\infty} k(\xi)\, i\, \omega\, u_0\, e^{i\omega(t-\xi)}\, d\xi. \tag{89}$$

or

$$T(t) = i\, \omega\, u_0\, e^{i\omega t} \int_0^{\infty} k(\xi)\ e^{-i\omega\xi}\, d\xi. \tag{90}$$

Since $k(t) = 0$ when $t < 0$, the lower limit of the integral in equation (90) can be replaced by $-\infty$, then the integration part in equation (90) can be

written in the conventional form of Fourier transformation :

$$\bar{k}(\omega) = \int_{-\infty}^{\infty} k(\tau)\ e^{-i\omega\tau}\, d\tau. \qquad (91)$$

Assuming that the Fourier integral exists, T(t) can be written as:

$$T(t) = i\ \omega\ u_0\ \bar{k}(\omega)\ e^{i\omega t}. \qquad (92)$$

Under a periodic forcing function the tension T(t) is also periodic. Let

$$T(t) = T_0\ e^{i\omega t}, \qquad (93)$$

then the following input-output ratio can be obtained:

$$\frac{T_0}{u_0} = i\ \omega\ \bar{k}(\omega). \qquad (94)$$

The ratio T_0 / u_0 is a complex number, which may be written as

$$\frac{T_0}{u_0} = \psi = i\ \omega\ \bar{k}(\omega) = \left|\omega\ \bar{k}(\omega)\right| e^{-i\delta}, \qquad (95)$$

where

ψ is called the 'complex modulus' of a viscoelastic material [17].

The angle δ is of particular interest. It represents the phase angle by which the stress lags the strain. The tangent of δ is often used as a measure of 'internal friction' (viscoelasticity) of a linear viscoelastic material.

Since

$$\tan \delta = \frac{\text{imaginary part of } \psi}{\text{real part of } \psi}, \qquad (96)$$

the internal friction can be easily computed when the Fourier transform of the relaxation function is known.

It might be interesting to investigate the viscoelastic effect on longitudinal tension variation. Even though the relaxation curve of web material is considered to be exponential from the investigation (see equations from (83) to (85)), it can be considered to be linear for some web material (e.g., Newsprint, Polypropylene) in order of half a minute (see Figures 24 and 25). For example, the relaxation characteristic of newsprint was given as follows in [18]:

$$T = A\,(E_1 \in - E_2 \in t), \qquad (97)$$

where

E_1 : Young's modulus, $E_1 \cong 5.12 \times 10^5$ psi

E_2 : Viscosity factor, $E_2 \cong 7.11 \times 10^3$ psi - sec $\cdot$

In equation (97), the magnitude of the viscosity term is only a few percent of that of elastic term, because the running time of the web in rotary press is usually a few seconds. Thus, the newsprint can be practically dealt with as elastic during the transport of the web.

As shown in this example, when the web transport speed is getting higher, the effect of viscoelastic properties on tension variation is negligible, and the web material can be considered as being linear.

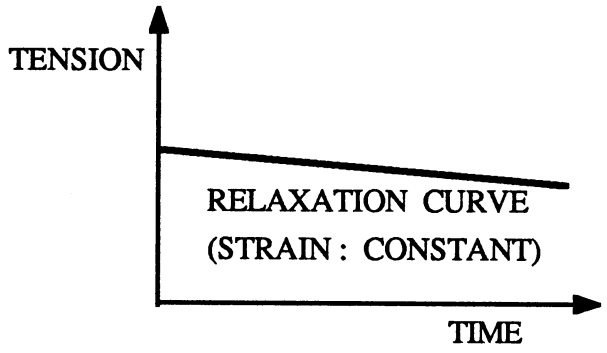

Figure 24. Measured Results of
Relaxation of Newsprint [18]

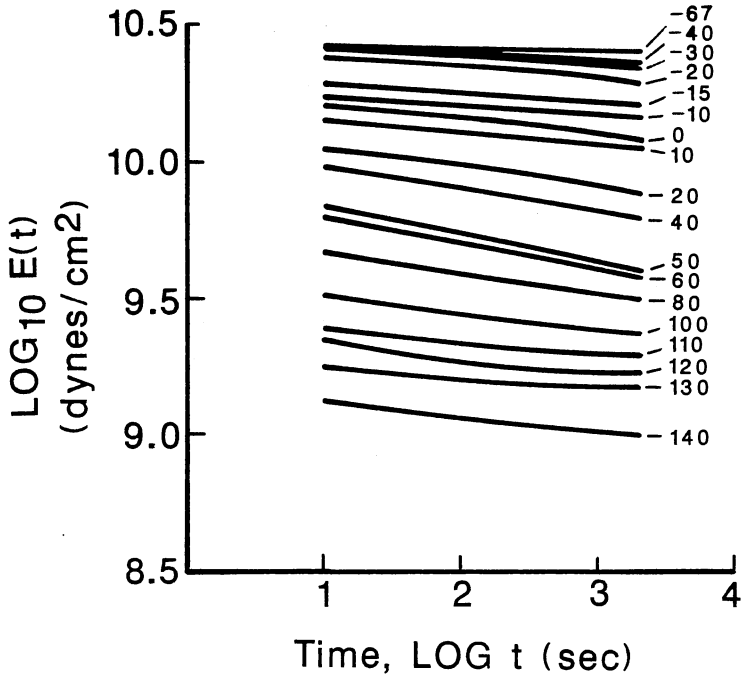

Figure 25. Stress Relaxation of Crystalline
Polypropylene [20] (Extended
5 %/min. to a Total Strain of
0.5 % on Instron Tester)

CHAPTER III

ANALYSIS OF A MULTI-SPAN SYSTEM WITH A DANCER

Primitive elements can be combined into subsystems as illustrated in Figure 26. Examples of subsystems are an idle roller with two free spans, an unwinding roll with a free span, and a winding roll with a free span, etc.. Systems can be configured using primitive elements and subsystems. An example system is shown in Figure 27.

Derivation of a Unified Model for A Multi-Span System

In this section, a "unified" open-loop dynamic model will be derived for an important multi-span system which includes a dancer as shown in Figure 27. This model includes the combined effects of slippage, temperature variation, and moisture variation. The model will be evaluated for a typical web material (Polypropylene) and typical web transport system operating conditions. The following assumptions were made in the derivation of the unified model:

(1) The vertical displacement of the dancer roll is very small

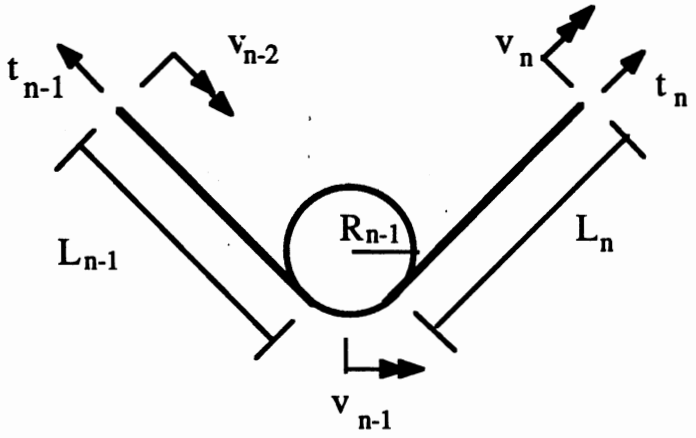

(a) Idle Roller with Two Free Spans

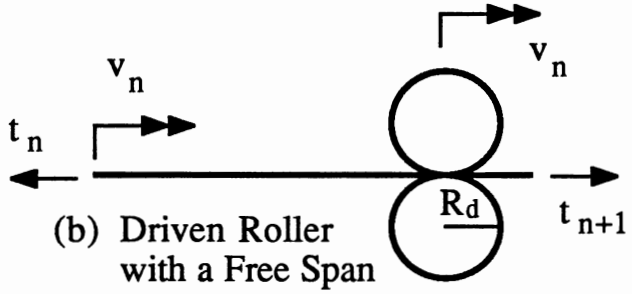

(b) Driven Roller with a Free Span

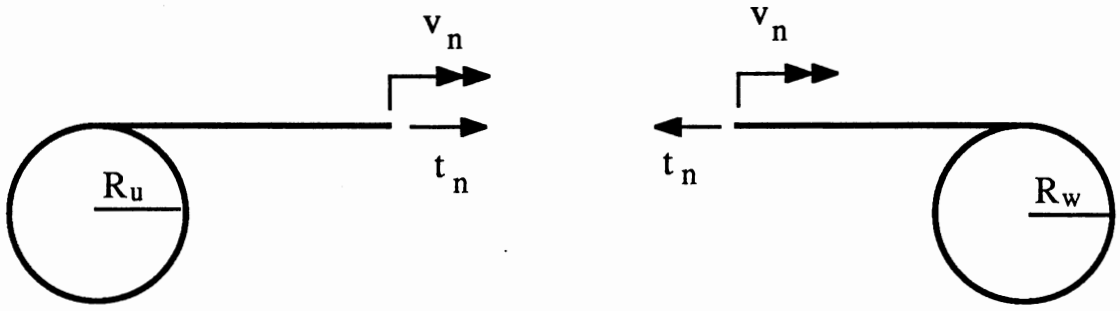

(c) Unwinding Roll with a Free Span (d) Winding Roll with a Free Span

Figure 26. Some Subsystems

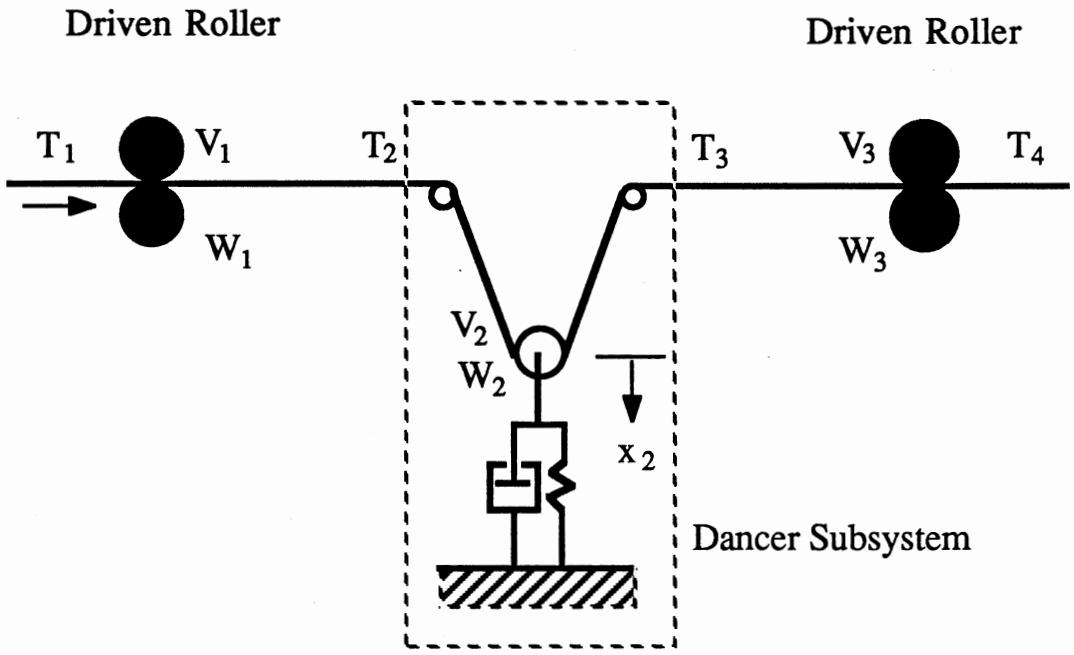

T_i : Change in web tension; i = 1, 2, 3, 4

V_i : Change in web velocity; i = 1, 2, 3

W_i : Change in tangential velocity of rollers; i = 1, 2, 3

x_2 : Vertical displacement of dancer subsystem

Figure 27. A Multi-Span System Which Includes a Dancer Subsystem

compared to the length of the web span,

(2) The change in the wrap angle of the web on the dancer roll due to the vertical displacement of the roll is negligible,

(3) No slippage occurs between the web and the dancer roll,

(4) The total elastic strain in the web is a linear combination of (a) the elastic strain due to the velocity difference between the two ends of the web, (b) the elastic strain due to the vertical displacement of the dancer roll, and (c) the elastic strain due to the angular displacement of dancer roll,

(5) The total strain in the web is the linear combination of the total elastic strain, the thermal strain, and the hygroscopic strain.

By using assumption (5), the total strain variations in the web spans of the system shown in Figure 27 can be written as:

$$\in_2(t) = \in_2^e(t) + \in_2^t(t) + \in_2^h(t), \tag{98}$$

$$\in_3(t) = \in_3^e(t) + \in_3^t(t) + \in_3^h(t), \tag{99}$$

where

$\in_i(t)$: Total change in strain

$\in_i^e(t)$: Total change in elastic strain

$\in_i^t(t)$: Total change in thermal strain

$\in_i^h(t)$: Total change in hygroscopic strain

and i = 2, 3.

The total change in elastic strains in the web spans are written as :

$$\in_2^e(t) = \in_{2d}^e(t) + \in_{2v}^e(t) + \in_{2a}^e(t). \tag{100}$$

$$\epsilon^{e}_{3}(t) = \epsilon^{e}_{3d}(t) + \epsilon^{e}_{3v}(t) + \epsilon^{e}_{3a}(t), \qquad (101)$$

where

$\epsilon^{e}_{id}(t)$: Change in elastic strain due to the velocity difference

$\epsilon^{e}_{iv}(t)$: Change in elastic strain due to the vertical displacement of the dancer roll

$\epsilon^{e}_{ia}(t)$: Elastic strain due to the angular displacement of the dancer roll

and i = 2, 3.

Dynamic models for web spans 2 and 3 are derived in Appendix C[1]. For web span 2, the model is:

$$\frac{d}{dt}\{\epsilon_2(t)\} = -\frac{v_{20}}{L_2}\epsilon_2(t) + \frac{v_{10}}{L_2}\epsilon_1(t) - \frac{V_1(t)}{L_2} + \frac{V_2(t)}{L_2} \qquad (102)$$

$$+ \frac{\sin\frac{\theta_{w2}}{2}}{L_2} x_{21}(t) + \frac{v_{20}\sin\frac{\theta_{w2}}{2}}{L_2^2} x_2(t) - \frac{v_{10}\sin\frac{\theta_{w1}}{2}}{L_1 L_2} x_1(t)$$

$$+ \frac{R_2}{L_2} y_{21}(t) + \frac{v_{20}R_2}{L_2^2} y_2(t) - \frac{v_{10}R_1}{L_1 L_2} y_1(t)$$

$$+ \alpha\frac{d}{dt}\{F_2(t)\} + \frac{v_{20}}{L_2}\alpha\{F_2(t) - F_{20}\} - \frac{v_{10}}{L_2}\alpha\{F_1(t) - F_{10}\}$$

$$+ \beta\frac{d}{dt}\{H_2(t)\} + \frac{v_{20}}{L_2}\beta\{H_2(t) - H_{20}\} - \frac{v_{10}}{L_2}\beta\{H_1(t) - H_{10}\}.$$

---

[1] Web span 2 is the web between the driven roller 1 and the dancer roll 2. Web span 3 is the web between the dancer roll 2 and the driven roller 3.

and, for web span 3 the model is:

$$\frac{d}{dt}\{\epsilon_3(t)\} = -\frac{v_{30}}{L_3}\epsilon_3(t) + \frac{v_{20}}{L_3}\epsilon_2(t) - \frac{V_2(t)}{L_3} + \frac{V_3(t)}{L_3} \qquad (103)$$

$$+ \frac{\sin\frac{\theta_{w2}}{2}}{L_3} x_{21}(t) + \frac{v_{30}\sin\frac{\theta_{w2}}{2}}{L_3^2} x_2(t) - \frac{v_{20}\sin\frac{\theta_{w2}}{2}}{L_2 L_3} x_2(t)$$

$$- \frac{R_2}{L_3} y_{21}(t) - \frac{v_{30}R_2}{L_3^2} y_2(t) - \frac{v_{20}R_2}{L_2 L_3} y_2(t)$$

$$+ \alpha \frac{d}{dt}\{F_3(t)\} + \frac{v_{30}}{L_3}\alpha\{F_3(t) - F_{30}\} - \frac{v_{20}}{L_3}\alpha\{F_2(t) - F_{20}\}$$

$$+ \beta \frac{d}{dt}\{H_3(t)\} + \frac{v_{30}}{L_3}\beta\{H_3(t) - H_{30}\} - \frac{v_{20}}{L_3}\beta\{H_2(t) - H_{20}\}.$$

where

b_2 : Damping constant in dancer subsystem

$F_n(t)$: Temperature of web

F_{n0} : Initial temperature of web

$H_n(t)$: Moisture of web

H_{n0} : Initial moisture of web

k_{s2} : Spring constant in dancer subsystem

L_n : Length of web span

M_2 : Mass of dancer roll

R_n : Radii of roller/roller

T_n : Change in web tension from a steady-state operating value

V_n : Change in web velocity from a steady-state operating value

v_{n0} : Steady-state operating value for web velocity

x_2 : Vertical displacement of dancer roll

x_{21} : Vertical velocity of dancer roll; $x_{21} \equiv \dot{x}_2$

y_2 : Angular displacement of dancer roll

y_{21} : Angular velocity of dancer roll; $y_{21} \equiv \dot{y}_2$

α : Coefficient of expansion of web with temperature

β : Coefficient of expansion of web with moisture

θ_{wn} : Wrap angle of web on dancer roll

and the subscript n is integer number,

and where

$$\dot{x}_2 = x_{21}, \tag{104}$$

$$\dot{y}_2 = y_{21}. \tag{105}$$

A force balance on the dancer roll taken in the vertical direction gives:

$$\frac{d\dot{x}_2}{dt} = -\frac{b_2}{M_2}x_{21} - \frac{k_{s2}}{M_2}x_2 - \frac{T_2 + T_3}{M_2}\sin\frac{\theta_{w2}}{2}. \tag{106}$$

A torque balance on the dancer roll gives:

$$\frac{d\dot{y}_{21}}{dt} = -\frac{B_{f2}}{J_2}y_{21} + \frac{R_2}{J_2}(T_3 - T_2), \tag{107}$$

where

B_{f2} : Rotary friction constant of bearing in dancer roll

J_2 : Polar moment of inertia of dancer roll.

Torque balances on the driven rollers results in the following equations:

$$\frac{d}{dt}\{W_1(t)\} = -\frac{B_{f1}}{J_1}W_1(t) + \frac{R_1^2}{J_1}\{T_2(t) - T_1(t)\} + \frac{R_1}{J_1}K_1U_1(t), \quad (108)$$

$$\frac{d}{dt}\{W_3(t)\} = -\frac{B_{f3}}{J_3}W_3(t) + \frac{R_3^2}{J_3}\{T_4(t) - T_3(t)\} + \frac{R_3}{J_3}K_3U_3(t), \quad (109)$$

where

B_{fn} : Rotary friction constant of bearing in dancer roll

J_n : Polar moment of inertia of dancer roll

U_n : Change in input to motors driving rollers 1 and 3.

From equation (28), the relationships between the motions of the web and rollers can be written as follows:

$$V_1(t) = W_1(t) - \frac{AE}{c_{s1}}[\{1 - k_\mu(1 - e^{-\mu_0\theta_{w1}}) - \epsilon_{20}^e\}\epsilon_1^e(t) - \epsilon_{10}^e\epsilon_2^e(t)]. \quad (110)$$

$$V_3(t) = W_3(t) - \frac{AE}{c_{s3}}[\{1 - k_\mu(1 - e^{-\mu_0\theta_{w3}}) - \epsilon_{40}^e\}\epsilon_3^e(t) - \epsilon_{30}^e\epsilon_4^e(t)]. \quad (111)$$

Since it assumed that there is no slippage between the dancer roll and the web (assumption (3)),

$$V_2(t) = W_2(t) . \quad (112)$$

Assumption (4) results in the following relations for the total elastic

strains:

$$\epsilon_2^e(t) = \epsilon_2(t) - \alpha \{F_2(t) - F_{20}\} - \beta \{H_2(t) - H_{20}\}. \quad (113)$$

$$\epsilon_3^e(t) = \epsilon_3(t) - \alpha \{F_3(t) - F_{30}\} - \beta \{H_3(t) - H_{30}\}. \quad (114)$$

From Hooke's law,

$$T_2(t) = AE\epsilon_2^e(t), \quad (115)$$

$$T_3(t) = AE\epsilon_3^e(t). \quad (116)$$

The unified model for the multi-span system in Figure 27 comprises equations (102) through (116). This unified model can be used to develop a mathematical model for a high order multi-span system which has more than one dancer. The following sections summarize results of analyses of systems which incorporate a dancer (1) for tension measurement and (2) for minimizing disturbances.

Analysis of a Multi-Span System Incorporating a Dancer Subsystem for Tension Measurement

The purpose of this section is to find guidelines for the selection or design of the dancer for tension measurement. The study is focused on how

much the dancer disturbs the system in which tension is to be measured. Consider a multi-span system which incorporates a dancer subsystem for tension measurement as shown in Figure 27. The following assumptions were made for the analysis.

(1) No variation of web temperature or moisture,

(2) No slippage between the web and the rollers,

(3) No change in the tangential velocity of driven roller 1

(i.e., $W_1 = 0.0$).

Natural frequencies due to the translational inertia (ω_t) and the rotational inertia (ω_r) are as follows[1]:

$$\omega_t = \sqrt{\frac{k_{s2}}{M_2}} . \tag{117}$$

$$\omega_r = \sqrt{\frac{AER_2^2}{J_2}\left(\frac{1}{L_2} + \frac{1}{L_2}\right)} . \tag{118}$$

Dynamic Model

With assumption (3), the change in tangential velocity of roller 1 is:

$$W_1(t) = 0.0 \text{ or } w_1 = \text{constant}. \tag{119}$$

The tangential velocity of roller 2 is:

$$W_2(t) = R_2 y_{21}(t). \tag{120}$$

[1] See Appendix D for the derivation

Equation (109) can be used for the tangential velocity of roller 3.

With assumption (2), the relations between the web velocities and roller velocities are:

$$V_1(t) = W_1(t)\,, \tag{121}$$

$$V_2(t) = W_2(t)\,, \tag{122}$$

$$V_3(t) = W_3(t)\,. \tag{123}$$

With assumption (1), equations (102) and (107) reduce to the following:

$$\frac{d}{dt}\{\in_2(t)\} = -\frac{v_{20}}{L_2}\in_2(t) + \frac{v_{10}}{L_2}\in_1(t) - \frac{V_1(t)}{L_2} + \frac{V_2(t)}{L_2} \tag{124}$$

$$+\frac{\sin\frac{\theta_{w2}}{2}}{L_2}x_{21}(t) + \frac{v_{20}\sin\frac{\theta_{w2}}{2}}{L_2^2}x_2(t) - \frac{v_{10}\sin\frac{\theta_{w1}}{2}}{L_1L_2}x_1(t)$$

$$+\frac{R_2}{L_2}y_{21}(t) + \frac{v_{20}R_2}{L_2^2}y_2(t) - \frac{v_{10}R_1}{L_1L_2}y_1(t),$$

and

$$\frac{d}{dt}\{\in_3(t)\} = -\frac{v_{30}}{L_3}\in_3(t) + \frac{v_{20}}{L_3}\in_2(t) - \frac{V_2(t)}{L_3} + \frac{V_3(t)}{L_3} \tag{125}$$

$$+\frac{\sin\frac{\theta_{w2}}{2}}{L_3}x_{21}(t) + \frac{v_{30}\sin\frac{\theta_{w2}}{2}}{L_3^2}x_2(t) - \frac{v_{20}\sin\frac{\theta_{w2}}{2}}{L_2L_3}x_2(t)$$

$$-\frac{R_2}{L_3}y_{21}(t) - \frac{v_{30}R_2}{L_3^2}y_2(t) - \frac{v_{20}R_2}{L_2L_3}y_2(t).$$

Equations (113) and (114) for the total elastic strains reduce to:

$$\epsilon_2^e(t) = \epsilon_2(t). \quad (126)$$

$$\epsilon_3^e(t) = \epsilon_3(t). \quad (127)$$

Equations (115) and (116) can be used to calculate tensions T_2 and T_3. The dynamic model for the analysis of the multi-span system using a dancer subsystem for tension measurement comprises equations (103) through (106), (109), (115), (116), (119), and (120) through (127).

Examples

The dynamic model for the multi-span system shown in Figure 27 was simulated with step input to the motor driving roller 3 and with different combinations of ω_t (frequency due to the translational inertia of the dancer) and ω_r (frequency due to the rotational inertia of the dancer). A typical web material (polypropylene) and typical web transport system operating conditions were used for the simulation (see Table 4). The conditions were chosen such that the natural frequency and the open-loop damping coefficient of the system without a dancer subsystem were ω_s = 6.5 rad/sec and ζ = 0.2 respectively.

Typical results of the simulation are shown in Figures 28, 29, and 30. Figure 28 shows a case when ω_t = 10 rad/sec and ω_r = 60 rad/sec. In this case, the dynamic tensions T_2 and T_3 are lightly damped without the dancer subsystem, and are well damped with the dancer subsystem in

operation. Figures 29 and 30 shows cases when $\omega_t > 3\omega_s$ and $\omega_r > 3\omega_s$. In these cases, the presence (or absence) of the dancer subsystem has little effect on the step responses T_2 and T_3. That is, the dancer subsystem is effective for tension measurement.

Based on a number of simulations, it was concluded that the dancer subsystem is useful for tension measurement, if it is designed such that:

$$\omega_t > 3\omega_s \quad \text{and} \quad \omega_r > 3\omega_s,$$

where $\omega_s = \sqrt{\frac{v_{30} B_{f3}}{(L_2+L_3)J_3} + \frac{A E R_3^2}{(L_2+L_3)J_3}}$: natural frequency of the system without a dancer subsystem.

Analysis of a Multi-Span System Incorporating a Dancer Subsystem for Minimizing Disturbances

The purpose of this section is to find guidelines for the selection or design of the dancer for minimizing disturbances. The study is focused on how much the dancer reduces the effect of disturbances in the system. Consider the multi-span system in Figure 31 which incorporates a dancer subsystem for disturbance minimization. The following assumptions are made for the analysis:

(1) No variation of web temperature or moisture,

(2) No slippage between the web and the rollers,

(3) No change in the tangential velocity of driven roller 1 (i.e., $W_1 = 0.0$).

TABLE 4

PARAMETER VALUES AND SYSTEM CONDITIONS
FOR SIMULATIONS IN SECTION 3.3

Parameter Values

A	$= 0.12$ in^2	c_2	$= 2300$ lbf-sec/ft
d	$= 120$ in	E	$= 350{,}000$ lbf/in^2,
h	$= 0.001$ in	K_i	$= 0.4$ lbf-ft/volt, $i = 1, 3$
L_i	$= 10$ ft, $i = 2, 3$	R_i	$= 5.0$ in., $i = 1, 2, 3$
v_{i0}	$= 1000$ ft/min, $i = 1, 2, 3$	μ	$= 0.1$
μ_{20}	$= 0.033$	θ_{w2}	$= 3.14$ Rad

where

L_2 : Web span between roller 1 and dancer roll

L_3 : Web span between dancer roll and roller 3

System Conditions

$T_i = 0$ lbf, $i = 1, 4$

$t_2(0^-) = 0$ lbf $\qquad$ $t_3(0^-) = 0$ lbf

Input U_3 = Input to motor driving roller 3

$U_3(0^-) = 0$, $U_3(0^+) = 1.0$ Volt

Conditions $\zeta = 0.2$, $\omega_s = 6.5$ rad/sec, $\omega_t = 10$ rad/sec,

$\omega_r = 60$ rad/sec

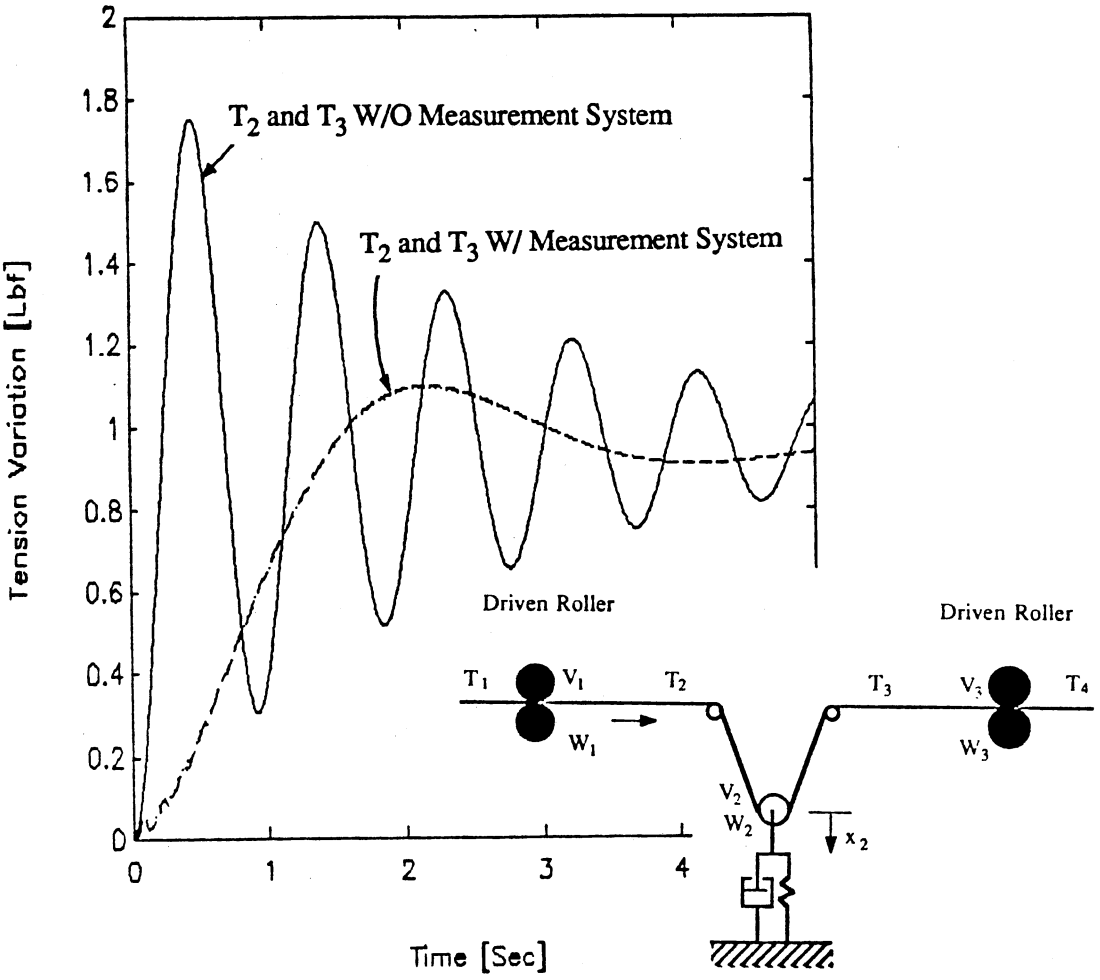

Figure 28. Performance of the Dancer as a Tension Measurement System for $\omega_t = 10$ rad/sec and $\omega_r = 60$ rad/sec

Input U_3 = Input to motor driving roller 3

$U_3(0^-) = 0$, $U_3(0^+) = 1.0$ Volt

Conditions $\zeta = 0.2$, $\omega_s = 6.5$ rad/sec, $\omega_t = 20$ rad/sec, $\omega_r = 20$ rad/sec

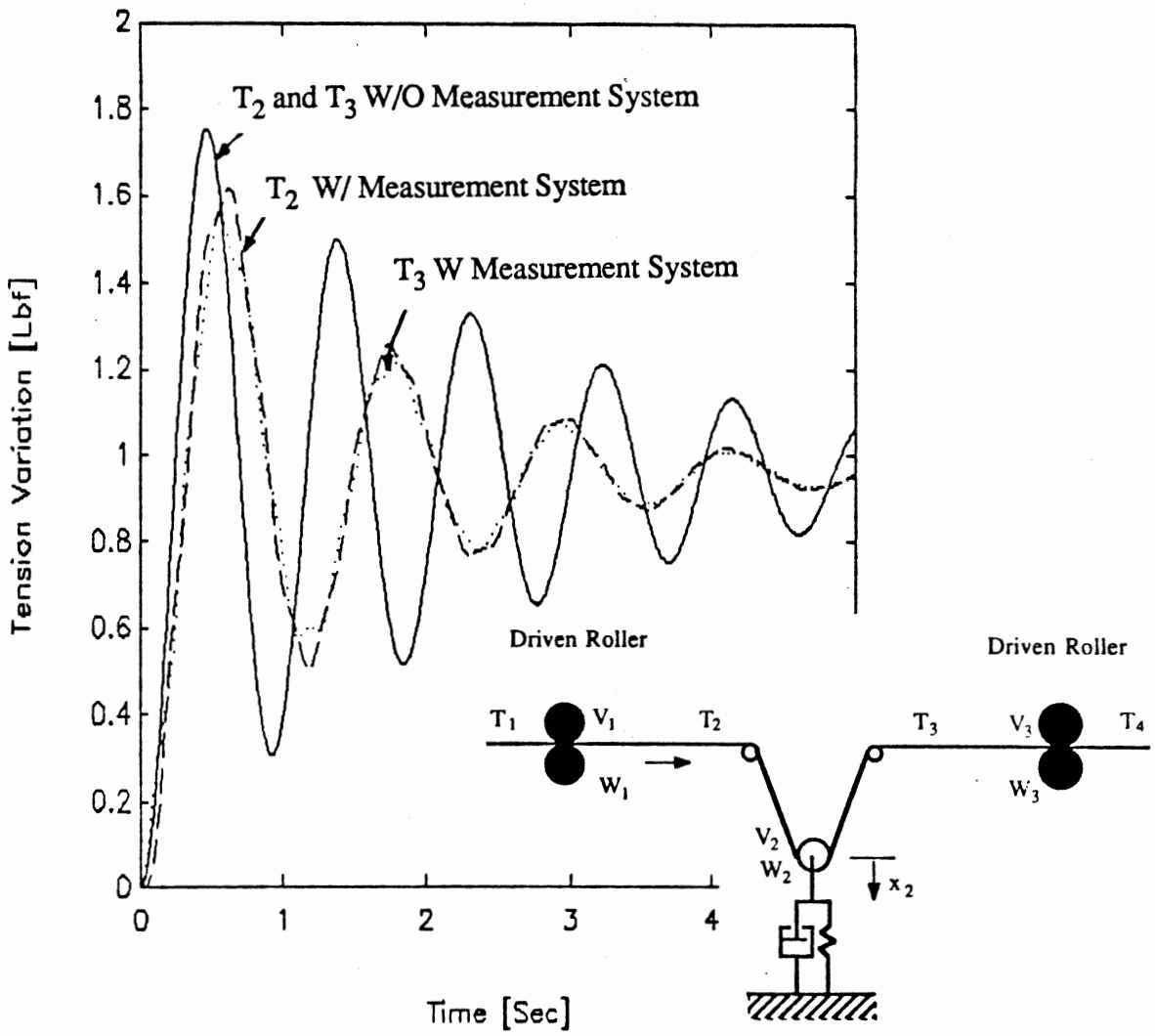

Figure 29. Performance of the Dancer as a Tension Measurement System for $\omega_t = 20$ rad/sec and $\omega_r = 20$ rad/sec

Input U_3 = Input to motor driving roller 3

$U_3(0^-) = 0$, $U_3(0^+) = 1.0$ Volt

Conditions $\zeta = 0.2$, $\omega_s = 6.5$ rad/sec, $\omega_t = 100$ rad/sec,

$\omega_r = 100$ rad/sec

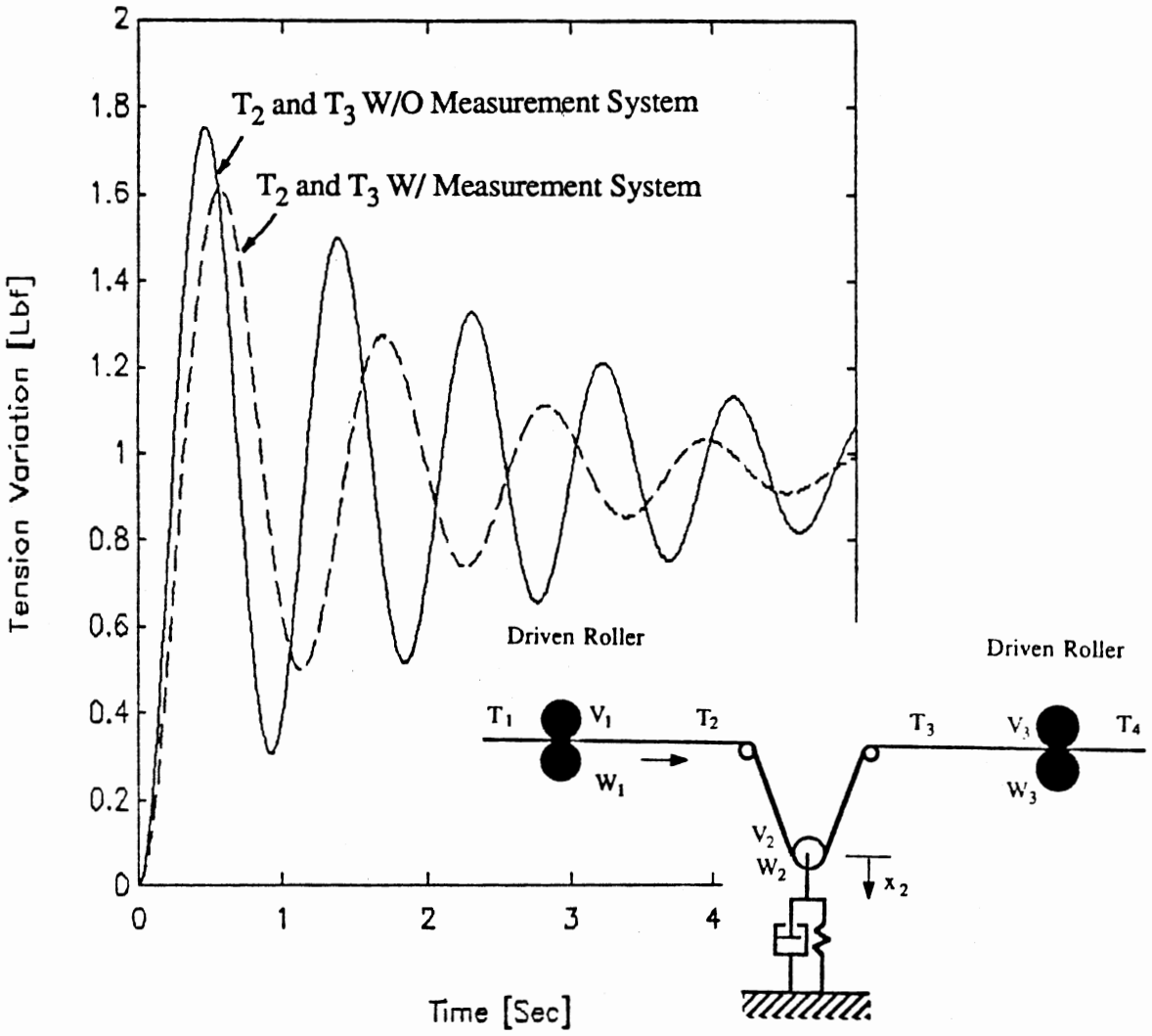

Figure 30. Performance of the Dancer as a Tension Measurement System for $\omega_t = 100$ rad/sec and $\omega_r = 100$ rad/sec

Dynamic Model

Equations (103) through (106), (109), (115), (116), (119), and (120) through (127) serve as the dynamic model for the system shown in Figure 31. It is of interest to evaluate the dancer subsystem as an effective means of minimizing the disturbance due to an eccentric unwinding roll, i.e.,

$$V_1(t) = V_{d0} \sin(\omega_d t). \tag{128}$$

Example

The dynamic model for the multi-span system shown in Figure 31 was simulated with a sinusoidal input (V_1) to the system and with different combinations of ω_t (frequency due to the translational inertia of the dancer) and ω_r (frequency due to the rotational inertia of the dancer). A typical web material (polypropylene) and typical web transport system operating conditions were used for the simulation (see Table 4). The conditions were chosen such that the natural frequency and the open-loop damping coefficient of the system without a dancer subsystem were ω_s = 6.5 rad/sec and ζ = 0.2 respectively. A sinusoidal input V_1 shown in equation (128) was provided to the multi-span system.

Typical results of the simulation are shown in Figures 32, 33, and 34. Figure 32 shows the case when the system does not have the dancer subsystem. Transient responses were shown for a couple of seconds of

period before the sinusoidal outputs reach to their steady-state values in Figure 32. Figures 33 and 34 shows cases when $\omega_t < \omega_s/3$ and $\omega_r > 3\omega_s$. In these cases, the presence of the dancer subsystem has great effect on the sinusoidal responses T_2 and T_3. That is, the dancer subsystem is excellent in minimizing the effect of disturbances.

Based on a number of simulations, it was concluded that the dancer subsystem is useful for minimizing the effect of disturbances, if it is designed such that:

If $\omega_d < \omega_s$, then $\omega_t > 3\omega_s$, $\omega_r < \frac{1}{3}\omega_d$

If $\omega_d > \omega_s$, then $\omega_t > 3\omega_d$, $\omega_r < \frac{1}{3}\omega_s$

where ω_d is the frequency of the disturbance.

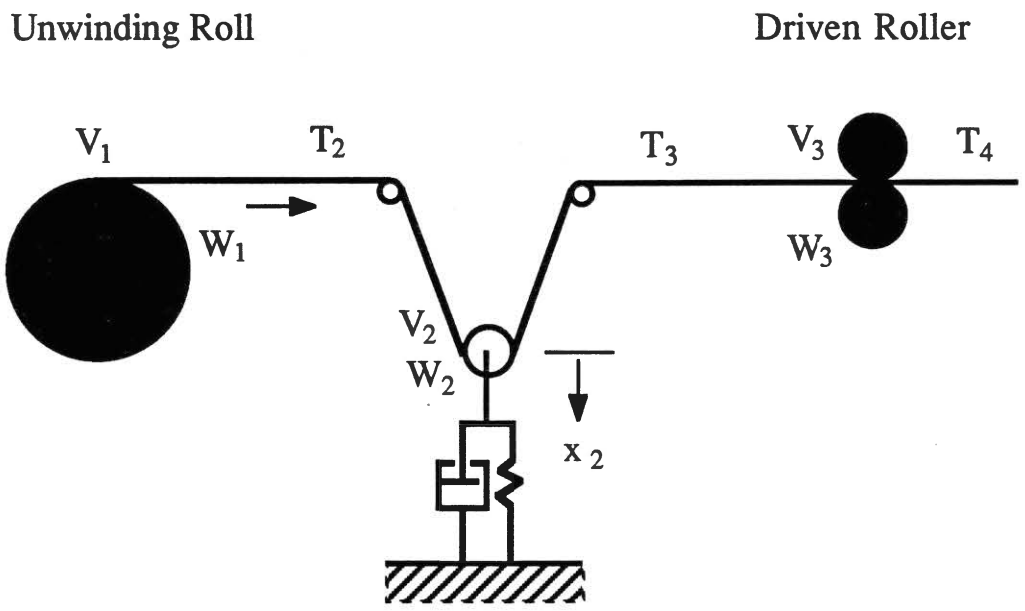

Figure 31. A Multi-Span Unwinding System Which Includes a Dancer Subsystem

Input $V_1(t) = V_{d0} \sin(\omega_d t)$, $V_{d0} = 0.01$ ft/sec, $\omega_d = 20$ rad/sec.

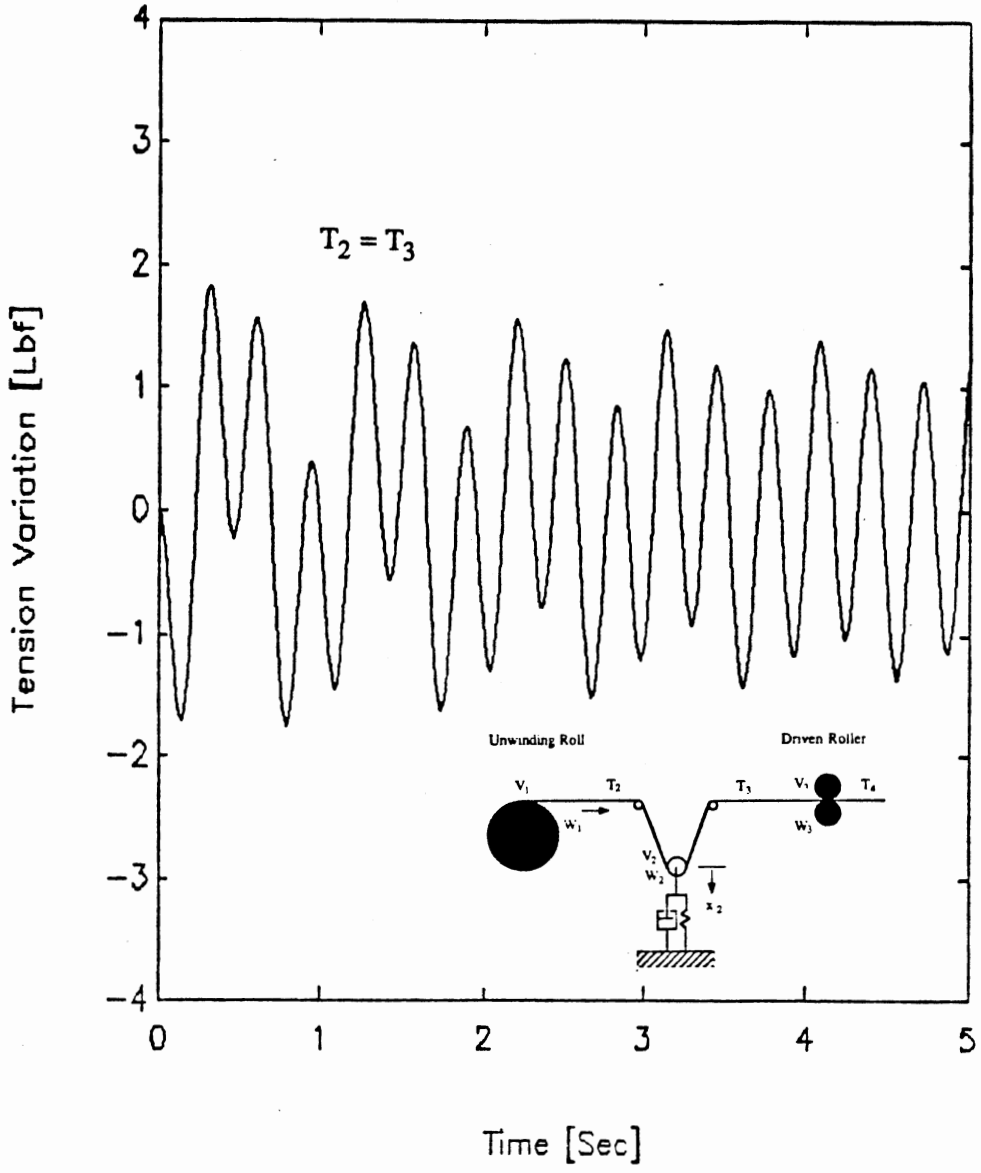

Figure 32. Tension Variation in a Web Span without a Dancer

Input $V_1(t) = V_{d0} \sin(\omega_d t)$, $V_{d0} = 0.01$ ft/sec, $\omega_d = 20$ rad/sec

Conditions $\zeta = 0.7$, $\omega_s = 6.5$ rad/sec, $\omega_t = 2$ rad/sec

$\omega_r = 60$ rad/sec.

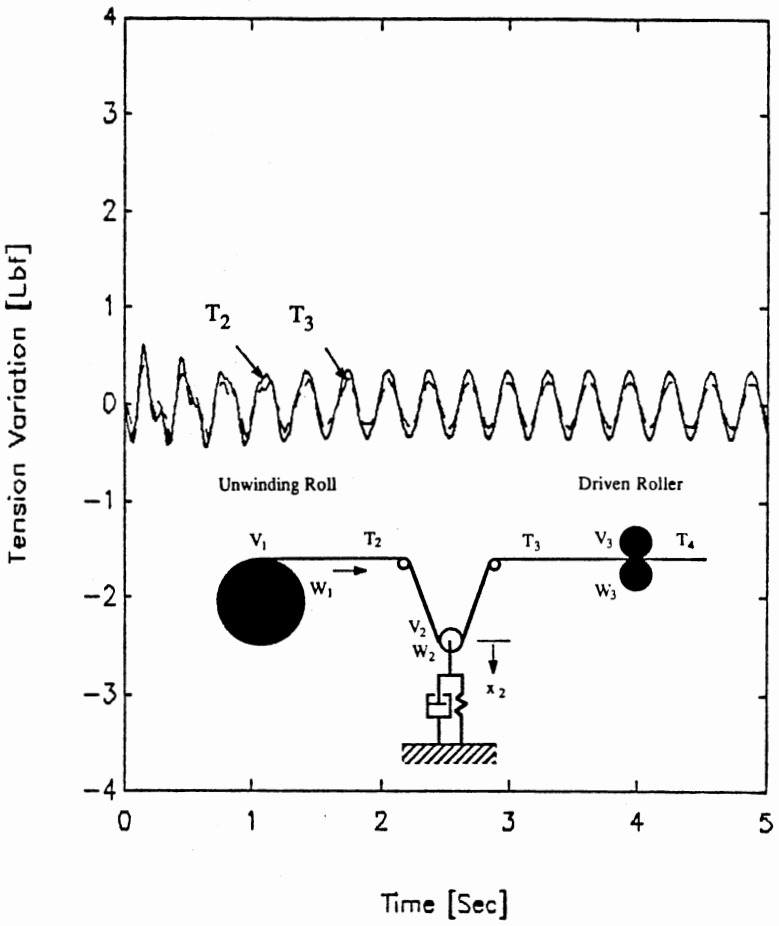

Figure 33. Performance of the Dancer as a Disturbance Minimizing System for $\omega_t = 2$ rad/sec and $\omega_r = 60$ rad/sec

Input $V_1(t) = V_{d0} \sin(\omega_d t)$, $V_{d0} = 0.01$ ft/sec, $\omega_d = 20$ rad/sec

Conditions $\zeta = 0.7$, $\omega_s = 6.5$ rad/sec, $\omega_t = 1$ rad/sec

$\omega_r = 100$ rad/sec.

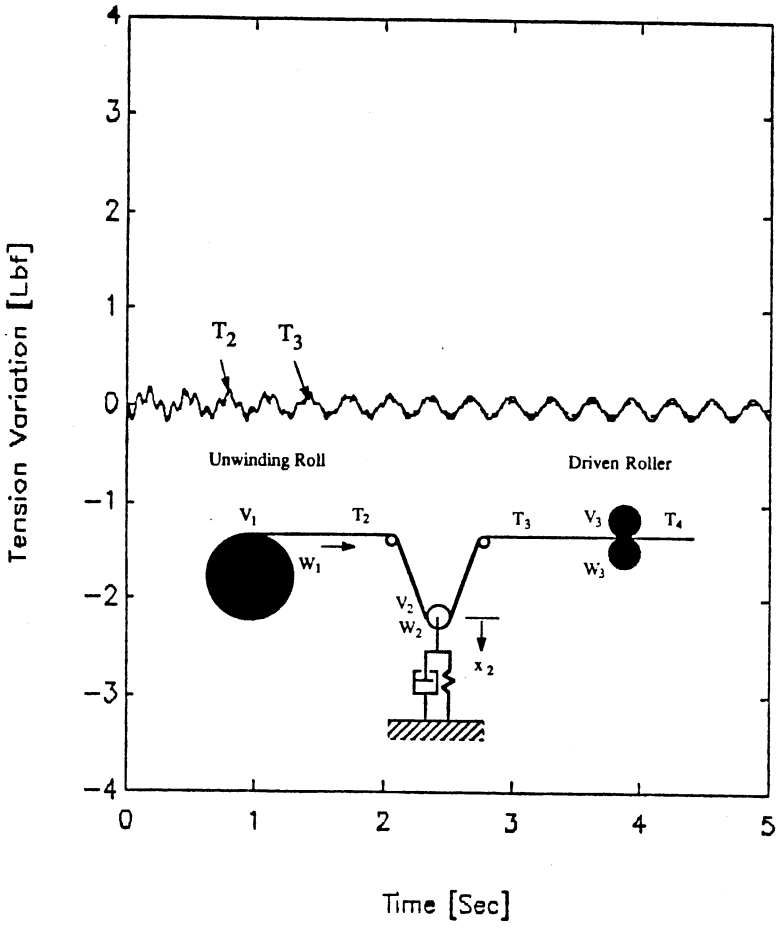

Figure 34. Performance of the Dancer as a Disturbance Minimizing System for $\omega_t = 1$ rad/sec and $\omega_r = 100$ rad/sec

CHAPTER IV

ANALYTICAL AND EXPERIMENTAL STUDY OF MULTI-SPAN SYSTEMS

This chapter presents results of (1) analyses of the interactions between adjacent web spans in two-span web transport systems and (2) experimental studies on an existing web processing plant.

Tension Transfer in a Multi-Span System

Consider the two-span system shown in Figure 35. By using the equation (22), the linearized mathematical models for web spans 2 and 3 can be written as:

$$\frac{dT_2}{dt} = -\frac{v_{20}}{L_2}T_2 + \frac{v_{10}}{L_2}T_1 + \frac{AE}{L_2}(V_2 - V_1). \qquad (129)$$

$$\frac{dT_3}{dt} = -\frac{v_{30}}{L_3}T_3 + \frac{v_{20}}{L_3}T_2 + \frac{AE}{L_3}(V_3 - V_2). \qquad (130)$$

In equation (129), the tension change T_2 is function of T_1, V_1, and V_2. That is, a change in the tension in the entering span (T_1) affects the tension in the

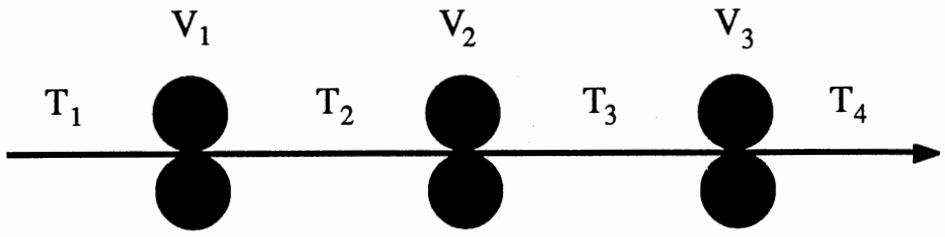

Figure 35. A Two-Span Web Transport System in Section 4.1

following span (T_2). This effect is called "tension transfer". All variables shown in Figure 35 are changes from the initial steady-state operating conditions. That is,

$$t_n = t_{n0} + T_n, \qquad v_n = v_{n0} + V_n$$

where

T_n : Change in web tension from a steady-state operating value

t_n : Web tension

t_{n0} : Steady-state operating value for web tension

V_n : Change in web velocity from a steady-state operating value

v_n : Web velocity

v_{n0} : Steady-state operating value for web velocity.

An example will illustrate the effect of tension transfer. Suppose that the two-span system in Figure 35 is operating in the steady state such that

$$v_{10} = v_{20} = v_{30},$$
$$V_1 = V_2 = V_3,$$
$$T_1 = T_2 = T_3.$$

Now suppose that t_1 is increased by an amount T_1. A solution of equation (129) for the final steady-state value of T_2 gives

$$T_2 = \frac{v_{10}}{v_{20}} T_1 = T_1.$$

That is, a change in t_1 results in an equal change in t_2. Similarly, a solution of equation (130) indicates that

$$T_3 = \frac{v_{20}}{v_{30}} T_2 = T_2.$$

Open-Loop Draw Control in Multi-Span Systems

In many web handling plants, an attempt is made to control web tension in a span by controlling the difference between the velocities of rollers at the ends of the span. This open-loop tension control approach is termed "draw control". Based on the results of the previous section, open-loop draw control cannot result in an accurate tension control in a span if

tension disturbances occur upstream of that span. That is, a tension disturbance will propagate "downstream" due to tension transfer. An example will illustrate this limitation of open-loop draw control.

Suppose that the two-span system in Figure 35 is operating in the steady state such that

$$v_{10} = v_{20} = v_{30},$$
$$V_1 = V_2 = V_3,$$
$$T_1 = T_2 = T_3.$$

Now suppose that v_2 is increased by an amount V_2 while $V_1 = V_3 = 0$. Equation (129) can be solved to determine the change in t_2 from the initial value of t_{20} The result is

$$T_2 = \frac{AE}{v_{20}} V_2.$$

That is, if v_2 is increased by V_2, t_2 is increased by T_2. Accurate control of t_2 depends on accurate control of v_2.

It might be expected in the example above that an increase in v_2 also would result in a decrease in t_3. That is, a steady-state analysis using equation (130) with $T_2 = 0$ and $V_3 = 0$ gives the result

$$T_3 = - \frac{AE}{v_{30}} V_2.$$

But, $T_2 \neq 0$. A simultaneous solution of equations (129) and (130) for

steady-state operation, with $V_1 = V_3 = 0$, and $T_1 = 0$, gives the result

$$T_3 = \frac{v_{20}}{v_{30}} T_2 - \frac{AE}{v_{30}} V_2.$$

But, since $T_2 = \frac{AE}{v_{20}} V_2$, $T_3 = 0$. That is, the expected decrease in T_3 is offset by an increase due to T_2.

In conclusion, even if the velocities of the rollers are controlled accurately, simple open-loop draw control cannot provide accurate control of the tensions in the various spans of a multi-span system if there are tension disturbances.

Master Speed Control in Multi-Span Systems

"Master speed control" is commonly used in multi-span web transport systems. In "master speed control", the velocity of a selected driven roller is set at a predefined constant value ("master speed"). Generally, a feedback control system is employed to produce accurate control of the velocity of the selected driven roller. In this case, the velocity of the output shaft of the motor driving the selected roller is measured and compared continuously with a reference or "set point". Other driving motors may be "slaved" to the "master". The velocities of the remaining driven rollers in the multi-span system may be varied in order to create the necessary velocity differences with respect to the "master speed" and to produce the desired tension levels in the various web spans. This approach is a form of open-loop draw control. As explained in

the previous section, tension control can only be achieved in the absence of tension disturbances and with accurate control of the velocities of the driven rollers.

In master speed control, selection of the driven roller for master speed is very important since the tension is transferred from an upstream span into downstream spans. Two numerical examples are presented below to illustrate the importance of the location of the driven roller selected for "master speed".

Example 1.

Consider the two-span system shown in Figure 36. The location of the roller for "master speed" (V_3) is downstream relative to the locations of the rollers for variable speeds (V_1 and V_2). Equations (129) and (130) can be used for the linearized mathematical models for web spans 2 and 3. It is assumed that $V_3 = 0$ for master speed.

Suppose that it is desired to maintain t_3 at a certain tension level lower than the initial operating tension (t_{30}) by using V_2. A simultaneous solution of equations (129) and (130) for steady-state operation with $V_1 = V_3 = 0$, and $T_1 = 0$ in the previous section can be used. That is, the expected decrease in T_3 was offset by an increase due to T_2.

In conclusion, when the location of the driven roller for "master speed" (V_3) is downstream relative to the driven roller for variable speed (V_2) as shown in Figure 36, the "master speed control" does not provide proper control even with accurate control of the velocities of the driven rollers.

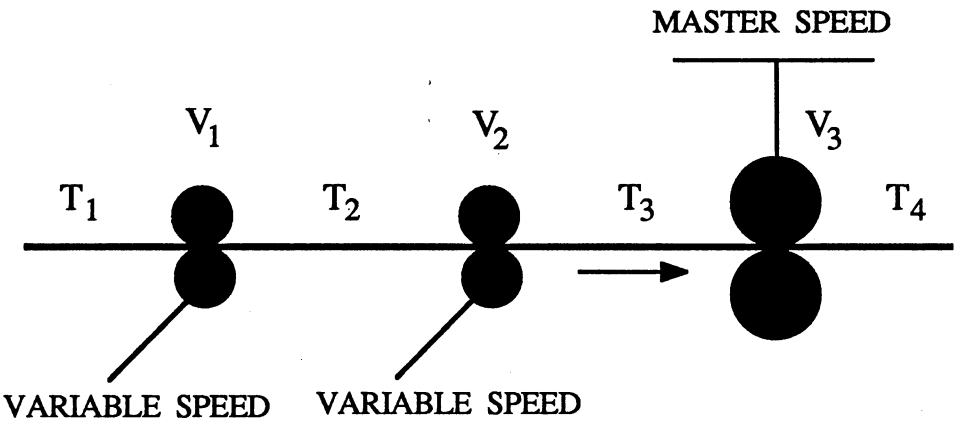

Figure 36. Master Speed Control: Example 1

Example 2.

Consider the two-span system as shown in Figures 37. The location of the roller for "master speed" (V_2) is upstream relative to the location of the roller for variable speed (V_3). Equations (129) and (130) can be used for the linearized mathematical models for web spans 2 and 3 again. It is assumed that $V_2 = 0$ for master speed.

Suppose the two-span in Figure 37 is operating in the steady state such that

$$v_{10} = v_{20} = v_{30},$$
$$V_1 = V_2 = V_3 = 0,$$
$$T_1 = T_2 = T_3 = 0.$$

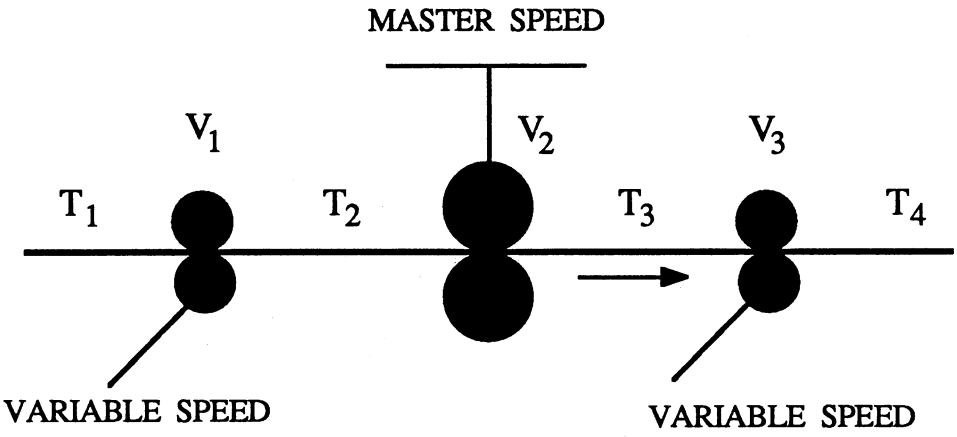

Figure 37. Master Speed Control: Example 2

Now suppose that v_3 is increased by an amount V_3 while $V_1 = V_2 = 0$. Equation (130) can be solved to determine the change in t_3 from the initial value of t_{30}. The result is

$$T_3 = \frac{AE}{v_{30}} V_3.$$

That is, if v_3 is increased by V_3, t_3 is increased by T_3.

In conclusion, when the location of the roller for "master speed" (V_2) is upstream relative to the roller for variable speed (V_3), the "master speed control" does provide proper control with accurate control of the velocities of the driven rollers.

In summary, the location of the driven roller for "master speed" should be upstream in a web span and the location of roller for variable speed should be downstream in the web span for the proper control of tension.

Analytical and Experimental Studies

Description of the System

Analytical and experimental studies were conducted on a Polypropylene processing line in the Mobil Chemical plant at Shawnee, Oklahoma. Figure 38 is a schematic of the relevant portion of the line. The web is spread in the machine direction (MD) and in the cross machine direction (CMD) before it reaches the entering section.

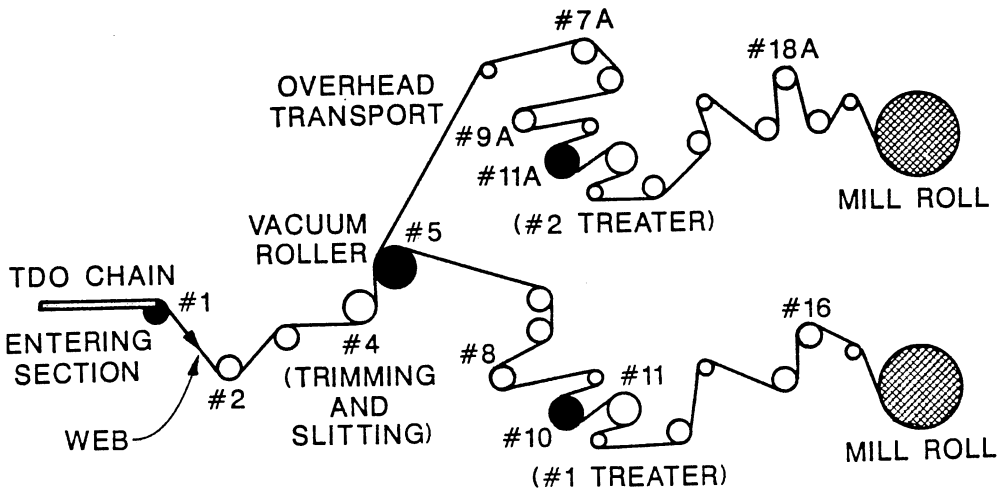

#2, #8, #9A, #16 and #18A are rollers equipped for tension measurement (load cell)

Figure 38. Polypropylene Processing Line

The "TDO" chain feeds the web to the trimming and slitting section. The web speed can be determined by measuring the TDO chain speed at the location of roller 1. The edges are trimmed off and the web is slit in half at roller 4. Roller 5 is a vacuum roller. Rollers 10 and 11A are treater rollers. The web is electrically treated to improve its surface characteristics and then wound into mill rolls.

An Avtron model PDC-5 digital control system is used to control tensions in the processing sections upstream from the mill rolls. Rollers 1, 5, 10 and 11A are driven in order to control web tension. Other rollers are idle rollers. The web tensions are measured at rollers 2, 8, 9A, 16, and 18A. The PDC-5 control system has both open-loop tension control (draw control) and closed-loop tension control modes. The open-loop tension control mode was used for the analytical and experimental studies.

The system shown in the Figure 38 was divided into two processing sections based on the locations of the driven rollers 1, 5, and 10 to facilitate the analytical and experimental studies. Processing section 1 is the web between rollers 1 and 5, processing section 2 is the web between rollers 5 and 10. A block diagram of the open-loop tension control system is shown in Figure 39. Load cells are used for monitoring tensions in the open-loop tension control mode. A distributed control strategy is used and is termed "progressive set-point coordination". For example, Set Point 1 is the sum of Set Point 0 and Local Input 0. That is, a change in Set Point 0 is progressively fed through the system. Likewise, a change in Local Input 0 is progressively fed through the system. This strategy is used (1) to provide smooth startup and shutdown of the line and (2) to reduce the effects of disturbances (slack or tighten web) from upstream processing sections.

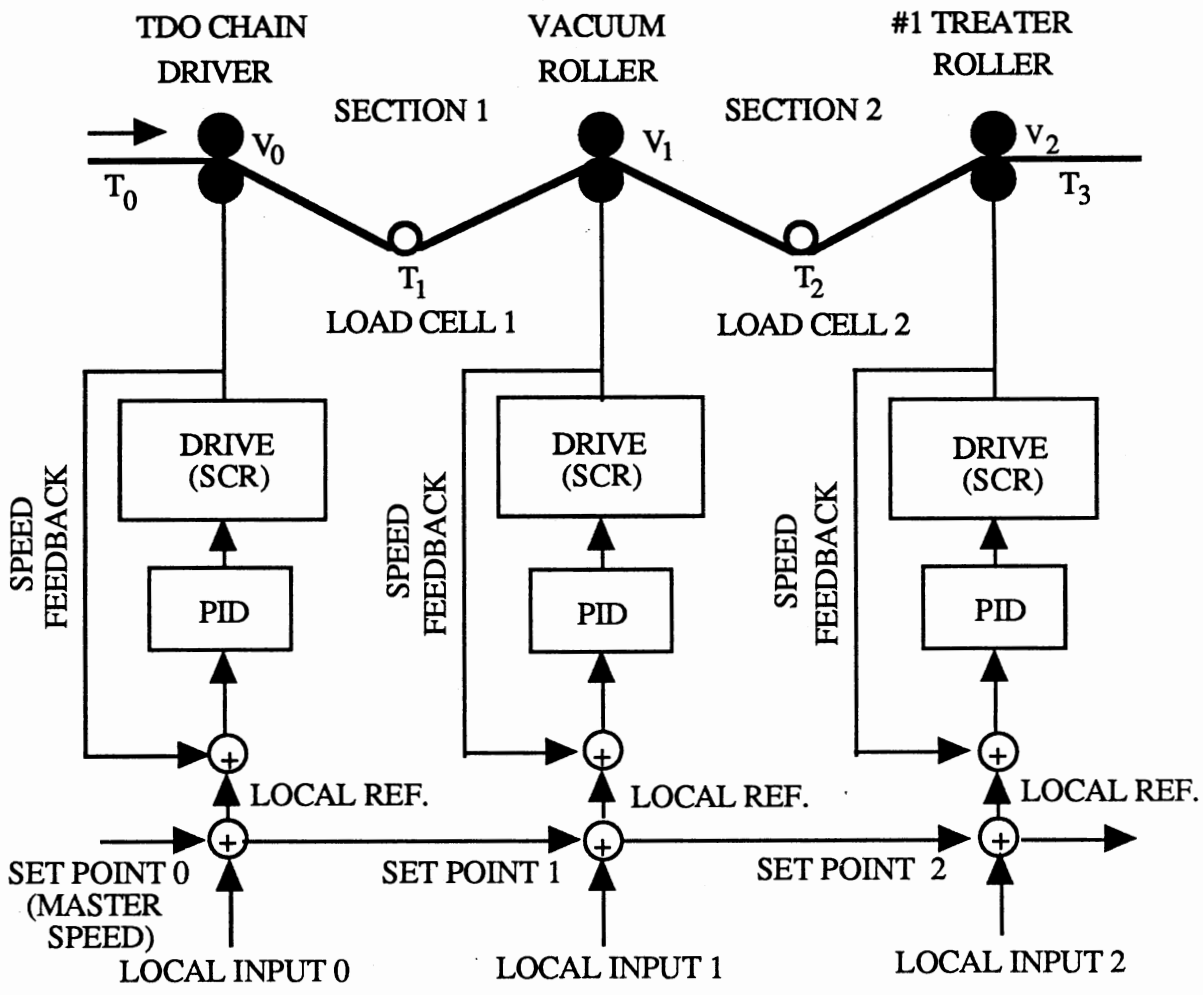

Figure 39. Block Diagram of Progressive Set-Point Coordination Scheme in Open-Loop Speed Control Mode

All variables shown in Figure 39 are changes from the initial steady-state operating conditions. That is,

$$t_n = t_{n0} + T_n, \qquad v_n = v_{n0} + V_n$$

where

T_n : Change in web tension from a steady-state operating value

t_n : Web tension

t_{n0} : Steady-state operating value for web tension

V_n : Change in web velocity from a steady-state operating value

v_n : Web velocity

v_{n0} : Steady-state operating value for web velocity

n : 1, 2, 3.

A velocity change in a particular driven roller (e.g., the vacuum roller) changes not only the tension in the upstream span but also the tension in the downstream span with respect to that roller. The progressive set point coordination feature results in a compensation for the tension change in the downstream span. For example, an increase in Local Input 1 results in an increase in the velocity of the vacuum roller, and therefore an increase in the tension in the span immediately upstream of the vacuum roller and a decrease in the tension in the span immediately downstream of the vacuum roller (and all successive spans). But, in this case, the control strategy results in an increase in Set Point 2 and therefore no steady-state change in the tension in the spans downstream of the vacuum roller.

The PDC-5 digital control system installed in the Polypropylene

process line also has a built-in function to provide a smooth ramp input at the Master Speed Input or at the Local Inputs; this gradually increasing input minimizes the potential for web breakage during line startup or following changes in any input(s). The approximate shape of the input used in the control system is shown in Figure 40.

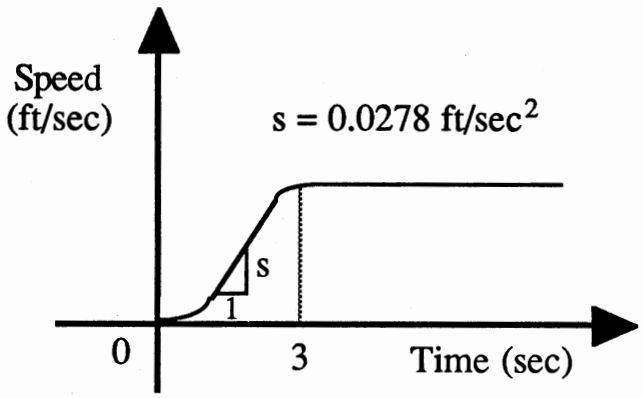

Figure 40. An Input Used in Control System

Analytical Study

Two cases of analytical studies were conducted using the Polypropylene processing line described above.

Case 1 : Analytical study on tension transfer.

Case 2 : Analytical study on slippage between the web and the vacuum roller.

First of all, some assumptions were made for the mathematical modeling of the system. Since the "TDO" chain feeds the web in the entering span and

the velocity of "TDO" chain is locked with roller 1, it was assumed that there was no slippage between the web and roller 1. The roller 5 is a vacuum roller to prevent slippage between the web and the roller. But, in the experiment, it was found out that there was slippage between the web and the vacuum roller. Even though a mathematical model for a system with slippage was developed in section 2.2, it was with the assumption that the model for the traction between the web and the roller was known. But, the model for the traction between the web and the roller in the Polypropylene processing line is not known. Thus, the analytical study will be carried out without considering slippage between the web and the vacuum roller for case 1 and with slippage for case 2 (using % slip, see equation (32) for % slip). The angle of wrap in the #1 treater roller was more than 270 degrees. It was assumed that there was no slippage between the web and roller 10 in the Figure 38. It was also assumed that load cells did not disturb the system. Since the length of the web span from the slitter roller to the vacuum roller is short (10 % of the length of web span in processing section 1), it was assumed that the strain in processing section 1 was uniform along the machine direction. The velocity of each driven roller in the Figure 38 is assumed to be controlled by PDC-5 speed control system. Thus, the dynamics of rollers was neglected. The effect of viscoelastic properties of web on tension variation is neglected based on the analysis in Chapter II. An average temperature within a processing section was used to select an appropriate Young's modulus for the web material (Polypropylene). With assumptions made above, the system shown in Figure 39 can be simplified further into a two-span system as shown in Figure 41.

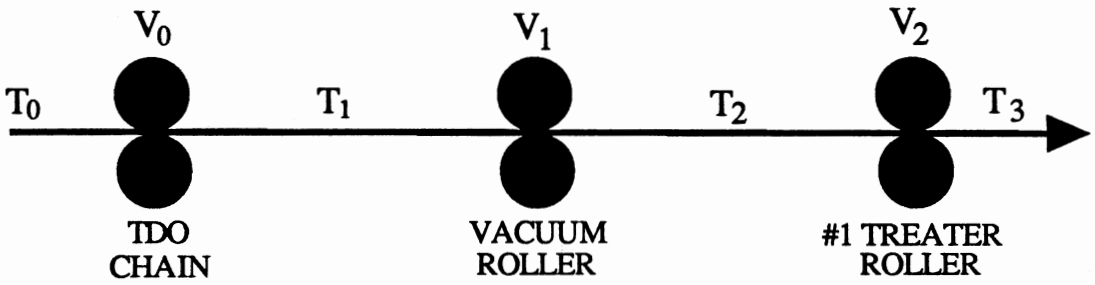

Figure 41. Two-Span System (Processing Sections 1 and 2 from Figure 39)

Case 1 : Analytical study on tension transfer. A linearized mathematical model for the system shown in Figure 41 can be written as follows:

Processing section 1:

$$\frac{d}{dt}[\epsilon_1(t)] = -\frac{v_{10}}{L_1}\epsilon_1(t) + \frac{v_{00}}{L_1}\epsilon_0(t) - \frac{V_0(t)}{L_1} + \frac{V_1(t)}{L_1}. \qquad (131)$$

$$T_1 = A_1 E_1 \epsilon_1, \qquad (132)$$

where A_1 : Cross-sectional area of web excluding edges to be trimmed[1].

Processing section 2:

$$\frac{d}{dt}[\epsilon_2(t)] = -\frac{v_{20}}{L_2}\epsilon_2(t) + \frac{v_{10}}{L_2}\epsilon_1(t) - \frac{V_1(t)}{L_2} + \frac{V_2(t)}{L_2}. \qquad (133)$$

1. See Appendix E for the analysis of non-uniform thickness web across its width

$$T_2 = A_2 E_2 \in_2. \qquad (134)$$

Because of the progressive set-point coordination scheme used in the control system, it was impossible to provide only one input in the two-span system for testing since an input in an upstream section is automatically fed to the following section. An example will be solved to provide an understanding of the system with complicated inputs and interactions between web spans.

Consider the two-span system shown in Figure 42-a. Assume that the progressive set-point coordination scheme is not installed. It was assumed that $T_1(0^-) = T_2(0^-) = T_3(0^-) = 0$. With the velocity inputs for each roller given in Figure 42-b, T_1 and T_2 might be expected to change as shown in Figure 42 - c and d. But, because of tension transfer from T_1, the actual change in tension T_2 will be as shown in Figure 42-e.

In the actual control system with progressive set-point coordination scheme, an input is automatically provided to the #1 treater roller when an input is provided to the vacuum roller (see Figure 43). It was also assumed that $T_1(0^-) = T_2(0^-) = T_3(0^-) = 0$. A computer simulation of the mathematical model (equations (131) through (134)) was carried out with the inputs (see Figure 44) to the vacuum roller and the #1 treater roller. It was assumed that there was no slippage between the web and the vacuum roller. System data used in simulation are given in Table 5. Output tensions from the simulations are shown in Figure 45.

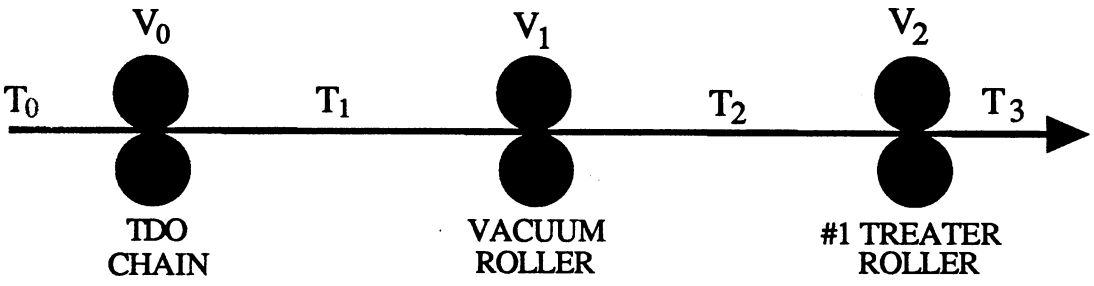

(a) Two-Span System Without Set-Point Coordination Scheme

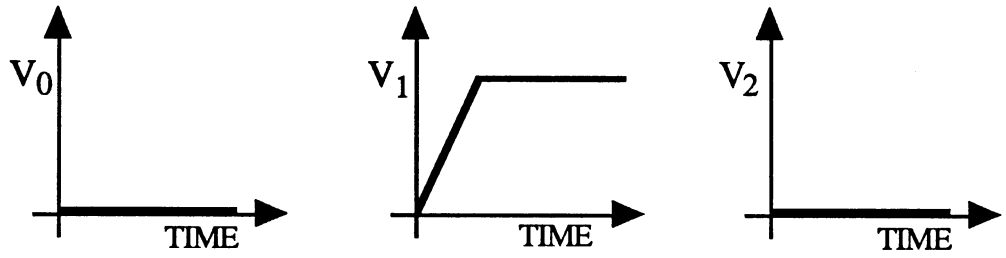

(b) Velocity Inputs to System

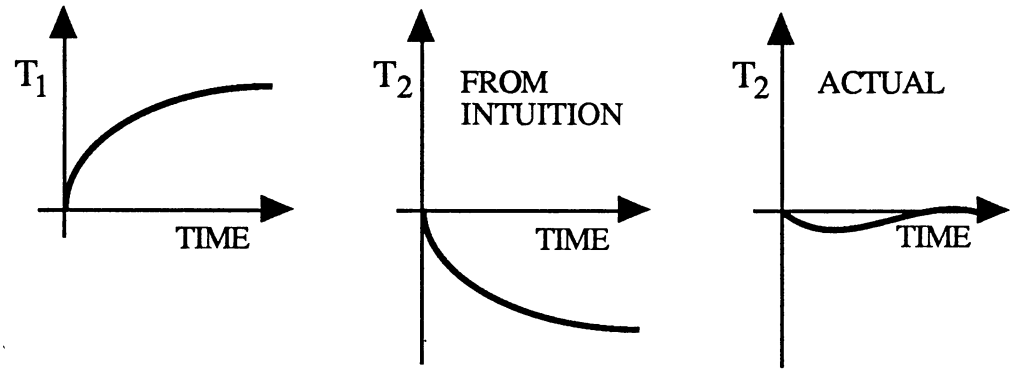

(c) (d) (e)

Outputs from System

Figure 42. Two-Span System :
without Set-Point Coordination Scheme

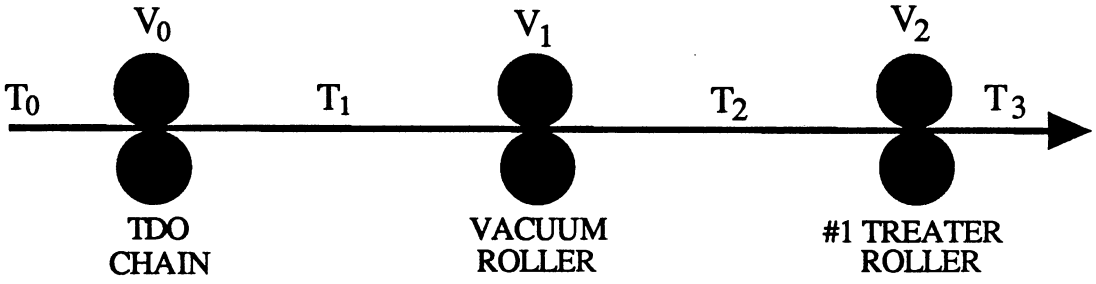

(a) Two-Span System with Set-Point Coordination Scheme

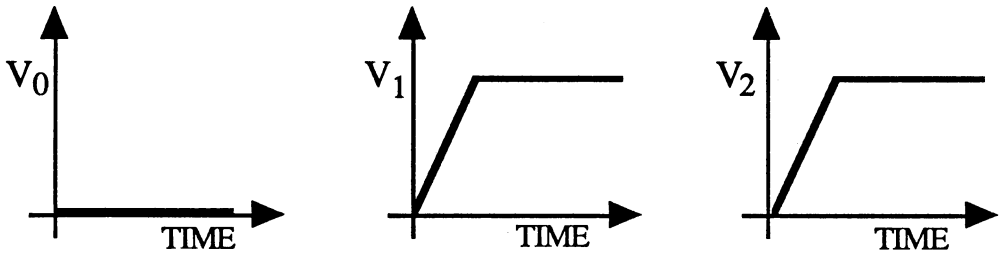

(b) Velocity Inputs to System

Figure 43. Two-Span System:
with Set-Point Coordination Scheme

TABLE 5

SYSTEM DATA USED FOR SIMULATION AND EXPERIMENT

Length of Span (inch)	Section 1 (L1)		190.8
	Section 2 (L2)		290.4
	Section 3 (L3)		224.4
Width of Web (inch)	Section 1	Edge	5.5
		Middle Part	263
	Section 2,3		126
Thickness of Web (inch)	Section 1	Edge	0.00625
		Middle Part	0.00125
	Section 2,3		0.00125
Initial Operating Speed (ft/min)	TDO Chain (V00)		459.1
	Vacuum Roller (V10)		459.1
	#1 Treater Roller (V20)		454.0
Average Temperature (Centigrade)	Section 1		67.0
	Section 2		46.3
	Section 3		35.0
Young's Modulus of Polypropylene (psi)	Section 1		116,000
	Section 2		258,000
	Section 3		304,000

* Room Temperature : 31 (Centigrade)

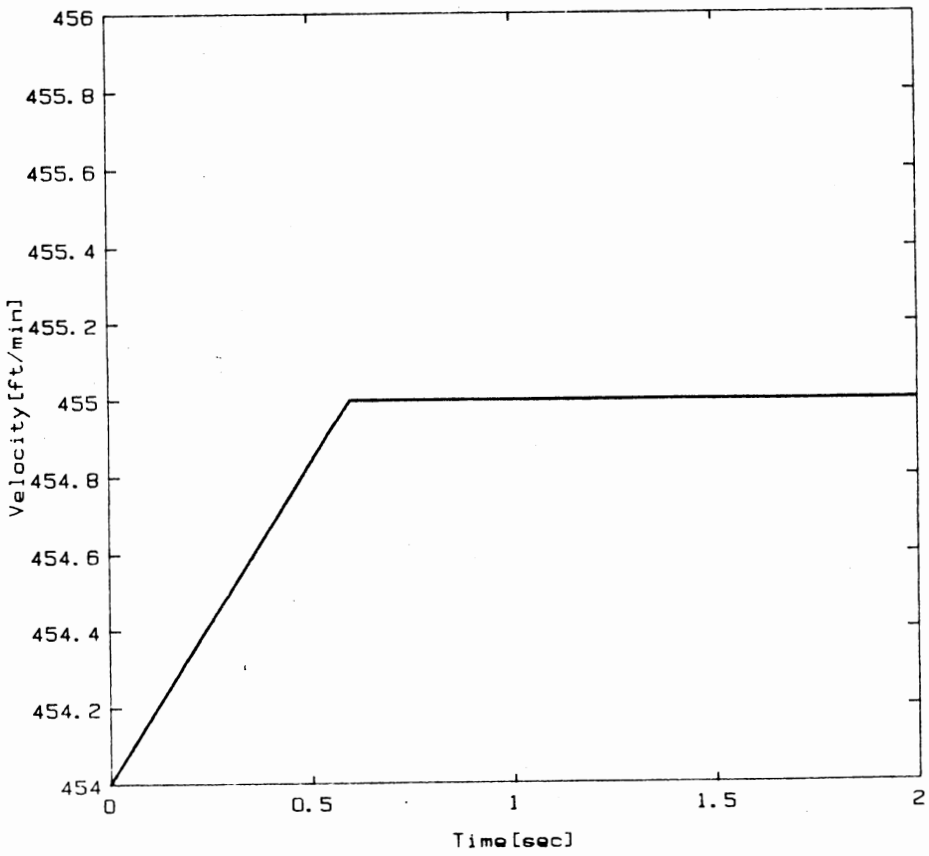

Figure 44. Velocity Input Used for Simulation and Experiment

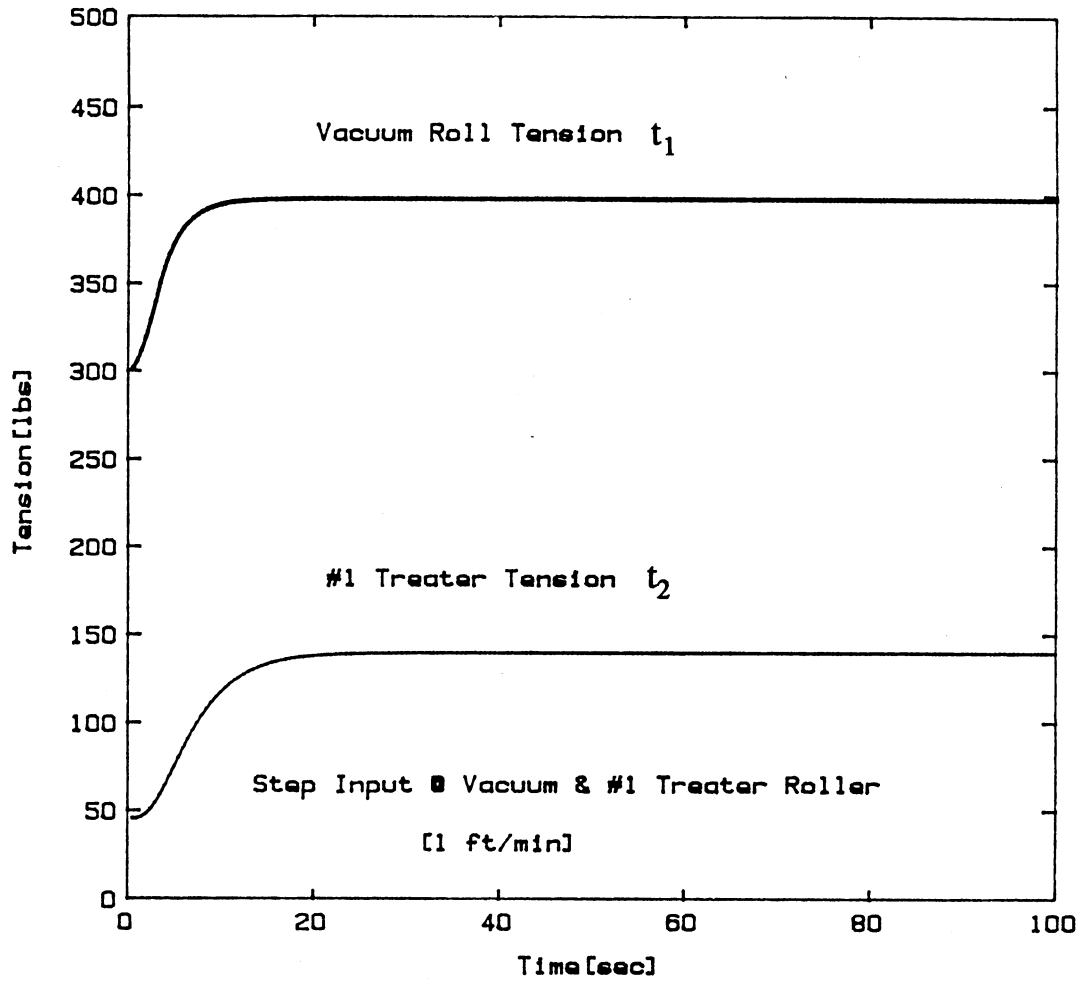

Figure 45. Output Tensions from Simulation: without Slippage between the Web and the Vacuum Roller

#1 treater tension t_2 might be expected to stay unchanged since the velocity inputs were provided to both the vacuum roller and #1 treater roller according to the set point coordination scheme. But, t_2 was actually changed from its steady-state operating value due to the tension transfer from upstream.

Case 2 : Analytical study on slippage between the web and the vacuum roller. Consider the section 2 in Figure 39 as shown in Figure 46.

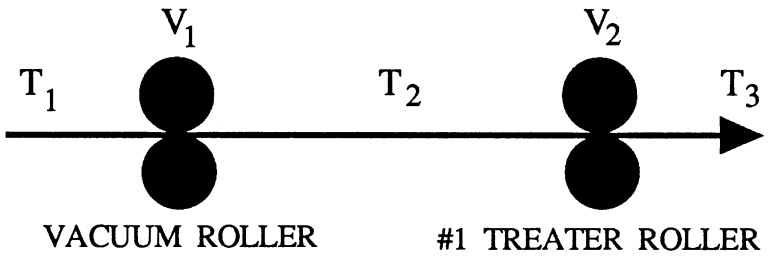

Figure 46. One-Span System

The mathematical model for the system shown in Figure 46 is:

$$\frac{d}{dt}[\epsilon_2(t)] = -\frac{v_{20}}{L_2}\epsilon_2(t) + \frac{v_{10}}{L_2}\epsilon_1(t) - \frac{V_1(t)}{L_2} + \frac{V_2(t)}{L_2}. \qquad (135)$$

$$T_2 = A_2 E_2 \epsilon_2. \qquad (136)$$

A computer simulation of the mathematical model (equations (135) and (136)) was carried out with the input (see Figure 44) to the #1 treater

roller to investigate the effect of slippage: (1) without slippage between the web and the vacuum roller, and (2) with slippage. The same data as that of case 1 was used for simulation. The simulation result without slippage between the web and the vacuum roller is shown in Figure 47. That is, it was assumed that tangential velocity of the vacuum roller is equal to the web velocity at 453 ft/min. When there was 0.16 % slip (see equation (32) for % slip, tangential velocity of the vacuum roller = 453 ft/min and the web velocity = 453.75 ft/min) between the web and the vacuum roller, output tension t_2 from the simulation is shown in Figure 48. The new steady-state value of t_2 with slippage was about 62 lbs lower than that without slippage between the web and the vacuum roller (see Figure 47). The effect of slippage between the web and the vacuum roller was significant.

Experimental Study

Two cases of experimental studies were conducted using the Polypropylene processing line.

Case 1 : Experimental study on tension transfer.

Case 2 : Experimental study on slippage between the web and the vacuum roller.

The MetraByte DAS-16 A/D board was used for data conversion with an IBM AT compatible computer. The LABTECK NOTEBOOK (a data acquisition software package for an IBM PC/XT/AT or compatible computers, developed by the Laboratories Technology Corp.) was used in

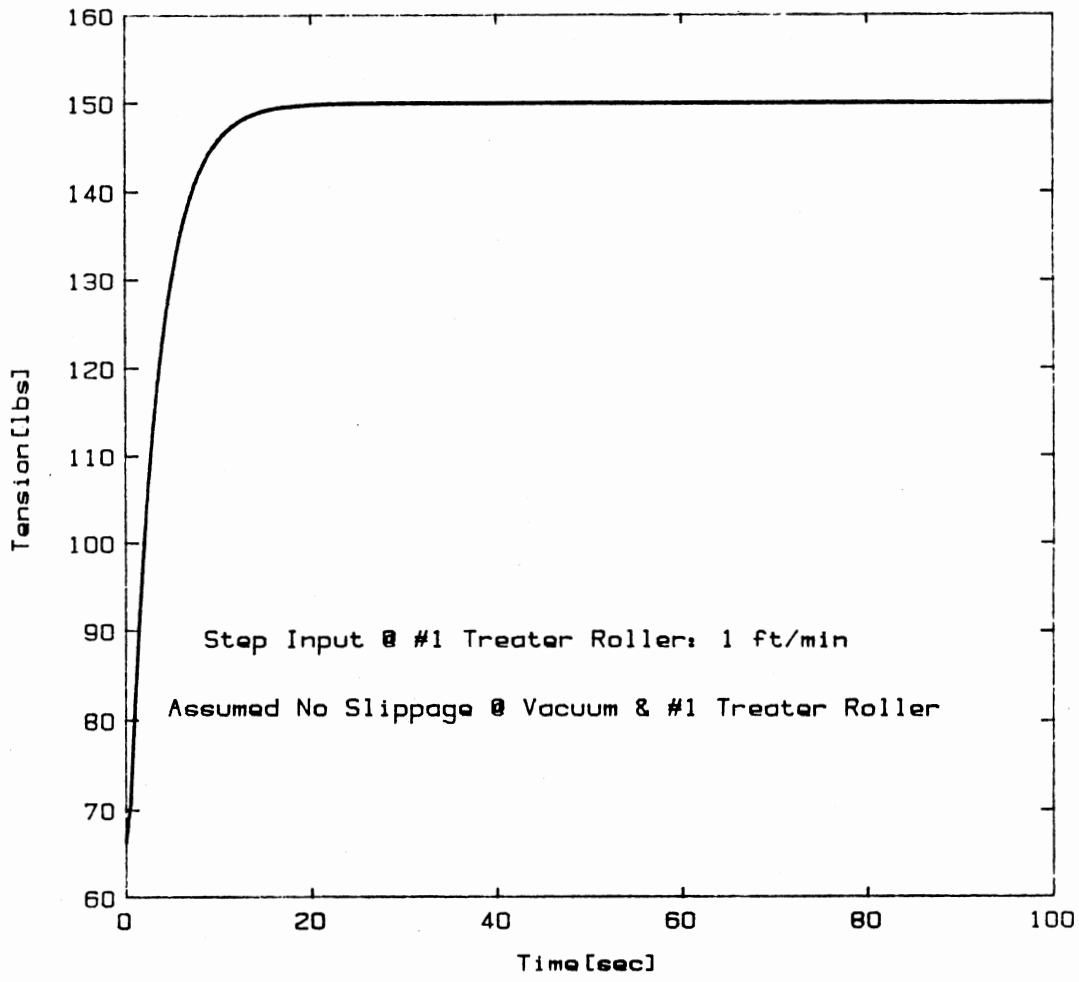

Figure 47. Tension t_2 from Simulation: without Slippage between the Web and the Vacuum Roller

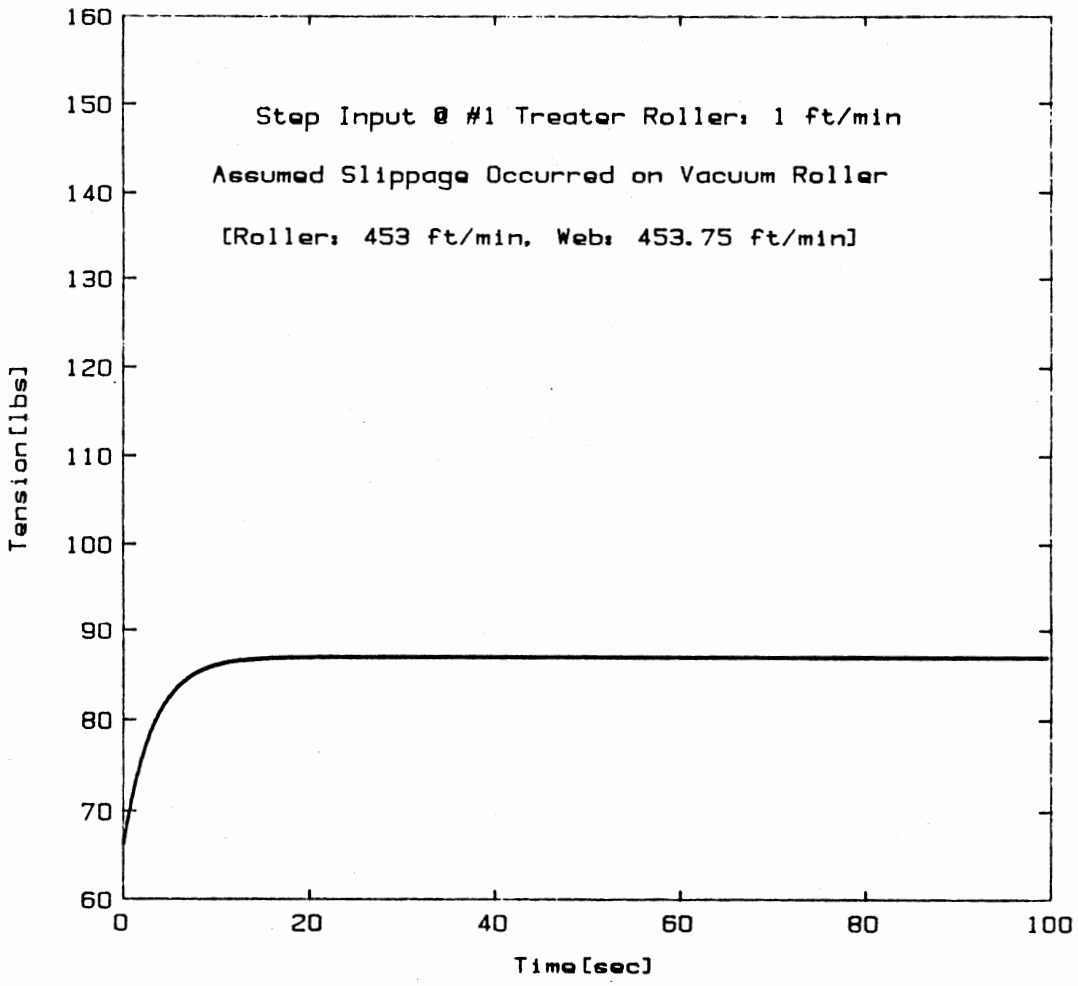

Figure 48. Tension t_2 from Simulation: with Slippage between the Web and the Vacuum Roller

conjunction with MetraByte DAS-16 for the data acquisition. The measured data was filtered using the Chebyshev Digital Filter built in the MatLab (interactive scientific and engineering computation package from the MATH WORKS Inc.).

Case 1 : Experimental study on tension transfer. An experimental study was carried out with an input shown in Figure 44 and the tensions were measured as shown in Figures 49.

The measured tensions are shown in Figures 50 and 51. As predicted from the simulation of the mathematical model, it was confirmed that the tension variation T_1 was transferred to affect the tension variation T_2. The actual tension variation was much lower than that predicted from simulation of mathematical model without slippage (see Figure 45). It was observed during the experiment that there was a difference between the web velocity and the tangential velocity of the vacuum roller, i.e., slippage between the web and the vacuum roller.

In conclusion, the mathematical model developed for the existing Polypropylene web processing line could predict tension transfer from upstream into downstream. The experimental study supported the prediction from mathematical model qualitatively.

Case 2 : Experimental study on slippage between the web and the vacuum roller. Another experiment was carried out to determine the effect of the slippage between the web and the vacuum roller on tension variation. The tension t_2 was measured from the Polypropylene processing system when the input (Figure 44) was provided to the #1 treater roller. The result is shown in Figure 52. The experimental result was fairly close to

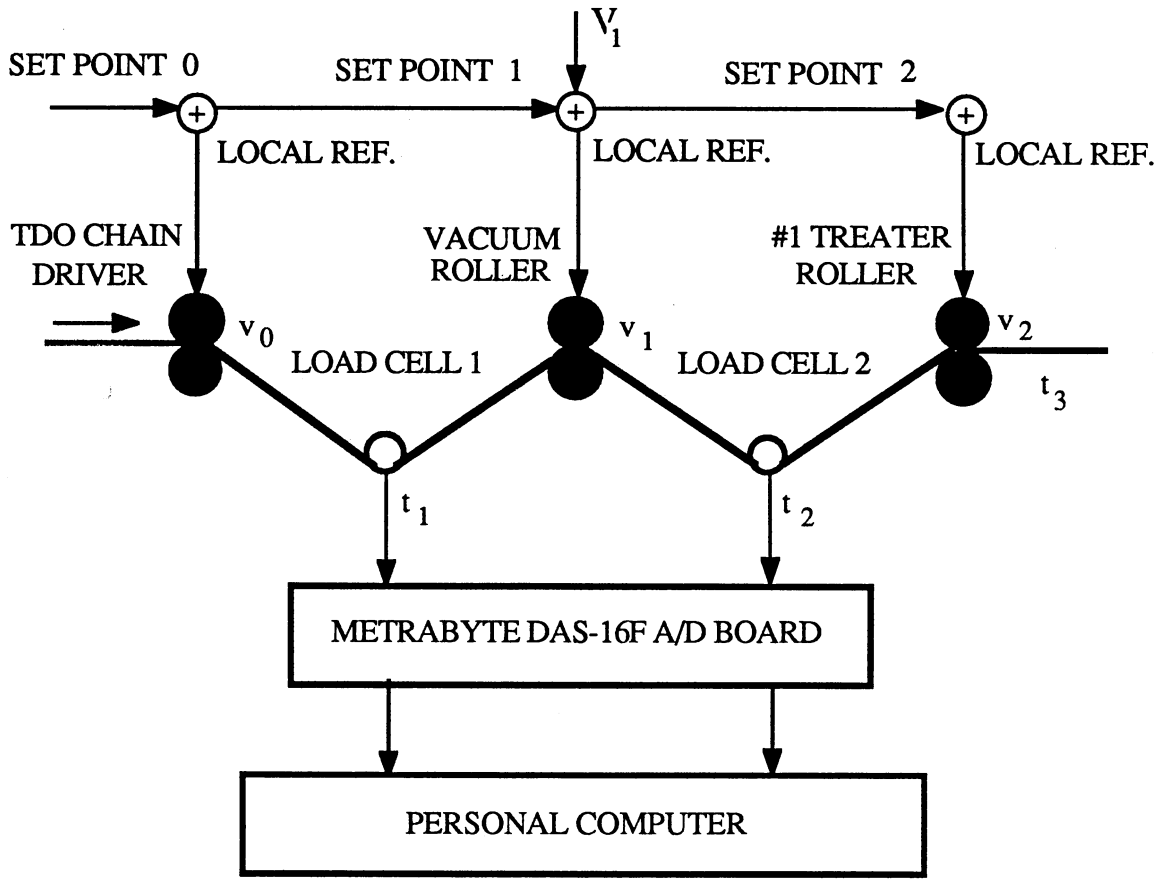

Figure 49. Experimental Set up for Tension Measurement

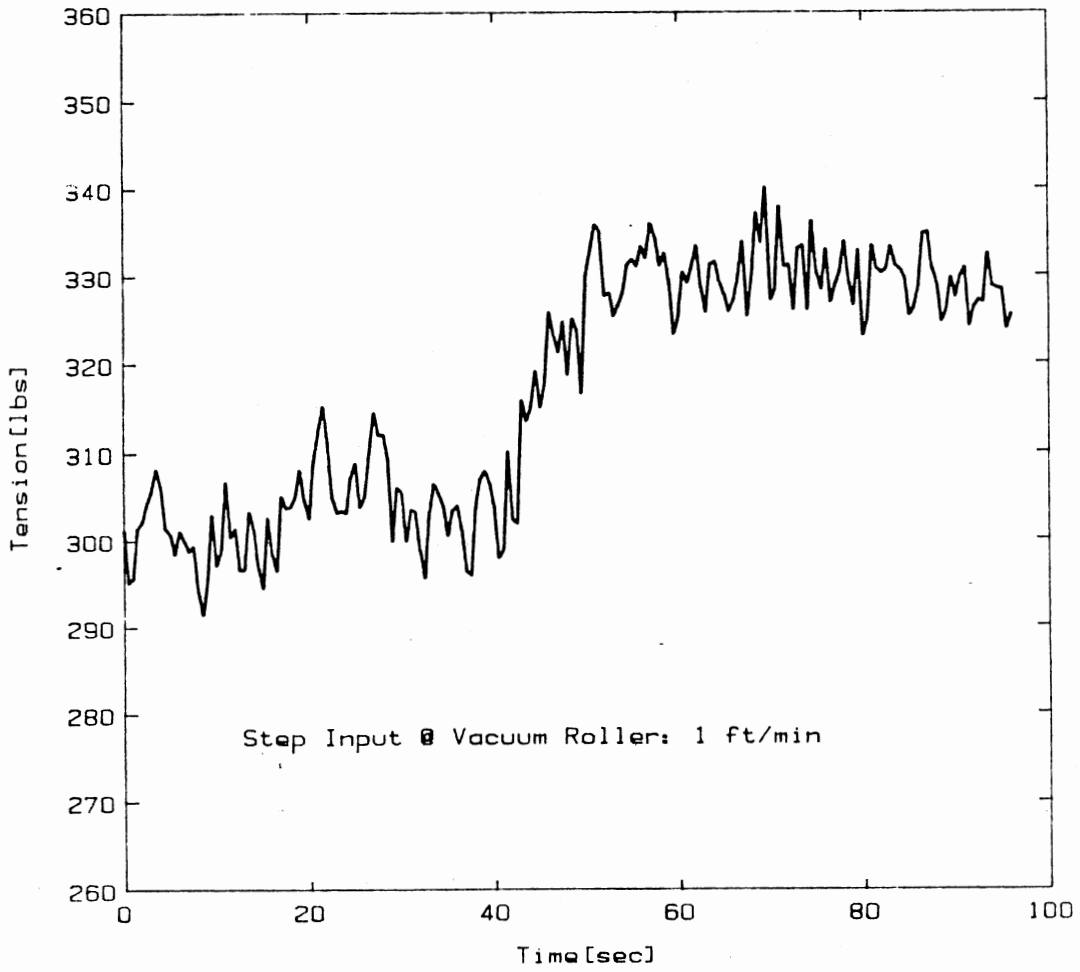

Figure 50. Output Tension t_1 from Experiment: Case 1

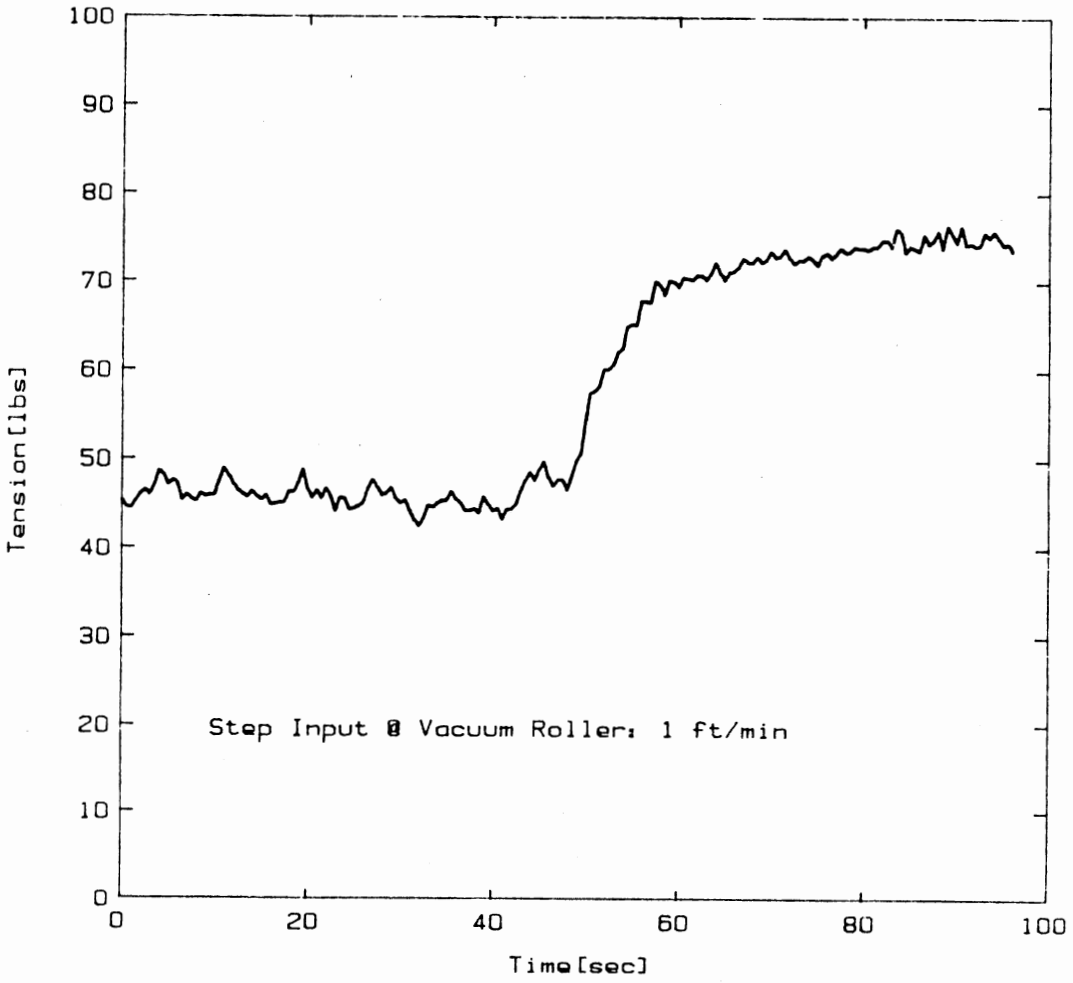

Figure 51. Output Tension t_2 from Experiment: Case 1

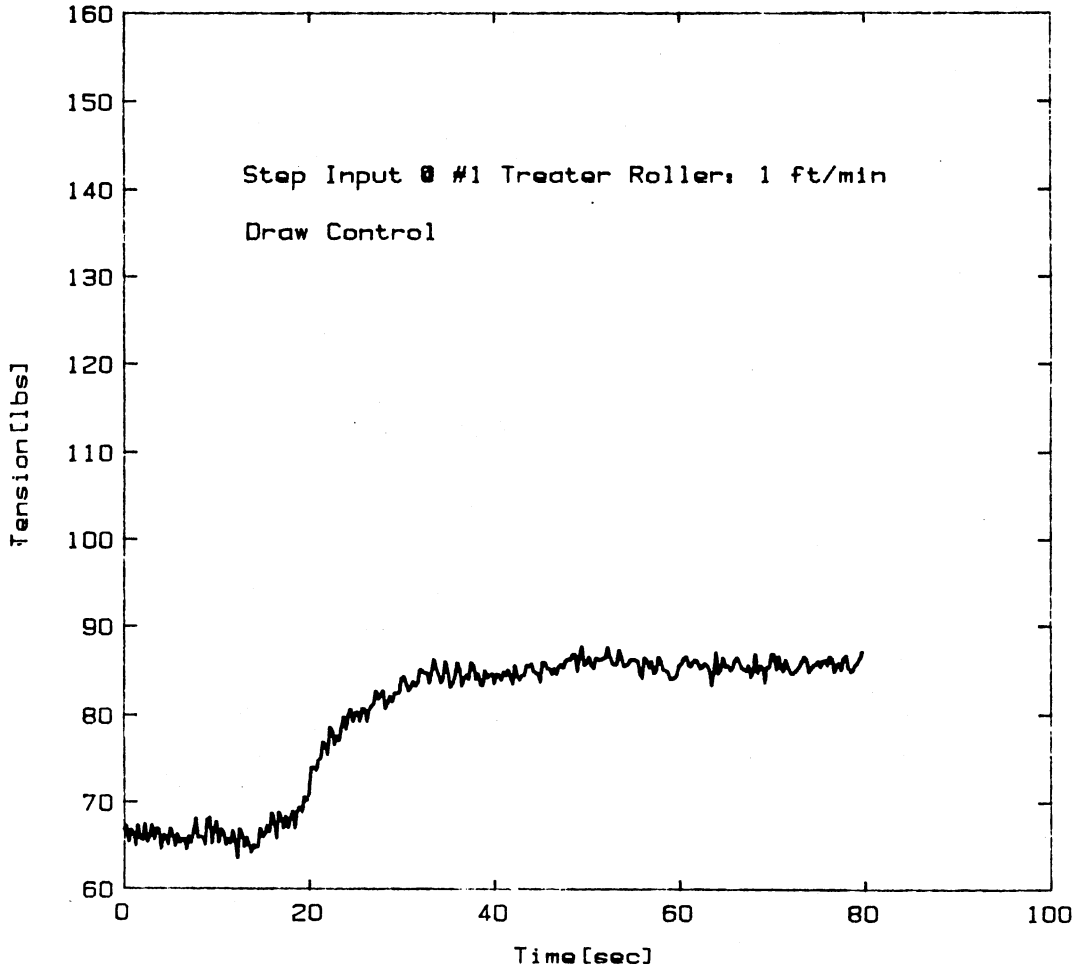

Figure 52. Output Tension t_2 from Experiment: Case 2

the simulation result when the slippage between the web and the vacuum roller was considered (see Figure 48).

In conclusion, the predicted tension from simulation was fairly close to the measured tension when the slippage between the web and the vacuum roller was taken into consideration in the simulation. Indeed, it was found that the effect of slippage between the web and the roller on tension variation is significant.

CHAPTER V

A COMPUTER-BASED ANALYSIS PROGRAM FOR WEB TRANSPORT SYSTEMS (WTS)

Objective of WTS

A computer-based analysis program for multi-span web transport systems (WTS) was developed by the author. The objective of WTS is to assist engineer and designer in the calculation of steady-state and dynamic longitudinal tension variations in multi-span web transport systems for different system configurations and operating conditions.

Essential Features of WTS

WTS is an interactive program which runs on IBM XT, AT, or 386 personal computers or other equivalent computers that run under the Disk Operating System (DOS) 2.0 or higher. WTS is a fully menu-driven program featuring a "Main Menu" (see Figure 53) and a "Sub Menu" (see Figure 54). Prior to using WTS, the user identifies the physical property data and operating conditions and sketches the system configuration using

the primitive elements shown in Figure 5.

To initiate use of WTS, the user selects the "Configure System" option from the "Main Menu". The user then inputs the system configuration through the "Sub Menu". That is, the user selects the primitive elements (subsystem) from the "Sub Menu" one by one starting at the upstream end of the previously synthesized system. The user inputs the physical property data through a separate data screen for each primitive element (subsystem). A typical data screen is shown in Figure 55. WTS automatically builds a mathematical model for the configured system using an algorithm to be discussed next section and the data provided by the user. The user then can select the "Confirm Configuration" option from the "Main Menu" for confirmation of the configured system. WTS automatically presents the configured system in a graphical form on the computer screen.

The "Steady-State Analysis" option must be selected from the "Main Menu" before the "Dynamic Analysis" option is selected. The results of steady-state analysis are used in the dynamic analysis. The user inputs operating conditions (e.g., tangential velocities of driven rollers, tension value for at least one web span) for the steady-state analysis. The user also inputs one or more voltage step inputs to the motors driving roller/rolls for the dynamic analysis. The steady-state and dynamic analysis for the configured system can be repeated as many times as the user wants.

A flow chart for WTS is shown in Figure 56. The essential features of WTS are as follows.

(1) Configure system: WTS assembles primitive elements selected by

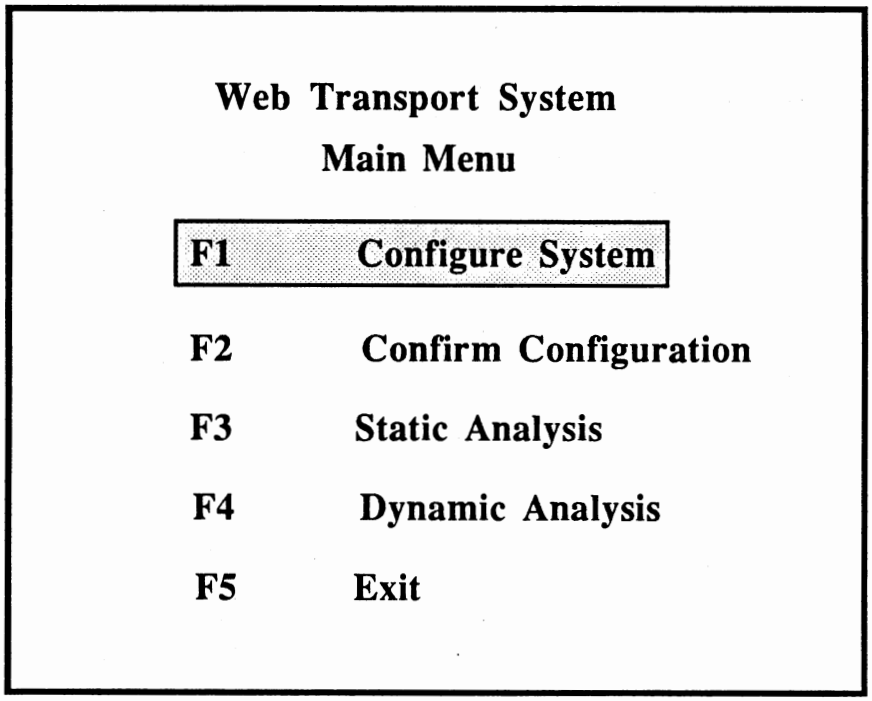

Figure 53. Main Menu of WTS

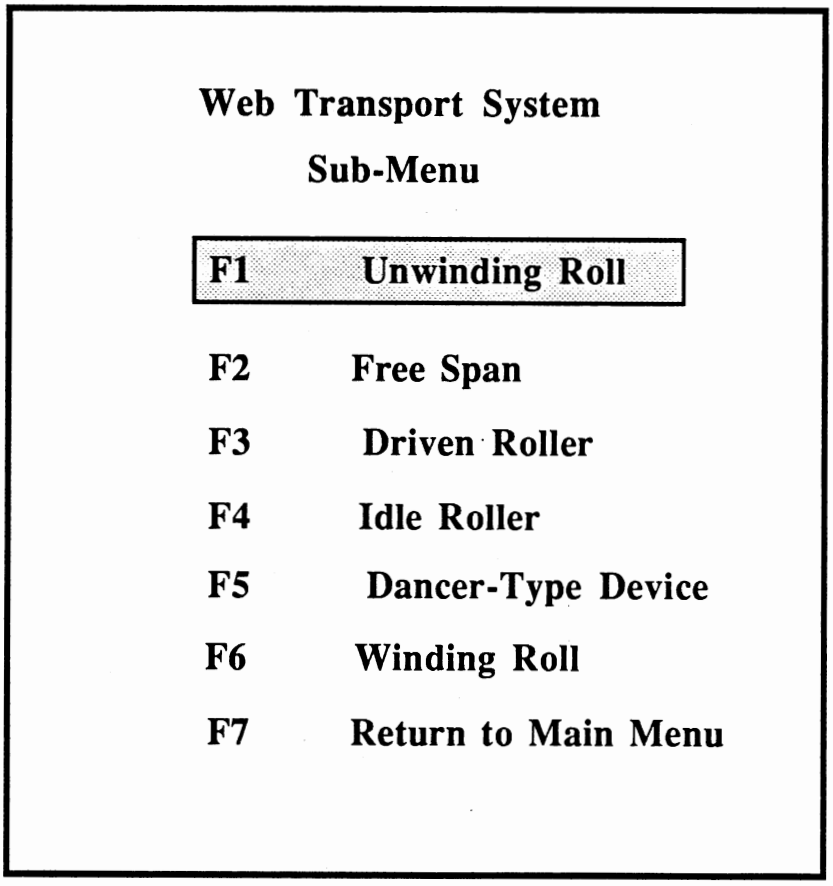

Figure 54. Sub Menu of WTS

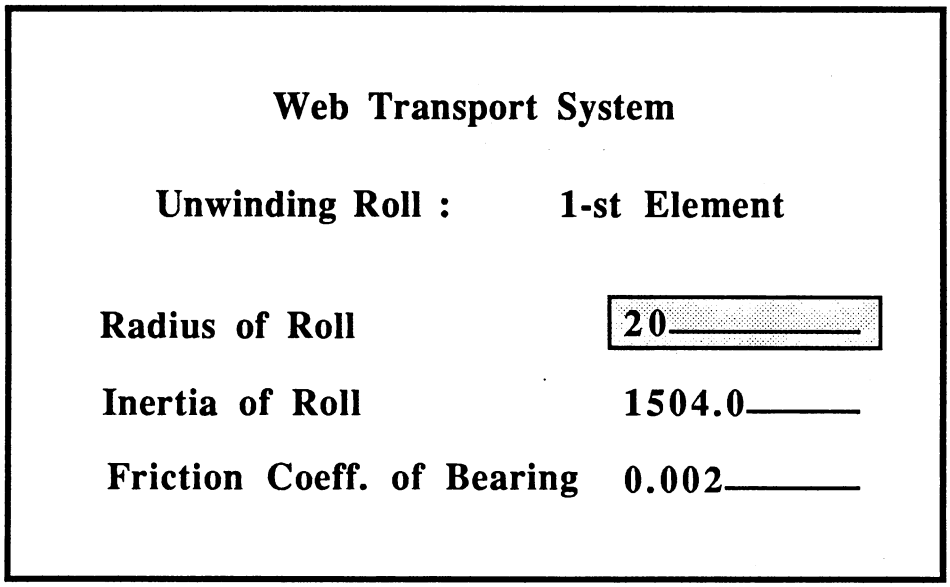

Figure 55. A Data Entry Screen for WTS: with Default Values

a user into a system and automatically generates a mathematical model of the assembled system using models for the primitive elements drawn from WTS library.

(2) Confirm configuration: the configured system is presented on the computer screen in a graphical form.

(3) Steady-state analysis: the configured system is analyzed to determine the steady-state web tensions for user-selected system parameters and operating conditions. The results are presented on the computer screen in a tabular form.

(4) Dynamic analysis: the mathematical model of the configured system is used to determine the dynamic response to a step change in one or more input variables. The results are presented on the computer screen in a graphical form.

The hardware requirements, instructions for use of WTS, and an example for each feature are given in the WTS User's Guide [79]. WTS Version 1.0 is available from Web Handling Research Center at Oklahoma State University. Later versions will be released once they have been fully evaluated.

Algorithm Used in WTS

The concept that a web transport system is composed of several primitive elements was vital for the development of WTS. This concept allowed WTS to have simple and effective procedures for the

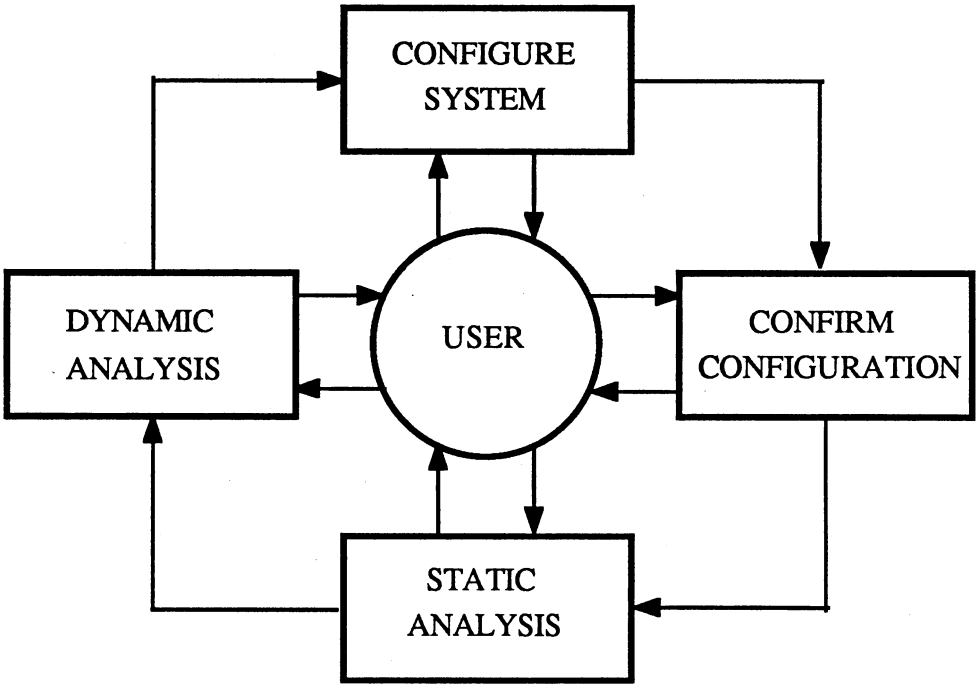

Figure 56. Flow Chart for WTS

configuration, graphical presentation, and mathematical modeling of a web transport system. If a group of primitive elements and subsystems is stored in the computer, a web transport system can be configured simply by combining these primitive elements and subsystems in the desired order.

In WTS, there are a "library" of subroutines for primitive elements and subsystems; there is one set of subroutines for each primitive element (or subsystem). When a primitive element (or subsystem) is selected for configuration, the corresponding set of subroutines will collect necessary physical property data about the primitive element (or subsystem). As the user configures the system, WTS keeps track of the number of the web spans, the number of the primitive elements, and the order that the primitive elements were selected. These data are used in the graphical representation and the automatic generation of the mathematical model of the configured system.

Each set of subroutines for a primitive element (or subsystem) also includes a subroutine for the graphic model of that element (or subsystem). Graphic models of primitive elements are drawn at designated positions on the screen to present the configured system. The position of the primitive element (or subsystem) depends on the order that the primitive elements (subsystems) were selected in the process of configuring a system.

Web transport systems were classified into four basic types of configurations to facilitate the automatic assembly of the system configuration and the automatic generation of the mathematical model of the assembled system. The first primitive element of the system is assumed to be either an unwinding roll or a driven roller and the last primitive

element is assumed to be either a driven roller or a winding roll. System types can be classified based on the first primitive element at the upstream end of the system and the last primitive element at the downstream end of the system. Four types of systems may occur as detailed in the Table 6 below and illustrated in Figure 57.

TABLE 6

FOUR TYPES OF SYSTEMS

Classification	First element	Last element
Type 1	unwind	wind
Type 2	unwind	driven
Type 3	driven	driven
Type 4	driven	wind

The total number of primitive elements relates to the the number of free web spans in the system as follows:

$$\text{Number of Primitive Elements} = 2\,N_s + 1, \qquad (137)$$

where N_s is the number of spans.

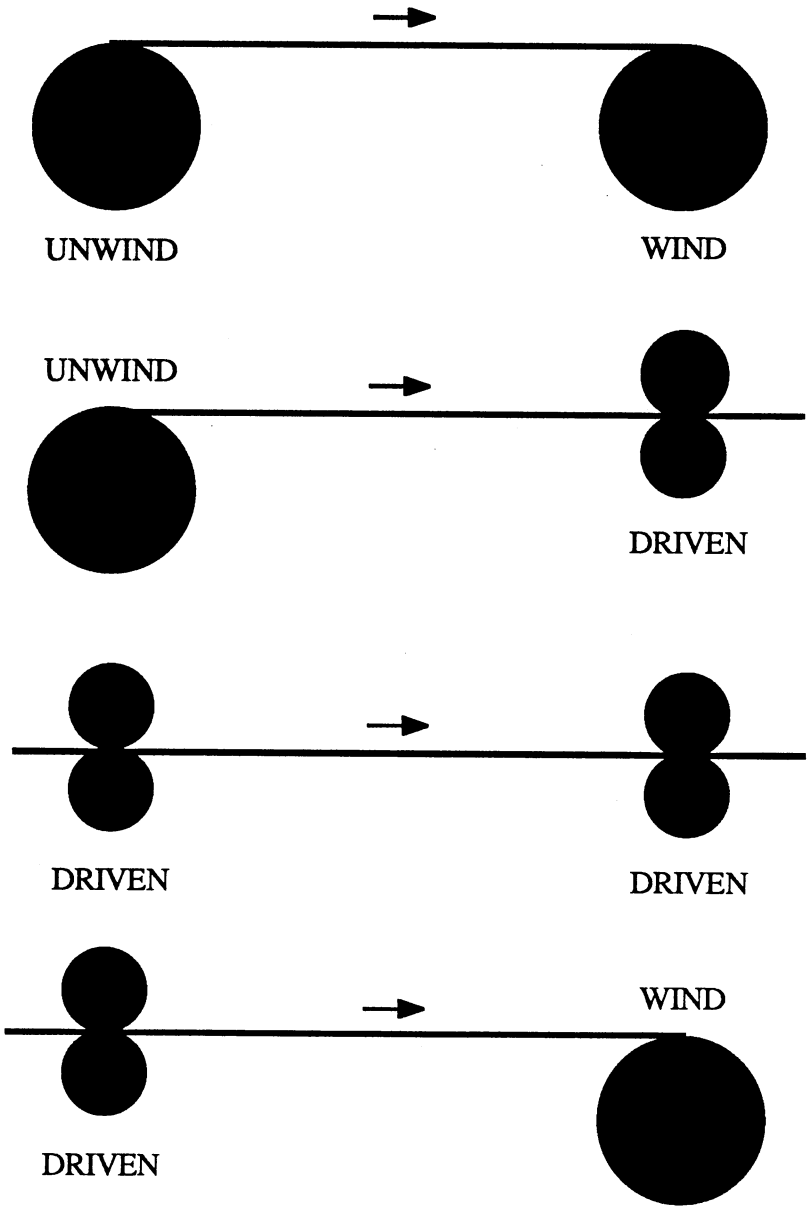

Figure 57. Four Basic Types of Web Transport Systems Used in WTS

Automatic Assembly of Primitive Element into a System and Automatic Generation of the System Mathematical Model

An algorithm for the automatic assembly of primitive elements into a system and automatic generation of mathematical models was developed by the author through the study of mathematical models of the web transport systems. Consider the multi-span web transport system shown in Figure 58.

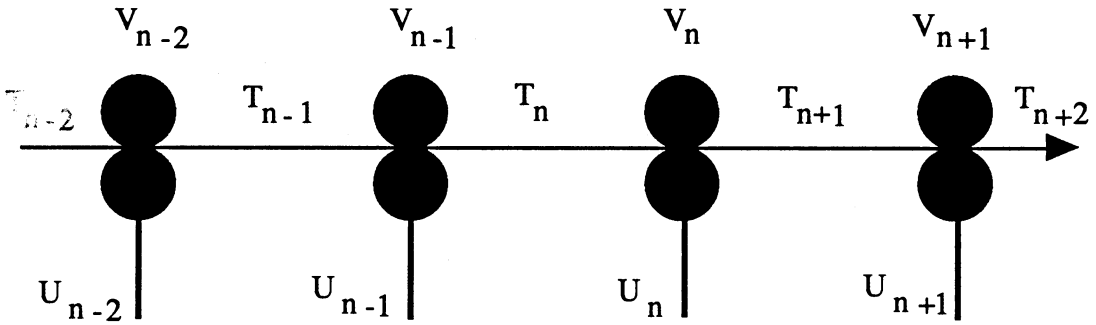

where

$$t_n = t_{n0} + T_n, \qquad u_n = u_{n0} + U_n, \qquad v_n = v_{n0} + V_n$$

and

T_n : Change in web tension from a steady-state operating value

t_{n0} : Steady-state operating value for web tension

U_n : Change in input to the motor

u_{n0}: Steady-state operating value for input to the motor

V_n : Change in web velocity from a steady-state operating value

v_{n0}: Steady-state operating value for web velocity.

Figure 58. A Multi-Span Web Transport System in Section 5.3

Usually, motors are used to change the tangential velocities of rollers in order to control the web tension in each processing section. Rollers with vertical bar mean that these rollers are driven by motors. The n-th subsystem is defined as the combination of the n-th span and the roller at the right end of the span in Figure 58.

The mathematical model describing the longitudinal dynamics of the n-th subsystem can be written in a state space form using equations (22) and (38) as follows.

$$\dot{X}_n = A_n X_n + B_n U_n, \tag{138}$$

where

A : Cross-sectional area of web

A_n : System matrix; $A_n = \begin{bmatrix} -\frac{v_{n0}}{L_n} & \frac{AE}{L_n} \\ -\frac{R_n^2}{J_n} & -\frac{B_{fn}}{J_n} \end{bmatrix}$

B_n : Input matrix; $B_n = \begin{bmatrix} 0 \\ \frac{R_n}{J_n} K_n \end{bmatrix}$

B_{fn}: Rotary friction constant of bearing

E : Young's modulus of web

J_n : Polar moment of inertia of roll

L_n : Length of web span

R_n : Radius of roller

X_n : State vector; $X_n = \begin{bmatrix} T_n \\ V_n \end{bmatrix}$.

It was assumed in the above mathematical model that the changes in tension in the entering and exiting spans were zero. It was also assumed that there is no slippage between the web and the rollers.

The user inputs the number of spans when he configures a system. Then the number of primitive elements can be obtained using equation (137). As the user selects the primitive elements one by one starting at the upstream end of the previously synthesized system, WTS keeps track of the order of the primitive elements selected. The mathematical model of each primitive element is called one by one from WTS library according to this order to assemble primitive elements into a system and to generate the mathematical model of the assembled system. The system matrix of the mathematical model of the assembled web transport system has a unique structure. The elements around the diagonal of the system matrix have non-zero values and the rest of elements have zero values. The user also inputs the physical data for each primitive element. Once the number of the primitive elements, the order a primitive is selected, and physical property data for primitive elements are known, the system matrix can be easily obtained by calculating the non-zero elements of the system matrix by using equation (138). The algorithm for the automatic assembly of primitive elements and generation of mathematical models is summarized as follows.

(1) Get the total number of web spans (N_s) from the user.

(2) Calculate the total number of primitive elements (subsystems) using the equation (137).

(3) Keep track of the order of the primitive elements selected by the user.

(4) Get the physical property data and the dimension of the primitive elements (subsystems) from the user.

(5) Calculate the elements of the system matrix (A_n) and input vector (B_n) by using equation (138).

Inputs and Outputs

Inputs

Input data for the configuration, steady-state analysis, and dynamic analysis can be entered through data entry screens. The input data can be changed easily or corrected on the data entry screen. Units for parameter values used in the simulation are shown at the bottom of each data entry screen.

Inputs to the WTS are :

Number of web spans
Young's modulus
Thickness of web
Width of web
Lengths of web spans
Web transport speed
Radii of rollers/rolls
Moments of inertia of rollers/rolls
Viscous friction coefficients in bearings
External restraining torque applied to unwinding roller (if

there is an unwinding roller in the system)
Input voltages to the driving motors
Torque Constants of the Motors
Steady-state operating tension (at least in one span of the system).

Outputs

The WTS has three kinds of outputs: graphical representation of the configured web transport system, steady-state analysis output, and dynamic analysis output. The steady-state analysis output contains the steady-state values of the system states (velocities of rollers/rolls, tensions), and the dynamic analysis output is composed of plots of dynamic responses of the system output variables.

An Example

This section demonstrates how to design and analyze a web transport system by following the procedure in the WTS User's Guide [79]. Consider an one-span system comprising an unwinding roll, a free span, and a winding roll as shown in Figure 59.

The default values of WTS given on pages 16 and 17 of WTS User's Guide [79] will be used for this example.

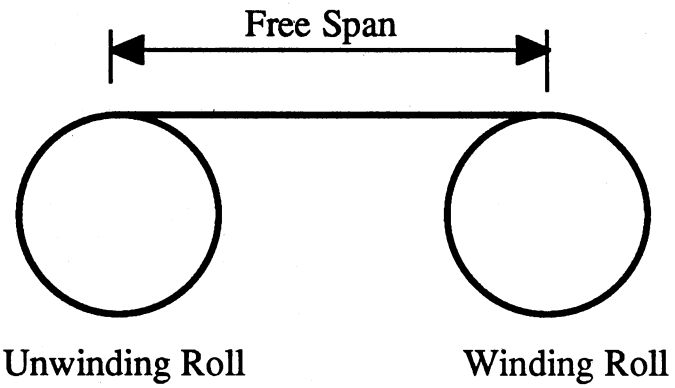

Figure 59. Unwinding - Rewinding System

- **Identify the data and operating conditions.**

No. of Spans = 1, Thickness of Web = 0.001 (in), Radii of Unwinding and Winding Rolls = 20 (in), Inertia of Rolls = 1504 (Lbf-in-sec-sec), Friction Coefficient of Bearings = 0.002 (Lbf-sec / in), Length of Span = 120 (in), Width of Web = 60 (in), Young's Modulus = 350,000 (Lbf / (in-in)), Initial Tangential Velocity of Rolls = 1,000 (ft / min), Initial Tension in Free Span = 0 (Lbf), External Restraining Torque at Unwinding Roll = 0.0 (Lbf-ft), Step Input in Voltage to Driving Motor = 1 (volts), Motor Constant = 4 (Lbf-ft / volt).

- **Sketch the system configuration using primitive elements shown in Figure 5.**

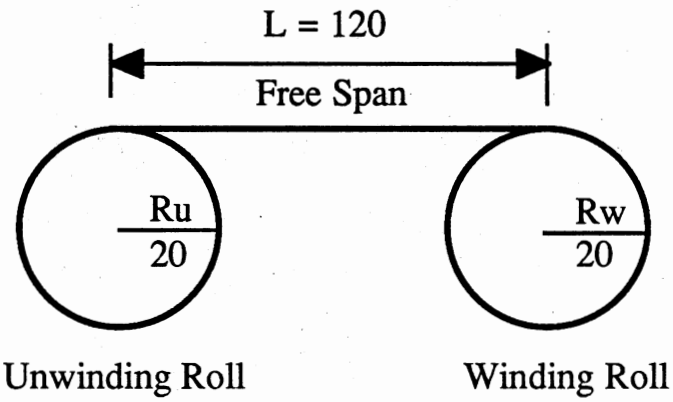

Figure 60. Sketch of Unwinding - Rewinding System

- **Prepare a data sheet for analysis using the standard form shown in Figure 6.**

1. General Data

Description	Data	Unit
Number of Spans	1	Integer
Thickness of Web	0.001	in

2. Unwinding Roll

Description	Data	Unit
Radius of Roll	20	in
Inertia of Roll	1504	Lbf-in-sec-sec
Friction Coeff. of Bearing	0.002	Lbf-sec / in

3. Free Span

Description	Data	Unit
Lengh of Span	120	in
Width of Web	60	in
Young's Modulus	350000	Lbf / (in-in)

Figure 61-1.2.3. Data Sheet for Analysis

4. Winding Roll

Description	Data	Unit
Radius of Roll	20	in
Inertia of Roll	1504	Lbf-in-sec-sec
Friction Coeff. of Bearing	0.002	Lbf-sec / in

5. Steady State Analysis

Description	Initial Tangential Velocity	Unit
1st Roll(er)	1000	ft / min
2nd Roll(er)	1000	ft / min

Description	Initial Tension	Unit
Entering Span	0	Lbf
1st Span	0	

Figure 61-4.5. Data Sheet for Analysis: Continued

6. Dynamic Analysis

Description	External Restraining Torque	Unit
1st Roll	0.0	Lbf-ft

Description	Step Input in Voltage to Driving Motor	Unit	Motor Constant	Unit
2nd Roll	1	Volts	4	Lbf-ft / volt

Figure 61-6. Data Sheet for Analysis: Continued

- **Boot the computer.**
- **If hard disk is available, enter the hard disk directory into which WTS has been copied using the CD command.**
  Or if hard disk is not available, place WTS Disk in Drive A. Make Drive A the default drive by typing A: and pressing RETURN key.
- **Type WTS and press RETURN key to start the program.**

The Main Menu will appear.

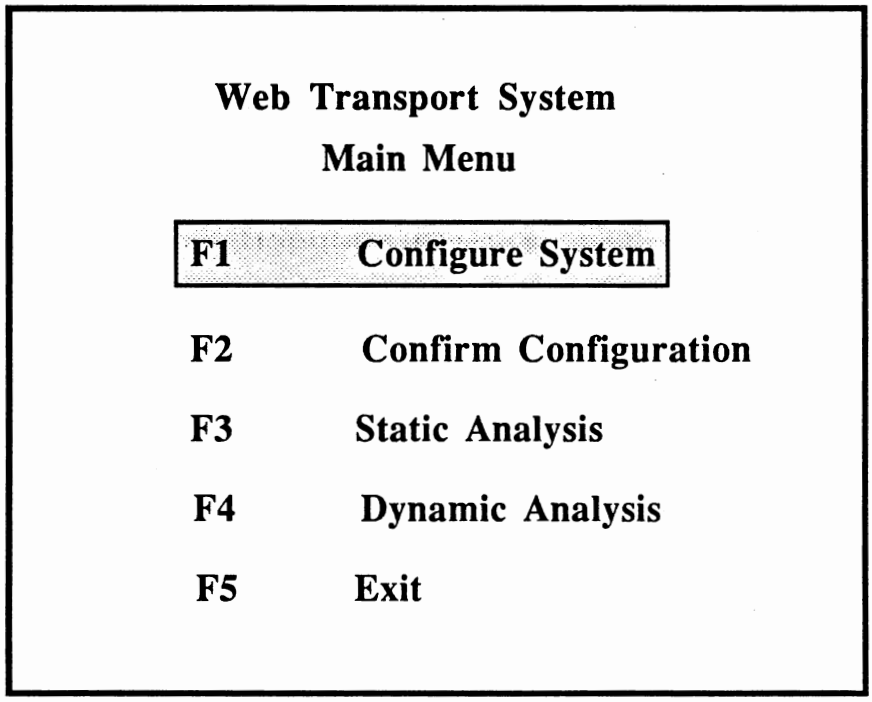

Figure 62. Main Menu of WTS: for Example

- **Select F1 for CONFIGURE SYSTEM and then press the RETURN key.**

The general data entry screen will appear.

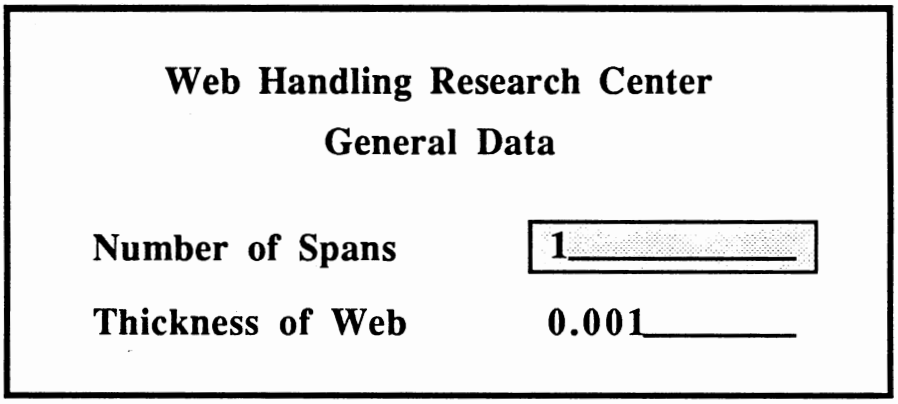

Figure 63. General Data Entry Screen

- **Press END key to leave the general data entry screen.**

The Sub-Menu will appear.

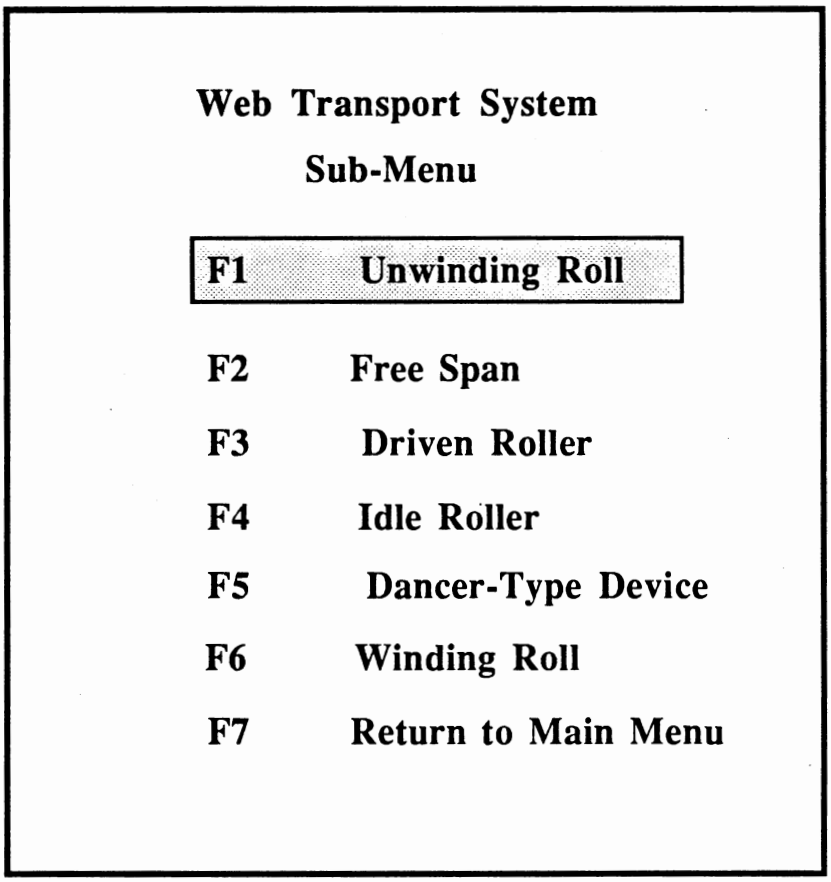

Figure 64. Sub Menu of WTS: for Example

- **Select F1 for Unwinding Roll and then press the RETURN key.**

The data entry screen will appear.

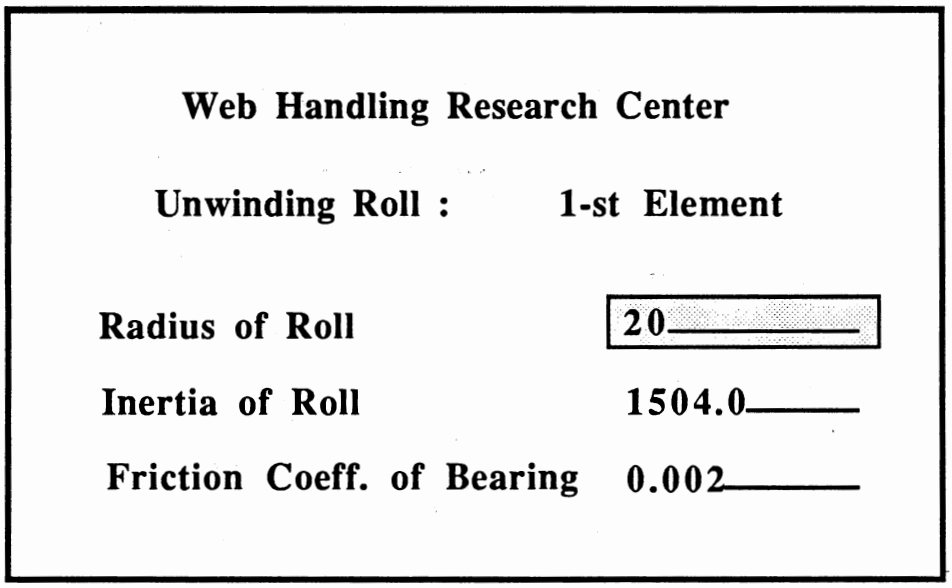

Figure 65. Data Entry Screen for Unwinding Roll

- **Press END key to leave the data entry screen.**

The Sub-Menu will re-appear.

- **Select F2 for Free Span and then press the RETURN key.**

The data entry screen will appear.

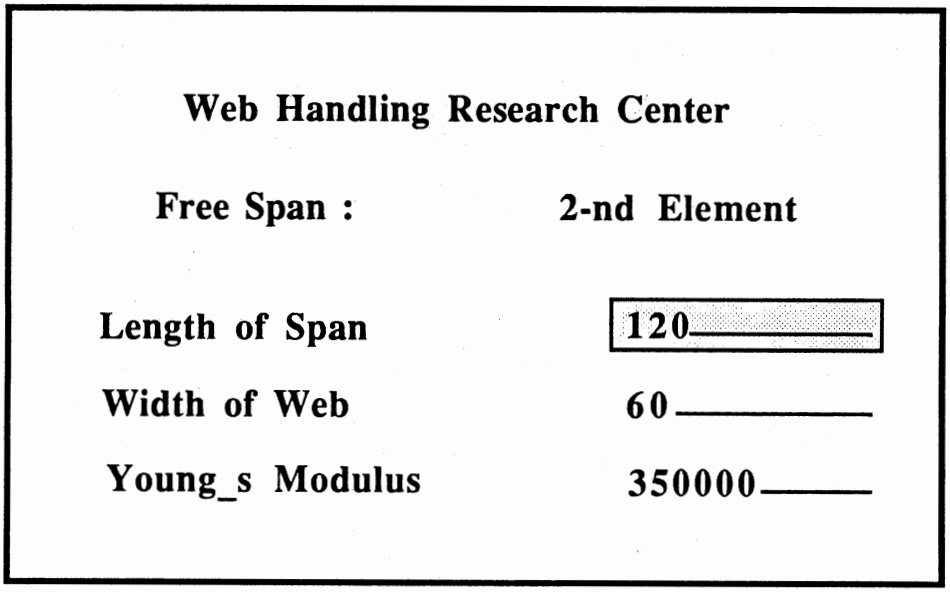

Figure 66. Data Entry Screen for Free Span

- **Press END key to leave the data entry screen.**

The Sub-Menu will re-appear.

- **Select F6 for Winding Roll and then press the RETURN key.**

The data entry screen will appear.

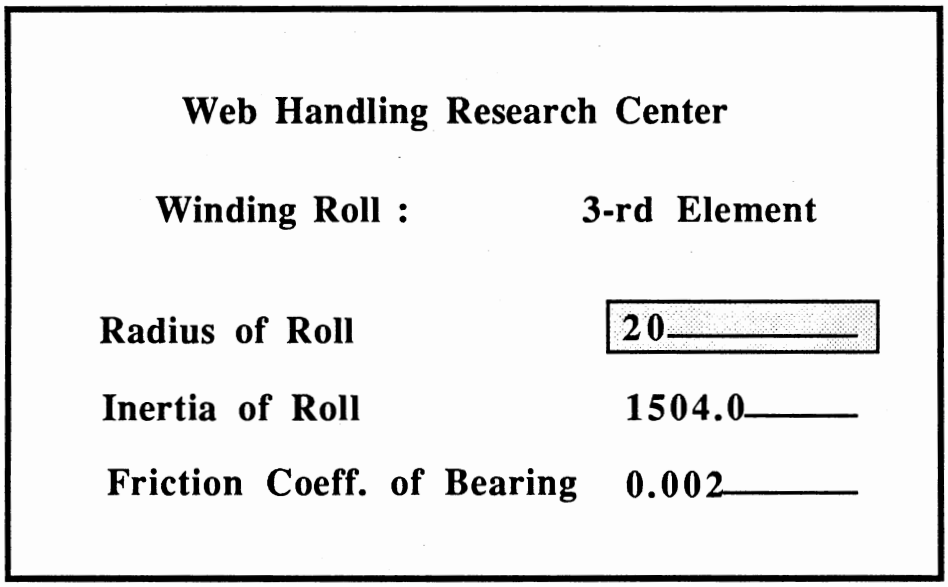

Figure 67. Data Entry Screen for Winding Roll

- **Press END key to leave the data entry screen.**

The Main Menu will re-appear.

- **Select F2 for CONFIRM CONFIGURATION and then press the RETURN key.**

Hit Any Key to Continue

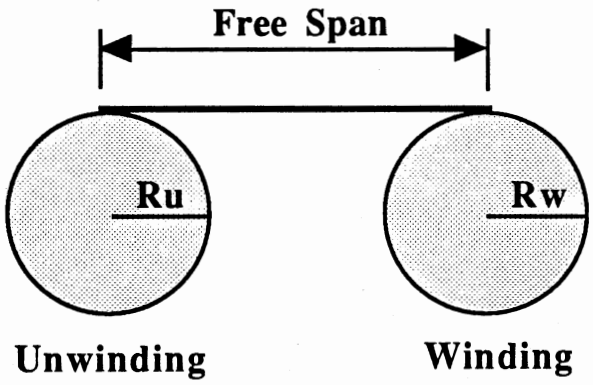

General Data

No. of Spans	1
Thick. of Web (in)	0.001

Element Data

Description	1st Elem	Sect. 1		
Young's Modulus (psi)		350000		
Width of Web (in)		60.0		
Length of Span (in)		120.0		
R. of Roll(er):Ru/Rd/Rw(in)	20.0	20.0		
Iner. of Roll(er)(Lb*in*s*s)	1504.0	1504.0		
Friction Coeff.(Lb*sec/in)	0.002	0.002		

Figure 68. Graphical Presentation of Configured System

- **Press any key to continue WTS.**

The Main Menu will re-appear.

- **Select F3 for STATIC ANALYSIS and then press the RETURN key.**

The data entry screen will appear.

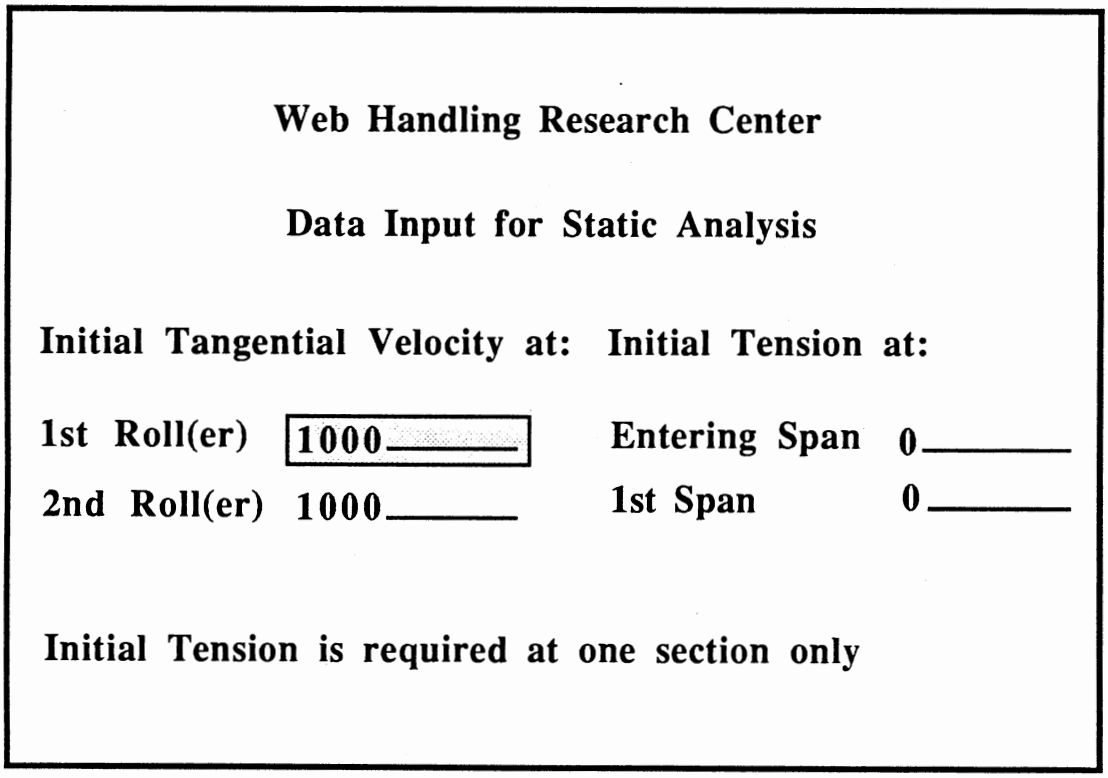

Figure 69. Data Entry Screen for Steady-State Analysis

o **Press END key to leave the data entry screen.**

The results of steady-state analysis will appear.

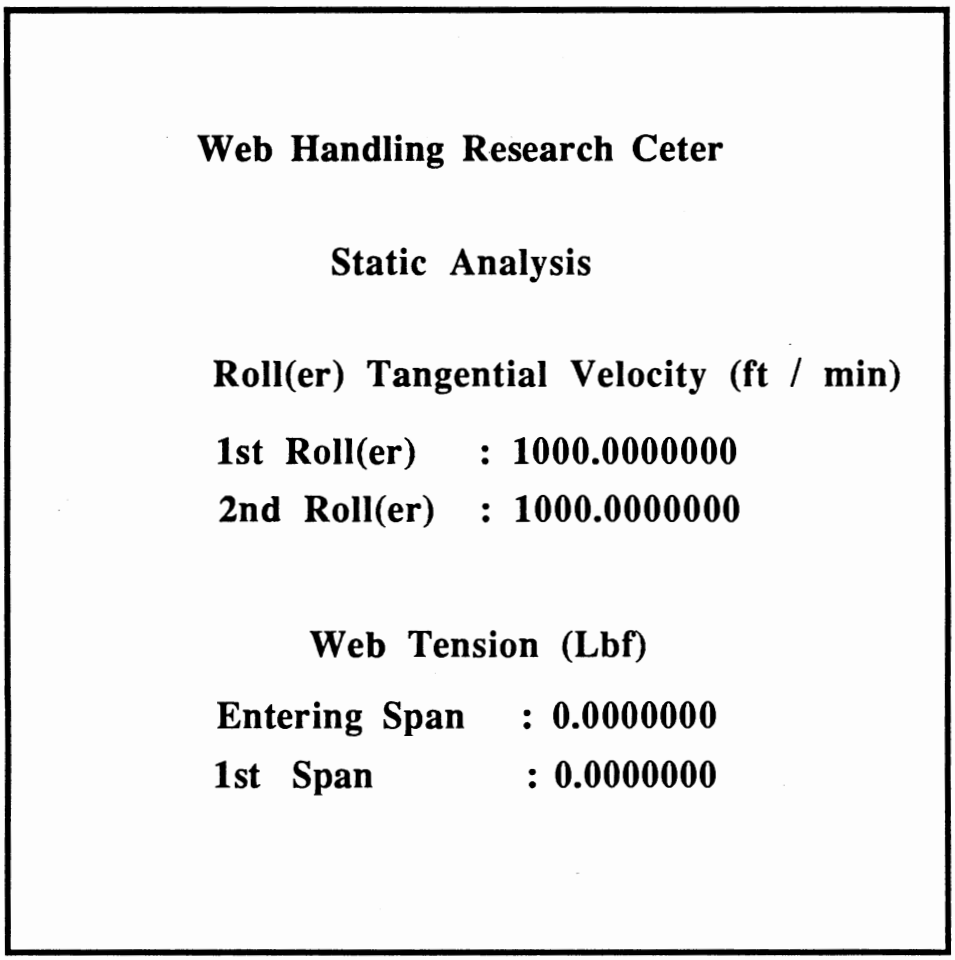

Figure 70. Steady-State Analysis Results

- **Press any key to continue WTS.**

The Main Menu will appear.

- **Select F4 for DYNAMIC ANALYSIS and then press the RETURN key.**

The data entry screen will appear.

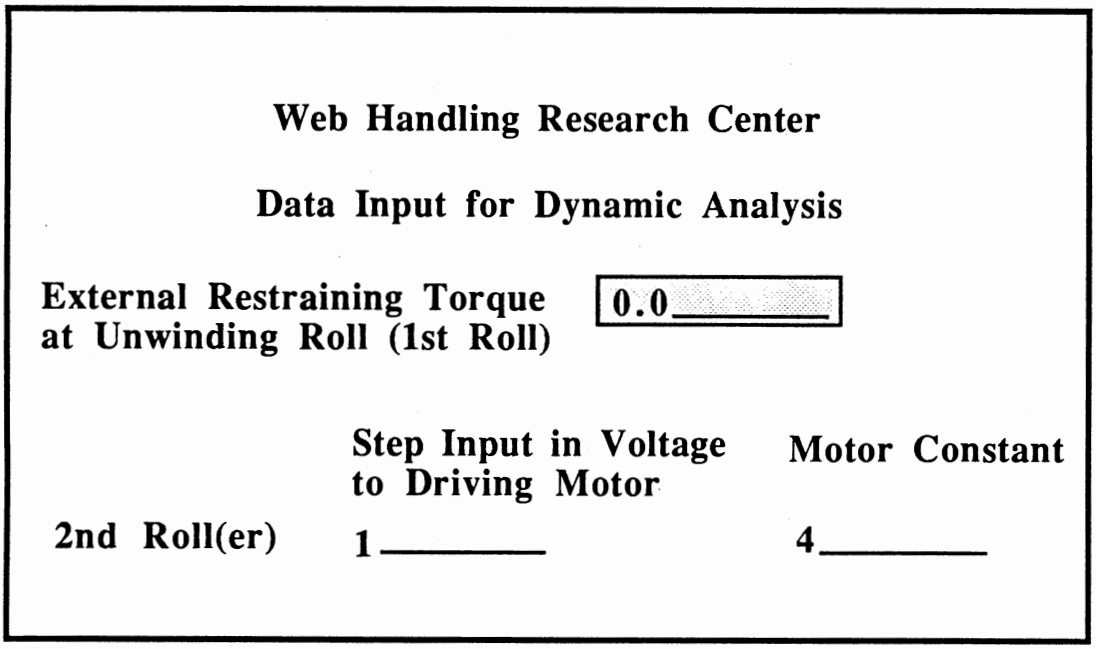

Figure 71. Data Entry Screen for Dynamic Analysis

o **Press END key to leave the data entry screen.**

The results of the dynamic analysis will appear as follows.

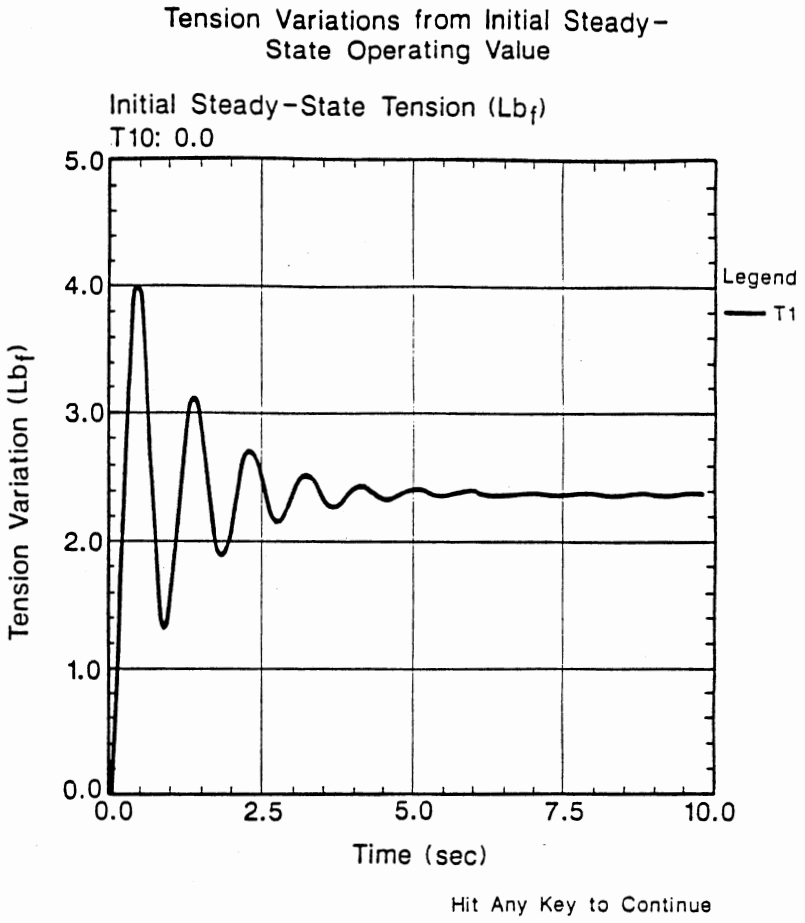

Figure 72. The Result of Dynamic Analysis

o **Press any key to continue WTS.**

The Main Menu will appear.

CHAPTER VI

TENSION CONTROL IN SINGLE-SPAN SYSTEMS

It was pointed out in Chapters I and IV that open-loop draw control may not produce accurate control of the web tension in a moving web. In this chapter, techniques for producing higher accuracy through closed-loop tension control in a moving web are discussed. Examples are presented to illustrate the use of a fixed-gain PID controller with feedforward controller for time invariant single-span web transport systems and a variable-gain PID controller for a time varying web transport system (winding section). The ability of these control strategies to overcome different types of disturbances is discussed.

Tension Control in a Single-Span System

Consider a schematic diagram of a closed-loop tension control system shown in Figure 73 for a single-span system. Suppose that the tension t_2 is to be controlled accurately. Two well-known approaches for implementing the controller are: (1) a fixed gain PID controller and (2) a fixed-gain PID controller with a feedforward element. An example is solved below to illustrate the advantages and disadvantages of these two

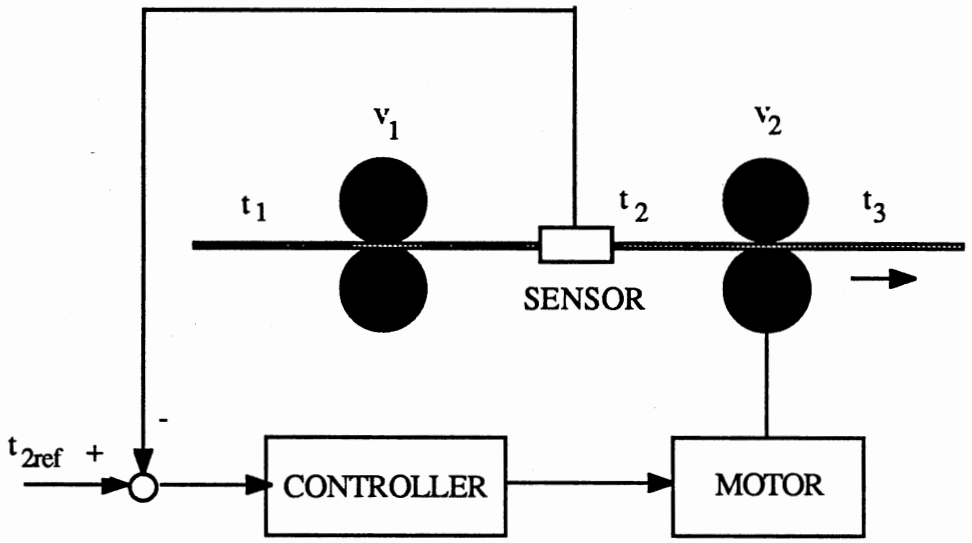

Figure 73. Schematic Diagram of a Tension Control System for a Typical Single-Span System

approaches.

Equations (22) and (38) constitute the linearized mathematical model for the open-loop system. For the case when $v_2 = w_2$ (i.e., no slippage occurs between the web and rollers) the dynamic model is given by the following equations:

$$\frac{d}{dt}[T_2(t)] = -\frac{v_{20}}{L}T_2(t) + \frac{v_{10}}{L}T_1(t) + \frac{AE}{L}(V_2(t) - V_1(t), \quad (139)$$

$$\frac{dV_2}{dt} = -\frac{B_{f2}}{J_2}V_2 + \frac{R_2^2}{J_2}(T_3 - T_2) + \frac{R_2}{J_2}K_2U_2, \quad (140)$$

where

K_2 : Motor constant

T_n : Change in web tension from a steady-state operating value

t_n : Web tension; $t_n = t_{n0} + T_n$

t_{n0} : Steady-state operating value for web tension

U_2 : Change in input to motor from a steady-state operating value

V_n : Change in web velocity from a steady-state operating value

v_n : Total web velocity; $v_n = v_{n0} + V_n$

v_{n0}: Steady-state operating value for web velocity.

PID Control

A closed-loop tension control system employing a PID controller is represented by the block diagram shown in Figure 74.

From the block diagram shown in Figure 74, the closed-loop transfer function can be written as follows:

$$T_2 = \frac{G_c G_p}{1 + G_c G_p} T_{2ref} + \frac{G_{T_3}}{1 + G_c G_p} T_3$$

$$+ \frac{G_{T_1}}{1 + G_c G_p} T_1 - \frac{G_{V_1}}{1 + G_c G_p} V_1. \qquad (141)$$

For simplicity, it is assumed that $T_1 = V_1 = T_3 = 0$. In this case the closed-loop transfer function reduces to:

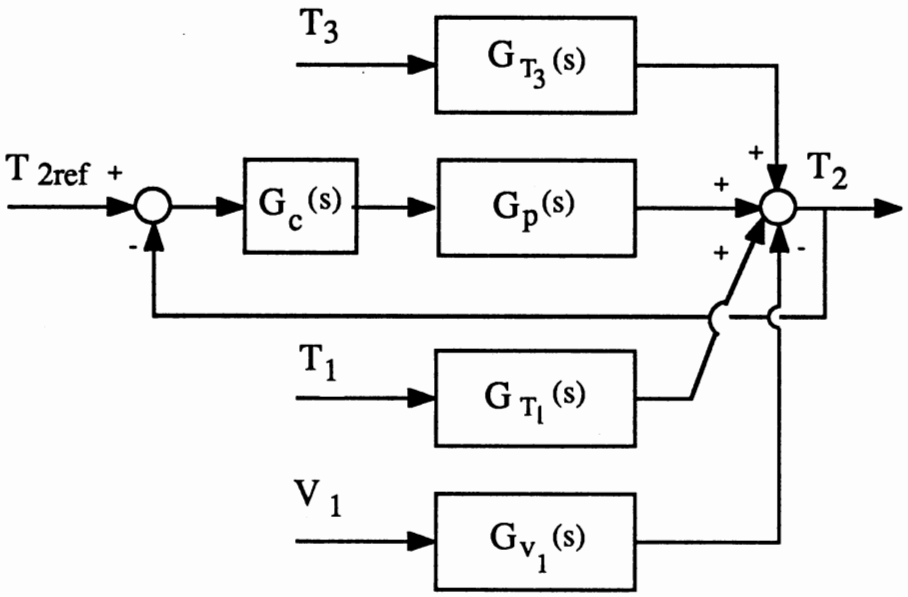

$$G_c(s) = K_p + \frac{K_i}{s} + K_d s : \text{PID controller}$$

$$G_P(s) = \frac{1}{\Delta} K_2 \frac{AER_2}{LJ_2}, \qquad G_{T_3}(s) = \frac{1}{\Delta} \frac{AER_2^2}{LJ_2}$$

$$G_{T_1}(s) = \frac{1}{\Delta} \frac{v_{20}}{L}(s + \frac{B_{f2}}{J_2}), \qquad G_{v_1}(s) = \frac{1}{\Delta} \frac{AE}{L}(s + \frac{B_{f2}}{J_2})$$

$$\Delta = s^2 + (\frac{v_{20}}{L} + \frac{B_{f2}}{J_2})s + \frac{v_{20}B_{f2}}{LJ_2} + \frac{AER_2^2}{LJ_2}.$$

Figure 74. Block Diagram of a Closed-Loop Tension Control System for the Single-Span System

$$\frac{T_2}{T_{2ref}} = \frac{G_c G_p}{1 + G_c G_p}, \tag{142}$$

or

$$\frac{T_2}{T_{2ref}} = \frac{b_2 s^2 + b_1 s + b_0}{s^3 + a_2 s^2 + a_1 s + a_0} = \frac{b_2 s^2 + b_1 s + b_0}{F(s)}, \tag{143}$$

where

$$a_0 = \beta_0 K_i , \qquad b_0 = \beta_0 K_i$$

$$a_1 = \alpha_0 + \beta_0 K_p , \qquad b_1 = \beta_0 K_p$$

$$a_2 = \alpha_1 + \beta_0 K_d , \qquad b_2 = \beta_0 K_d$$

and

$$\alpha_0 = \frac{v_{20} B_{f2}}{L J_2} + \frac{AER_2^2}{L J_2}, \quad \alpha_1 = \frac{v_{20}}{L} + \frac{B_{f2}}{J_2}$$

$$\beta_0 = K_2 \frac{AER_2}{L J_2}.$$

Suppose the specifications for the second order closed-loop tension control system are given in terms of a steady-state error (i.e., $e_{ss} = 0$), a damping coefficient (ζ), and a natural frequency (ω_n). The characteristic equation of the closed-loop tension control system derived is the third order (see equation (143)). The third order characteristic equation of the desired closed-loop tension control system can be rewritten in terms of ζ and ω_n as follows [24].

$$F(s) = (s + r)(s^2 + 2\zeta\omega_n + \omega_n^2) = 0, \tag{144}$$

where

$$r = k_r |\zeta\omega_n| , \qquad k_r > 10.$$

The gains of the PID controller can be obtained by comparing terms in equations (143) and (144). That is,

$$K_i = \frac{1}{\beta_0} k_r \zeta \omega_n^3, \tag{145}$$

$$K_p = \frac{1}{\beta_0}\left(\frac{2\zeta\omega_n\beta_0 K_i}{\omega_n^2} + \omega_n^2 - \alpha_0\right), \tag{146}$$

$$K_d = \frac{1}{\beta_0}\left(\frac{\beta_0 K_i}{\omega_n^2} + 2\zeta\omega_n - \alpha_1\right). \tag{147}$$

Using equations (145) through (147), a PID controller can be designed for given system parameter values and specifications for the closed-loop tension control system.

A PID controller was designed for the closed-loop tension control system assuming that $T_1 = V_1 = T_3 = 0$. An example was solved to demonstrate the performance of the closed-loop tension control system with the PID control when a disturbance $T_3 = 0.001$ lbf is introduced. The desired specifications for the closed-loop tension control system are given in Table 7. The desired step response was obtained by simulating equation (143) and is shown in Figure 76. $T_{2ref}(t) = 0$ @ $t = 0^-$ and $T_{2ref}(t) = 1.0$ lbf @ $t = 0^+$. The parameter values and system conditions used for the simulations are given in Table 1. The simulation results are shown in Figure 76 (curve for $T_3 = 0.001$). The transient performance of the closed-loop tension control system with a PID controller was not satisfactory when the disturbance T_3 was introduced.

TABLE 7

SPECIFICATIONS FOR A CLOSED-LOOP TENSION CONTROL SYSTEM

Steady-State Error	$e_{ss} = 0$
Damping Coeff. of Closed-Loop System	$\zeta = 0.7$
Natural Frequency of Closed-Loop System	$\omega_n = 10$

PID Control with Feedforward

Simple PID control of tension in the span does not result in rejecting disturbances due to V_1, T_1, and T_3. A PID controller with an additive feedforward control element will reject the disturbance T_3 under the assumption that T_3 is measurable. But, the feedforward control cannot be implemented for disturbances T_1 and V_1. When feedforward controllers were designed for T_1 and V_1, feedforward controllers were noncausal. Figure 75 is a block diagram of a closed-loop tension control system with a feedforward feature.

With the feedforward control feature in addition to the PID controller, the output of the closed-loop system can be written as the follows when T_1 and V_1 are assumed to be zero.

$$T_2 = \frac{G_c G_p}{1 + G_c G_p} T_{2ref} + \frac{G_{ff} G_p + G_{T_3}}{1 + G_c G_p} T_3. \qquad (148)$$

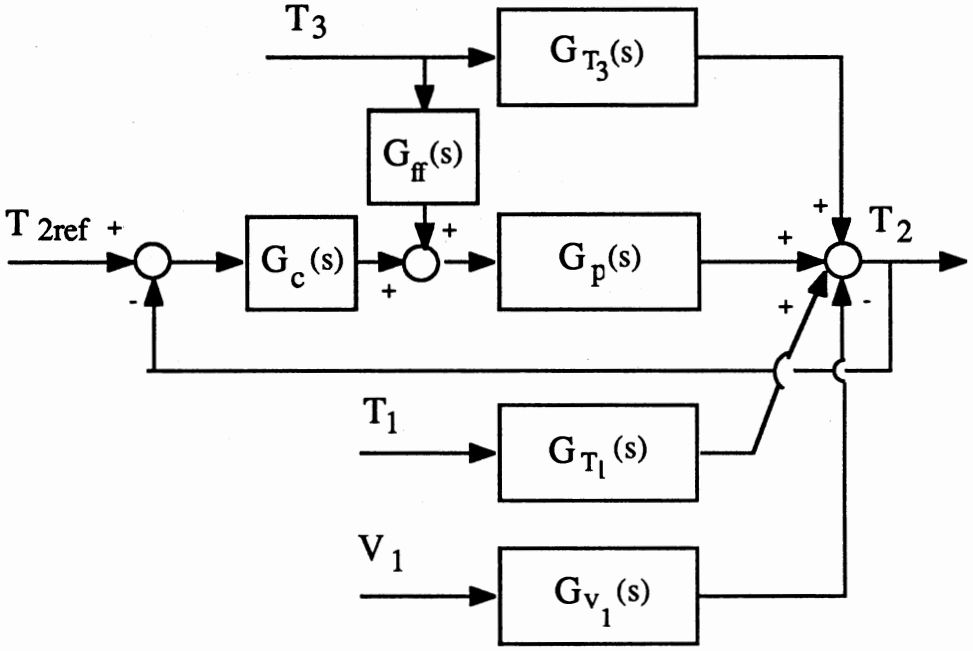

Figure 75. Block Diagram of a Closed-Loop Tension Control System for the Single-Span System: with PID and Feedforward Control

Since the feedforward controller G_{ff} can be designed such that:

$$G_{ff} G_p + G_{T_3} = 0. \qquad (149)$$

the disturbance, T_3, can be rejected.

A PID controller with feedforward control feature was designed for

the closed-loop tension control system assuming that $T_1 = V_1 = 0$. An example was solved to demonstrate the performance of the closed-loop control system with PID and feedforward control. The desired specifications for the closed-loop tension control system are given in Table 7. The parameter values and system conditions used for the simulations are given in Table 1. $T_{2ref}(t) = 0$ @ $t = 0^-$ and $T_{2ref} = 1.0$ lbf. A disturbance T_3 (0.001 lbf) was introduced to the closed-loop system. The simulation result is shown in Figure 76 (curve for $T_3 = 0.001$ lbf). The disturbance T_3 was rejected when the feedforward controller was added to the PID controller.

In summary, a fixed-gain PID controllers with and without feedforward feature were designed for a single-span system. The tension in the single-span system can be properly controlled by using the fixed-gain PID controller when disturbances are not considered. Feedforward control can be used to reject some types of disturbances and to improve the dynamic performance.

Tension Control in a Winding Section

The purpose of this section is to illustrate an important application where a fixed-gain PID controller may be an improper choice. The application involves a time-varying parameter and lends itself well to the use of a variable-gain PID controller.

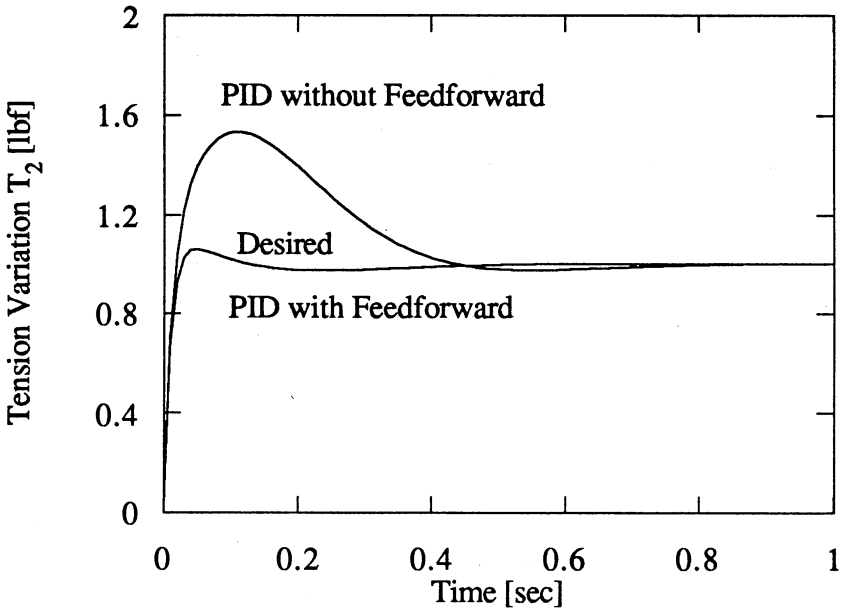

Figure 76. Performances of Closed-Loop Control Systems with PID Control: with and without Feedforward Control

A schematic diagram of a tension control system for a winding section is shown in Figure 77. Equation (141) is the transfer function for the system in Figure 77 when PID control is used. For the simplified case when $T_1 = V_1 = T_3 = 0$, equation (143) also represents the system in Figure 77. Unlike in the previous example, the radius of roll, R_2, are time-varying. Therefore the parameters a_2, a_1, and a_0 in the system characteristic equation are time varying.

The polar moment of inertia of the winding roll can be expressed as a function of the radius of the roll if the density of roll is known. A "build-up ratio" R_b is defined as:

$$R_b = \frac{R_2}{R_{c2}},$$

where

R_2 = Radius of winding roll,

R_{c2} = Initial radius of winding roll.

The system parameters α_0, α_1, and β_0 in equation (143) can be rewritten as functions of the build-up ratio, R_b, as follows.

$$\alpha_0 = \frac{v_{20}B_{f2}}{LJ_{20}}\frac{1}{R_b^4} + \frac{AER_{20}^2}{LJ_{20}}\frac{1}{R_b^2}, \qquad (150)$$

$$\alpha_1 = \frac{v_{20}}{L} + \frac{B_{f2}}{J_{20}}\frac{1}{R_b^4}, \qquad (151)$$

$$\beta_0 = K_2 \frac{AER_{20}}{LJ_{20}} \frac{1}{R_b^3} , \qquad (152)$$

where J_{20} represents the initial moment of inertia when $R_b = 1.0$.

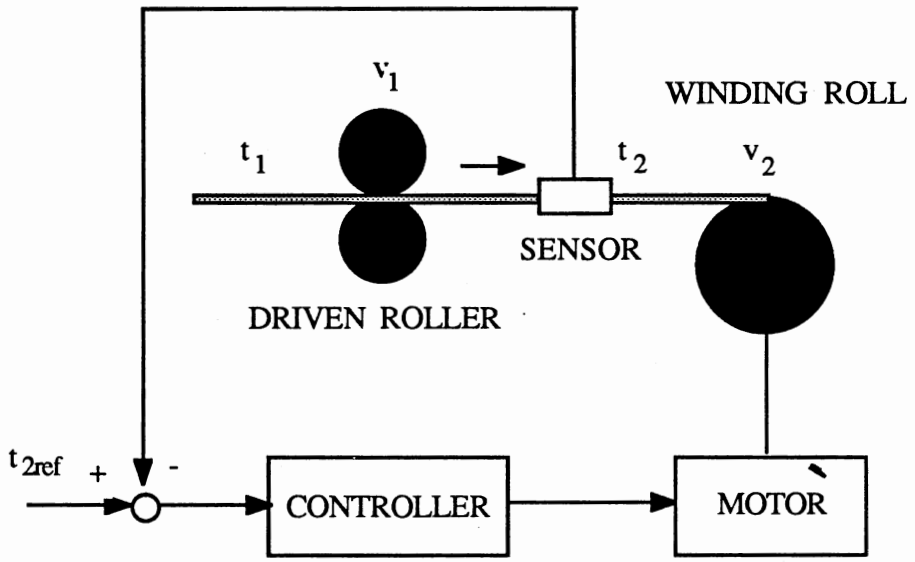

Figure 77. Schematic Diagram of a Tension Control System for a Winding Section

An example was solved to demonstrate the performance of the closed-loop tension control system with a fixed-gain PID controller when the parameters a_2, a_1, and a_0 in the system characteristic equation are time varying. The desired specifications for the closed-loop tension control system are given in Table 7. The desired step response was obtained by

simulating equation (143) and is shown in Figure 78. The parameter values and system conditions used for the simulations are given in Table 1. Equation (143) with system parameters α_0, α_1, and β_0 in equations (150) through (152) were used for the simulation. $T_{2ref}(t) = 0$ @ $t = 0^-$ and $T_{2ref} =$ 1.0 lbf @ $t = 0^+$. The simulation result is shown in Figure 78. Since the parameters change as the build-up ratio changes, the fixed-gain PID controller designed in the previous section cannot meet the desired specifications any more in the winding section (see Figure 78).

A simple adaptive control technique may be used to overcome the deficiency of the fixed-gain PID controller. The idea of the simple adaptive control technique is to continuously update the gains of a PID controller (variable-gain PID controller) according to the change of the time-varying parameter, build-up ratio. A schematic diagram of an variable-gain tension control system is shown in Figure 79. A block diagram for the adaptive control system is shown in Figure 80.

Equations (145) through (147) that were used to design the fixed-gain PID controller in the previous section can be used to design a variable-gain PID controller for the winding section. The gains (K_i, K_p, K_d) of the variable-gain PID controller can be calculated as follows:

$$K_i = \frac{1}{\beta_0} k_r \zeta \omega_n^3, \tag{153}$$

$$K_p = \frac{1}{\beta_0}\left(\frac{2\zeta\omega_n\beta_0 K_i}{\omega_n^2} + \omega_n^2 - \alpha_0\right), \tag{154}$$

$$K_d = \frac{1}{\beta_0}\left(\frac{\beta_0 K_i}{\omega_n^2} + 2\zeta\omega_n - \alpha_1\right), \tag{155}$$

and

$$\alpha_0 = \frac{v_{20}B_{f2}}{LJ_{20}}\frac{1}{R_b^4} + \frac{AER_{20}^2}{LJ_{20}}\frac{1}{R_b^2}, \tag{156}$$

$$\alpha_1 = \frac{v_{20}}{L} + \frac{B_{f2}}{J_{20}}\frac{1}{R_b^4}, \tag{157}$$

$$\beta_0 = K_2\frac{AER_{20}}{LJ_{20}}\frac{1}{R_b^3}. \tag{158}$$

J_{20} represents the initial moment of inertia when $R_b = 1.0$. α_0, α_1, and β_0 are functions of the build-up ratio and, therefore, are functions of time. As the radius of the roll is continuously updated through measurement, the α_0, α_1, and β_0 in equations (153) through (155) are calculated from equations (156) through (158). Then, the variable-gain PID controller can be designed from equations (153) through (155). The objective of the algorithm is to continuously position the poles of the closed-loop transfer function in the specified locations in the left half s-plane as one or more system parameters are changing with time.

An example was solved to illustrate the performance of a variable-gain PID controller for tension control in a winding section. It was assumed that $T_1 = T_3 = V_1 = 0$. The desired specifications for the closed-loop tension control system are given in Table 7. The desired step response was obtained by simulating equation (143) and is shown in Figure 81. The parameter values and the system operating conditions used for the simulation are given in Table 1. $T_{2ref}(t) = 0$ @ $t = 0^-$ and $T_{2ref}(t) = 1.0$ lbf @ $t = 0^+$.

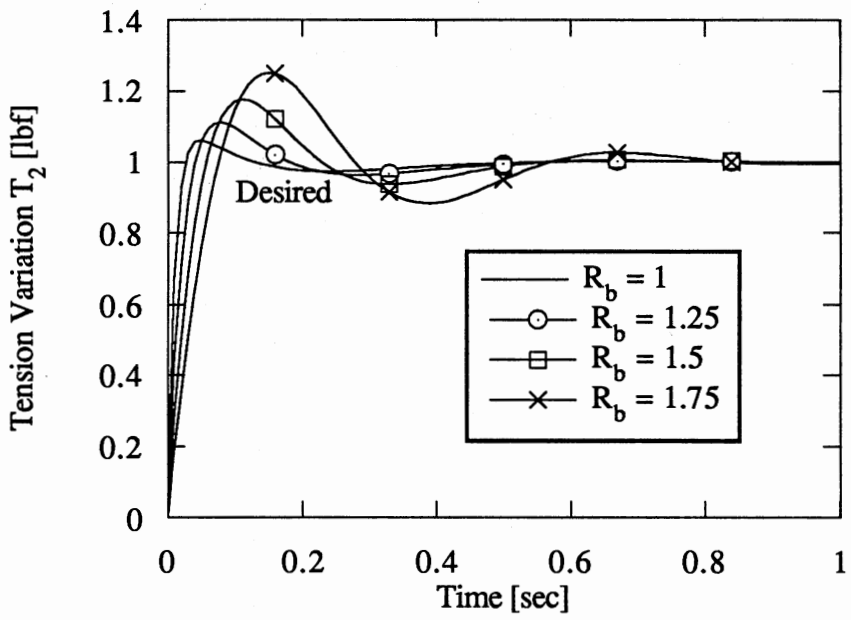

Figure 78. Tension Outputs for System with a Fixed-Gain PID Controller

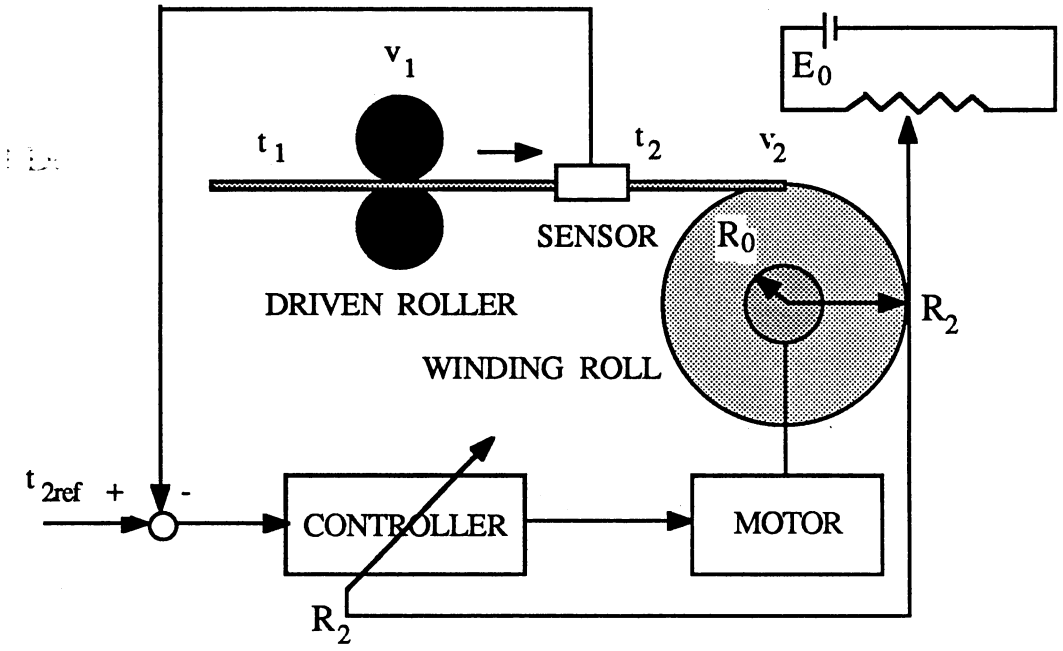

Figure 79. Schematic Diagram of an Adaptive Tension Control System

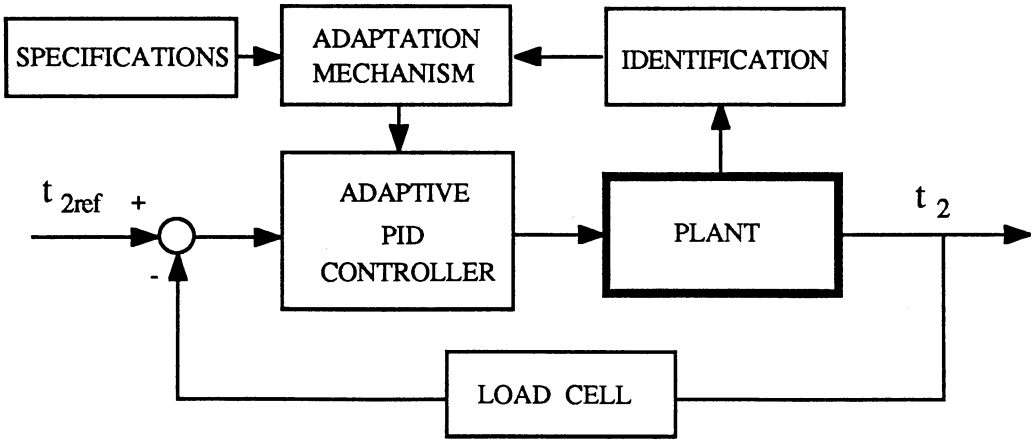

Figure 80. Block Diagram for an Adaptive PID Control System

Outputs are step response,T_2, for the build-up ratios R_b = 1.5, 1.75. The outputs from the tension control system with a variable-gain PID controller is compared with the outputs for the case with a fixed-gain PID controller in Figure 81. As shown in Figures 81, the step response of the model system with variable-gain PID controller satisfies the desired specifications very accurately, but the fixed-gain PID controller is not capable of providing adequate performance except at one fixed value of build-up ratio, R_b = 1.0.

In summary, a variable-gain PID controller was designed for the tension control in a winding section. The variable-gain PID controller produced a desired solution for a system with a time-varying parameter (i.e., a winding roll with increasing radius).

The idea used for the adaptive control in the winding section is also called as the gain scheduling approach. An advantage of this approach compared with other adaptive control techniques is its simplicity. This approach is easy to implement and shows promise for applications where the time-varying parameter is easily measured. However, the weakness of this approach is that it is not robust against measurement noise or unmodeled disturbances.

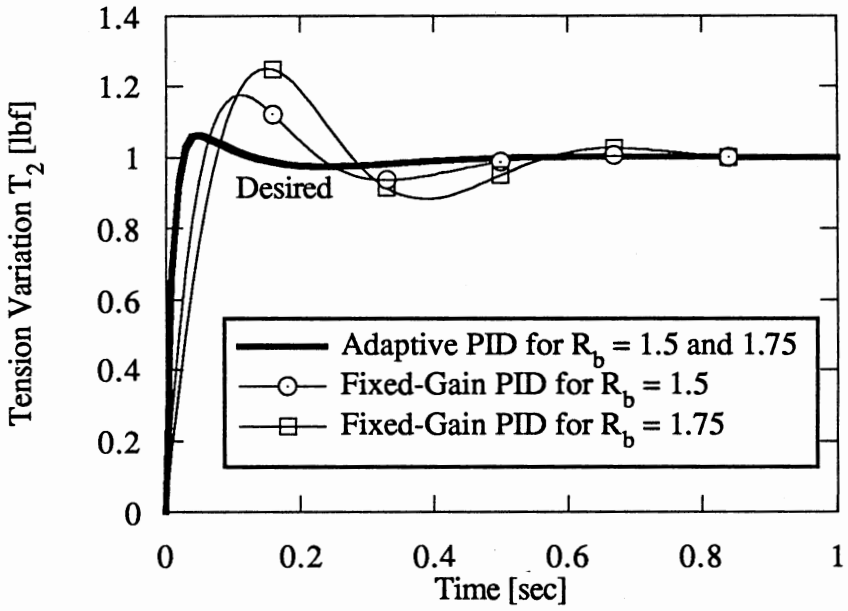

Figure 81. Tension Outputs for System with PID and Adaptive Controller

CHAPTER VII

TENSION CONTROL IN MULTI-SPAN SYSTEMS

A web may have to pass through several consecutive processing sections (e.g., cleaning, coating, drying, etc.) in the manufacture of an intermediate or final product. Different web processing sections may require different conditions, e.g., different tension levels. A typical control problem in a multi-span web transport system is maintaining the required longitudinal tension level in each processing section, and at same time stabilizing the overall web transport system. Some type of distributed control is required. Two primary techniques are used in the web processing industries for the distributed control of tension: they are open-loop "draw control" and "progressive set-point coordination" control (open-loop and closed-loop).

The problem with open-loop control of tension is that disturbances are not rejected and precise control may not be achieved. The progressive set-point coordination control forces tensions in the downstream web spans to be automatically changed when the tension in an upstream web span is changed. In order to overcome these deficiencies, a method for designing a closed-loop distributed control system for the control of web tension in a multi-span web transport system is developed in this chapter.

Open-Loop Draw Control

In open-loop "draw control", tension in a web span is controlled by controlling the velocities of rollers at either end of the web span. Control of web tension using draw control requires extremely accurate control of the roller velocities, a requirement which may be very difficult or expensive (see section 1.3). Also, when open-loop draw control is used, a disturbance from an adjacent web span cannot be rejected no matter how accurately the web velocity is controlled (see section 1.3).

Progressive Set-Point Coordination Control

In progressive set-point coordination control, once an input is provided to an upstream driven roller, an input of the same magnitude is automatically provided to each of the driven rollers which follow downstream (see section 1.3). Progressive set-point coordination control is effective for the start-up or shut-down of a system. But, it is not a desirable technique for normal operation of a multi-span web transport system. This technique forces tensions in the downstream web spans to be automatically changed when the tension in an upstream web span is changed. That is, unwanted disturbances are automatically introduced to downstream web spans when there is an input to an upstream processing section. The problem with the progressive set-point coordination control was fully analyzed through the simulation of models and experimental studies in

section 4.3.

Closed-Loop Control

In order to overcome deficiency of open-loop draw control and progressive set-point coordination control, a method for designing a closed-loop distributed control system for the control of web tension in a multi-span web transport system is developed in this section. The objectives of the control system are to produce the desired performance in each subsystem and to guarantee stability of the overall system in the presence of interactions between adjacent web spans.

Multi-span web transport systems generally can be simplified as shown in Figure 82. Usually, motors are used to change the tangential velocities of the rollers in order to control the web tension in each processing section. U_n denotes the change in the input to the n-th driving motor, V_n denotes the change in the tangential velocity of the n-th driven roller, and T_n denotes the change in the longitudinal tension in the n-th span.

The system shown in the Figure 82 can be considered as a set of interconnected subsystems. Each subsystem consists of a web span and a driven roller at the right end of the web span. The n-th subsystem will be called as s_n.

By using equations (22) and (38), a linearized mathematical model for the n-th subsystem, s_n, can be written as [11];

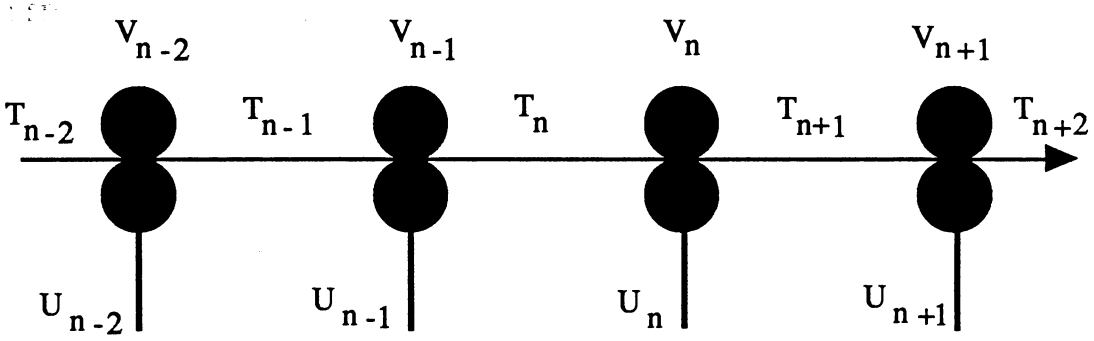

$$t_n = t_{n0} + T_n, \qquad u_n = u_{n0} + U_n, \qquad v_n = v_{n0} + V_n$$

Figure 82. A Multi-Span Web Transport System

$$\frac{dT_n}{dt} = -\frac{v_{n0}}{L_n} T_n + \frac{v_{n-1\,0}}{L_n} T_{n-1} + \frac{AE}{L_n}(V_n - V_{n-1}). \qquad (159)$$

$$\frac{dV_n}{dt} = -\frac{B_{fn}}{J_n} V_n + \frac{R_n^2}{J_n} (T_{n+1} - T_n) + \frac{R_n}{J_n} K_n U_n. \qquad (160)$$

The problem is to design controls U_n , n= 1,...,N, such that these controls together guarantee precise control of tension in each subsystem and the stability of the overall system. N is the total number of subsystems.

The mathematical model for the n-th subsystem given in equations (159) and (160) can be rewritten in a more compact form as shown below :

$$\dot{X}_n = A_n X_n + A_{n\,n-1} X_{n-1} + A_{n\,n+1} X_{n+1} + B_n U_n, \qquad (161)$$

$$Y_n = C_n X_n , \qquad (162)$$

where

$$X_n = \begin{bmatrix} T_n \\ V_n \end{bmatrix},$$

$$A_n = \begin{bmatrix} -\frac{v_{n0}}{L_n} & \frac{AE}{L_n} \\ -\frac{R_n^2}{J_n} & -\frac{B_{fn}}{J_n} \end{bmatrix}, \quad B_n = \begin{bmatrix} 0 \\ \frac{R_n}{J_n} K_n \end{bmatrix}, \quad C_n = [\,1 \;\; 0\,]$$

$$A_{n\,n-1} = \begin{bmatrix} \frac{v_{n-1\,0}}{L_n} & -\frac{AE}{L_n} \\ 0 & 0 \end{bmatrix}, \; A_{n\,n+1} = \begin{bmatrix} 0 & 0 \\ \frac{R_n^2}{J_n} & 0 \end{bmatrix}.$$

A_n and B_n are the system matrix and the input vector, respectively. The matrix $A_{n\,n-1}$ and $A_{n\,n+1}$ are called "interconnection matrices". All pairs (A_n, B_n) are controllable, and all pairs (A_n, C_n) are observable in the above equations.

The problem is to design a set of local controllers for the subsystems of distributed system. Each local controller includes feedback and feedforward control. Feedforward control may be used to reject some types of disturbances as discussed in section 6.1. Each local controller has the form of:

$$U_n = - F_n X_n - G_n X_{n+1} ,$$

where n = 1,..., N.

F_n and G_n are the gains for the feedback and the feedforward control respectively.

The pole assignment technique is quite commonly used for controller design. This technique may be used in the design of a local controller for each subsystem in a multi-span web transport system. It must be assumed that all the states are accessible by either measurement or estimation. Only states and inputs of corresponding subsystem and adjacent subsystems are used in designing local controllers.

Closed-Loop Control Using an Auxiliary Dynamic Model

Derivation of an Auxiliary Dynamic model

Coupling between the equations which describe the longitudinal dynamics of the web in a multi-span system, complicates the design of a distributed control system. In this section, the describing equations will be modified such that they are decoupled. The set of modified equations will be referred to the "auxiliary dynamic model".

Using equations (159) and (160), the mathematical models for the subsystems s_{n-1} and s_n can be written as:

$$\frac{dT_{n-1}}{dt} = - \frac{v_{n-10}}{L_{n-1}} T_{n-1} + \frac{v_{n-20}}{L_{n-1}} T_{n-2} + \frac{AE}{L_{n-1}} (V_{n-1} - V_{n-2}) . \qquad (163)$$

$$\frac{dV_{n-1}}{dt} = -\frac{B_{fn-1}}{J_{n-1}} V_{n-1} + \frac{R_{n-1}^2}{J_{n-1}} (T_n - T_{n-1}) + \frac{R_{n-1}}{J_{n-1}} K_{n-1} U_{n-1} . \quad (164)$$

$$\frac{dT_n}{dt} = -\frac{v_{n0}}{L_n} T_n + \frac{v_{n-1\,0}}{L_n} T_{n-1} + \frac{AE}{L_n} (V_n - V_{n-1}) . \quad (165)$$

$$\frac{dV_n}{dt} = -\frac{B_{fn}}{J_n} V_n + \frac{R_n^2}{J_n} (T_{n+1} - T_n) + \frac{R_n}{J_n} K_n U_n . \quad (166)$$

Observing the mathematical models in equation (165) reveals that the velocity difference ($V_n - V_{n-1}$) between the ends of the n-th span can be used as a control variable, instead of the individual velocities. An "auxiliary dynamic model" may be derived from the mathematical model of the system by introducing a new state variable ($V_{n\,n-1} \equiv V_n - V_{n-1}$).

The auxiliary dynamic model can be derived as follows.

Let

$$V_{n\,n-1} = V_n - V_{n-1}, \quad (167)$$

where n =1,...,N.

Using equation (167) in equation (165) yields:

$$\frac{dT_n}{dt} = -\frac{v_{n0}}{L_n} T_n + \frac{v_{n-1\,0}}{L_n} T_{n-1} + \frac{AE}{L_n} V_{n\,n-1} . \quad (168)$$

The tension in the n-th span depends only on the velocity difference ($V_{n\,n-1}$) instead of the absolute tangential velocities (V_n and V_{n-1}) of the rollers in

the n-th subsystem. And substituting equation (167) into equation (166) yields:

$$\frac{d(V_{n-1} + V_{n\,n-1})}{dt} = -\frac{B_{fn}}{J_n}(V_{n-1} + V_{n\,n-1}) + \frac{R_n^2}{J_n}(T_{n+1} - T_n)$$

$$+ \frac{R_n}{J_n} K_n U_n \,. \tag{169}$$

Subtracting equation (164) from (169) gives:

$$\frac{dV_{n\,n-1}}{dt} = -\frac{B_{fn}}{J_n} V_{n\,n-1} - \left(\frac{B_{fn}}{J_n} - \frac{B_{f\,n-1}}{J_{n-1}}\right) V_{n-1} \tag{170}$$

$$+ \left[\frac{R_n^2}{J_n} T_{n+1} - \left(\frac{R_n^2}{J_n} + \frac{R_{n-1}^2}{J_{n-1}}\right) T_n + \frac{R_{n-1}^2}{J_{n-1}} T_{n-1}\right]$$

$$+ \frac{R_n}{J_n} K_n U_n - \frac{R_{n-1}}{J_{n-1}} K_{n-1} U_{n-1} \,.$$

By using equation (167), V_{n-1} in equation (170) can be written as:

$$\begin{aligned} V_{n-1} &= V_{n-2} + V_{n-1\,n-2} \\ &= V_{n-3} + V_{n-2\,n-3} + V_{n-1\,n-2} \\ &\;\;\vdots \\ &= V_0 + \sum_{i=1}^{N-1} V_{i\,i-1} \,. \end{aligned} \tag{171}$$

where V_0 is the tangential velocity of the driven roller under master speed control, $V_{i\,i-1}$ is the change in the velocity difference associated with the i-th span, and N is the total number of spans (subsystems) in a multi-span system.

And in equation (170), let the input difference ($U_{n\,n-1}$) between the n-th and (n-1)-th subsystem:

$$U_{n\,n-1} = \frac{R_n}{J_n} K_n U_n - \frac{R_{n-1}}{J_{n-1}} K_{n-1} U_{n-1} . \qquad (172)$$

Substituting equations (171) and (172) in equation (170) gives:

$$\frac{dV_{n\,n-1}}{dt} = - \frac{B_{fn}}{J_n} V_{n\,n-1} - \left(\frac{B_{fn}}{J_n} - \frac{B_{f\,n-1}}{J_{n-1}}\right)\left(V_0 + \sum_{i=1}^{N-1} V_{i\,i-1}\right)$$

$$+ \left[\frac{R_n^2}{J_n} T_{n+1} - \left(\frac{R_n^2}{J_n} + \frac{R_{n-1}^2}{J_{n-1}}\right) T_n + \frac{R_{n-1}^2}{J_{n-1}} T_{n-1}\right]$$

$$+ U_{n\,n-1} . \qquad (173)$$

Equations (168) and (173) constitute the "auxiliary dynamic model" for the n-th subsystem. The input difference $U_{n\,n-1}$ in equation (172) is defined as the "auxiliary control".

Design of Local Controllers Using the Auxiliary Model

In this section, a procedure for designing each local controller in the distributed control system is developed. The advantage of using the auxiliary dynamic model in the design of the distributed control system will be illustrated using a numerical example.

To simplify the problem, it is assumed that $J_n = J$, $R_n = R$, $B_{fn} = B_f$, and $K_n = 1$ for n=1,...,N in equation (173). Then, the auxiliary model for the n-th subsystem s_n, represented by equations (168) and (173), can be rewritten in a compact form as:

$$\dot{X}_n = A_n X_n + A_{n\,n-1} X_{n-1} + A_{n\,n+1} X_{n+1} + B_n U_{n\,n-1}, \qquad (174)$$

$$Y_n = C_n X_n , \qquad (175)$$

where

$$X_n = \begin{bmatrix} T_n \\ V_{n\,n-1} \end{bmatrix} , \quad B_n = \begin{bmatrix} 0 \\ 1 \end{bmatrix}, \; C_n = [\,1 \;\; 0\,]$$

$$A_n = \begin{bmatrix} -\frac{v_{n0}}{L_n} & \frac{AE}{L_n} \\ -2\frac{R^2}{J} & -\frac{B_f}{J} \end{bmatrix}, \; A_{n\,n-1} = \begin{bmatrix} \frac{v_{n-1\,0}}{L_n} & 0 \\ \frac{R^2}{J} & 0 \end{bmatrix}$$

$$A_{n\,n+1} = \begin{bmatrix} 0 & 0 \\ \frac{R^2}{J} & 0 \end{bmatrix}.$$

The block diagram for the closed-loop subsystems shown in Figure 83 can be obtained using equations (167), (168), and (172) through (175). The block diagram shows the structures of two closed-loop subsystems (second and third subsystems) which use the auxiliary dynamic models in the design of local controllers. The purpose is to design local controls U_n, n=1,..N, such that Y_n , n=1,..,N can be controlled at the desired level within given performance specifications and such that the overall system is stable.

Auxiliary controls $U_{n\,n-1}$, n= 1,...,N, which were defined in equation (172) may be designed using the auxiliary dynamic model represented by equations (168) and (173) and the specifications for each subsystem. The control for each subsystem is calculated from equation (172) as follows:

$$U_n = \frac{J_n}{R_n K_n}(U_{n\,n-1} + \frac{R_{n-1}}{J_{n-1}} K_{n-1}\, U_{n-1}). \qquad (176)$$

Feedforward control may be used in the design of local controller to reject some types of disturbances as discussed in section 6.1. Each local controller incorporates both feedback and feedforward control. Let the auxiliary local control be:

$$U_{n\,n-1} = H_n(U_{nc} - F_n X_n - G_n X_{n+1}), \qquad (177)$$

where $U_{n\,n-1}$ is the auxiliary control for the n-th subsystem

U_{nc} is the reference input for n-th subsystem

F_n is the feedback gain vector for the n-th subsystem

G_n is the feedforward gain vector for the n-th subsystem

H_n is the overall gain for the local controller.

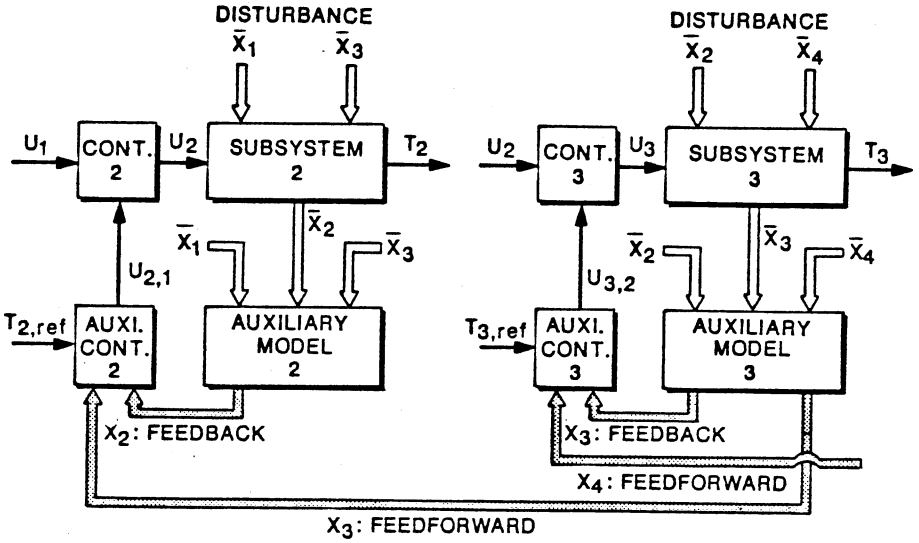

$$\bar{X}_1 = \begin{bmatrix} T_1 \\ V_1 \end{bmatrix} \quad \bar{X}_2 = \begin{bmatrix} T_2 \\ V_2 \end{bmatrix} \quad \bar{X}_3 = \begin{bmatrix} T_3 \\ V_3 \end{bmatrix} \quad \bar{X}_4 = \begin{bmatrix} T_4 \\ V_4 \end{bmatrix}$$

$$X_1 = \begin{bmatrix} T_1 \\ V_{10} \end{bmatrix} \quad X_2 = \begin{bmatrix} T_2 \\ V_{21} \end{bmatrix} \quad X_3 = \begin{bmatrix} T_3 \\ V_{32} \end{bmatrix} \quad X_4 = \begin{bmatrix} T_4 \\ V_{43} \end{bmatrix}$$

Figure 83. Block Diagram for Closed-Loop Subsystems

Substituting equation (177) into equation (174) gives:

$$\dot{X}_n = \overline{A}_n X_n + A_{n\ n-1} X_{n-1} + \overline{A}_{n\ n+1} X_{n+1} + B_n H_n U_{nc} , \qquad (178)$$

where

$$\overline{A}_n = A_n - B_n H_n F_n ,$$

$$\overline{A}_{n\ n+1} = A_{n\ n+1} - B_n H_n G_n .$$

$A_{n\ n+1}$ in equation (178) can be factored by B_n and H_n as:

$$A_{n\ n+1} = B_n\ H_n\ G_n . \qquad (179)$$

By using equation (178), G_n can be selected such that

$$\overline{A}_{n\ n+1} = 0 . \qquad (180)$$

H_n and F_n can be selected by the pole placement technique such that the closed-loop local subsystem meets the performance specifications.

Examples for the Design of Local Controllers

To illustrate the advantage of using the auxiliary dynamic model, simple numerical examples in the design of a distributed control system were solved for a two-span web transport system. Two cases were considered.

Case 1: Using the auxiliary dynamic model.

Case 2: Using the original mathematical model.

Consider the two-span system as shown in Figure 84. The control U_1 is considered as the master speed control and assumed to be controlled perfectly to guarantee no velocity variance in v_1, i.e. $V_1 = 0.0$.

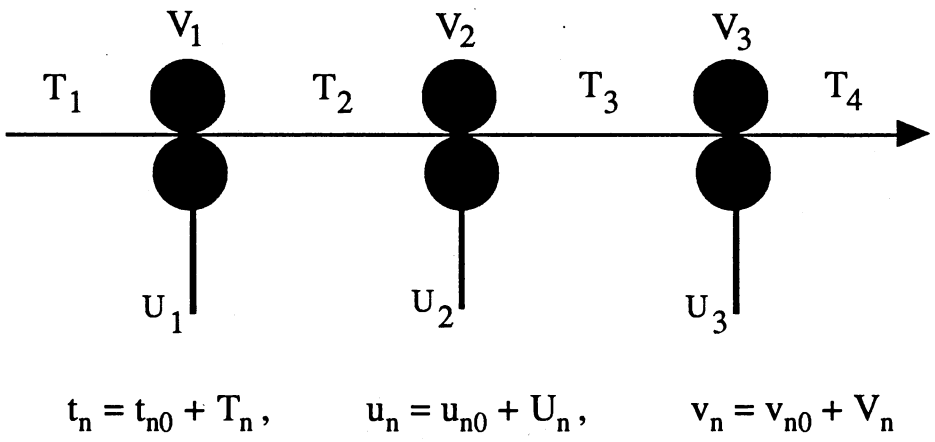

Figure 84. A Two-Span Web Transport System

Assume that desired closed-loop transfer functions for subsystems s_n, n=2,3, were given as:

$$Y_n = \frac{100}{s^2 + 14\,s + 100}\ U_{nc}\ ,\ \text{for } n = 2, 3\ , \qquad (181)$$

And $U_{2c} = T_{2ref} = 0$, and $U_{3c} = T_{3ref} = 0.0$.

Case 1: Using the auxiliary dynamic model.

The auxiliary dynamic model for the two-span system shown in Figure 84 is:

$$\dot{X}_n = A_n X_n + A_{n\,n-1} X_{n-1} + A_{n\,n+1} X_{n+1} + B_n U_{n\,n-1}, \qquad (182)$$

$$Y_n = C_n X_n , \qquad (183)$$

where

$$X_n = \begin{bmatrix} T_n \\ V_{n\,n-1} \end{bmatrix}, \quad B_n = \begin{bmatrix} 0 \\ 1 \end{bmatrix}, \quad C_n = [\,1 \;\; 0\,]$$

$$A_n = \begin{bmatrix} -\frac{v_{n0}}{L_n} & \frac{AE}{L_n} \\ -2\frac{R^2}{J} & -\frac{B_f}{J} \end{bmatrix}, \; A_{n\,n-1} = \begin{bmatrix} \frac{v_{n-1\,0}}{L_n} & 0 \\ \frac{R^2}{J} & 0 \end{bmatrix}$$

$$A_{n\,n+1} = \begin{bmatrix} 0 & 0 \\ \frac{R^2}{J} & 0 \end{bmatrix}$$

and n = 2, 3.

The operating conditions and parameter values used for the design are given in Table 1.

When X_{n-1} and X_{n+1} are assumed zero, the closed-loop transfer function for the n-th subsystem can be obtained using equations (178)

through (180) as:

$$Y_n = \frac{a_0}{s^2 + a_1 s + a_0} U_{nc},\ n = 2,3\ , \qquad (184)$$

where

$$a_0 = \frac{v_{n0}}{L_n}\left(\frac{B_f}{J} + H_n f_n^2\right) + \frac{AE}{L_n}\left(2\frac{R^2}{J} + H_n f_n^1\right),$$

$$a_1 = \frac{v_{n0}}{L_n} + \frac{B_f}{J} + H_n f_n^2, \text{ and } \quad F_n = [\, f_n^1 \ \ f_n^2\,].$$

Equating equation (183) and (184) allows us to select H_n and F_n. First of all, by using equation (178), G_n can be selected as:

$$G_n = \frac{1}{H_n}\left[\frac{R^2}{J}\ 0\right],\ n=2,3\ . \qquad (185)$$

The designed controls for local subsystems are:

$$H_n = 0.02381\ ,\ n = 2,3\ . \qquad (186)$$

$$F_n = [\ -1.0661 \quad 517.8496],\ n = 2, 3\ . \qquad (187)$$

With H_n and F_n from equations (186) and (187), the auxiliary control can be obtained by using equation (177) as :

$$U_{n\,n-1} = H_n(U_{nc} - F_n X_n - G_n X_{n+1})\ ,\ n = 2, 3\ .$$

With the auxiliary control $U_{n\,n-1}$, the local control can be obtained as follows using equation (176).

$$U_n = \frac{J_n}{R_n}\,(U_{n\,n-1} + \frac{R_{n-1}}{J_{n-1}}\,U_{n-1})\,,\quad n= 2,\,3\,.$$

It was assumed that $K_n = 1.0$, n= 2, 3. The performance of the controller designed based on the auxiliary dynamic model were determined for a step change in u_1 (i.e., $U_1(0^-) = 0$, $U_1(0^+) = 0.1$ for this example).

Case 2: Using the original model.

The original mathematical model for the system shown in Figure 84 is:

$$\dot{X}_n = A_nX_n + A_{n\,n-1}X_{n-1} + A_{n\,n+1}X_{n+1} + B_nU_n, \qquad (188)$$

$$Y_n = C_nX_n\,,\ n = 2,\,3, \qquad (189)$$

where

$$X_n = \begin{bmatrix} T_n \\ V_n \end{bmatrix},\quad B_n = \begin{bmatrix} 0 \\ \frac{R}{J} \end{bmatrix},\quad C_n = [\,1\ \ 0\,]$$

$$A_n = \begin{bmatrix} -\frac{v_{n0}}{L_n} & \frac{AE}{L_n} \\ -\frac{R^2}{J} & -\frac{B_f}{J} \end{bmatrix},\ A_{n\,n-1} = \begin{bmatrix} \frac{v_{n-1\,0}}{L_n} & -\frac{AE}{L_n} \\ 0 & 0 \end{bmatrix},\ A_{n\,n+1} = \begin{bmatrix} 0 & 0 \\ \frac{R^2}{J} & 0 \end{bmatrix}.$$

With original mathematical model represented by equations (188) and

(189), the control for the n-th subsystem can be given as:

$$U_n = H_n(U_{nc} - F_nX_n - G_nX_{n+1}) . \qquad (190)$$

Following similar procedures as those of case 1,

$$G_n = \frac{1}{H_n}[R \;\; 0] \;, n = 2, 3 \;, \qquad (191)$$

And

$$H_n = 0.4475 \;, n = 2, 3 \qquad (192)$$

$$F_n = [\; -0.138 \quad 517.8496] \;, n = 2, 3 \;. \qquad (193)$$

The performance of the controller designed based on the original model were determined for a step change in u_1 (i.e., $U_1(0^-) = 0$, $U_1(0^+) = 0.1$ for this example).

The solutions for the examples are given in Figures 85 and 86. When the auxiliary model is used in the controller design, control signals (U_2, U_3) are generated such that they induce necessary velocity difference between rollers just enough for the required tension variations in the web span.

In conclusion, when the auxiliary model was used in the control design, a change in control, U_1 (from 0.0 to 0.1) did not affect the closed-loop system performance in T_2 and T_3, whereas it did in the case when the original model was used in the design of control system.

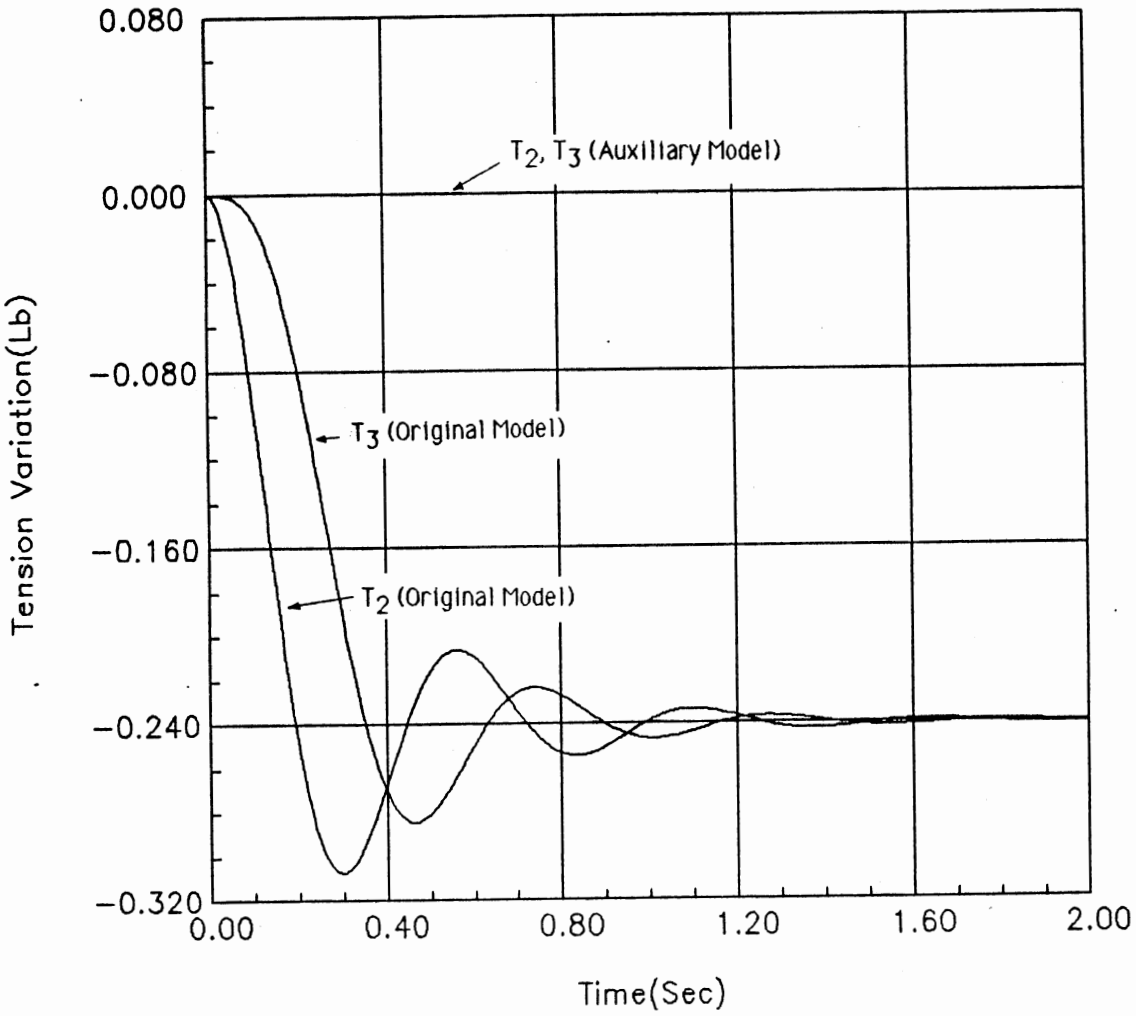

Figure 85. Tension Variations: with Auxiliary and Origin Model

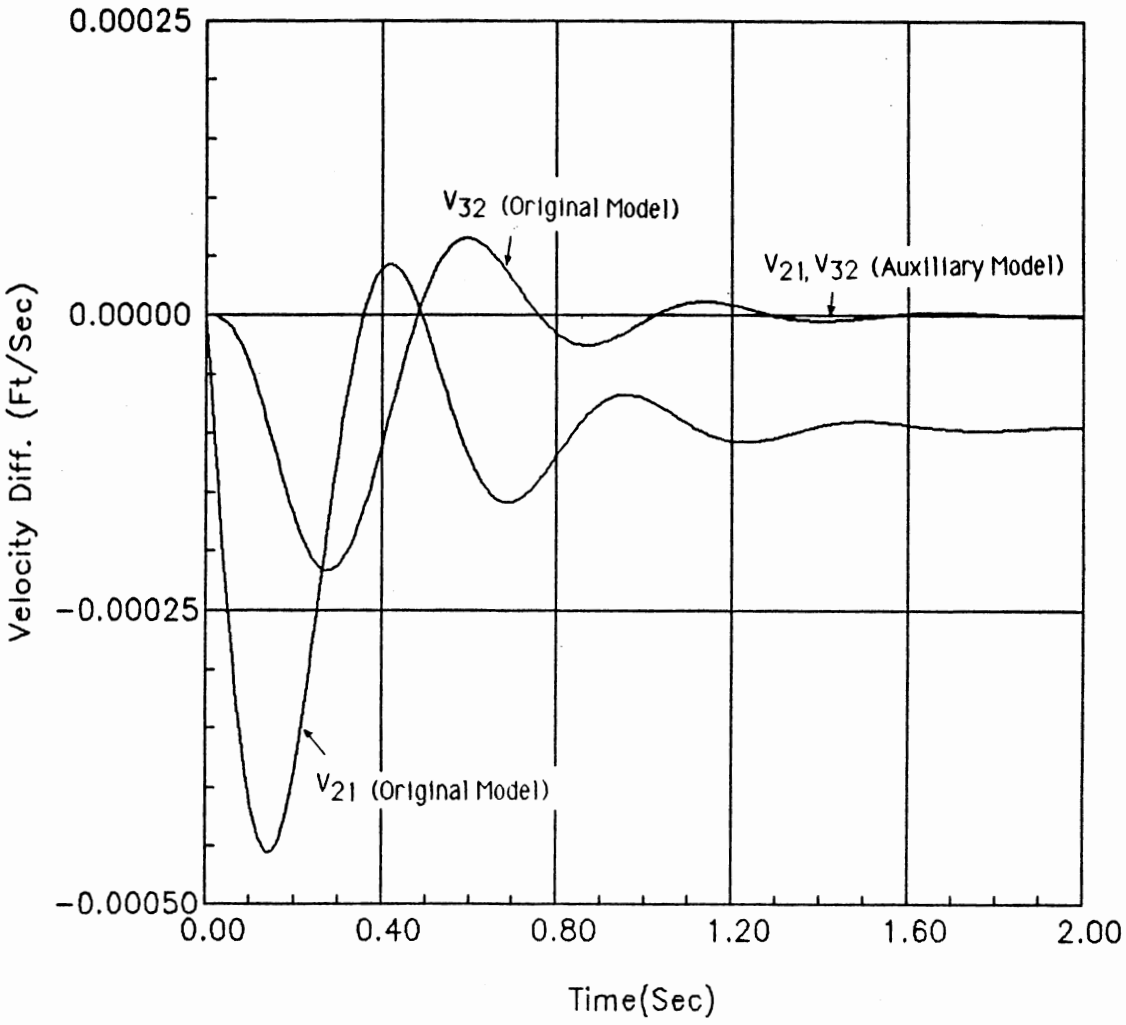

Figure 86. Differences between the Roller Velocities at the Ends of a Web Span: with Auxiliary and Original Model

One disadvantage of using velocity difference as a control variable for tension control is that the magnitude of velocity difference is very small, and so measurement must be very accurate.

Stability of Overall System

A set of local controllers to be designed for the distributed tension control system should guarantee not only the required performance specifications for each subsystem but also the stability of the overall combined system. The problem of designing local controllers in the distributed control system was considered in section 7.3. In this section the problem of stability of the overall system will be considered when all closed-loop subsystems are combined.

Practically, it is almost impossible to completely reject disturbances from adjacent subsystems when each local controller is designed for a multi-span system. Even though each subsystem is designed to be stable, the stability of the overall closed-loop multi-span system is not generally guaranteed since the subsystems are coupled through the continuous web. The basic idea is to find the eigenvalues of the closed-loop local controllers in the overall system which reduce the effect of interactions between subsystems to the minimum. The concept of global BIBO (bounded-input bounded-output) stability where, whenever the input and the initial conditions are bound, the output is guaranteed to be bounded [28] will be used to develop a stability condition for the combined overall web transport system. An essential tool in establishing BIBO stability

mathematically is the use of inequalities. The Bellman-Gronwall inequality [29] will be employed to treat the problem of overall system stability in the proposed study. And it is necessary to define the norm of a real vector in order to use the Bellman-Gronwall inequality.

Let R^n denote the n-dimensional vector space. If a certain norm of a real vector $X \in R^n$ is defined as $\| X \|$, then the induced matrix norm $\| A \|$ of a matrix $A \in R^{mn}$ is defined as [30]:

$$\| A \| = \sup_{\substack{x \neq 0 \\ x \in R^n}} \frac{\| AX \|}{\| X \|} = \sup_{\|X\|=1} \| AX \| = \sup_{\|X\|<1} \| AX \| . \qquad (194)$$

Selecting the definition of $\| X \|$ as :

$$\| X \| = \sum_i | X_i | , \qquad \text{(absolute sum)} \qquad (195)$$

where X_i, i=1,2,...,n denotes the elements of the vector.

The corresponding induced norm is given by:

$$\| A \| = \max_j \{ \sum_i | a_{ij} | \} \text{ (column sum)} \qquad (196)$$

where a_{ij}, i = 1, 2,..,m, j = 1, 2,...,n denotes the entry of the matrix A.

Now, consider the mathematical model for the n-th closed-loop subsystem developed in section 7.3 (equation 178) again:

$$\dot{X}_n = \overline{A}_n X_n + A_{n\,n-1} X_{n-1} + \overline{A}_{n\,n+1} X_{n+1} + B_n H_n U_{nc} \,, \qquad (197)$$

where

$$\overline{A}_n = A_n - B_n H_n F_n \,,$$

$$\overline{A}_{n\,n+1} = A_{n\,n+1} - B_n H_n G_n .$$

Define the transition matrix of the n-th closed-loop subsystem as:

$$\Phi_n(t) \equiv \exp (\overline{A}_n t) . \qquad (198)$$

Then, the solution for equation (197) can be written as :

$$X_n(t) = \Phi_n(t)\, X_{n0} + \int_0^t \Phi_n(t-h)\left[B_n H_n U_{nc}(h) + A_{n\,n-1} X_{n-1}(h) + \overline{A}_{n\,n+1} X_{n+1}(h)\right] dh \qquad (199)$$

The problem is to find the control law represented as :

$$U_{n\,n-1} = H_n(U_{nc} - F_n X_n - G_n X_{n+1}), \qquad (200)$$

where n=1,2,...,N such that the combined system is asymptotically stable.

The eigenvalues of the $\overline{A}_n = A_n - B_n H_n F_n$ can be selected by using the pole placement technique in the left half of the s-plane so that the transition matrix satisfies the following inequality:

$$\| \Phi_n(t) \| \le \beta_n \exp (- \alpha_n t) , \text{ for } \alpha_n > 0 \text{ and } \beta_n > 0 . \qquad (201)$$

where - α_n denotes the negative real part of eigen value nearest to the j ω-axis of the n-th closed-loop subsystem matrix $\overline{A}_n$.

Performing norm to both sides of equation (199) gives:

$$\| X_n(t) \| = \| \Phi_n(t) \| \| X_{n0} \| + \int_0^t \| \Phi_n(t-h) \| \left[\| B_n \| \| H_n \| \| U_{nc}(h) \| + \| A_{n\,n-1} \| \| X_{n-1}(h) \| + \| \overline{A}_{n\,n+1} \| \| X_{n+1}(h) \| \right] dh \tag{202}$$

Assume that the reference inputs for the subsystem are bounded, and let

$$\| U_{nc}(t) \| \leq \delta_{nc} \| X_n(t) \| \ , \tag{203}$$

where δ_{nc} is a positive constant. Equations (199) and (201) make this assumption possible.

Substituting equations (201) and (203) into equation (202) gives:

$$\| X_n(t) \| = \beta_n \exp (- \alpha_n t) \| X_{n0} \| + \int_0^t \beta_n \exp[-\alpha_n(t-h)] \left[\| B_n \| \| H_n \| \delta_{nc} \| X_n(h) \| + \| A_{n\,n-1} \| \| X_{n-1}(h) \| + \| \overline{A}_{n\,n+1} \| \| X_{n+1}(h) \| \right] dh \tag{204}$$

Aggregating N equations of equation (204), the inequality of the combined system is formed as:

$$X(t) \le M X_0 + \int_0^t M P(t-h) Q X(h)\ dh\ , \qquad (205)$$

where

$$X = [\ \| X_1 \| ,..., \| X_N \|\ ]^T$$

$$X_0 = [\ \| X_{1,0} \| ,..., \| X_{N,0} \|\ ]^T$$

$$M = \text{diag}\ \{\ \beta_1,...,\beta_N\ \}$$

$$P(t) = \text{diag}\{\ \exp\ (\ -\ \alpha_1\ t\ ),..., \exp\ (\ -\ \alpha_N\ t\ )\}$$

$$Q = \begin{bmatrix} q_{11} & q_{12} & 0 & \dots & \dots & 0 \\ q_{21} & q_{22} & q_{23} & 0 & \dots & 0 \\ \dots & \dots & \dots & \dots & \dots & \dots \\ 0 & \dots & q_{N-2\ N-3} & q_{N-2\ N-2} & q_{N-2\ N-1} & 0 \\ 0 & \dots & 0 & q_{N-1\ N-2} & q_{N-1\ N-1} & q_{N-1\ N} \\ 0 & \dots & \dots & 0 & q_{N\ N-1} & q_{NN} \end{bmatrix}$$

and

$q_{11} = \|B_1\|\ \|H_1\|\ \delta_{1,c}$, $\quad q_{12} = \|\bar{A}_{1,2}\|$

$q_{21} = \|A_{21}\|$, $\quad q_{22} = \|B_2\|\ \|H_2\|\ \delta_{2c}$, $\quad q_{23} = \|\bar{A}_{23}\|$

$q_{N-2\ N-3} = \|A_{N-2\ N-3}\|$, $\quad q_{N-2\ N-2} = \|B_{N-2}\|\ \|H_{N-2}\|\ \delta_{N-2\ c}$, $\quad q_{N-2\ N-1} = \|\bar{A}_{N-2\ N-1}\|$

$q_{N-1\ N-2} = \|A_{N-1\ N-2}\|$, $\quad q_{N-1\ N-1} = \|B_{N-1}\|\ \|H_{N-1}\|\ \delta_{N-1\ c}$, $\quad q_{N-1\ N} = \|\bar{A}_{N-1\ N}\|$

$q_{N\ N-1} = \|A_{N\ N-1}\|$, $\quad q_{NN} = \|B_N\|\ \|H_N\|\ \delta_{Nc}$.

Applying the norm operation to equation (205) yields:

$$\| X(t) \| \leq \| M \| \| P(t) \| \| X_0 \| + \int_0^t \| M \| \| P(t-h) \| \| Q \| \| X(h) \| dh \tag{206}$$

Using the definition of the induced norm operation gives:

$$\| M \| = \max \{ \beta_1, \ldots, \beta_N \} = \beta_{max}, \tag{207}$$

$$\| P(t) \| = \max \{ \exp (- \alpha_1 t), \ldots, \exp (- \alpha_N t) \} = \exp (- \alpha_{min} t), \tag{208}$$

$$\| Q \| = \max_j \{ \| B_j \| \| H_j \| \delta_{jc} + \| \overline{A}_{j-1\, j} \| + \| A_{j+1\, j} \| \}, \tag{209}$$

where $j = 1, \ldots, N$, and $\| \overline{A}_{01} \| = 0$, $\| A_{N+1\, N} \| = 0$.

Note that $\| \overline{A}_{j-1\, j} \| = 0$, $j = 1, \ldots, N$ in the closed-loop system since feedforward control gain G_n was designed such that $\overline{A}_{n\, n+1} = 0$, $n = 1, \ldots, N$ in equation (197).

Substituting equations (207) and (208) into (206) yields:

$$\| X(t) \| \leq \beta_{max} \exp(- \alpha_{min} t) \| X_0 \| + \int_0^t \beta_{max} \exp [- \alpha_{min} (t - h)] \| Q \| \| X(h) \| dh \tag{210}$$

Multiplying both sides of equation (210) by $\exp(\alpha_{min} t)$ gives:

$$\exp(\alpha_{min}\, t)\| X(t) \| \le \beta_{max} \| X_0 \| + \int_0^t \beta_{max} \| Q \| \exp(\alpha_{min}\, h) \| X(h) \| dh \tag{211}$$

Using the Bellman-Gronwall Lemma [29] in equation (211) gives:

$$\exp(\alpha_{min}\, t)\| X(t) \| \le \beta_{max} \| X_0 \| \exp\left[\int_0^t \beta_{max} \| Q \| dh \right] . \tag{212}$$

or

$$\exp(\alpha_{min}\, t)\| X(t) \| \le \beta_{max} \| X_0 \| \exp[\beta_{max} \| Q \| t] . \tag{213}$$

Multiplying both sides of equation (213) by $\exp(-\alpha_{min}\, t)$ gives:

$$\| X(t) \| \le \beta_{max} \| X_0 \| \exp[-(\alpha_{min} - \beta_{max} \| Q \|) t] . \tag{214}$$

Thus, in order to have the combined system asymptotically stable in equation (214), the following condition should be met:

$$\alpha_{min} > \beta_{max} \| Q \|, \tag{215}$$

where

$\| Q \| = \max_j \left\{ \| B_j \| \| H_j \| \delta_{jc} + \| \overline{A}_{j-1\, j} \| + \| A_{j+1\, j} \| \right\}$, $j = 1,...,N$, and

$\| \overline{A}_{01} \| = 0$, $\| A_{N+1\, N} \| = 0$.

From the stability condition represented in inequality (215), it is interesting

to note that the asymptotic stability of the overall closed-loop system depends on the local control (α_n, H_n), the magnitude of local inputs, and the degree of interconnections between subsystems, $\| A_{ij} \|$.

In summary, a set of local controls in the distributed control system represented in equations (176) and (177) asymptotically stabilizes the combined overall system if the control parameters H_n, F_n, G_n, n = 1,...,N are selected such that:

(1) Reference input U_{nc} , n = 1,...,N are bounded,

(2) $\| \Phi_n(t) \| \leq \beta_n \exp (- \alpha_n t)$, for $\alpha_n \geq 0$ and $\beta_n \geq 0$, n = 1,..., N

where $- \alpha_n$ denotes the negative real part of eigen value of the n-th closed-loop subsystem matrix $\bar{A}_n$ nearest to the j ω-axis,

(3) Let $\alpha_{min} = \min_j \{\alpha_j\}$, and $\beta_{max} = \max_j \{\beta_j\}$, then

$\alpha_{min} > \beta_{max} \| Q \|$, where $\| Q \| = \max_j \{ \| B_j \| \| H_j \| \delta_{jc} + \| \bar{A}_{j-1\, j} \| + \| A_{j+1\, j} \| \}$,

j = 1,..., N and $\| \bar{A}_{01} \| = 0$, $\| A_{N+1\, N} \| = 0$.

The dominant pole of the required closed-loop subsystem α_n can be selected as shown in (2) in the above summary. But, also note that the local controls may be readjusted further to the left in the left-half of the s-plane according to the magnitude of inputs and gains of a local controller, and the degree of interconnections between subsystems as shown in (3) and in Figure 87. The feedforward control was used to reject disturbances from adjacent subsystems, which makes it possible to reduce the feedback control effort to overcome the interaction at each subsystem.

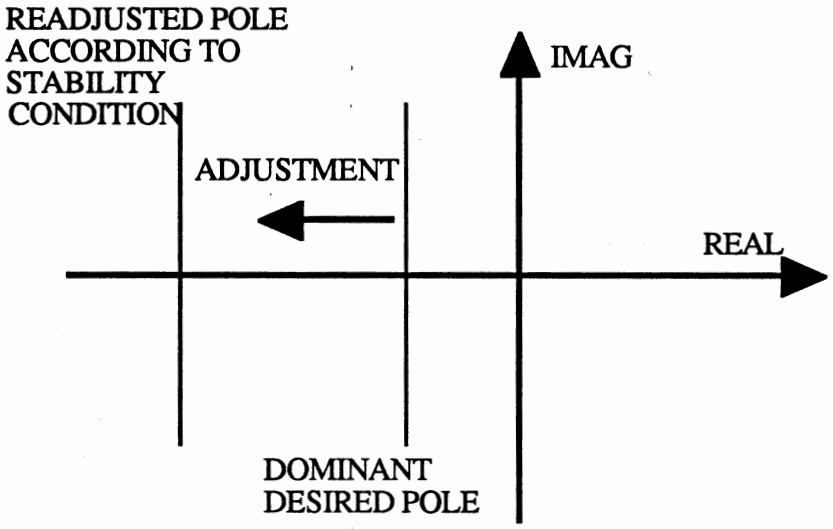

Figure 87. Readjustment of Local Control

Once the set of local controllers is designed such that they together meet the stability condition (3) above, the stability of the overall system is guaranteed even though there is a small change of control in one of subsystems as far as the magnitude of change in control does not violate the stability condition (215).

The auxiliary model can be seen as a different representation of the original mathematical model for the same physical system by introducing a new state variable for the velocity difference between two rollers at both ends of a web span. Thus, even though the stability condition (215) was derived using the auxiliary model, it still holds with the original mathematical model.

Distributed Tension Control System

The structure of the distributed tension control system is shown in Figure 88.

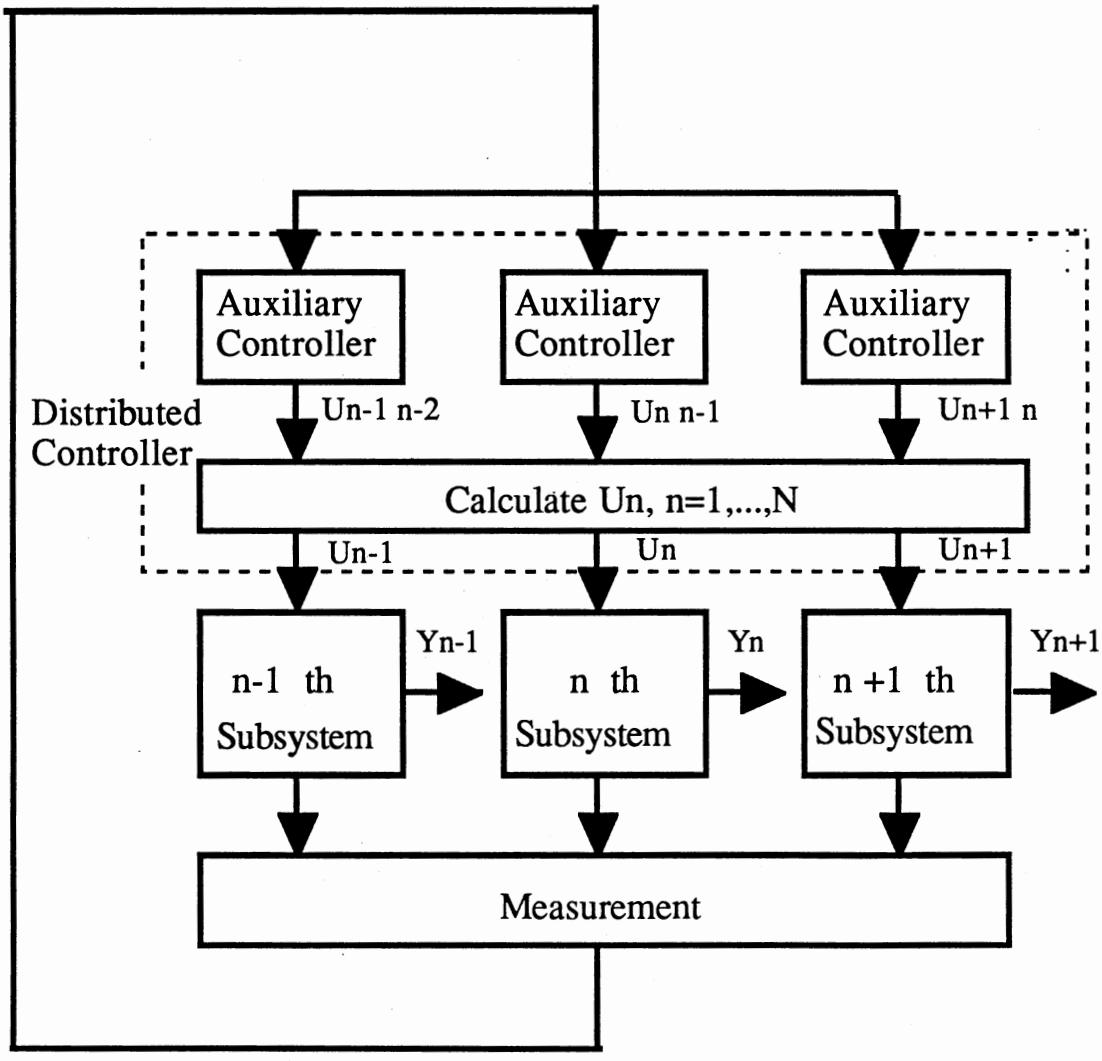

Figure 88. Structure of Distributed Tension Control System

The algorithm of the proposed method for the design of a distributed tension control system can be summarized as follows:

(1) Derive an auxiliary dynamic model from the mathematical model for a unit process by defining a new state variable based on the relative velocity of the ends of the web span.

(2) Design auxiliary local controls which meet the required closed-loop performance specifications of subsystems assuming there are no interactions.

(3) Combine closed-loop subsystems into a composite system and check whether the set of local controllers designed together meet the stability condition for the overall system. If the local controls meet the stability condition then go to (4), otherwise go to the step (2).

(4) Design local controllers using auxiliary controls and the control in the corresponding up-stream subsystem.

A flow chart of the algorithm is shown in Figure 89.

Even though the proposed method of designing the distributed control system was initially developed for the tension control in the multi-span web transport system, this approach can be applied to the control design for the class of the large-scale system in which the subsystems are interconnected. An example will be presented to illustrate an application of the proposed method of design in section 7.6.

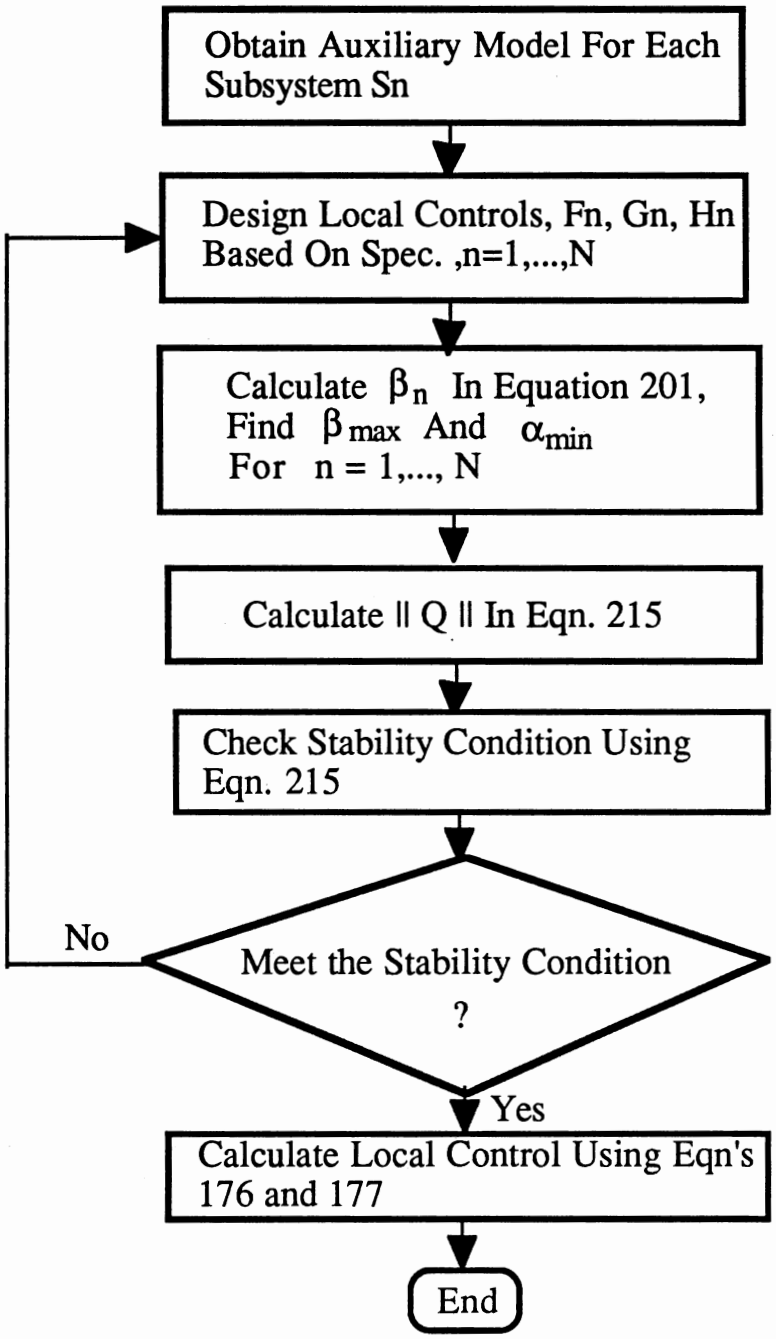

Figure 89. A Flow Chart of the Distributed Tension Control Algorithm

An Example

A method for designing a closed-loop distributed system for the control of web tension in a multi-span web transport system is developed in sections 7.1 through 7.4. The algorithm of the method for the design of distributed control system was summarized in section 7.5. The purpose of this section is (1) to show an application of the method to the design of a distributed control system and (2) to compare the performance of the distributed control system designed by using the proposed method with the performances of existing distributed control systems through computer simulation. Consider a multi-span web transport system which consists of four web spans as shown in Figure 90. The control purpose is to have $T_2 = 1.0$ @ $t = \infty$ without disturbing tensions in other web spans or stability of the overall system. Parameter values and conditions of the system used are in Table 1.

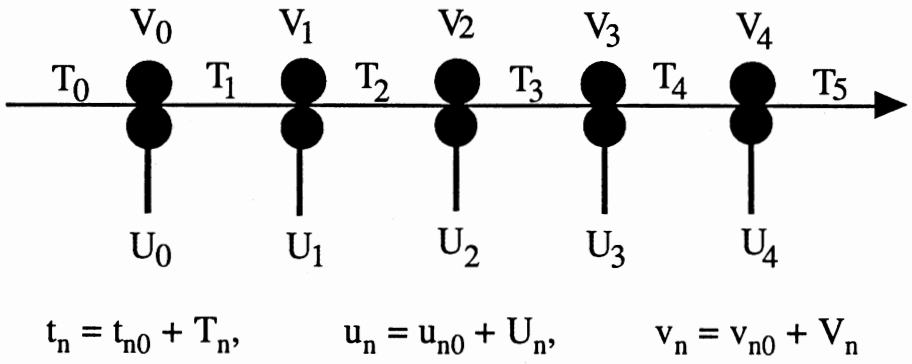

Figure 90. A Multi-Span System: for Example

It is assumed that all four spans have the same length, and all rollers have same moment of inertia, same radius, same frictional coefficient in the related bearing.

Draw Control

Wolfermann and Schroder [5] suggested an application of decoupling and state space control of the speed of the driven roller to improve the performance of draw control. In this example, the tangential velocity of roller is even assumed to be controlled perfectly.

Using equation (22), the mathematical model for the draw control system can be written as:

$$\frac{dT_1}{dt} = -\frac{v_{10}}{L}T_1 + \frac{v_{00}}{L}T_0 + \frac{AE}{L}(V_1 - V_0) . \qquad (216)$$

$$\frac{dT_2}{dt} = -\frac{v_{20}}{L}T_2 + \frac{v_{10}}{L}T_1 + \frac{AE}{L}(V_2 - V_1) . \qquad (217)$$

$$\frac{dT_3}{dt} = -\frac{v_{30}}{L}T_3 + \frac{v_{20}}{L}T_2 + \frac{AE}{L}(V_3 - V_2) . \qquad (218)$$

$$\frac{dT_4}{dt} = -\frac{v_{40}}{L}T_4 + \frac{v_{30}}{L}T_3 + \frac{AE}{L}(V_4 - V_3) . \qquad (219)$$

It was found that 0.0238 ft/min of velocity difference at both ends of web span produced 1.0 lb of steady-state tension variation with the system described by equations (216) through (219). A step velocity input (only in v_2 i.e., V_2 = 0.0238 ft/min) from a steady-state operating condition (1000 ft/min) was provided to the draw control system in order to achieve $T_2(t)$ = 1.0 lb @ t = ∞. Parameter values and conditions of system for simulation are in Table 1. Results from computer simulation is shown in Figure 91. As shown in Figure 91, there were significant unwanted transient tension variations (T_3 and T_4) due to the interactions among web spans.

Draw Control with Progressive Set-Point Coordination Scheme

Open-loop draw control with a progressive set-point coordination scheme is a common distributed control strategy for multi-span web transport systems in the field. In this example, the tangential velocity of roller is also assumed to be controlled perfectly. The mathematical model represented by equations (216) -(219) is still valid, but the set-point for the control of roller velocity in the second span (e.g., v_2) is automatically propagated to the downstream. That is, a step input in v_2 (V_2 = 0.0238 ft/min) to achieve $T_2(t)$ = 1.0 lb @ t = ∞ will cause $V_3 = V_4$ = 0.0238 ft/min. The results from computer simulation are shown in Figure 92. As shown in Figure 92, there were significant unwanted steady-state tension variations (T_3 and T_4) due to the interactions and propagation of disturbances from upstream.

v_{n0} = 1000 for i = 0...5, $V_2(0^-)$ = 1000, $V_2(0^+)$ = 1000.0238 ft/min,

t_{i0} = 0 lbs for i = 0...4, $T_0 = T_5 = 0$ lb

Desired Tension Values: $T_{ides} = 0$ for i = 1,3,4, and $T_{2des} = 1$ lb

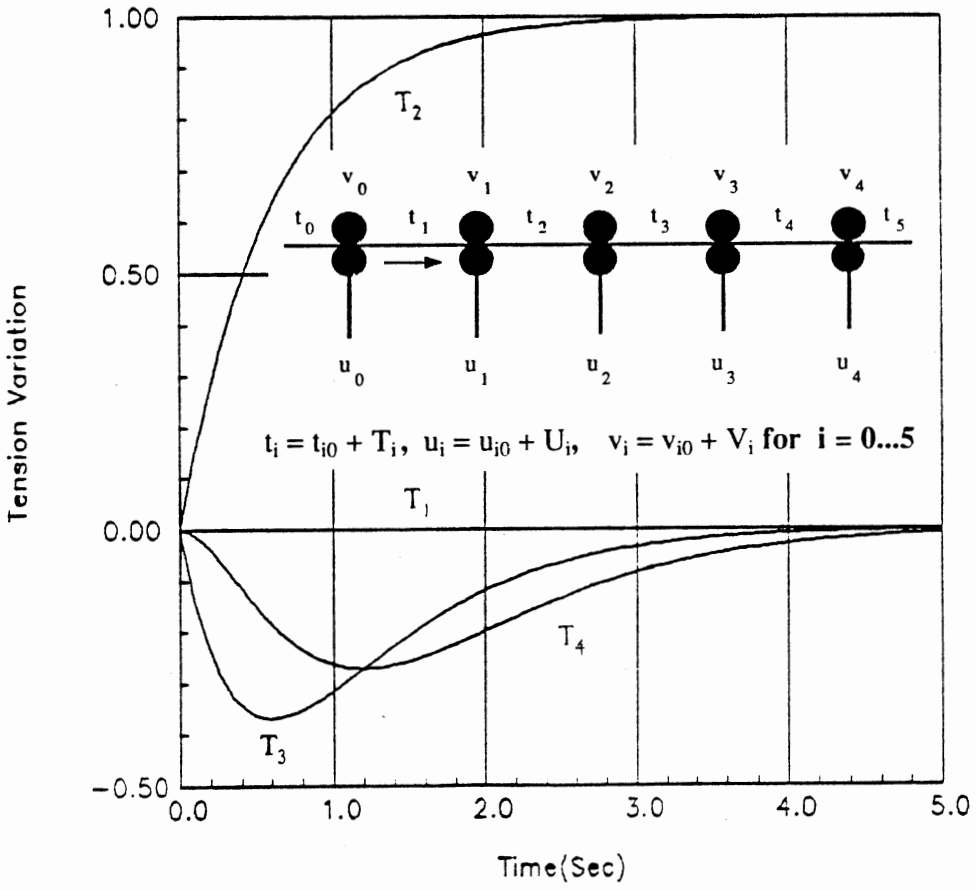

Figure 91. Performance of Distributed Control: Draw Control

v_{n0} = 1000 for i = 0...5, $V_2(0^-)$ = 1000, $V_2(0^+)$ = 1000.0238 ft/min,

t_{i0} = 0 lbs for i = 0...4, $T_0 = T_5 = 0$ lb

Desired Tension Values: $T_{ides} = 0$ for i = 1,3,4, and $T_{2des} = 1$ lb

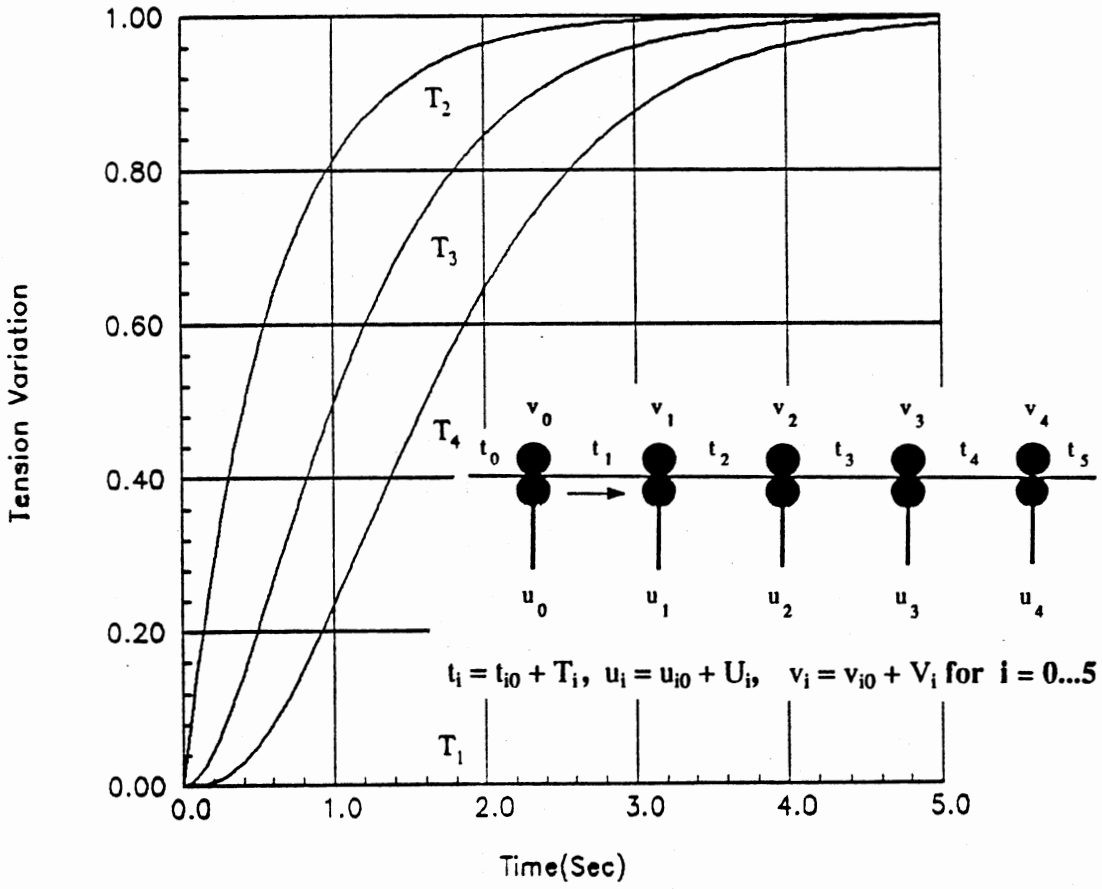

Figure 92. Performance of Distributed Control: Draw Control with Progressive Set-Point Coordination Scheme

Distributed Control System Proposed

All four subsystems are assumed to have the same desired closed-loop behavior for the given system shown in Figure 90 as:

$$Y_n = \frac{100}{s^2 + 14\,s + 100}\,U_{nc} \quad , \text{for} \quad n=1,...,4, \qquad (220)$$

where Y_n is output tensions and U_{nc} is the reference input tensions.

Input tensions, U_{nc}, n = 1,...,4 are assumed to be :

$U_{1c} = 0.0$ lbf.

$U_{2c} = 1.0$ lbf

$U_{3c} = 0.0$ lbf

$U_{4c} = 0.0$ lbf

$\delta_{nc} = 1.0$, n = 1,...,4.

Following the algorithm shown in Figure 89:

(1) Derive auxiliary model [use equation (174) for n=1,...,4] ,

(2) Design F_n, H_n, G_n [use equations (176)- (179)] ,

$H_n = 0.02381$, for n=1,..,4 ,

$F_n = [-1.0661, 517.8496\ ]$, for n=1,...,4 ,

$G_n = \frac{1}{H_n}\,[\frac{R^2}{J}\quad 0\ ]$, for n=1,...,4 ,

(3) Calculate β_{max} and α_{min} [use equation. (201)] ,

$\beta_{max} \cong 589.399$ and $\alpha_{min} = 7$,

(4) Calculate $\| Q \|$ [use equation (215)] ,

$\| Q \| \cong 1.6928$,

(5) Check stability condition [see equation. (215)] ,

$\beta_{max} \| Q \| \cong 997.735 > \alpha_{min} = 7$.

The set of local controllers(F_n, G_n, H_n) designed does not meet the stability condition [inequality equation (215)]. Thus the local controller gains was readjusted. And the poles in desired transfer function was moved farther left in the left-half s-plane to find a control set which together meet the stability condition for the overall system.

Let the new poles be moved to -25 and -4000. Then, the revised desired behavior to be tried became:

$$Y_n = \frac{100000}{s^2 + 4025\, s + 100000}\ U_{nc} .$$

(1) Derive auxiliary model [use equation (174) For n=1,...,4] ,

(2) Design F_n, H_n, G_n [use equations (176)- (179)] with 10 % steady state error ,

$H_n = 21.4286$, for n=1,..,4 ,

$F_n = [1.0345 \ , \ 187.755]$, for n=1,...,4 ,

$G_n = \frac{1}{H_n} [\frac{R^2}{J} \ \ 0]$, for n=1,...,4 ,

(3) Calculate β_{max} and α_{min} [use equation (201)] ,

$\beta_{max} \cong 1.06$ and $\alpha_{min} = 25$,

(4) Calculate $\| Q \|$ [use equation (215)] ,

$\| Q \| \cong 23.1176$,

(5) Check stability condition [see equation. (215)] ,

$\beta_{max} \| Q \| \cong 24.5 < \alpha_{min} = 25$.

This set of local controllers (F_n, G_n, H_n) designed meets the stability condition [inequality (215)] .

Simulation results are shown in Figures 93 and 94. When local controllers together meet the stability criteria (see inequality (215)), tensions were controlled as intended as shown in Figures with 10% of the steady state error. Since the stability condition for this example was so strict in the design of local controllers, 10% of the steady-state error was forced in designing the set of local controllers which meets the stability condition (see inequality (215)).

It is interesting to see that velocity differences, V_{21} and V_{32} (see Figure 94), are negative values even though tension T_2 and T_3 (see Figure 94) are positive. It is hard to imagine negative velocity difference between the ends of a span for positive tension variation in the "draw control". But the negative velocity differences V_{21} and V_{32} in this example are the results of control effort to compensate the tension disturbances due to the tension transfer from the upstream span.

In conclusion, the proposed design method has the capability to design a stable distributed control system for a class of web transport system. And the distributed control system designed based on the author's proposed method outperformed the draw control system with and without

progressive set-point coordination scheme.

Disadvantages of the proposed method are that the design method is iterative, and it is not easy to find a set of local controllers which meet the stability condition when the number of subsystems is growing.

v_{n0} = 1000 ft/min for i = 0...5, t_{i0} = 0 lbs for i = 0...4, $T_0 = T_5 = 0$ lb

Desired Tension Values: $T_{iref} = 0$ for i = 1,3,4, and $T_{2ref} = 1$ lb

$U_{2c}(0^-) = 0$, $U_{2c}(0^+) = 1$ lb

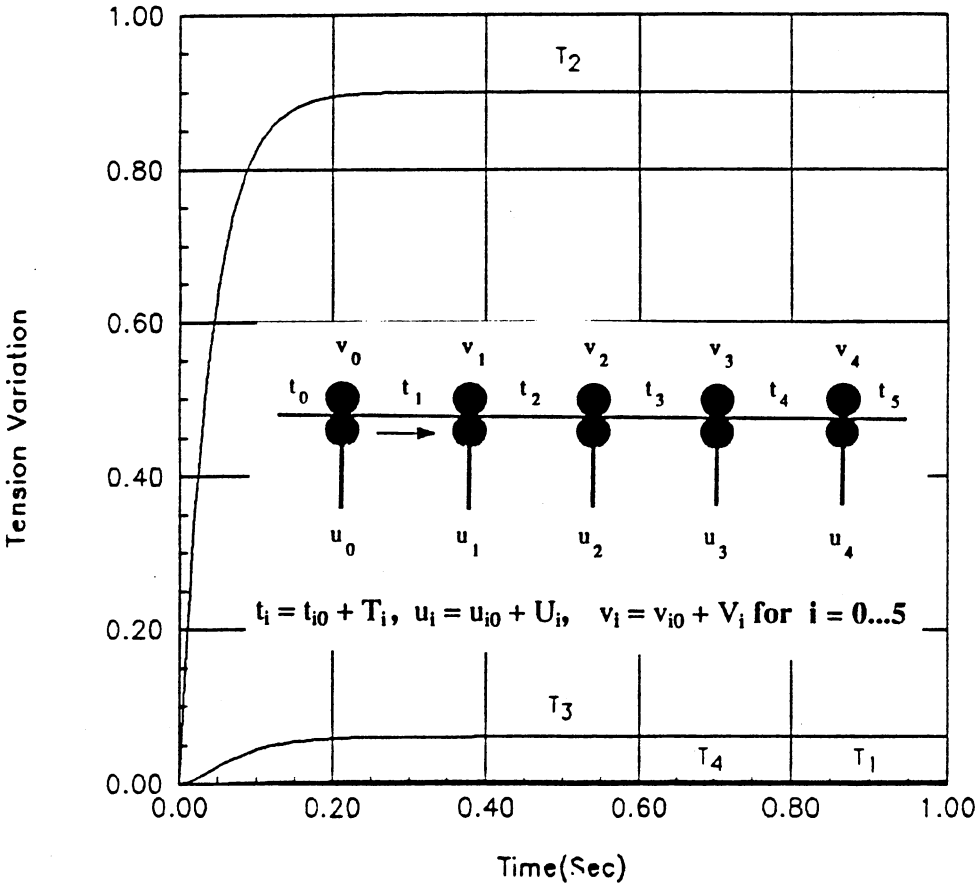

Figure 93. Performance of Distributed Control: with Proposed Method

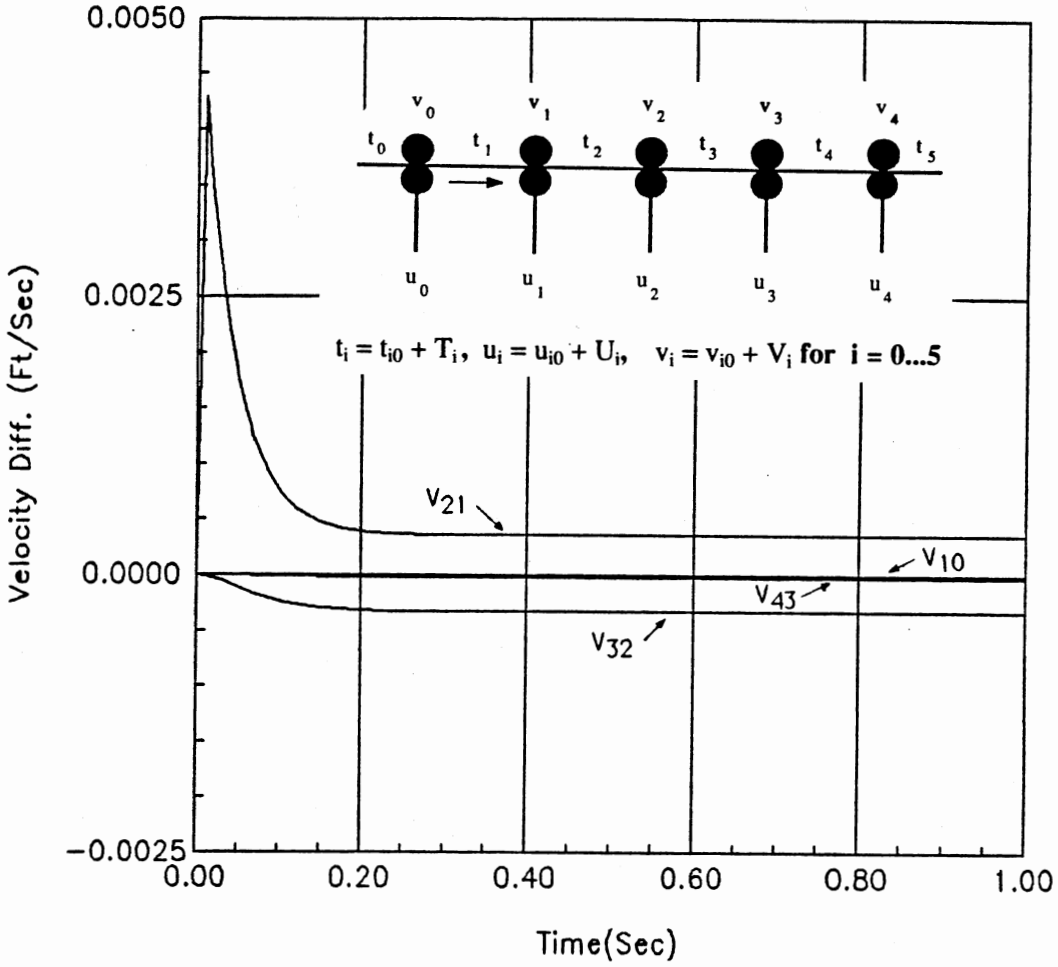

Figure 94. Differences between the Roller Velocities at the Ends of a Web Span: with Proposed Method

CHAPTER VIII

SUMMARY AND CONCLUSIONS

Because of limited previous understanding of longitudinal behavior of the moving web, broad topics related to the problem of tension control have been dealt with in this thesis. The concept of a primitive element was established (see Chapter 2). Primitive elements and multi-span systems were analyzed. Design methods of the tension control systems were developed for single-span systems and for multi-span systems. A computer-based analysis program for web transport systems (WTS) was also developed to help a web handling system engineer/designer analyze the open-loop steady-state and dynamic longitudinal tension variations in multi-span web transport systems.

In Chapter II, mathematical models for primitive elements were derived, and non-ideal effects on tension variations were analyzed. It was found that the effect of cross-sectional area change of web due to Poisson's ratio on tension variation is negligible if the magnitude of strain is small. It was also found that the effect of temperature change on tension variation is significant in plastic film and the effect of moisture variation is significant in paper. The effect of the viscoelastic properties of the web on tension variation was found to be negligible when the web transport speed is high,

and thus, the duration time of the web within a web span is short (less than half a minute). The effect of slippage between the web and a roller on tension variation was studied. A mathematical relation between the velocity of the web and the tangential velocity of a roller was derived when there is slippage. When there is slippage between the web and a roller, the tension is transferred not only from upstream to downstream, but also from downstream to upstream across the roller. A change in the tangential velocity of the roller (W_2, Figure 14) produces smaller degree of dynamic interaction between t_2 and t_3 (see Figure 15) than would occur with no-slippage.

In Chapter III, a "unified" open-loop dynamic model was derived for an important multi-span system that includes a dancer. This model includes the combined effects of slippage, temperature variation, and moisture variation. The model was evaluated for a typical web material (Polypropylene) and typical web transport system operating conditions. By using the unified model developed, the dancer was evaluated as a tension measuring system or a disturbance minimizing system. Guidelines for designing a dancer were obtained for either a tension measuring system or a disturbance minimizing system.

In Chapter IV, the interaction between web spans in multi-span web transport systems was analyzed by using the mathematical model developed. It was found that the tension is transferred from an upstream span down to the following web span. Adjacent web spans interact through the intermediate roller. These interactions, tension transfer and interaction of adjacent web spans through the intermediate roller, were confirmed through experimental work at a Polypropylene web processing system.

In Chapter V, a computer-based analysis program for web transport systems (WTS) was developed. WTS has features of (1) automatic assembly of primitive elements into a system or a subsystem, (2) automatic generation of a mathematical model of the assembled system, (3) steady-state and dynamic analysis of the configured system (assembled system), (4) graphical presentation of the configured system and analysis output, (5) user friendly interfaces.

In Chapter VI, a fixed-gain PID controller for a typical single-span system (time-invariant system) and a variable-gain PID controller for a winding section (time-varying system) were designed to overcome disturbances and produce accurate tension control in the appropriate span. It was demonstrated that the feedforward scheme would reject certain disturbances. A fixed-gain PID controller with feedforward feature was shown to be adequate for a time-invariant unit process. A variable-gain PID controller produced a desired solution for a system with a time-varying parameter (i.e., a winding roll with increasing radius).

In Chapter VII, a method for the design of a distributed system for the tension control in multi-span systems was developed. A new concept of an "auxiliary dynamic model" was introduced in the design of the distributed control system. The auxiliary dynamic model was derived from the original mathematical model by introducing a new state variable. This new state variable denotes the relative velocity between the ends of a web span. The auxiliary dynamic model is used to design an "auxiliary control" for each local controller, which makes it possible to maintain the desired tension level in each web span and to guarantee the stability of the overall

system. A stability condition was derived for the design of a closed-loop distributed control system for a multi-span web transport system. It was found that the asymptotic stability of the overall closed-loop system depends on the gains of local controllers, the magnitude of local inputs, and the degree of interconnections.

Contributions of Most Significance

The most significant contribution of this thesis is the development of a method for the design of a distributed control system for the tension control in multi-span web transport systems (Chapter VII). A stability condition derived for the design of a distributed control system says that the asymptotic stability of an overall closed-loop system depends on the gains of local controllers, the magnitude of local inputs, and the degree of interconnections between subsystems. The distributed control system designed by using the method developed in this study could reject disturbances from adjacent web spans due to the tension transfer and interactions of web spans.

The derivation of a "unified" open-loop dynamic model for an important system that includes a dancer is also a significant result. It was assumed that there is no slippage between the web and the dancer roll. This model includes the combined effects of slippage, temperature variation, and moisture variation. By using the model, a dancer was evaluated as a tension measuring system and a disturbance minimizing system. A typical web material (Polypropylene) and typical web transport system operating

conditions were used for the evaluations. Conclusions from the evaluation are as follows:

(a) When the dancer is used for tension measurement, the dancer should be designed such that:

$\omega_t > 3\omega_s$ and $\omega_r > 3\omega_s$

where

ω_r is the natural frequency associated with the rotational inertia of the dancer roll and the effective elastic spring constant of the web entering and exiting the dancer roll,

ω_s is the natural frequency of the system,

ω_t is the natural frequency associated with the translational inertia of the dancer roll and the dancer system spring.

(b) When the dancer is used for minimizing the effects of disturbances on tension in a web span, the dancer should be designed such that:

If $\omega_d < \omega_s$, then $\omega_t > 3\omega_s$, $\omega_r < \frac{1}{3}\omega_d$

If $\omega_d > \omega_s$, then $\omega_t > 3\omega_d$, $\omega_r < \frac{1}{3}\omega_s$

where

ω_d is the frequency of the disturbance.

Various non-ideal effects (e.g., temperature change, moisture change, viscoelastic properties of web) on tension variation and the effect of slippage between the web and rollers on tension variation were investigated. Results indicate that the effect of temperature change on

tension variation was significant in plastic film and the effect of moisture change was significant in paper. The effects of viscoelastic properties of web turned out to be not significant on the tension variation if the duration time of web in a processing section is very short (a few seconds). The effect of slippage between the web and the roller on tension variation was found to be significant.

The interactions between web spans were studied through the computer simulations of the derived mathematical model and experimentally confirmed. The significant effects of slippage between the web and the roller, and the effect of temperature on tension variation in plastic film were confirmed in experimentation.

Finally, the development of a computer-based analysis program for web transport systems (WTS) is another significant contribution from a practical point of view. WTS allows an extensive numerical simulation of several versions of the system, which provides critical information about steady-state and dynamic system behavior without constructing a real version.

Suggestions for Further Study

This thesis concerned itself with aspects of steady-state and dynamic longitudinal behavior of a straight moving web between parallel cylindrical rollers or rolls. Further research is necessary in the area of steady-state and dynamic behavior of a non-straight moving web (e.g., moving web with slack part of web or slack edges) and a moving web between non-

parallel cylindrical roller or rolls.

The analysis of the effects of the uncertainties owing to the imperfection of the mathematical model on tension variation should be studied. For example, the Young's modulus of the web material might have uncertainty in its value. The effects of temperature, moisture, and viscoelastic properties of the web on tension variations have been analyzed individually, but these effects together may increase the degree of imperfection in the mathematical model.

The design method for a distributed control system developed in Chapter VII needs to be improved. The method requires highly accurate measurement of the web velocity. The performance of the control system designed by using this method is very sensitive to the noise in the velocity of the web. An observer to estimate the web velocity using the measurement of tension might be a solution, since tension variation is much less sensitive to the noise in measurement.

There were some limitations in the experimental work for the validation of mathematical model in this thesis since an existing web production line was used. More thorough experimental work using a dedicated experimental set-up is necessary in order to develop and validate a more complete mathematical model with non-ideal effects for various operating conditions and web materials.

WTS needs to be extended to include more features of system analysis (e.g., closed-loop analysis), system optimization, and expert system.

Furthermore, all the analyses and design in this thesis were carried out in the linear continuous region. The areas of nonlinear and discrete

analysis and design require additional study.

Register is the relative position of the impression made by a press unit to the position of the first press unit on the final copy [27]. The area of print register control was not covered but might be interesting.

Finally, all the analysis and design were based on the assumption that the web span can be assumed as being one-dimensional. The area of two-dimensional analysis and design remains wide open to future researchers.

A SELECTED BIBLIOGRAPHY

[1] Grenfell, K.P., "Tension Control on Paper-making and Converting Machinery", Proc., IEEE Ninth Annual Conference on Electrical Engineering in the Pulp and Paper Industry, Boston, Mass. June 20-21, 1963.

[2] Brandenburg, G. "New Mathematical Models for Web Tension and Register Error", Proc. 1, 3rd International IFAC Conf. on Instrumentation and Automation in the Paper, Rubber and Plastics Industries, Brussels, 24-26 May, 1976.

[3] Campbell, D. P. Process Dynamics. John Wiely & Sons, Inc. 1958.

[4] King, D. L. "The Mathematical Model of a Newspaper Press", Newspaper Techniques., pp 3-7, Dec. 1969.

[5] Wolfermann, W. and Schroder, D. "Application of Decoupling and State Space Control in Processing Machines with Continuous Moving Webs", Proc., International Federation of Automatic Control, 1987, Munhen.

[6] Aoki, M., "On Feedback Stabilizability of Decentralized Dynamic System", Automatica, Vol. 8, pp. 163-173. Pergamon Press, 1972.

[7] Wang, S. H. and Davison, E.J. " On the Stabilization of Decentralized Control Systems", IEEE Trans. Automat. Contr., VOl. AC-18, pp,473-478, Oct. 1973.

[8] Siljak, D. and Vukcevic, M. B. "Decentralized Stabilizable Linear and Bilinear Large-Scale Systems", Int. J. Control, Vol. 26,

1977. 289-305.

[9] Chen, B-S. and Lu, H-C. "State Estimation of Large-Scale System", Int. J. Control, Vol. 47, 1988. pp1613-1632.

[10] Sezer, M. E. and Huseyn, O., " Stabilization of Linear Time-Invariant Interconnected Systems Using Local State Feedback", IEEE Trans. Syst. Man Cyber., 8, pp. 751, 1980.

[11] Reid, K. N. , Shelton, J. J. and Shin, K-H. "Distributed Tension Control in Multi-span Web Transport System", Unpubl. Executive Summary for WHRC, 1988.

[12] Plummer, D. W., Modelling and Sensitivity Analysis of the Rewind Portion of a Web Handling Machine, Thesis, Oklahoma State Univ., 1985.

[13] Timoshenko, Young, Weaver, Vibration Problems in Engineering, John Wiley & Sons, New York, 1974

[14] Crandall, H. Stephen, Dahl, Norman C. An Introduction to the Mechanics of Solids, McGraw-Hill Book Company, Inc., New York,1959.

[15] Edited by R. M. Ogorkiewicz, Engineering Properties of Thermoplastics, Wiley-Interscience, A Division of John Wiley & Sons Ltd. London., 1970.

[16] Jantunen, J., "Visco-Elastic Properties of Wet Webs Under Dynamic Conditions", The Finnish Pulp and Paper Research Institute

[17] Fung, Y. C. Foundations of Solid Mechanics, New Jersey, Prentice Hall, 1965.

[18] Taguchi, T, Morimoto, K., Terada, Y.,and Sakamoto, Y. "Web Behavior on Newspaper Web Rotary Presses", Technical

Review , Mitsubishi Heavy Industries LTd., Tokyo Japan, October 1985.

[19] Ferry, J. D. Viscoelastic Properties of Polymers, New York, John Wiley & Sons, Inc., 1961.

[20] Faucher, J. A. "Viscoelastic Behavior of Polyethylene and Polypropylene", Transaction of The Society of Rheology, Vol. 3, pp 81-93, 1959.

[21] McDermott, J., "R1: A Rule-Based Configurer of Computer Systems", Artificial Intelligence, North-Holland, 19:39-88, 1982.

[22] Dixon, J. R. and Simmons, M. K., Computers That Design: Expert Systems for Mechanical Engineers, Computers in Mechanical Engineering, The ASME, New York, NY, 2, 3:3:10-18, 1983.

[23] Mittals S., Dym, C. L., and Morjaria, M., "PRIDE: An Expert System for the Design of Paper Handling Systems", Computer, Vol. 19, No. 7, pp. 102-114, 1986.

[24] Dorf, R. C., Modern Control Systems, Third Ed. Addision Wesley, 1981.

[25] Chen, Y. H. "Large-Scale Uncertain Systems Under Insufficient Decentralized Controllers", Proc. ACC, 1988.

[26] Wahlstrom, B., Juusela, A., Ollus, M. , Narvainen, P. , Lehmus, I. and Lonnqvist, P., "A Distributed Control System and Its Application to a Board Mill", Proc. International Federation of Automatic Control, pp 1-14, 1983.

[27] Oppenheimer, R. H. and George, H. F. "Transfer Equations of the Gravure Press System", Gravure Nip Mechnics, TAGA Proc., 1964, pp 348-360.

[28] Hahn, W. Theory and Application of Lyapunov's Direct Method,

New Jersey: Prentice-Hall, 1963.

[29] Hsu, J. C. and Meyer, A. U. Modern Control Principles and Applications, New York: McGraw-Hill, 1968.

[30] Desoer, C. A. and Vidyasagar, M. Feedback Systems: Input-Output Properties, New York: Academic, 1975.

[31] George, Harvey F, Kimball, John J., and Oppenheimer, Robert H., "Web Tensiometer Frequency Response", Proceedings - Technical Association of the Graphic Arts, 1963, pp 85-101.

[32] Beloit, "Hygroscopic Testing", Beloit Research, Intenal Report, #D85-32, Oct., 1985

[33] Shelton, J. J., Lateral Dynamics of Moving Web, Thesis, Oklahoma State Univ. , 1966

[34] Reski, D. A., " Constant Tension Drives Speed Vinyl Production", Power Transmission Design, Feb. 1979.

[35] Pfeiffer, J. D. "Nip Forces and Their Effect on Wound-in Tension", TAPPI, vol. 60, No. 2, Feb. 1977.

[36] Haglov, Nils J. E. "Web Tension, Rollstandings, and Reel Changing", Proceedings of the PATRA(Printing, Packing and Allied Trades Res. A), pp 65-114, Oct. 1987.

[37] Shin, K-H. "Tension Control in A Moving Web", Unpubl. M.S. Report., Oklahoma State Univ., 1985.

[38] Sandell, Jr. N. , Varaiya, P., Athans, M., and Safonov, M. G. "Survey of Decentralized Control Methods for Large Scale Systems", IEEE Transactions on Automatic Control, 23 (1978), 108-128.

[39] Lasley, E.J. and Michel, A.N. "Input-Output Stability of Interconnected Systems", IEEE Trans. Automat. Contr.,

vol.,AC-21, pp. 84-89, Feb. 1976.

[40] Looze, D. P., Houpt, P. K., Sandel, Jr. N.R. , and Athans, M. "On Suboptimal Decentralized Estimation and Control with Application to Freeway Ramp Monitoring", in Proc. 1977 Joint Automatic Control Conf., San Francisco, CA, !977.

[41] Kosut, R.L. "Suboptimal Control of Linear Time-invarient System Subject to Control Structure Constraints", IEEE Trans., Automat. Contr., Vol. AC-15, pp 557-563, Oct., 1970.

[42] Siljak, D. D., "Stability of Large Scale System", Proceedings of the Fifth IFAC, Congress, pp c-32:1-11, Paris 1972.

[43] Bailey F. N. , "The Application of Lyapunov's Second Method to Interconnected Systems", J. SIAM Control, Ser. A, vol. 3 pp 443-463, 1965.

[44] Luenberger, D. G. "Canonical Forms for Linear Multivariable System", IEEE Trans. Automat. Contr, June. 1967. pp 290-293.

[45] Chen, C. T. Linear System Theory and Design, New York: CBS college. 1984

[46] Sternad, M. and Soderstrom, T., "LQG-Optimal Feedforward Regulators", Accepted for Publication in Automatica, 1988.

[47] Geromel, Jose C. and Yamakami, Akebo, "Stabilization of Continuous and Discrete Linear Systems Subjected to Control Structure Constraints", Int. J. Control, 1982, vol. 63, No. 3, 429-444.

[48] Golub, G. H. and Van Loan, C. F. Matrix Computations, Baltimore, The Johns Hopkins Univ. Press, 1983.

[49] Davison, E. J. , "The Decentralized Stabilization and Control of a

Class of Unknown Non-Linear Time-Varying Systems", Automatica, vol. 10, pp 309-314, May 1974.

[50] Davison, E. J., " Large Scale Control System Design", Proc., FAC Theory and Application of Digital Control, pp 23-30, New Delhi, India 1982.

[51] Ikeda, M. and Siljak, D. D., " Decentralized Stabilization of Linear Time-Varying Systems", IEEE Transactions on Automatic Control, vol. AC-25, No. 1, pp 106-107. Feb. 1980.

[52] Lee, T. N. and Radovic, U. L., "Decentralized Stabilization of Linear Continuous and Discrete-Time Systems with Delays in Interconnections", IEEE Transactions on Automatic Control, vol. 33, No. 8, pp. 757-761.Aug., 1988.

[53] Kwakernaak, H. and Sivan, R., Linear Optimal Control Systems, New York. Wiley-Interscience, a Division of John Wiley & Sons, Inc. 1972.

[54] King, D. L. "The Battle Against Web Breaks", Newspaper Techniques, pp 3-1 & 4-21, March. 1972.

[55] King, D. L. "Web Tension Study at Perscombinatie NV", Newspaper Techniques, pp 8-18, Nov. 1972.

[56] Whitworth, D. P. D. and Harrison, M. C., "Tension Variations in Pliable Material in Production Machinery", Appl. Math. Modeling, Vol. 7. 1983, pp 189-196.

[57] Veits, V. L., Beilin, I. Sh., and Merkin, V. M.,"Mathematical Models of an Elastic Strip in Mechanisms with Flexible Couplings", Soviet Applied Mechanics, Vol. 19, No. 8, pp. 721-726, Aug. 1983.

[58] Soong, T. C. and Li, C., "An Elastic Analysis of Multiroll Endless Web Systems", ASME. Trans. on Journal of Dynamic Systems Measurement and Control, Vol. 101, pp. 308-313,

Dec. 1979.

[59] Martin, J. R., "Tension Control for Web-Off-Set", The Penrose Graphic Arts and International Annual, Vol. 66, pp. 209-214. 1973.

[60] Bryant, G. F. and Higham, J. D., "A Method of Realizable Non-Interactive Control Design for a Five Stand Cold Rolling Mill", Proc., FAC/IFIP Conference on Digital Computer Applications to Process Control, Helsinki, Finland, June, 1971.

[61] Endersby, D. C. and Zucker, E., "Direct Tension Control by Strain Gauges and Disc Brakes for Rewinders", Pulp and Paper Magazine of Canada, Vol. 67, No. 9, pp. 393-398, Sept. 1966.

[62] Henderson, G. M. and Hung, J. C., "Automatic Tension Control for Winding Superconducting Coils", Proc. Southeastconf. Reg. 3. Conf., Roanoke, Va. Apr. 1-4, 1979, Publ. by IEEE (Cat n 79chol432-4 Reg 3), pp 148-153, New York. coden;psrccd.

[63] Sen, P. C. and MacDonald, M. L., "Thyristorized DC Drives with Regenerative Braking and Speed Reversal", IEEE Trans. on Industrial Electronics and Control Instrumentation, Vol. IECI-25, No. 4, Nov. 1978.

[64] Daly, D. A. "Factors Controlling Traction between Webs and Their Carrying Rolls", Tappi, Vol. 48, No. 9, pp 88-90, Sept 1965

[65] Good, K. and Ducotey K. S. "Measurement of Traction between Webs and Rollers", Unpubl. Executive Summary for WHRC, Oct. 1988.

[66] Shelton, J. J. "Dynamics of Web Tension Control with Velocity or Torque Control", Proc. ACC, 1988.

[67] Marhauer, H. H. " The Dynamics of Web-Tension Measurement",

ISA Transaction, Vol. 5. No. 3, pp 242-247, July 1966.

[68] Sezer, M. E. and Siljak, D. D. " Structural Decomposition and Stabilization of Large-Scale Control Systems", Allerton Conf. on Communication Control and Computing Proc., 17th, pp 54-63, 1977.

[69] Davision, E. J. and Ozguner, U. "Characterizations of Decentralized Fixed Modes for Interconnected Systems", Automatica, Vol. 19, No. 2. pp 169-182, 1983.

[70] Chan, W. S. and Desoer, C. A., "Eigenvalue Assignment and Stabilization of Interconnected Systems Using Local Feedbacks", IEEE Transaction on Automatic Control, Vol. AC-24, No. 2, Apr. 1979.

[71] Saeks, R. "On the Decentralized Control of Interconnected Dynamical Systems", IEEE Transactions on Automatic Control, Vol. AC-24, No.2, Apr. 1979.

[72] Melzer, S. M. and Kuo, B. C. "Optimal Regulation of Systems Described by a Countably Infinite Number of Objects", Automatica, Vol. 7, pp 359-366, 1971.

[73] Richter, S., Lefebvre, S, and DeCarlo, R.,"Control of a Class of Nonlinear Systems by Decentralized Control", IEEE Transactions on Automatic Control, Vol. AC-27, No. 2, Apr. 1982.

[74] Chen, Y. H. "Decentralized Robust Control System Design for Large-Scale Uncertain Systems", Int. J. Control, Vol. 47, No. 5, pp 1195-1205, 1988.

[75] Chu, K-C. " OPtimal Decentralized Regulation for a String of Coupled Systems", IEEE Transactions on Automatic Control, June 1974.

[76] Linder, D. K. "Decentralized Control of a Class of Interconnected Systems", Proc. ACC, 1985.

[77] Bhattacharyya, S. P., Del Nero Gomes, A. C., and Howze, Jo. W. "The Structure of Robust Disturbance Rejection Control", IEEE Transactions on automatic Control, Vol. AC-28, No. 9, Sept. 1983.

[78] Reid, K. N. , Shelton, J. J. and Shin, K-H. "Distributed Tension Control in Multi-span Web Transport System." Unpubl., Executive Summary for WHRC, May 1990.

[79] Shin, K. H., Cho, S. H., "A Computer-Based Analysis Program for Multi-Span Web Transport Systems", WHRC Project 8600-10.Report, Oklahoma State Univ., 1990.

APPENDIXES

APPENDIX A

FORCE BALANCE EQUATION

Consider an infinitesimal element of web in region of slip as shown in Figure 95. The forces and angles in the region of slip are shown.

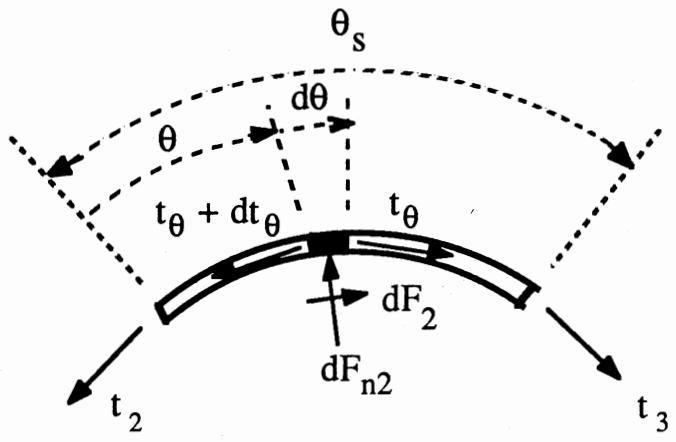

Figure 95. Infinitesimal Element of Web in Region of Slip

Force balance equations can be written as:

$$(t_\theta + dt_\theta) \sin\frac{d\theta}{2} + t_\theta \sin\frac{d\theta}{2} - dF_{n2} = 0 \ . \qquad (221)$$

$$(t_\theta + dt_\theta) \cos\frac{d\theta}{2} - t_\theta \cos\frac{d\theta}{2} - dF_2 = 0 \ . \qquad (222)$$

Angle conditions are:

$$\text{For } d\theta << 1, \ \sin\frac{d\theta}{2} \cong \frac{d\theta}{2} \ , \ \cos\frac{d\theta}{2} \cong 1 \ .$$

From equation (221), since $dt_\theta \frac{d\theta}{2} \cong 0$

$$dF_{n2} = t_\theta \, d\theta \ . \qquad (223)$$

Using angle conditions, equation (222) can be simplified as:

$$dF_2 = dt_\theta \ . \qquad (224)$$

Frictional force can be written as:

$$dF_2 = \mu \, dF_{n2} \ . \qquad (225)$$

From equations (224) and (225)

$$dt_\theta = \mu \, dF_{n2} \, . \tag{226}$$

Combining equations (226) and (223) gives:

$$\frac{dt_\theta}{t_\theta} = \mu \, d\theta \, . \tag{227}$$

Integrating equation (227) gives:

$$\int_{t_\theta}^{t_2} \frac{dt_\theta}{t_\theta} = \int_0^\theta \mu \, d\theta \, , \tag{228}$$

or the tension in the web at location θ

$$t_\theta = t_2 \, e^{-\mu\theta} \quad \text{for} \quad t_2 > t_3 \, . \tag{229}$$

Combining equations (229) and (223) gives:

$$dF_{n2} = t_2 \, e^{-\mu\theta} \, d\theta \, . \tag{230}$$

Integrating equation (230) gives:

$$\int dF_{n2} = \int_0^{\theta_2} t_2 \, e^{-\mu\theta} \, d\theta \, ,$$

or

$$F_{n2} = \frac{1}{\mu}\left(1 - e^{-\mu\theta_s}\right) t_2 \qquad \text{for } t_2 > t_3 ,$$

where

$$0 \le \theta_s \le \theta_w .$$

When $\theta_s = \theta_w$,

$$F_{n2} = \frac{1}{\mu}\left(1 - e^{-\mu\theta_w}\right) t_2, \qquad \text{for } t_2 > t_3 .$$

APPENDIX B

FORCE VELOCITY RELATION

A model of friction between a web and roller with only Coulomb friction is shown Figure 96.

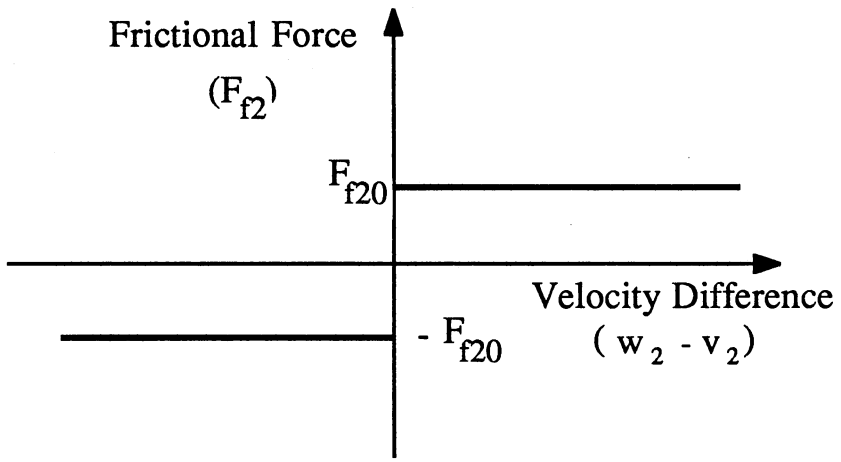

Figure 96. A Model of Friction between a Web and a Roller with only Coulomb Friction

When

$$F_2 = F_{20} \qquad \text{for } |w_2 - v_2| > 0 ,$$

$$t_2 = t_3 + F_{20} .$$

In conclusion, t_2 is not affected by w_2 when there is only Coulomb friction; w_2 cannot be used as a control variable for tension control.

APPENDIX C

STRAIN IN A UNIFIED MODEL

Recall the multi-span system shown in Figure 27. The elastic strain due to the velocity difference in the first web span can be written as:

$$\frac{d}{dt}\{\epsilon^{e}_{2d}(t)\} = -\frac{v_{20}}{L_2}\epsilon^{e}_{2d}(t) + \frac{v_{10}}{L_2}\epsilon^{e}_{1d}(t) - \frac{V_1(t)}{L_2} + \frac{V_2(t)}{L_2}. \qquad (235)$$

$$\frac{d}{dt}\{\epsilon^{e}_{3d}(t)\} = -\frac{v_{30}}{L_3}\epsilon^{e}_{3d}(t) + \frac{v_{20}}{L_3}\epsilon^{e}_{2d}(t) - \frac{V_2(t)}{L_3} + \frac{V_3(t)}{L_3}. \qquad (236)$$

When the dancer has a vertical displacement of x_2, the geometry of the multi-span system is shown in Figure 97. Elastic strain due to the vertical displacement of the dancer can be written as:

$$\epsilon^{e}_{2x}(t) \cong \frac{x_2(t)\sin\frac{\theta_{w2}}{2}}{L_2}. \qquad (237)$$

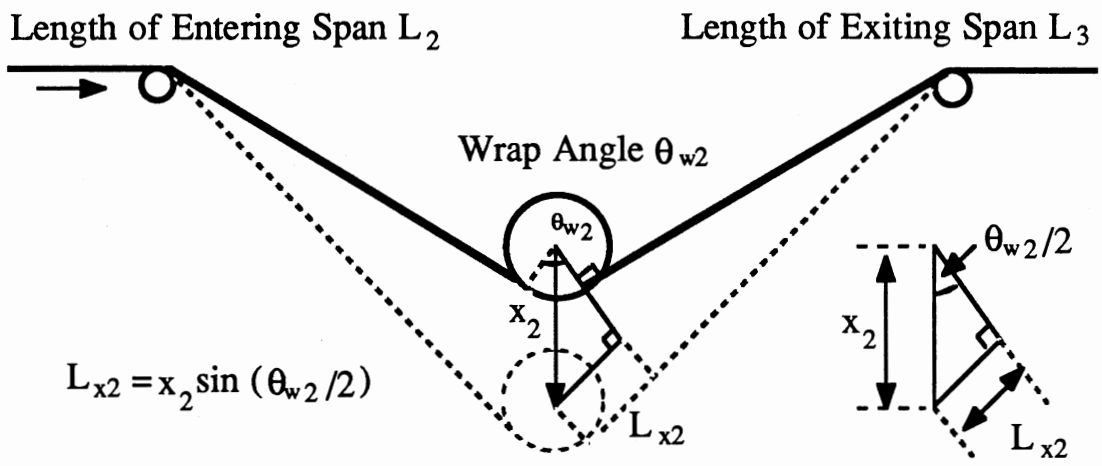

Figure 97. Geometry of the System with a Vertical Displacement of the Dancer in Figure 27

$$\epsilon_{3v}^{c}(t) \cong \frac{x_2(t) \sin\frac{\theta_{w2}}{2}}{L_3}, \qquad (238)$$

where

θ_{w2} : Wrap angle in dancer

x_2 : Vertical displacement of dancer from the equilibrium point.

A free body diagram of the dancer roll is shown in Figure 98. The following equations can be written from the force balance on the roll.

$$M_2\ddot{X}_2 + b_2\dot{X}_2 + k_{s2}X_2 = -(T_2 + T_3)\sin\frac{\theta_{w2}}{2}.$$

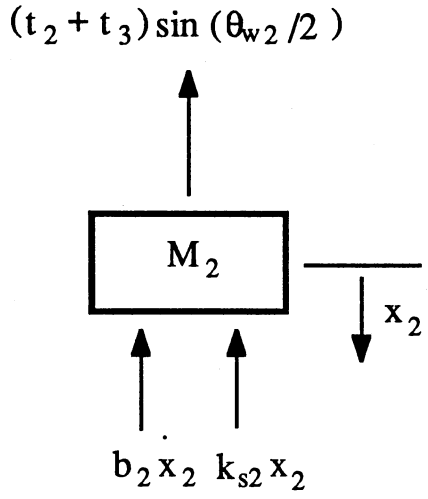

Figure 98. Free Body Diagram of the Dancer Roll: for Force Balance

where $t_n = t_{n0} + T_n$, n = 2, 3.

or let $x_{21} = \dot{x}_2$

$$\dot{x}_2 = x_{21} , \tag{239}$$

$$\dot{x}_{21} = -\frac{b_2}{M_2}x_{21} - \frac{k_{s2}}{M_2}x_2 - \frac{T_2 + T_3}{M_2}\sin\frac{\theta_{w2}}{2} , \tag{240}$$

where $x_{21} = \dot{x}_2$ is the vertical velocity of dancer.

When the dancer has a angular displacement of θ_2, the geometry of the multi-span system is shown in Figure 99. Elastic strain due to the angular displacement of the dancer can be written as:

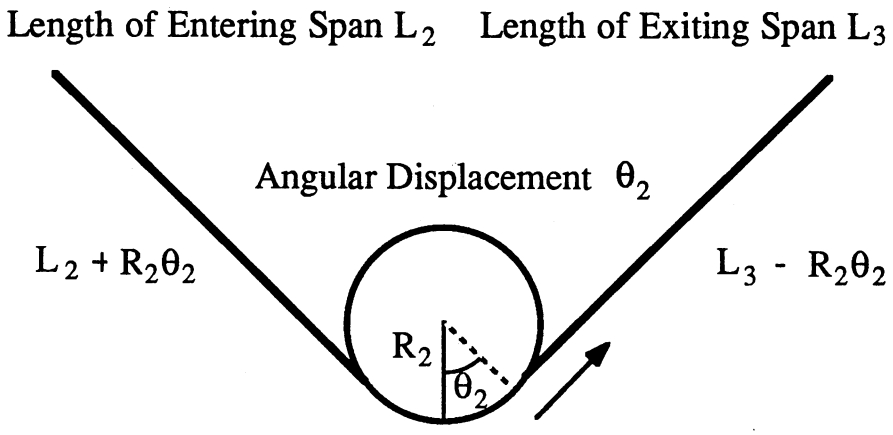

Figure 99. Geometry of the System with an Angular Displacement of the Dancer in Figure 27

$$\epsilon^{e}_{23}(t) \cong \frac{R_2\,\theta_2(t)}{L_2}, \tag{241}$$

$$\epsilon^{e}_{33}(t) \cong -\frac{R_2\,\theta_2(t)}{L_3}, \tag{242}$$

where

θ_2 : Angular disp. of roll .

A free body diagram of the dancer roll is shown in Figure 100. Torque balance in roll can be written as:

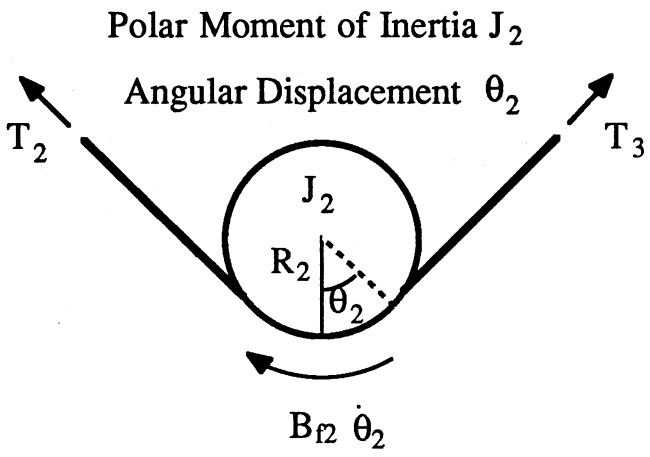

Figure 100. Free Body Diagram of the Dancer Roll: for Torque Balance

$$J_2\ddot{\theta}_2 + B_{f2}\dot{\theta}_2 = R_2(T_3 - T_2) \ ,$$

where

$$J_2 = \frac{1}{2}M_2R_2^2 \ .$$

Or let $y_2 = \theta_2$.

$$\dot{y}_2 = y_{21} \ , \tag{243}$$

$$\dot{y}_{21} = - \frac{B_{f2}}{J_2} y_{21} + \frac{R_2}{J_2}(T_3 - T_2) \ , \tag{244}$$

and

$$W_2 = R_2 y_{21} \ . \tag{245}$$

Thermal Strain

$$\epsilon^t_2(t) = \alpha \ \{F_2(t) - F_{20}\} \ , \tag{246}$$

$$\epsilon^t_3(t) = \alpha \ \{F_3(t) - F_{30}\} \ , \tag{247}$$

where

α : Coefficient of expansion with temperature.

Hygroscopic Strain

$$\epsilon^m_2(t) = \beta \ \{H_2(t) - H_{20}\} \ , \tag{248}$$

$$\epsilon^m_3(t) = \beta \ \{H_3(t) - H_{30}\} \ , \tag{249}$$

where

β : Coefficient of expansion with moisture.

Combining equations (98) - (101) and (235) - (249) gives total strain in spans 2 and 3 as:

$$\frac{d}{dt}\{\epsilon_2(t)\} = -\frac{v_{20}}{L_2}\epsilon_2(t) + \frac{v_{10}}{L_2}\epsilon_1(t) - \frac{V_1(t)}{L_2} + \frac{V_2(t)}{L_2}$$

$$+ \frac{\sin\frac{\theta_{w2}}{2}}{L_2} x_{21}(t) + \frac{v_{20}\sin\frac{\theta_{w2}}{2}}{L_2^2} x_2(t) - \frac{v_{10}\sin\frac{\theta_{w1}}{2}}{L_1 L_2} x_1(t)$$

$$+ \frac{R_2}{L_2} y_{21}(t) + \frac{v_{20}R_2}{L_2^2} y_2(t) - \frac{v_{10}R_1}{L_1 L_2} y_1(t)$$

$$+ \alpha \frac{d}{dt}\{F_2(t)\} + \frac{v_{20}}{L_2}\alpha\{F_2(t) - F_{20}\}$$

$$- \frac{v_{10}}{L_2}\alpha\{F_1(t) - F_{10}\}$$

$$+ \beta \frac{d}{dt}\{H_2(t)\} + \frac{v_{20}}{L_2}\beta\{H_2(t) - H_{20}\}$$

$$- \frac{v_{10}}{L_2}\beta\{H_1(t) - H_{10}\} , \qquad (250)$$

where

$X_{21}(t) = \dot{X}_2(t)$ and $y_2(t) = \theta_2(t)$, $y_{21}(t) = \dot{y}_2(t)$.

Similarly

$$\frac{d}{dt}\{\in_3(t)\} = -\frac{v_{30}}{L_3}\in_3(t) + \frac{v_{20}}{L_3}\in_2(t) - \frac{V_2(t)}{L_3} + \frac{V_3(t)}{L_3}$$

$$+ \frac{\sin\frac{\theta_{w2}}{2}}{L_3} x_{21}(t) + \frac{v_{30}\sin\frac{\theta_{w2}}{2}}{L_3^2} x_2(t) - \frac{v_{20}\sin\frac{\theta_{w2}}{2}}{L_2 L_3} x_2(t)$$

$$- \frac{R_2}{L_3} y_{21}(t) - \frac{v_{30}R_2}{L_3^2} y_2(t) - \frac{v_{20}R_2}{L_2 L_3} y_2(t)$$

$$+ \alpha \frac{d}{dt}\{F_3(t)\} + \frac{v_{30}}{L_3}\alpha\{F_3(t) - F_{30}\}$$

$$- \frac{v_{20}}{L_3}\alpha\{F_2(t) - F_{20}\}$$

$$+ \beta \frac{d}{dt}\{H_3(t)\} + \frac{v_{30}}{L_3}\beta\{H_3(t) - H_{30}\}$$

$$- \frac{v_{20}}{L_3}\beta\{H_2(t) - H_{20}\} . \qquad (251)$$

APPENDIX D

NATURAL FREQUENCY OF A SUBSYSTEM COMPRISING A DANCER ROLL SEPARATING TWO FREE SPANS

Consider a dancer roll seperating two free spans shown in Figure 101.

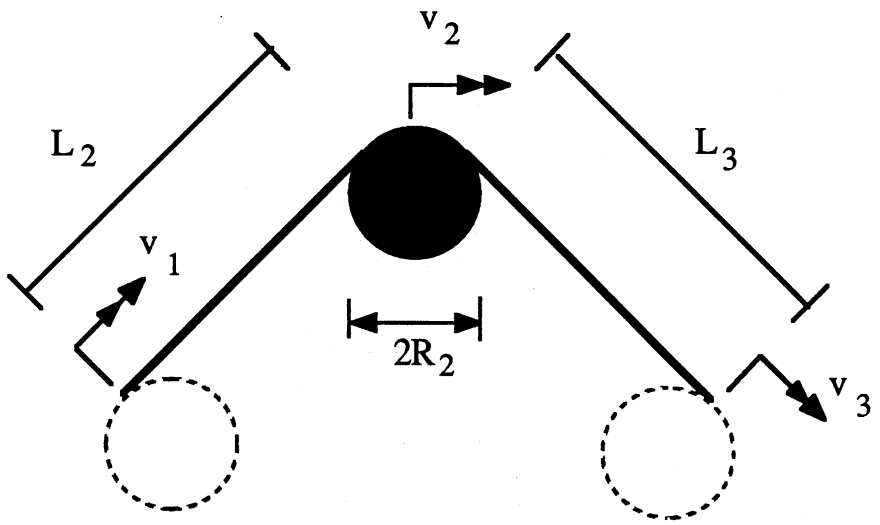

Figure 101. A Dancer Roll Separating Two Free Spans

Assumptions made were:

(1) Web mass is negligible,

(2) Web cross-sectional area is constant,

(3) A no slip region exists between the web and roller,

(4) Transport of strain is neglected,

(5) Friction in the roller bearing is viscous.

Based on these assumptions, the subsystem shown in Figure 101 can be represented by the lumped-parameter model shown in Figure 102. Each web span is represented as a massless elastic spring.

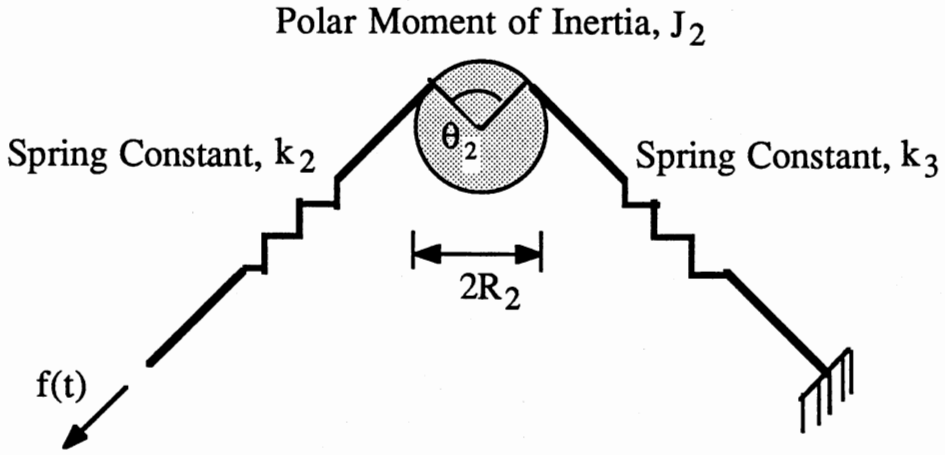

Figure 102. A Lumped-Parameter Model for the Subsystem Shown in Figure 101

A torque balance equation can be written as:

$$J_2 \ddot{\theta}_2 + B_{f2} \dot{\theta}_2 + K \theta_2 = f(t) R_2 , \qquad (252)$$

where

$$K = (k_2 + k_3) R_2^2 , \; k_2 = \frac{A E}{L_2} , \; k_3 = \frac{A E}{L_3} ; \; A2 = A3 = A = d h ,$$

and

B_{f2} is the bearing viscous friction coefficient.

The natural frequency of the subsystem is :

$$\omega_r = \sqrt{\frac{K}{J_2}} = \sqrt{\frac{A E R_2^2}{J_2} \left(\frac{1}{L_2} + \frac{1}{L_3} \right)} . \qquad (253)$$

APPENDIX E

TENSION VARIATION IN A WEB SPAN WITH NON-UNIFORM THICKNESS ACROSS ITS WIDTH

The thickness of a web typically varies across its width. Consider an idealized web span which has a non-uniform thickness in the CMD of the web span as shown in Figure 103. It is assumed that there is the same amount of strain on the edges as in the middle portion.

By using the equation (20), the linearized relationship between the strain in the web and web-velocity for the web span between rollers 0 and 1 in Figure 103 is:

$$\frac{d}{dt}[\epsilon_1(t)] = -\frac{v_{10}}{L_1}\epsilon_1(t) + \frac{v_{00}}{L_1}\epsilon_0(t) - \frac{V_0(t)}{L_1} + \frac{V_1(t)}{L_1}. \qquad (254)$$

According to the results of analyses from Chapter 2.7, the effect of the viscoelastic properties of a web on tension variation will be neglected in the mathematical modeling. Using equation (21), the tension loaded in the non-uniform thickness web span is :

$$T = A\,E\,\epsilon_1. \qquad (255)$$

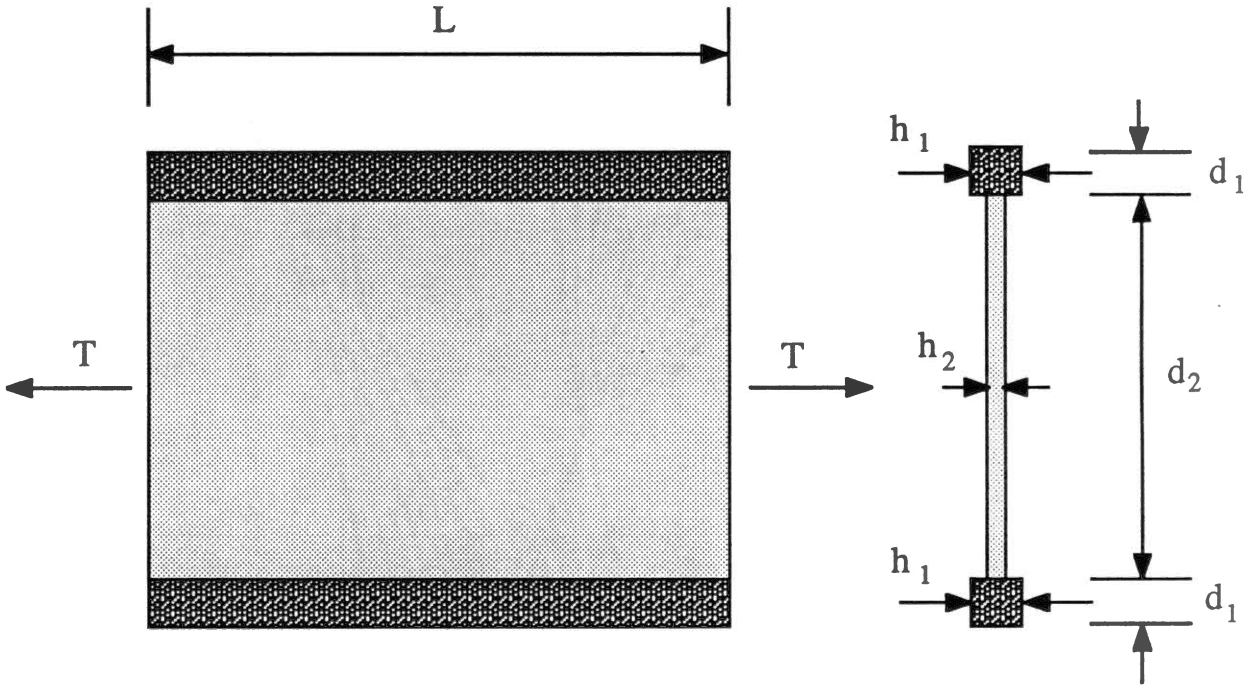

where

L : Length of the free span

T : Tension loaded

h_1 : Thickness of web edges

h_2 : Thickness of the web in the middle portion

d_1 : Width of web edges

d_2 : Width of the center portion of the web.

Figure 103. A Free Web Span with Non-Uniform Thickness in CMD

Assume that stress and strain in the cross-sectional area are uniform across its width. Since the thickness of the web is non-uniform across its width, the tension T can be written as follows:

$$T = T_1 + T_2 ,$$

where

$$T_1 = A_1 E \in_1 = d_2 h_2 E \in_1 , \qquad (256)$$

$$T_2 = A_2 E \in_1 = 2 d_1 h_1 E \in_1 , \qquad (257)$$

and

A_1 : Cross-sectional area of the web in the middle portion

A_2 : Sum of cross-sectional areas of the web edges

T_1 : Tension loaded in the middle portion

T_2 : Sum of tension loaded web edges

$\in_1$: Strain .

By solving equations (254) through (257) simultaneously, tensions in the edges and middle portion of the web can be calculated separately.

VITA

Kee-Hyun Shin

Candidate for the Degree of

Doctor of Philosophy

Thesis: DISTRIBUTED CONTROL OF TENSION IN MULTI-SPAN WEB TRANSPORT SYSTEMS

Major Field: Mechanical Engineering

Biographical:

Personal Data: Born in Jeom-Chon City, Kyung-Book Korea, September 27, 1953, the son of Jin-Joo Hong and Young-Kyu Shin.

Education: Graduated from Seoul High School, Seoul, Korea in January 1974; received the Bachelor of Science degree in Mechanical Design and Production Engineering from Seoul National University at Seoul, Korea in February 1981; received the Master of Science degree in Mechanical Design and Production Engineering from Seoul National University in February 1983; received the Master of Science degree in Mechanical Engineering from Oklahoma State University in December 1987; completed requirements for the Doctor of Philosophy degree in May 1991.

Professional Experience: US Army in Korea, operation and maintenance of Nike Hercules Missile Launching System,

August 1975, to April 1978; Research Associate, Korea Institute of Industrial Economy in Seoul, production management, management information system, December 1981, to December 1982; Research Assistant and Teaching Assistant, Mechanical Design and Production Engineering, Seoul National University, March 1981 to February 1983; Lecturer, Mechanical Design and Production Engineering, National Gyung-Gi Open College, Seoul, automatic control, hydraulic system design, March 1983, to February 1984; Teaching Assistant, Mechanical Engineering, Oklahoma State University, January 1985, to June 1989; Graduate Research Associate, Web Handling Research Center, Oklahoma State University, analysis and control of web transport systems, January 1986, to August 1990; Presently Post Doctoral Research Fellow, Web Handling Research Center, Oklahoma State University, design and implementation of real-time process control systems, analysis and control of web handling systems, development of computer-based tools for web handling systems.

Professional Societies and Honors: Member of the American Society of Mechanical Engineers; Member of the Institute of Electrical and Electronics Engineers; Received travel award from the American Society of Mechanical Engineers to attend 1988 Winter Annual Meeting; Member of Phi Kappa Phi.